

ЖУРНАЛ
ПРИКЛАДНОЙ ХИМИИ

Volume 32, No. 4

April 1959

JOURNAL OF
APPLIED CHEMISTRY
OF THE USSR

(ZHURNAL PRIKLADNOI KHIMII)

IN ENGLISH TRANSLATION



CONSULTANTS BUREAU, INC.

SYNTHESES OF HETEROCYCLIC COMPOUNDS

Volumes 1 and 2 Edited by
A. L. MNDZHOIAN

TRANSLATED FROM RUSSIAN

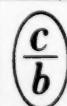
THE lack of a practical guide to the laboratory preparation of heterocyclic compounds is being met by this series of collections of synthesis methods, originally published by the Armenian Academy of Sciences.

The translation of Volumes 1 and 2 of this series is combined in this convenient handbook, devoted exclusively to the synthesis of furan derivatives.

Subsequent volumes in the series will be published in translation by Consultants Bureau promptly after their appearance in the original Russian.

1959 cloth 6 x 9 155 pp. illus. \$6.00

Book Division



CONSULTANTS BUREAU, INC.

227 WEST 17TH STREET, NEW YORK 11, N. Y.

Volume 32, No. 4

April 1959

JOURNAL OF
APPLIED CHEMISTRY
OF THE USSR

(ZHURNAL PRIKLADNOI KHIMII)

A publication of the Academy of Sciences of the USSR

IN ENGLISH TRANSLATION

Year and issue of first translation:

Vol. 23, No. 1

January 1950

	<i>U. S. and Canada</i>	<i>Foreign</i>
<i>Annual subscription</i>	<i>\$60.00</i>	<i>\$65.00</i>
<i>Annual subscription for libraries of nonprofit academic institutions</i>	<i>20.00</i>	<i>25.00</i>
<i>Single issue</i>	<i>7.50</i>	<i>7.50</i>

Copyright 1960

CONSULTANTS BUREAU INC.
227 W. 17th ST., NEW YORK 11, N. Y.

Editorial Board
(ZHURNAL PRIKLADNOI KHIMII)

P. P. Budnikov, S. I. Vol'fkovich, A. F. Dobrianskii,
O. E. Zviagintsev, N. I. Nikitin (Editor in Chief),
G. V. Pigulevskii, M. E. Pozin, L. K. Simonova
(Secretary), V. V. Skorchelletti, N. P. Fedot'ev

*Note: The sale of photostatic copies of any
portion of this copyright translation is expressly
prohibited by the copyright owners.*

Printed in the United States of America

CONTENTS

	PAGE	RUSS. PAGE
Realization of D. I. Mendeleev's Idea Concerning the Underground Gasification of Coal. <u>A. M. Terpigorev and M. P. Korsh</u>	731	705
The Hydrolysis Rate of Monocalcium Phosphate in Aqueous Solutions. <u>M. E. Pozin, B. A. Kopylev and D. F. Zhil'tsova</u>	736	710
The Hardening of Sorel Cements. <u>I. P. Vyrodov and A. G. Bergman</u>	742	716
Decomposition of Silver Halides and Determination of Their Silver, Bromine and Iodine Contents. <u>G. I. Barannikov</u>	749	724
Elution of Noble Metals From Anion Exchangers After Adsorption. <u>A. B. Davankov and V. M. Laufer</u>	753	727
Comparative Study of the Thermal Stability of Sulfonated Cation Exchangers Heated in Water. <u>N. G. Polyanskii</u>	760	735
Physicochemical Properties of Glassy Lithium Silicates and Aluminosilicates. <u>S. K. Dubrovo and Yu. A. Shmidt</u>	767	742
Production of Acid-Resistant Material Based on Corundum With Additions of Organosilicon Polymers. <u>I. D. Abramson, V. A. Bork and I. I. Kornblit</u>	774	750
Kinetics of Formation of Nickel Carbonyl From Ammine Sulfate Solutions. <u>G. N. Dobrokhotov</u>	780	757
Methods for Production of Aluminum Hydroxide and the Deformation and Strength Characteristics of Its Pastes in Petrolatum. <u>A. A. Trapeznikov and A. M. Tolmachev</u>	786	763
Effects of Hydrodynamic Factors on the Carbonation of Ammoniacal Brines in Gas Lift Equipment. <u>G. N. Gasyuk, A. G. Bol'shakov, A. V. Kortnev and P. Ya. Krainii</u>	792	770
The Physical Chemistry of Foams. <u>V. G. Gleim and I. K. Shelomov</u>	799	778
Calculation of the Height of Equipment for Chemical Interaction of Gases With Liquids. <u>L. A. Mochalova and M. Kh. Kishinevskii</u>	806	785
Phase-Contact Area of Immiscible Liquids During Agitation by Mechanical Stirrers. <u>V. V. Kafarov and B. M. Babanov</u>	810	789
Investigation of the Dust-Absorbing Properties of Solutions of Wetting Agents in a Dust Chamber. <u>S. Kh. Zakieva and A. B. Taubman</u>	817	797
Methods for Calculation of Mass Transfer in Equipment With Continuous Variation of Driving Force in Apparatus of the Stepwise Type. <u>V. M. Govorkov and Ya. D. Averbukh</u>	820	800

CONTENTS (continued)

	PAGE	RUSS. PAGE
General Form of Criterial Equations for Mass Transfer in Equipment with Fixed Interfacial Area. <u>L. D. Berman</u>	826	807
Apparatus for Determination of Liquid-Vapor Equilibria. <u>I. N. Bushmakín</u>	831	812
Effects of Fused Lithium, Sodium, and Potassium Hydroxides on Nickel, Copper, Iron, and Stainless Steel. <u>E. I. Gurovich</u>	836	817
Cathodic Liberation of Zinc From Zinc Sulfate Solutions With High Contents of Iron Ions. <u>O. A. Khan and L. S. Dukhankina</u>	841	823
Hydrogen Overvoltage at a Porous Iron-Nickel Cathode. <u>I. B. Barmashenko and V. I. Shapoval</u>	845	827
Mechanism of Formation of Bright Nickel Deposits in Baths With Sulfur-Containing Additives. <u>R. M. Morgart and O. É. Panchuk</u>	851	833
Production of Bright Coating in Electrodeposition of Copper-Gold Alloys. <u>B. S. Krasikov and Yu. D. Grin</u>	855	837
The State of Nickel in Ammoniacal Tartrate and Citrate Solutions. <u>T. F. Frantsevich-Zabludovskaya, A. I. Zayats, and V. T. Barchuk</u>	859	842
Separation of Mixtures of Alcohols and Hydrocarbons by Extraction. <u>V. B. Kogan, V. M. Fridman, and T. G. Romanova</u>	864	847
Main Laws Governing the Hydrolysis of Polysaccharides in Homogeneous and Heterogeneous Media. <u>A. A. Konkin and Z. A. Rogovín</u>	868	852
Polymerization of Styrene in Presence of 1-Hydroxy-1'-Hydroperoxodicyclohexyl Peroxide and Cobalt Naphthenate. <u>R. K. Gavurina, P. A. Medvedeva, Sh. G. Yanovskaya and Z. A. Granova</u>	873	857
Investigation of Certain Epoxy Stabilizers for Polyvinyl Chloride. <u>A. A. Berlin, E. N. Zil'berman, N. A. Rybakova, A. M. Sharetskii and D. M. Yanovskii</u>	880	863
Polycondensation of Phenoxyacetic Acid With Formaldehyde and Synthesis of a Weakly Acidic Ion Exchanger From Them. <u>A. A. Vansheidt and N. N. Kuznetsova</u>	885	868
Hypochlorination of Propylene. <u>V. S. Étlis and L. N. Grobov</u>	891	874
Certain Reactions Carried Out With Methylene Chloride Without The Use of Pressure in Benzyl Alcohol as a High-Boiling Solvent. <u>E. D. Laskina</u>	895	878
Arylation of Methylchlorosilane by Aromatic Hydrocarbons. <u>K. A. Andrianov, I. A. Zubkov, V. A. Semenova, and S. I. Mikhailov</u>	900	883
Oxidation of a Mixture of Cyclohexane and Cyclohexanol to Adipic Acid. <u>I. V. Berezin, E. T. Denisov, E. N. Suvorova, Z. S. Smolyan and N. M. Emanuéľ</u>	906	888
Influence of Chemical Structure of Sulfenamide Compounds on Vulcanization Activity. <u>M. S. Fel'dshtein, B. A. Dogadkin, I. I. Éitingon, G. P. Shcherbachev and N. P. Strel'nikova</u>	910	893
Composition of the Products of Cyclohexanol Dehydrogenation Over A Zinc Catalyst and Conversion of the Resultant Still Residue Into Cyclohexanone. <u>L. Kh. Freidlin, V. Z. Sharf, and Z. S. Smolyan</u>	918	901

CONTENTS (continued)

	PAGE	RUSS. PAGE
Antiseptic Properties of Coal-Tar Components. <u>G. D. Kharlampovich, M. V. Gofman, M. M. Raukas, and N. D. Rus'yanova.</u>	922	905
Determination of Molecular Weights of Humic Preparations Cryoscopically in Pyrocatechol. <u>T. A. Kukharensko and L. N. Ekaterinina</u>	926	909
Production of Formaldehyde in a Flow Unit By Oxidation of Methane, Catalyzed By Nitrogen Oxides. <u>N. S. Enikolopyan, N. A. Kleimenov, L. V. Karmilova, A. M. Markevich, and A. B. Nalbandyan.</u>	930	913
Synthesis of α, β -Cyclopentamethylenetetrazole (Corazole). <u>R. G. Glushkov and E. S. Golovchinskaya</u>	937	920
A New Synthesis of Sulfanthrol. <u>N. N. Dykhanov and A. S. Dykhanova</u>	941	924
Brief Communications		
Preparation of Spectrally Pure Rhodium. <u>V. V. Lebedinskii, E. V. Shenderetskaya, and A. G. Maforova.</u>	944	928
Preparation of Spectrally Pure Palladium. <u>A. M. Rubinshtein and S. K. Sokol.</u>	947	930
Electrolytic Preparation of Potassium Perborate. <u>N. E. Khomutov and A. T. Sklyarov</u>	949	931
Separate Determination of Cyclohexanone and Cyclohexanol in Aqueous Solutions. <u>A. S. Maslennikov.</u>	951	933
Apparatus for Preparation of Salts by Anodic Solution of Metals. <u>V. I. Kravtsov and Yu. N. Polovoi</u>	954	935
Reaction of Ammonia With the Oxide of Petroselinic Acid. <u>G. V. Pigulevskii, I. L. Kuranova, and É. V. Sokolov</u>	957	937
Condensation of Isophthalic Aldehyde With Nitromethane. <u>V. V. Perekalin and O. M. Lerner.</u>	959	939



REALIZATION OF D. I. MENDELEEV'S IDEA CONCERNING THE UNDERGROUND GASIFICATION OF COAL

A. M. Terpigorev and M. P. Korsh

D. I. Mendeleev was the originator of the notable idea of underground gasification of coal as a chemical method for utilization of the energy of coal without the need to bring it to the surface.

He wrote in 1888: "... a time will probably come when coal will not be taken out of the earth, but a method will be devised for converting it into inflammable gases underground, and for distributing these gases by pipes over long distances" [1].

In subsequent years Mendeleev repeatedly returned to the idea of the underground gasification of coal. In a discussion of individual aspects of this method of coal utilization, he stated in 1897 that "... in my opinion, the cost of coal fuel can be greatly lowered in the future only if the coal is converted underground, if possible, in the actual seams (without excavation), into producer gas and then distributed by pipelines; I do not foresee any significant difficulties in this" [2].

The great scientist not only formulated the principle that coal seams can be converted into gaseous fuel, but also indicated a solution for the engineering aspects of the problem. Of course, this was merely a remote prototype idea of the modern underground gasification plants, but the principles stated by Mendeleev formed the basis of production schemes subsequently proposed by others.

In studying underground fires in coal mines, he reached the conclusion that, if the fires can be controlled so that the combustion takes place in the same way as in a gas producer, i.e., with limited air access, producer gas can be made in the seam. "Several orifices should be drilled in the seam; some of these should be used for introduction of air, even by blowing, and others for the exit or withdrawal (for example, by a suction fan) of the inflammable gases, which can then easily be taken to furnaces, even over long distances" [3].

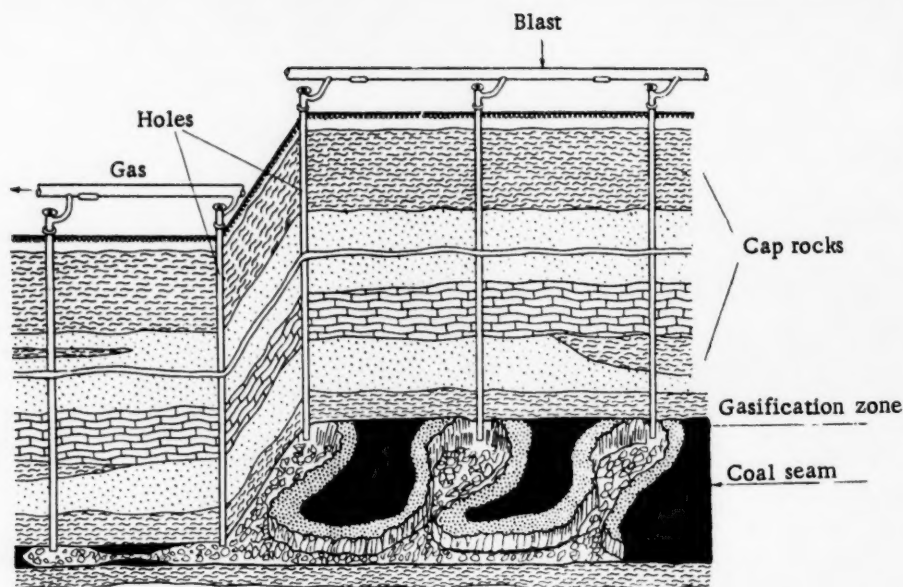
Mendeleev did not see his idea realized, and even the idea of underground gasification itself remained forgotten for some time.

It was only in 1912, five years after Mendeleev's death, that the English chemist William Ramsay, with whom Mendeleev was personally acquainted, remembered the idea of underground gasification of coal. It is likely that Ramsay got the idea from Mendeleev, especially as Mendeleev's work and his views on this subject had been published extensively at that time. However, Mendeleev's idea was not put into practice either in Tsarist Russia or in England. Ramsay's communication on the underground gasification of coal attracted the attention of Vladimir Il'ich Lenin. He appreciated fully the colossal social and technical advantages of underground gasification over the pit method of coal winning.

In an article entitled "One of the Great Victories of Technology," Lenin wrote in 1913, as follows on the discovery of this process: "An enormous amount of human labor now used in winning and transportation of coal would be saved. Even the poorest coal deposits, and new unworked fields could be utilized. Costs of domestic heating and lighting would be greatly lowered.

The industrial revolution caused by this discovery will be enormous" [4].

Prospecting, planning, and scientific research work on underground gasification of coal commenced in the Soviet Union in 1933.



Underground gasification scheme for horizontal coal seams.

The outbreak of war arrested further development in this field. In the postwar period more extensive and diverse investigations on underground gasification were started. A number of difficulties was encountered, such as are inevitable in any new project, and especially in the solution of such a complex problem as underground gasification. Several institutes of the Academy of Sciences, USSR, joined in the work: the Institute of Combustible Minerals, Mining, G. M. Krzhizhanovskii Power Engineering, Automation and Telematics, Geophysics, Geological Sciences, and the F. P. Savarenskii Laboratory of Hydrogeological Problems. By a Government decision, a special Scientific Research and Planning Institute for Underground Gasification of Fuels (VNIIP) was established in 1949.

In addition, work is in progress in scientific sectors and at underground gasification stations under various geological and mining conditions.

Numerous scientific, engineering, and technological workers are engaged on the realization in our country of the idea of underground gasification of coal, which was highly appraised by V. I. Lenin.

A blast containing oxygen, such as air, is supplied to an ignited coal seam through a blow-hole. When oxygen comes in contact with a region of the coal seam heated above the ignition temperature, the following principal reactions take place:



In presence of oxygen the carbon monoxide in the gas phase is oxidized to the dioxide:

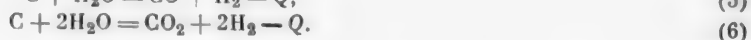
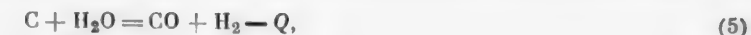


These reactions are accompanied by evolution of much heat. Therefore, the temperature of the gas in the oxidation (oxygen-containing) zone increases as these reactions develop.

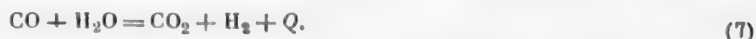
The carbon dioxide formed is reduced to carbon monoxide in the subsequent regions of the coal channel along the course of the blast:



If water vapor is present in the reducing zone, it undergoes decomposition according to the equations:



Under certain conditions the conversion reaction of carbon monoxide with water vapor may also become significant in underground gasification:



If heat is supplied continuously and in adequate quantity to the reducing zone, mainly from the products formed in Reactions (1)-(3), and if this zone (heated coal channel) is of sufficient length, the endothermic reactions (4)-(6) will be intensive. Toward the end of the reducing zone, considerable amounts of combustible components — carbon monoxide and hydrogen — are formed in the gas, and these, together with the other gasification products (N_2 , CO_2 , CH_4 , H_2S , C_nH_m) leave through the gas outlet hole and enter the gas pipe.

First a shaft method and subsequently a combined method was used for preparation of coal seams for gasification, i.e., for formation of underground gas producers. This required underground human labor, and the underground gas producers were not always satisfactorily airtight. Therefore, a great advance in underground gasification was the development by Soviet scientists and engineers, of shaftless methods for preparation of coal seams for gasification [5]. Underground gas producers are now constructed by the shaftless method, and consist of surrounded regions of the coal seam penetrated by a number of holes, gasification channels, and in some cases holes for drainage of ground water.

The design of the gas producers may vary considerably, and depends mainly on the geological situation of the seam and of the gasification system adopted.

Air, steam-air, oxygen-enriched, and steam-oxygen blasts are used in gasification. Formation of the original gasification channel, i.e., connection of the holes along the coal seam, is effected by means of air-flame crosscutting along the seam under different air pressures, electrical crosscutting (by means of an electric current), and by means of directed drilling; successful experiments are being carried out on channel formation by hydraulic fracturing of the seam.

The use of hydraulic fracturing is of great interest in relation to underground gasification of coal. Adoption of this method would allow wider spacing between the holes, and would shorten the crosscutting time and decrease power consumption in compression of the blast.

Neither the composition and properties of the coal, nor the stratification conditions now place any limitations on the gasification of coal seams. Underground gasification can be applied to the most varied combustible minerals, from bituminous shales to anthracites, at all depths down to hundreds of meters.

Three underground gasification plants are now operating in the Soviet Union: Podmoskovnaya in the Moscow coal field, Lisichanskaya in the Donetsk coal field, and Yuzhno-Abinskaya in the Kuznetsk coal field [6].

The Podmoskovnaya plant has already been in operation for 16 years. It produces about 420,000,000 cubic meters of gas per year, with a calorific value of 800 kcal/m^3 , which is supplied to several undertakings in the city of Tula.

The Lisichanskaya plant is working a coal deposit of complex structure. It is producing 100,000,000-120,000,000 cubic meters of gas per year, with a calorific value of 800 kcal/m^3 . It is used as boiler fuel in the North Donetsk Regional Electric Power Plant. In the future this station will be used as an experimental unit for scientific research work.

Steeply dipping seams are gasified at the Experimental Industrial Yuzhno-Abinskaya plant. Air blast is used to produce gas of calorific value of 900-1000 kcal/m^3 . The output is 160,000,000 cubic meters per year.

In addition to the existing plants, two industrial plants (Shatskaya and Angrenskaya) and one experimental (Kamenskaya) are now under construction.

The Shatskaya plant is being built in conjunction with a gas-turbine electric power plant of 24,000 kw capacity. This is the first gas-turbine power plant in the world to run on gas made by underground gasification. The gas output is rated at 634,000,000 m^3 annually.

The Angrenskaya plant is being built in the Uzbek SSR at a brown-coal deposit. Its planned gas output is 2,320,000 m³ per year, with a calorific value of 100 kcal/m³. This gas will supply the Angrenskaya Regional Electric Power Plant.

The Kamenskaya experimental unit is intended for experimental and development work on gasification of lean coals of the Donets field under natural conditions.

Development work on underground gasification must proceed by way of construction of industrial units in conjunction with extensive theoretical research and experimental work under natural conditions. Work is going on continuously in the Institute of Combustible Minerals of the Academy of Sciences, USSR, [7], in VNIIP, and at the operating stations, in order to improve existing and develop new methods of underground gasification and ways of controlling the process. Thus, as the result of investigations (at VNIIP) of underground gasification of brown coal, new technological processes were developed and tested on the pilot scale: a process with preliminary thermal preparation of the coal by means of the sensible heat of the gases [7], and a process with directed blast in the plane of the seam [8]. The principle of underground gasification with thermal preparation is that currents of hot gas are directed in such a way that the regions of the coal seam to be gasified are preheated. This lowers the natural moisture content of the coal and increases the number of crevices in it. The reactive surface of the coal is thereby increased; this is very important in relation to the heterogeneous reactions taking place in the formation of combustible gases.

In all sections in which thermally prepared coal was gasified, the calorific value of the gas made with the use of air blast reached 1000 kcal/m³, and gasification was almost complete. Moreover, coals of ash content up to 70% were gasified.

Theoretical calculations and experiments with VNIIP models showed that the quality of the gas can be improved and the gasification process intensified by variations of the blast velocity and structure.

In experiments with directed blast in the plane of the seam, the gas had a higher carbon monoxide content and higher calorific value than gas made by the usual blast through a hole. During the entire trial period the average calorific power of the gas was over 1000 kcal/m³.

The methods described above are by no means the only ones possible, and there are probably more effective methods for underground gasification of coal, which will undoubtedly be devised by Soviet scientists and engineers.

At present the gases made by underground gasification are used mainly as fuel in the generation of electric power. However, gases made by this process may also serve as raw materials in the synthesis of various chemicals.

As the result of theoretical and experimental investigations, conducted in the Institute of Combustible Minerals of the Academy of Sciences, USSR, and VNIIP, methods have been discovered and verified for the production of synthesis gases by underground gasification of coal. Experiments on the production of synthesis under natural conditions fully confirmed the theoretical findings. Gas suitable for ammonia synthesis was obtained from brown coal of the Moscow region [9].

One promising method to be studied for increasing the total efficiency of underground gasification by utilization of the sensible heat of gases is the use of semiconductors for direct conversion of heat into electrical energy (based on the work of Academician A. F. Ioffe and his associates). As was noted by Lavrov and Kirichenko [10], the use of semiconductors will enable semifurnace and furnace processes to be operated by the underground gasification of coal, so that thin and high-ash coal seams can be utilized, the gasification of which for production of good-quality gas is in practice impossible or difficult.

Success in the development of underground gasification of coal in the Soviet Union has attracted the attention of many foreign countries. Recently our country has been visited by representatives from Britain, the United States, Czechoslovakia, Bulgaria, Rumania, Poland, and the Chinese People's Republic, who desire to acquaint themselves with work in the field of underground gasification. Particular interest in this problem has been displayed by British business circles, representatives of which have made repeated visits to scientific research institutes working in this field, and to working gasification plants at different coal fields of the Soviet Union [11].

The Soviet Union is at present the only country in the world where underground gasification has been developed industrially.

More than 400 scientific papers have been published in the USSR on the subject of underground gasification; a list is given in Bakulev's monograph [12].

We believe that the time is not far distant when underground gasification of coal will take one of the leading positions in the utilization of coal energy for the good of our people.

LITERATURE CITED

- [1] D. I. Mendelev, *Collected Works*, 9 [in Russian] (Izd. AN SSSR, 1949) p. 66.
- [2] D. I. Mendelev, *Collected Works*, 9 [in Russian] (Izd. AN SSSR, 1949).
- [3] D. I. Mendelev, *Collected Works*, 2 [in Russian] (Izd. AN SSSR, 1949) p. 542.
- [4] V. I. Lenin, *Collected Works*, 4th Edn. 9 [in Russian] (State Political Literature Press, 1953). p. 41.
- [5] I. S. Garkusha and V. P. Yurchenko, *Bull. Sci. Tech. Information, TsITI Coal Industry* 7 (1957).
- [6] V. A. Matveev, *Bull. Underground Gasification of Coal* 2 (1957).
- [7] *Trans. Inst. Combustible Minerals* 7 (Izd. AN SSSR, 1957); G. O. Nusinov, N. É. Brunshtein and M. N. Kulakova, *Bull. Underground Gasification of Coal* 3 (1957).
- [8] K. M. Leonovich, *Bull. Underground Gasification of Coal* 3 (1957).
- [9] N. É. Brunshtein and M. A. Kulakova, *Bull. Underground Gasification of Coal* 4 (1957).
- [10] N. V. Lavrov and I. P. Kirichenko, *J. Acad. Sci. USSR* 6, 56 (1958).
- [11] *Mining, Electrical and Mechanical Eng.* 38, 448 (1958); *Colliery Eng.* 35, 408 (1958).
- [12] G. D. Bakulev, *Economic Analysis of the Underground Gasification of Coal*, with preface by Academician A. M. Terpigorev (editor) [in Russian] (Izd. AN SSSR, 1957).

Received November 3, 1958

THE HYDROLYSIS RATE OF MONOCALCIUM PHOSPHATE IN AQUEOUS SOLUTIONS

M. E. Pozin, B. A. Kopylev and D. F. Zhil'tsova

The Leningrad Technological Institute, Leningrad

A knowledge of the properties of the ternary system $\text{CaO}-\text{P}_2\text{O}_5-\text{H}_2\text{O}$ is required for effective performance of most technological processes in the production of phosphate fertilizers.

Solubility in this system has been studied at 20, 25, 40, 50, 70, 80° [1-6]. The equilibrium diagram can be used to calculate the degree of decomposition of monocalcium phosphate at various temperatures and water-salt ratios. Experimental data are available on the degree of hydrolysis of monocalcium phosphate under equilibrium conditions. However, the time required to reach equilibrium is several hours. It is known [1, 7] that

monocalcium phosphate has a great tendency to form supersaturated solutions from which disubstituted calcium phosphate crystallizes only after some time. Because of this, the attainment of equilibrium in the interaction of monocalcium phosphate with water is hindered; equilibrium is attained relatively easily in the interaction of anhydrous dicalcium phosphate with phosphoric acid. This demonstrates the importance of the time factor in studies of the interaction of monocalcium phosphate with water. However, we did not find any information in the literature on the hydrolysis rate of monocalcium phosphate under various conditions. Moreover, in a number of processes, such as the continuous conversion of phosphates by means of sulfuric or phosphoric acid [8], we are concerned with systems which have not reached equilibrium. Studies of the hydrolysis rate of monocalcium phosphate are therefore important.

The results of studies of the hydrolysis rate of monocalcium phosphate in water and phosphoric acid solution at different water-salt ratios and various temperatures are given below.

EXPERIMENTAL

Calculated quantities of the original substances — distilled water and monocalcium phosphate — were put into test tubes in a thermostat. After the water and salt had been stirred together for

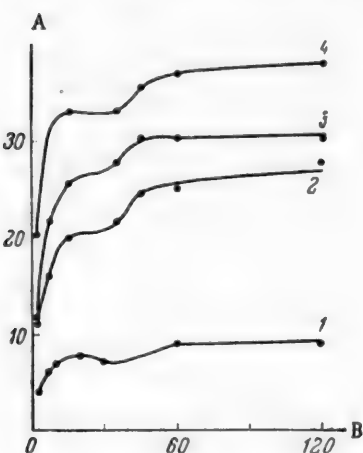


Fig. 1. Degree of decomposition of monocalcium phosphate in water at 20° and at different salt-water ratios: A) degree of decomposition (%); B) time (minutes). S:W ratio: 1) 0.05; 2) 0.25; 3) 0.43; 4) 1.5.

a definite time, the liquid phase was separated from the solid residue by centrifugation and analyzed by titration with caustic soda solution.

The degree of decomposition was calculated from the equation

$$A = \frac{a}{a + y} \cdot 100,$$

where a is the amount of monocalcium phosphate hydrolyzed, and y is the amount of monocalcium phosphate in solution.

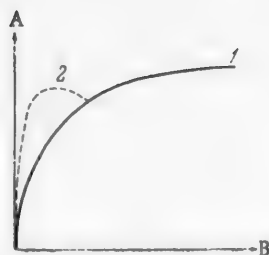


Fig. 2. Qualitative representation of the hydrolysis of monocalcium phosphate: A) degree of decomposition; B) time; 1) hydrolysis without supersaturation of the solution; 2) hydrolysis with supersaturation of the solution by dicalcium phosphate.

Fig. 1 shows variations of the degree of decomposition of monocalcium phosphate by water as a function of time at 20° and at different salt-water (S:W) ratios. It is seen that equilibrium was not reached in 2 hours at any of the S:W ratios taken. Comparison of these results with the equilibrium values calculated from the diagram for 20° [1] shows that for S:W ratio of 0.25, the degree of decomposition of monocalcium phosphate at equilibrium reaches 40.51%, and after 2 hours it is only 27.9%; during the first 15 minutes 20% of the monocalcium phosphate is decomposed. The rate varies analogously for other S:W ratios.

At S:W ratio of 0.1, 10% is hydrolyzed during the first six minutes, and only 1.7% during the subsequent 10 minutes. The hydrolysis rate is relatively high during the first 5-10 minutes of contact between monocalcium phosphate and water. Subsequently hydrolysis slows down with accumulation of phosphoric acid in solution. The subsequent decomposition of monocalcium phosphate in presence of free phosphoric acid is relatively slow. The curves for degree of decomposition as a function of time (Fig. 1) follow a peculiar course, which is observed in all experiments, both in duplicate and under different conditions.

The first relatively short period of rapid decomposition of the salt is followed by some retardation (or arrest) of hydrolysis for about 20 minutes. Subsequently the degree of hydrolysis gradually increases with time of stirring and asymptotically approaches its equilibrium value.

A possible explanation of this character of the curves is that the degree of decomposition of monocalcium phosphate by water at any instant is determined by a number of processes taking place at different rates. These include dissolution of the salt, its reaction with water, and crystallization of dicalcium phosphate. The tendency of mono- and dicalcium phosphates to form supersaturated solutions [1, 7] must also be taken into account. It is possible that during the initial period the solution is supersaturated with respect to dicalcium phosphate, and the decomposition rate of monocalcium phosphate is determined by the rate of its dissolution. The amount of monocalcium phosphate which dissolves and undergoes hydrolysis is somewhat greater than the amount which would be dissolved and hydrolyzed in absence of supersaturation. The dicalcium phosphate formed does not yet have time to crystallize. Subsequently supersaturation ceases because of the interaction of phosphoric acid with dicalcium phosphate (Fig. 2).

Hydrolysis of the Products of Incomplete Decomposition of Apatite by Phosphoric Acid

Time (min)	Degree of decomposition (%) at different temperatures and S:W ratios				
	0.75	0.5	1.5	0.75	0.5
	40°		80°		
10			4.8	18.8	18.8
20			17.2	20.0	21.0
30	Nil	Nil	17.4	—	26.3
60			20.7	25.6	29.2
180	1.1	2.5	22.5	26.4	34.1
240	1.6	7.5	—	—	—
300	—	8.5	26.0	—	—

As a result, the degree of hydrolysis diminishes somewhat during the second period. This is also confirmed by the fact that the amount of phosphoric acid in solution decreases during the period when the increase of the degree of decomposition is retarded. This is accompanied by a decrease in the amount of monocalcium phosphate because of its crystallization as the result of even greater supersaturation of the solution owing to the occurrence of the reverse reaction (removal of supersaturation).

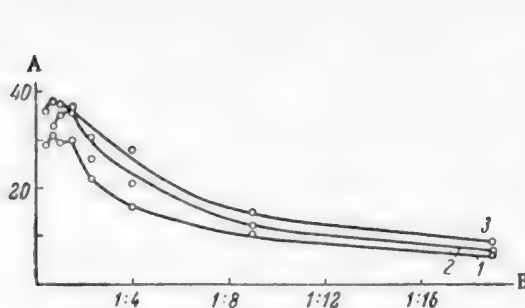


Fig. 3

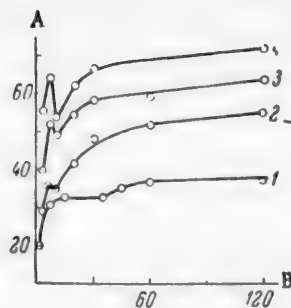


Fig. 4

Fig. 3. Isotherm-isochrones for the degree of decomposition of monocalcium phosphate by water at 20° as a function of the S:W ratio: A) degree of decomposition of monocalcium phosphate (%); B) S:W ratio. Time (minutes): 1) 7; 2) 30; 3) 120.

Fig. 4. Degree of decomposition of monocalcium phosphate by water at S:W ratio 1.5 and various temperatures: A) degree of decomposition (%); B) time (minutes). Temperature (°C): 1) 20; 2) 50; 3) 60; 4) 80.

The highest degree of decomposition at 20° during 2 hours is reached at S:W ratio 1.5 (Fig. 3).

The degree of decomposition in a given time decreases with change of this ratio.

The curve for variations of the degree of hydrolysis with S:W ratio for a 2-hour period is analogous to the curve for equilibrium conditions. However, with decrease of the reaction time (the 7- and 30-minute isochrones) the change in the degree of hydrolysis in the region of high S:W ratios is somewhat different in character. Thus, for the 30-minute isochrone, the maximum degree of decomposition is somewhat further to the right, at a lower S:W ratio. The 7-minute isochrone has two maxima; the reasons for this were discussed above.

Variation of the degree of decomposition of monocalcium phosphate with time at different temperatures are plotted in Fig. 4.

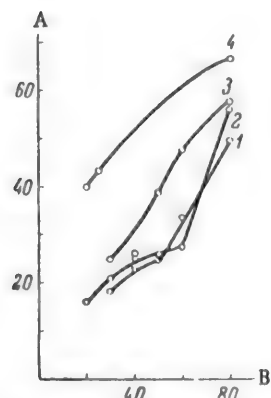


Fig. 5. Isochrones for the degree of decomposition of monocalcium phosphate by water as a function of temperature at S:W ratio 0.25: A) degree of decomposition of monocalcium phosphate (%); B) temperature (°C). Time (min): 1) 10; 2) 7; 3) 120; 4) at equilibrium.

The degree of decomposition increases with rise of temperature from 20° to 80°. At S:W ratio 1.5 the degree of decomposition in 2 hours is 38.5% at 30°, 49% at 40°, 55.4% at 50°, 64.5% at 60°, and 72.5% at 80°.

A similar relationship holds at other S:W ratios. For example, at S:W ratio 0.05, the degree of decomposition for the same time is 9.0% at 20°, 22.5% at 30°, 25.8% at 40°, 29.5% at 50°, 34.65% at 60°, and 47.2% at 80°.

The curves for variations of the degree of decomposition with time each have these three regions for all the temperatures studied. Supersaturation of the solution with dicalcium phosphate increases during the first period with rise of temperature, and accordingly the degree of decomposition shows a greater decrease during the second period. The influence of the time factor in hydrolysis is illustrated in Fig. 5, which shows isochrones for 7, 10, and 120 minutes compared with the equilibrium curve for variations of the degree of decomposition with temperature.

The 7-minute isochrone lies somewhat higher than the 10-minute curve. The degree of hydrolysis increases little with increase of temperature in the 20-40° range. There is a sharp increase of the degree of decomposition in the 40-80° range. Accordingly, the system is much further from equilibrium at low than at high temperatures. This accounts for the observed greater change of the degree of hydrolysis during the second period of interaction between the salt and water.

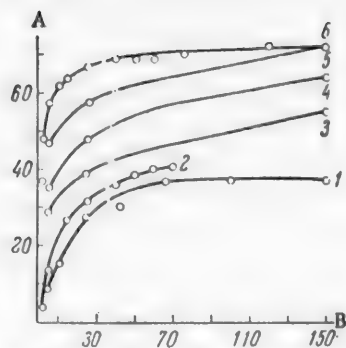


Fig. 6. Two-hour and equilibrium isotherms for the degree of decomposition of monocalcium phosphate by water as a function of S:W ratio: A) degree of decomposition of monocalcium phosphate (%); B) amount of $\text{Ca}(\text{H}_2\text{PO}_4)_2$ (in grams per 100 g water). Temperature ($^{\circ}\text{C}$): 1) 20; 2) 20 (equilibrium, after Sanfourch); 3) 50; 4) 60; 5) 80; 6) 80 (equilibrium, after Belopol'skii).

In Fig. 6 the results are compared with the data of Belopol'skii et al. [1] and of Sanfourch [6]. Their results refer to systems at equilibrium.

Curves 1 and 3-5 represent variations of the degree of decomposition of monocalcium phosphate with the S:W ratio for a 2-hour period. It is seen that the curves for 20 and 80° , based on our experimental data lie somewhat below the corresponding equilibrium curves; this is because, as already stated, equilibrium was not reached during the time of the experiments.

Variations of the solution composition with time at S:W ratios 1.5 and 0.25 at 80° are represented by the isotherms in Fig. 7.

The solution composition varies in the course of hydrolysis along the saturation line, approaching the equilibrium points A and B.

At S:W ratios, such that the salt does not dissolve completely at once, but only as hydrolysis proceeds, the point for the equilibrium solution (A) lies to the right of the points for nonequilibrium solutions (1, 2, 3) in the direction of higher P_2O_5 contents. At S:W ratio 0.25 the salt dissolves completely in water, and therefore the point for the equilibrium solution (B) lies in a region of lower P_2O_5 content, i.e., to the left of the equilibrium point (4, 5, 6).

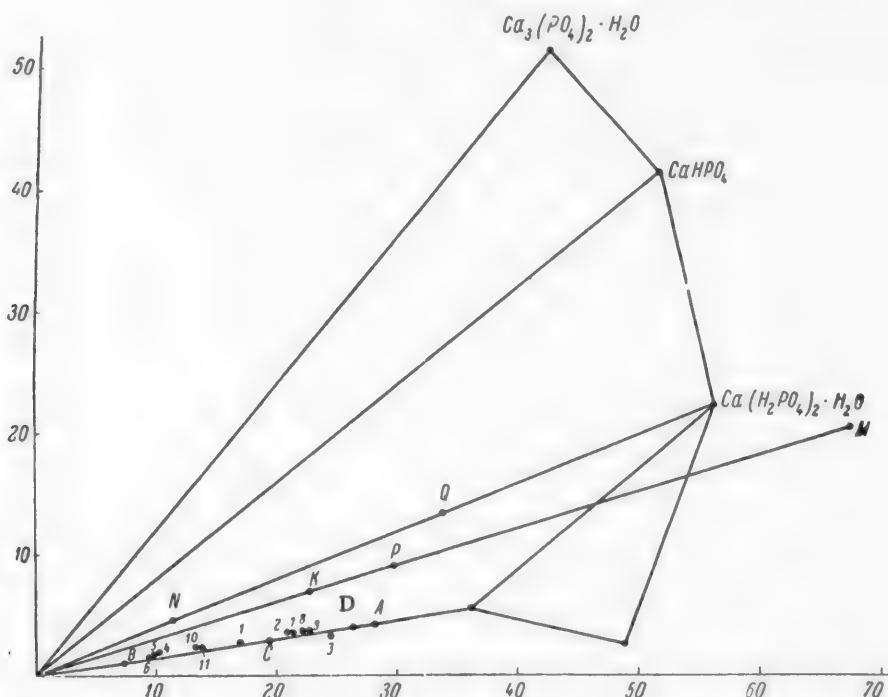


Fig. 7. Variation of solution composition with decomposition of monocalcium phosphate, represented in the equilibrium diagram for the system $\text{CaO}-\text{P}_2\text{O}_5-\text{H}_2\text{O}$ at 80° : ordinates) CaO contents (%); abscissas) P_2O_5 contents (%); M) composition of the soluble portion in incomplete decomposition of apatite by phosphoric acid. Compositions of the system at S:W ratios: Q) 1.5; N) 0.25; P) 0.8; K) 0.5. Times from start of experiment (min): for System Q: 1) 3; 2) 10; 3) 30; for System N: 4) 7; 5) 60; 6) 120; for System P: 7) 10; 8) 20; 9) 60; for System K: 10) 10; 11) 180.

It follows from these data that hydrolysis of monocalcium phosphate begins immediately upon mixing the reagents, at all temperatures and ratios of the starting substances. In the cyclic process of phosphate conversion one stage of the process is leaching of the monocalcium phosphate formed in water.

The yield of the product would be considerably lowered if hydrolysis took place. However, in the material leached, the degree of decomposition of apatite is approximately 70%. Moreover, it is to be expected that in presence of free phosphoric acid hydrolysis would be retarded. The composition of the soluble portion of the system after 70% decomposition of apatite (Fig. 7, point M) is: CaO 20.4%, P_2O_5 67.5%, and H_2O 12.1%.

This composition was taken as the basis for preparation of solutions of $Ca(H_2PO_4)_2$ and phosphoric acid with different amounts of added water, for studies of monocalcium phosphate hydrolysis at 20, 40, and 80°.

The results are given in the table.

No decomposition of monocalcium phosphate was observed at 20° at any S:W ratio, and at 40° at S:W ratio 1.5. At 40° and S:W ratios 0.75 and 0.5 hydrolysis was observed only after 3 hours. No hydrolysis could be detected at the same temperature in 5 hours as S:W ratio 1.5. Thus, the lower the free phosphoric acid concentration in the solution, the earlier does hydrolysis begin and the higher is the degree of decomposition in a given time.

Figure 7 shows the compositions of solutions obtained at 80° after 10, 20, and 180 minutes at S:W ratio 0.75 (7, 8, 9) and after 10 and 80 minutes at S:W ratio 0.5 (10, 11).

The solutions had not reached equilibrium composition, but were gradually approaching it along the saturation line (points D and C).

The results obtained in this study of hydrolysis in presence of phosphoric acid show that monocalcium phosphate can be leached at 20 and 40° out of the products formed by the decomposition of apatite by phosphoric acid without loss of P_2O_5 as the result of hydrolysis.

SUMMARY

1. The degree of decomposition of monocalcium phosphate by water depends on the time of contact between the reagents.

The hydrolysis rate is highest during the first 5-10 minutes of interaction between the salt and water. Thus, at S:W ratio 1.5, the degree of decomposition at 20° is 32.5% during the first 10 minutes, and 7.5% during the subsequent 10 minutes. At S:W ratio 0.1, the degree of decomposition over the corresponding periods is 10 and 1.7%, respectively.

2. The degree of decomposition at a given S:W ratio and decomposition time increases with rise in temperature. At S:W ratio 1.5, the degree of decomposition in 2 hours is 38.5% at 30°, 49% at 40°, 55.4% at 50°, 64.5% at 60°, and 72.5% at 80°. At S:W ratio 0.05, the degree of decomposition is 9% at 20°, 22.5% at 30°, 25.8% at 40°, 29.5% at 50°, 34.65% at 60°, and 47.2% at 80°.

3. The degree of decomposition of monocalcium phosphate is considerably lower in presence of free phosphoric acid than in pure water under the same conditions. At 20° and S:W ratios 0.75 and 0.5, no hydrolysis was observed over a period of 5 hours (the composition of the original system was: P_2O_5 67.5%, CaO 20.4%, H_2O 12.1%). At 40° and the same S:W ratios hydrolysis was observed only 3 hours after the start of the experiment.

4. Variations of the degree of decomposition of monocalcium phosphate with time show three different regions. A first, relatively short period of rapid decomposition is followed by some retardation (or cessation) of hydrolysis, followed by a slow increase of the degree of decomposition. It is suggested that this effect is caused by supersaturation of the solution with dicalcium phosphate.

LITERATURE CITED

- [1] A. P. Belopol'skii, A. A. Taperova, M. T. Serebrennikova and M. N. Shul'gina, J. Chem. Ind. 14, 7, 504 (1937).
- [2] H. Basset, Z. anorg. Chem. 53, 34,49 (1907); 59, 1 (1908).
- [3] K. L. Elmore and T. D. Farr, Ind. Eng. Chem. 32,580 (1940).
- [4] F. K. Cameron and Seidel, J. Am. Chem. Soc. 27, 1503 (1905).

- [5] F. K. Cameron and J. M. Bell, *J. Am. Chem. Soc.* **27**, 1512 (1905).
- [6] A. Sanfourch, and B. Fout, *Bull. Soc. Chim. France*, (4), **53**, 974 (1933).
- [7] M. L. Chepelevetskii, *J. Phys. Chem.* **13**, 5, 561 (1939).
- [8] M. E. Pozin, B. A. Kopylev and D. F. Zhil'tsova, *J. Appl. Chem.* **32**, No. 3, 509 (1959). *

Received April 10, 1958

*Original Russian pagination. See C. B. Translation.

THE HARDENING OF SOREL CEMENTS*

I. P. Vyrodov and A. G. Bergman

Despite the inexhaustible reserves of magnesium chloride and magnesites, and also of dolomites, our production and utilization of magnesium oxychloride (Sorel) cements is still at a low level.

Economic calculations [3, 4] show that the production costs of mass-produced goods, such as floor coverings (xylolith, Sorel cement with sawdust filler), wall partitions (fibrolite, Sorel cement with wood shavings), and other products [5] can be lowered considerably.

Therefore, deeper investigations into the nature of Sorel cements are of great technological importance.

The present communication contains some of our data obtained by differential thermal, tensimetric, and x-ray structural analyses.

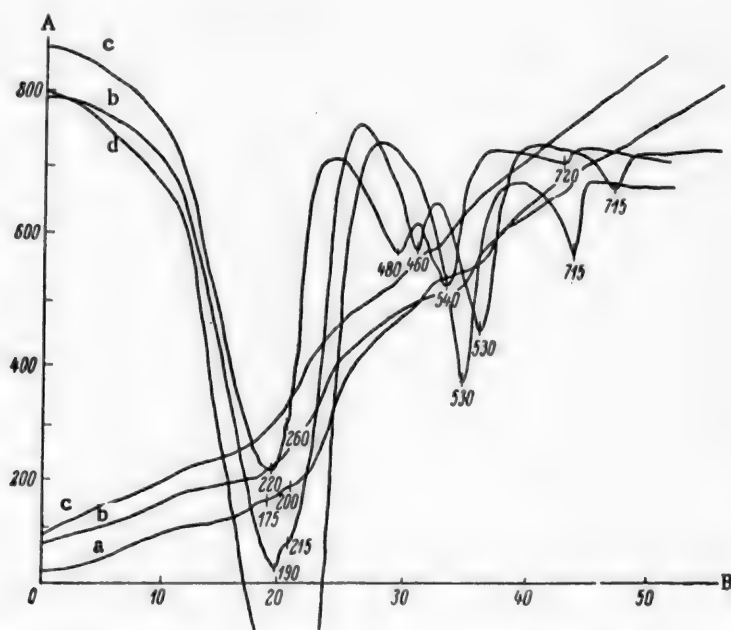


Fig. 1. Thermograms for cements of different compositions: A) temperature ($^{\circ}\text{C}$); B) time (minutes). a) $\text{MgO} \cdot \text{MgCl}_2 \cdot 10\text{H}_2\text{O}$; b) $2\text{MgO} \cdot \text{MgCl}_2 \cdot 10\text{H}_2\text{O}$; c) $3\text{MgO} \cdot \text{MgCl}_2 \cdot 10\text{H}_2\text{O}$.

EXPERIMENTAL

1. Samples of Sorel cements prepared as described previously [1, 2] were studied by means of differential thermal analysis. Thermograms of samples made with 35% magnesium chloride solutions are given in Figs. 1 and 2.
2. The $\text{MgO}:\text{MgCl}_2$ ratios for these samples were 1:1, 2:1, 3:1, 5:1, 7:1. The first sample ($\text{MgO}:\text{MgCl}_2 = 1:1$)

* Communication III [1, 2].

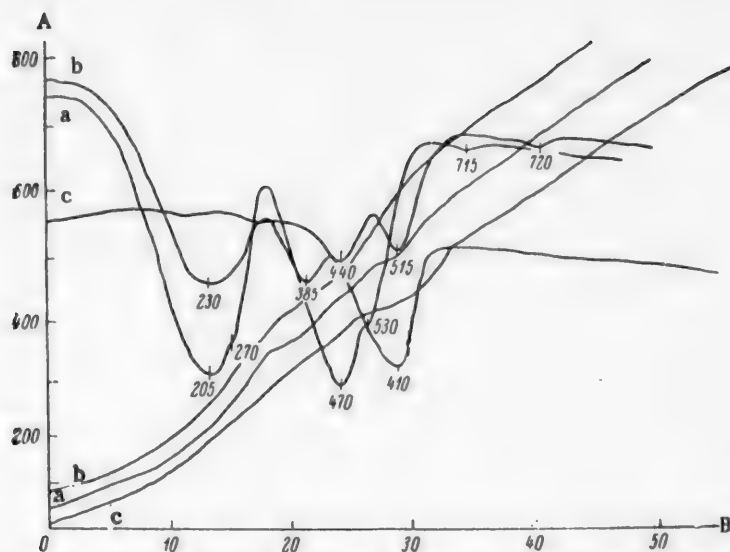


Fig. 2. Thermograms for cements of different compositions and for $\text{Mg}(\text{OH})_2$: A) temperature ($^{\circ}\text{C}$); B) time (minutes); a) $5\text{MgO} \cdot \text{MgCl}_2 \cdot 10\text{H}_2\text{O}$; b) $7\text{MgO} \cdot \text{MgCl}_2 \cdot 10\text{H}_2\text{O}$; c) $\text{Mg}(\text{OH})_2$.

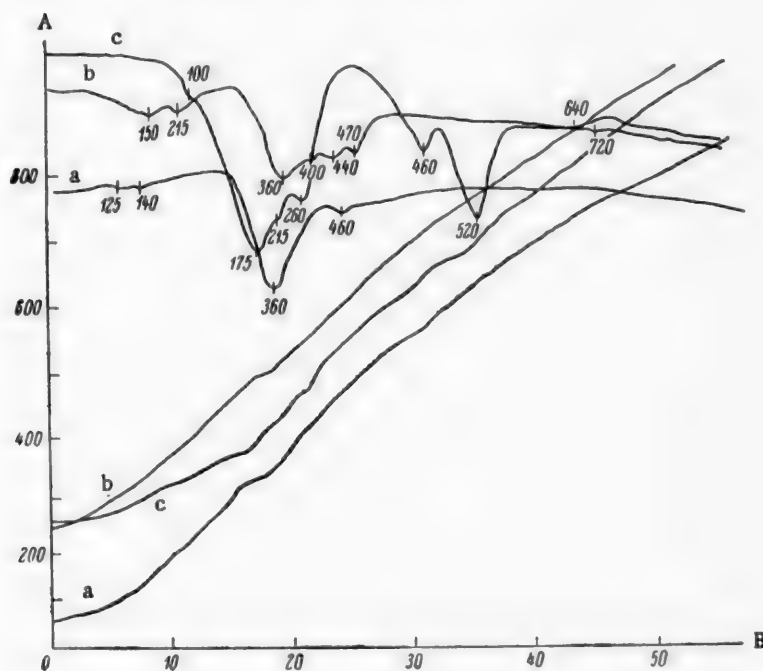


Fig. 3. Thermograms of precipitates formed from different MgCl_2 solutions: A) temperature ($^{\circ}\text{C}$); B) time (minutes). MgCl_2 contents (%): a) 10; b) 15; c) 20.

as Fig. 1 (curve a) shows, exhibits four distinct endothermic effects at 175, 200, 530, and 715°. The second sample ($\text{MgO} : \text{MgCl}_2 = 2 : 1$), represented by curve b, Fig. 1, shows five sharp endothermic effects at 190, 215, 460, 530, and 715°. The third sample ($\text{MgO} : \text{MgCl}_2 = 3 : 1$), represented by curve c, Fig. 1, has four pronounced endothermic effects at 220, 480, 540, and 720°, and an indistinct endothermic effect at 260°. A characteristic feature for these

three samples is the shift of the series of endothermic effects in the direction of higher temperatures. The endothermic effect at 175° for the first sample is shifted to 190° for the second sample and to 220° for the third. The endothermic effect at 200° for the first sample is shifted to 215° for the second and to 260° for the third. The second sample shows a new endothermic effect at 560°, which is shifted to 480° for the third. The endothermic effect at 530° is shifted to 540°, and the endothermic effect at 715°, to 720°.

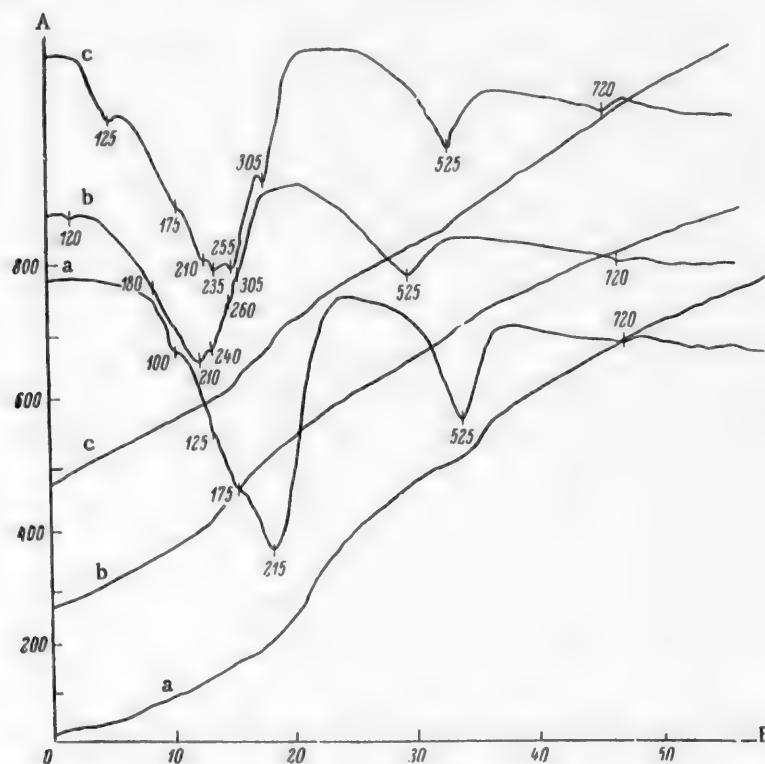


Fig. 4. Thermograms of precipitates formed from different MgCl_2 solutions: A) temperature ($^{\circ}\text{C}$); B) time (minutes). MgCl_2 contents (%): a) 25; b) 30; c) 35.

The sample with the composition $\text{MgO}:\text{MgCl}_2 = 5:1$ (curve a, Fig. 2) shows a new pronounced endothermic effect at 385°. In addition, there are strong endothermic effects at 205, 440, 515, and 720°, and a weak one at 270°. The sample with the composition $\text{MgO}:\text{MgCl}_2 = 7:1$ (Fig. 2, curve b) has only two strong endothermic effects, at 230 and 470°, and two weak effects, at 530 and 715°. Thus samples with $\text{MgO}:\text{MgCl}_2$ ratios of 1:1, 3:1, 5:1, and 7:1 are distinguished from each other. The endothermic effects, corresponding to these compositions persist over relatively wide concentration ranges (at constant $\text{MgO}:\text{MgCl}_2$ ratios).

The solid precipitates formed when 0.5 g MgO was shaken with 100 cc lots of magnesium chloride solutions of different concentrations were subjected to differential thermal analysis. It is clear from Figures 3 and 4 that the differential curves for the precipitates formed after 3 days in 10, 15, 20, 25, 30, and 35% solutions did not show the endothermic effects (at 410°) characteristic of $\text{Mg}(\text{OH})_2$ (Fig. 2, curve c).

It also follows from Figs. 3 and 4 that the oxychlorides formed in the precipitates from 10, 15, and 20% solutions differ appreciably from each other, whereas the oxychloride formed in the precipitate from 25% solution is also found in the 35% solution.

Since none of these thermograms shows an endothermic effect, corresponding to $\text{Mg}(\text{OH})_2$, it follows that magnesium hydroxide is not formed as an intermediate phase in the hardening of Sorel cements. Comparison of the x-ray patterns for a sample made with 35% solution at $\text{MgO}:\text{MgCl}_2$ close to 5:1 and heated to above 200, 480, and 530°, shows that the compositions formed as the result of heating give new lines in the x-ray patterns,

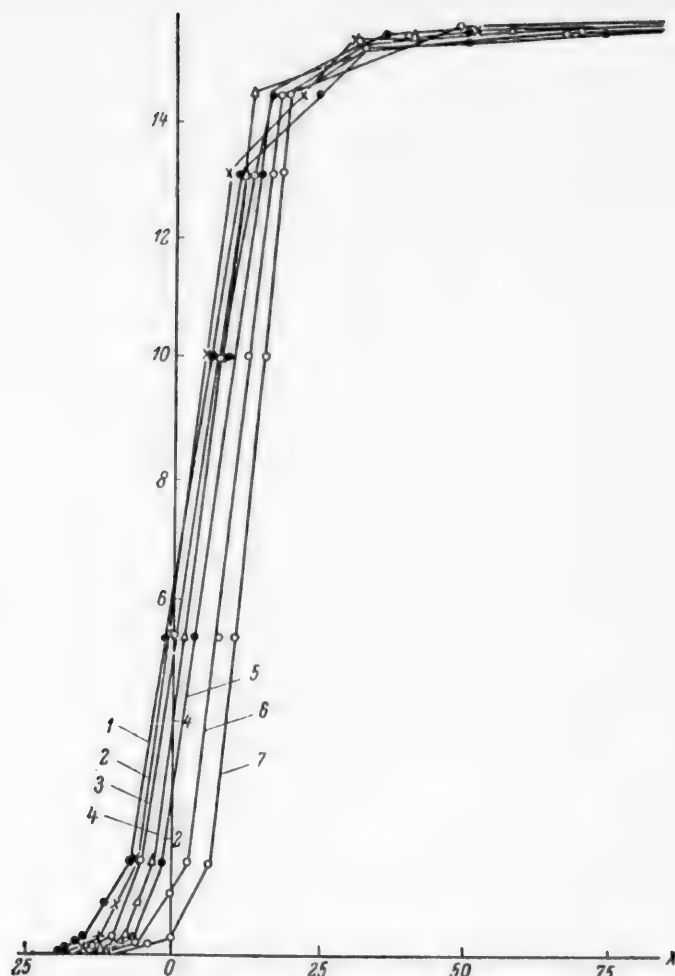


Fig. 5. $P = f(X)$ isotherms: P) water-vapor pressure (mm Hg), X) composition (%). Values of n (% MgO): 1) 35; 2) 40; 3) 45; 4) 50; 5) 60; 6) 75; 7) 105.

TABLE 1

Interplanar Spacing for the Oxychloride $3MgO \cdot MgCl_2 \cdot 10H_2O$

Heating temperature (°C)	I	$2L$ (mm)	θ°	$\frac{d}{n}$ (ln kX)	Heating temperature (°C)	I	$2L$ (mm)	θ°	$\frac{d}{n}$ (ln kX)
200	w	43	21.5	2.64	480	m	47.0	23.5	2.42
	s	47.4	23.7	2.41		m	49.65	24.82	2.29
	s	55.2	27.6	2.09		vs	54.9	27.45	2.096
	vw	59.15	29.6	1.955		m	72.3	36.15	1.638
	s	81.65	40.82	1.482		vs	81.2	40.0	1.494
	m	73.9	53.05	1.210		w	87.6	46.2	1.338
	w	46.0	67.0	1.0495		m	80.5	49.75	1.265
480	vw	40.3	20.15	2.80		s	74.3	52.85	1.212
	vw	43.15	21.57	2.62		s	46.0	67.0	1.0495
						vw	42.0	69.0	1.0347

Note: vw = very weak, w = weak, m = medium, s = strong, vs = very strong.

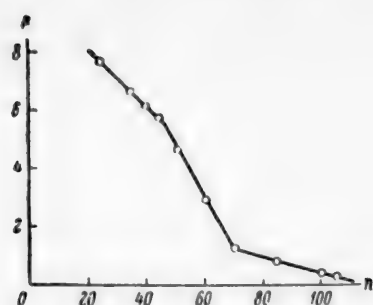


Fig. 6. $P = f(n)$ isotherm: P) water-vapor pressure (mm Hg); n) composition (% MgO).

not found in the patterns for the preceding compositions. It was found that the crystal system of the sample heated to above 200° is hexagonal. When the sample is heated to above 480° , the system is changed to tetragonal (Table 1).

2. The hypothesis which had been put forward by a number of workers, concerning the possibility of formation of $Mg(OH)_2$ during hardening of Sorel cements, made with the use of concentrated solutions, was not confirmed by our experiments. To test this, x-ray structural analysis of hardening specimens was performed, polished sections being photographed. The focusing angle was calculated by Kurdyumov's method [6]. The x-ray patterns were taken at intervals of 1.5 hours and then 24 hours after the mixing. The formation of $Mg(OH)_2$ should be revealed by very intense lines, corresponding to interplanar spacings $d/n = 4.75, 2.36$ and 1.79 kX.

However, such lines were not detected either during the period up to the temperature maximum of the reaction (3-4 hours) or after the maximum (Table 2). The exposures were 30 minutes with a Cu anode, in an RKD camera, $D = 57.3$ mm. Nevertheless, a brucite layer ($d/n = 2.36$ A) is formed in mixtures with $MgO:MgCl_2$ ratios less than 3:1 soon after the temperature maximum is reached. The somewhat high values for (d/n) of the brucite layer for the sample with $MgO:MgCl_2$ ratios of 5:1 ($d/n = 2.42$ kX) and the broadening of the reflection, corresponding to this interplanar spacing, may be attributed to deviations of the composition of the oxychlorides formed during hardening from the stoichiometric ratio, owing to lattice defects. The anion sites in the forming lattice are statistically distributed between OH^- and Cl^- ions, the radii of which conform to the expression $\Delta r/r \approx 15\%$ [7]. In consequence the x-ray patterns of the cements have no reflections in the precision region (small d/n and large θ). As the solution concentration decreases, lines begin to appear in the precision region too, and

TABLE 2

Interplanar Spacings $\left(\frac{d}{n}\right)$ for a Hardening Sample of the Composition $3MgO \cdot MgCl_2 \cdot 10H_2O$

Diagram No.	Time from mixing of MgO with $MgCl_2$ solution	I	I , (mm)	θ°	$\frac{d}{n}$ (in kX)
1	1.5 hours	vs	7	7.07	6.24
		vs	10	10.1	4.38
		s	19.6	19.8	2.269
		m	29	29.3	1.570
2	3 hours	vs	7	7.07	6.24
		vs	10	10.1	4.38
		s	19.6	19.8	2.269
		m	29	29.3	1.570
3	4.5 hours	vs	7	7.07	6.24
		vs	10	10.1	4.38
		vw	15.8	15.9	2.805
		vw	17.2	17.3	2.599
		s	19.6	19.8	2.269
4	One day	m	29	29.3	1.570
		vs	11	11.1	3.99
		vw	16.5	16.6	2.675
		w	18.8	18.5	2.42
		s	21.2	21.3	2.116
		w	31.0	31.3	1.479

the interplanar spacing (d/n) of 2.42 kX diminishes to 2.36 A. In x-ray investigations of Sorel cements difficulties arise as the result of the presence of large amounts of water, producing a strong background effect on the patterns,

in the higher hydrates; this makes identification and interpretation of the patterns difficult. The use of a combination of physicochemical methods proves extremely effective in studies of such systems. It was noted in our earlier papers [1, 2] that broadening of the x-ray lines is caused more by lattice defects than by the high degree of dispersion of the oxychlorides. This is also confirmed by the form of the isotherms (Fig. 5) [8].

3. Samples conforming to the general formula $[q\% \text{MgCl}_2 + (100 - q)\% \text{H}_2\text{O}] + n\% \text{MgO}$ were subjected to tensimetric analysis. The samples were kept in desiccators for 14 months. The $P - (\Delta m/m)$ (Fig. 5) were used to plot $P - n$ isotherms [9] (Fig. 6).

Results for $q = 35\%$, are given in this paper. The samples of the composition $3\text{MgO} \cdot \text{MgCl}_2 \cdot 10\text{H}_2\text{O}$, and samples containing 35, 40, and 50% MgO, all exhibit five hydration steps. For the sample of the composition $3\text{MgO} \cdot \text{MgCl}_2 \cdot 10\text{H}_2\text{O}$ the first hydration step (0.01–0.3 mm) corresponds to dehydration of the sample formed at $P = 0.3$ mm by 1.35 molecules of water. The second step corresponds to dehydration of the sample formed at $P = 1.6$ mm, also by 1.35 molecules of water. The third step corresponds to dehydration of the sample formed at $P = 14.5$ mm by 5.7 molecules of water, and finally, the last step corresponds to hydration of the sample formed at $P = 14.5$ mm by 8.25 molecules of water (to $P = 15.3$ mm).

Samples were not kept in desiccators at higher water-vapor pressures because this caused such strong hydration that drops of water appeared on the surface of the samples. Thus, it follows from these results that samples of the composition $3\text{MgO} \cdot \text{MgCl}_2 \cdot 10\text{H}_2\text{O}$, formed at 21° , may be dehydrated, losing 4.2 molecules of water, or hydrated adding 12.5 molecules of water. The stability of the oxychloride $3\text{MgO} \cdot \text{MgCl}_2 \cdot 10\text{H}_2\text{O}$ (with small deviation from 10 molecules of water), when kept in the air at about room temperature, can be ascribed to the presence of the highest hydration step (1.6–14.5 mm). The oxychloride made with 35% MgCl_2 solution with $\text{MgO} : \text{MgCl}_2$ ratio of 5 : 1 ($5\text{MgO} \cdot \text{MgCl}_2 \cdot 10\text{H}_2\text{O}$) has these properties when hydrated up to two molecules of water (Fig. 5); this corresponds to a shift of the coordinate origin to the point $\Delta m/m_0$, representing +4%. If the same is applied to the sample with the composition $7\text{MgO} \cdot \text{MgCl}_2 \cdot 10\text{H}_2\text{O}$, we find 14 molecules of water. Thus, samples stable when stored in air at about room temperature correspond to the formulas: $3\text{MgO} \cdot \text{MgCl}_2 \cdot 10\text{H}_2\text{O}$, $5\text{MgO} \cdot \text{MgCl}_2 \cdot 12\text{H}_2\text{O}$, $7\text{MgO} \cdot \text{MgCl}_2 \cdot 14\text{H}_2\text{O}$.

Because of small variations of P and T under room conditions, there should be some deviations from these numbers of water molecules. This accounts for the discrepancies between the values found by a number of workers [10–13] for the number of water molecules in the oxychloride $3\text{MgO} \cdot \text{MgCl}_2 \cdot 10\text{H}_2\text{O}$.

Within the limits of each step in the isotherm the pressure P as a function of the relative change of mass $\Delta m/m_0$ can be represented by the formula

$$P = k \frac{\Delta m}{m_0} + C_1(n), \quad (1)$$

where C_1 is a constant which depends on the percentage composition of MgO in the cement (n), and Δm is the difference between the initial mass and the mass corresponding to pressure P , such that $\Delta m = m - m_0$. Represent-

ing the variable $\frac{\Delta m}{m_0} = \frac{m}{m_0} - 1 = X$, we have $\frac{dX}{dm} = \frac{1}{m_0}$.

From Equation (1) we have

$$dP = k dX \quad \text{or} \quad \frac{dm}{dP} = \frac{m_0}{k}. \quad (2)$$

Thus, for a given sample the variation of pressure with mass (dp/dm) is inversely proportional to the initial mass m_0 , whereas dP/dX is independent of the mass m_0 . We used this criterion for plotting the graphs and for analysis of our results.

SUMMARY

1. Differential heating curves for the oxychlorides were found to exhibit endothermic effects characterizing different compositions of oxychlorides and their hydrates.

2. It is shown that the positions of OH^- and Cl^- ions are not differentiated in the crystal lattice of the oxychlorides formed.

3. It is shown that the crystal system of the decomposition product of the oxychloride of the general formula $3\text{MgO} \cdot \text{MgCl}_2 \cdot 10\text{H}_2\text{O}$ changes from hexagonal to tetragonal on heating.

4. Magnesium hydroxide is not formed as an intermediate phase during the hardening of cements.

5. It follows from P-X and P-n isotherms that Sorel cements form nonstoichiometric hydrated oxychlorides. The smallest deviations from stoichiometric composition are found for samples with vapor pressures in the range of 1.6-14.5 mm.

6. The reasons for the discrepancies between the results obtained by different workers in determination of the formula of the oxychloride $3\text{MgO} \cdot \text{MgCl}_2 \cdot 10\text{H}_2\text{O}$ have been found and it is shown that data on oxychloride composition must be augmented by the conditions of the investigation: water-vapor pressure and temperature.

LITERATURE CITED

- [1] A. G. Bergman and I. P. Vyrodov, J. Appl. Chem. 31, No. 1, 19 (1958).*
- [2] A. G. Bergman and I. P. Vyrodov, J. Appl. Chem. 32, No. 3, 478 (1959). *
- [3] Ya. M. Kheifets, Solikamsk Carnallites [in Russian] (ONTI, Moscow-Leningrad, 1935) p. 25.
- [4] D. O. Bernshtein and Ya. R. Krass, Building Ind. 6, 32 (1956).
- [5] Trans. State Inst. Appl. Chem. 25 (1935).
- [6] G. V. Kurdyumov, J. Russ. Phys.-Chem. Soc. 43 (1926).
- [7] F. Seitz, Modern Theory of Solids (State Tech. Press, 1949) [Russian translation].
- [8] A. L. G. Rees, Chemistry of the Defect Solid State (IL, 1956) [Russian translation].
- [9] A. G. Bergman, J. Russ. Phys. - Chem. Soc. 56, 5-9, 177 (1925).
- [10] W. O. Robinson and W. A. Waggaman, J. Phys. Chem. 13, 673 (1909).
- [11] Maeda and J. Yamone, Bl. Phys. Chem. Res., Tokyo, 7, 340 (1928).
- [12] C. R. Bury and R. H. Davies, Soc. 2008 (1932).
- [13] W. Feitknecht and F. Held, Helv. Chim. Acta, 27, 1480 (1944).

Received February 24, 1958

* Original Russian pagination. See C. B. Translation.

DECOMPOSITION OF SILVER HALIDES AND DETERMINATION OF THEIR SILVER, BROMINE, AND IODINE CONTENTS

G. I. Barannikov

The Perm' Pharmaceutical Institute

Volumetric and gravimetric methods for determination of silver by means of halides, and vice versa, lead to accumulation of considerable quantities of silver residues for recovery in chemical laboratories. The author of this paper was interested in practical possibilities of decomposing silver halides remaining at the end of titration and their reconversion into useful substances.

Fairley [1] used hydrogen peroxide for reduction of silver from its oxide, and Kleinstück [2] showed qualitatively that hydrogen peroxide in an alkaline medium (KOH) also reduces silver chloride to the metal; Karyakin [3] lists glucose, formaldehyde, zinc and iron in metallic form, and zinc in contact with silver or platinum wire as reducing agents for silver halides; Shchigol' [4] used arsenite in an alkaline medium for the same purpose, and Shat'ko [5] used chromous salts; Zolotavin and Troitskaya reduced silver in solution by means of thallous nitrate, while Nikitina [7] and Erdey and Buzas [8] used ascorbic acid for this purpose.

In our experiments we used a mixture of caustic soda and hydrogen peroxide to decompose silver halides and simultaneously to reduce silver to the metal. In contrast to arsenites and thallium compounds, this solution does not contain toxic elements, is readily available and has good reducing properties.

EXPERIMENTAL

Determination of Silver and Its Chloride. 10.0 ml of 0.1 N sodium chloride solution was titrated in a 250 ml conical flask with silver nitrate solution in presence of dichlorofluorescein. One and one half the volume of 3 N NH_4OH solution was added without undue delay to the precipitate. The precipitate dissolved within one hour when shaken at intervals; solution was more rapid in concentrated ammonia solutions. A freshly-prepared mixture consisting of 2-2.5 ml of 30% NaOH and 5 ml of 30% hydrogen peroxide was added to the clear ammoniacal solution and the liquid was stirred. The reduction of silver to the metal proceeded smoothly at room temperature. When the liquid was heated in an inclined vessel on a sand bath under draft, the reaction rate obviously increased with increase of temperature and decrease of ammonia concentration.

When evolution of oxygen bubbles ceased, which showed that decomposition of hydrogen peroxide was complete, the vessel was placed in the vertical position and ammonia was completely removed by gentle boiling (tested with mercurous nitrate). 200-250 ml of water was then added to the vessel and the contents brought to the boil. The liquid was cooled and passed through an ashless filter (without the precipitate as far as possible); at the end of the filtration the filter was washed several times with water. The silver precipitate was washed three times by decantation with boiling water, transferred to the filter, and washed with cold water to a negative reaction for alkali and chloride. The filter was dried and ashed in a crucible together with the precipitate, which was then heated strongly in a muffle until the silver began to melt, cooled, and weighed.

The results of silver determinations in chloride solutions are given in Table 1; the amounts of chloride corresponding to the amounts of silver found were determined by calculation.

Decomposition and Analysis of Silver Bromide. In contrast to silver chloride, silver bromide is decomposed to an appreciable extent by the action of excess alkaline hydrogen peroxide mixture at room temperature only on

standing. If the liquid is warmed, the reduction is fairly rapid but not quantitative because particles of the original substance become clogged by its reduction product. The reaction proceeds satisfactorily if silver bromide is first dissolved by means of ammonia before the reduction.

Several authors [4, 9, 10] consider that the solubility of silver bromide in ammonia, in absence of excess amounts of soluble bromides, is a linear function of the ammonia concentration; this was reflected in the experiments described below.

TABLE 1

Determination No.	Taken (g)		Found		Corresponding chloride content (g)
	silver	chloride	in g	in %	
1	0.1085	0.0357	0.1079	99.44	0.0355
2	0.1085	0.0357	0.1089	100.37	0.0358
3	0.1079	0.0355	0.1074	99.54	0.0353
4	0.1079	0.0355	0.1078	99.91	0.0354
5	0.1079	0.0355	0.1075	99.63	0.0354
Average				99.78	0.0355

10.0 ml of 0.1 N sodium bromide solution was titrated with silver nitrate solution in presence of fluorescein, and the precipitate was dissolved in a twofold volume of 30% aqueous ammonia. A freshly-prepared clear mixture, consisting of 2.5 ml of 30% caustic soda and 7.5 ml of 30% hydrogen peroxide, was added to the ammoniacal solution and the liquid was stirred.

The vessel was heated and the silver precipitate washed and separated from the liquid as described for the preceding experiment. The filtrate and wash waters were kept for determination of their bromide contents. The alkaline filtrate containing bromide was transferred to a flask with a ground-glass stopper, and evaporated to a small volume; to it an equal volume of concentrated hydrochloric acid followed by 10 ml of 0.1 N potassium chlorate solution were added. The liquid was stirred, left to stand for 5 minutes in the stoppered flask, and 10 ml of 0.1 N potassium iodide solution was then added.

TABLE 2

Expt. No.	Taken silver bromide (g)	Found silver bromide	
		in g	in %
I	0.1079	0.1081	100.19
	0.0852	0.0831	97.54
II	0.1079	0.1079	100.00
	0.0852	0.0838	98.36
III	0.1079	0.1080	100.09
	0.0852	0.0840	98.59
IV	0.1079	0.1078	99.91
	0.0852	0.0832	97.65
V	0.1079	0.1080	100.09
	0.0852	0.0817	95.89
Average	0.1079	0.1080	100.06
	0.0852	0.0832	97.65

After a few minutes the liberated iodine was titrated with sodium thiosulfate, with vigorous shaking. Starch was added at the end of the titration.

The results of silver (upper line) and bromide (lower line) determinations are given in Table 2.

Analysis of Silver Iodide. In contrast to the chloride and bromide, silver iodide is reduced to the metal by the action of hydrogen peroxide at elevated temperatures only in a strongly alkaline medium (containing about 5-10% alkali relative to the whole volume of the liquid). However, because of clogging of the silver iodide particles by the reduction products, the reaction is not quantitative and depends to a considerable extent on the particle size of the original material.

Without using solvents, such as potassium cyanide, we decomposed silver iodide and determined its components by the following procedure.

10 ml of 0.1 N potassium iodide solution was titrated with silver nitrate solution in presence of fluorescein. 5 ml of 30% caustic soda solution and 2.5 ml of 30% hydrogen peroxide were added to the precipitate and the mixture was warmed and then boiled until the hydrogen peroxide was decomposed.

A mixture of 2.5 ml of alkali and the same volume of hydrogen peroxide solution was then added to the liquid, which was boiled until the peroxide was decomposed; this procedure was then repeated once more. The reduced silver spontaneously aggregated into loose gray lumps while the liquid became colorless and clear. The liquid was cooled, neutralized by means of concentrated hydrochloric acid, and decanted from the precipitate through a filter; the silver was washed 3 times with boiling water by decantation, transferred to the filter, and washed with water to a negative reaction for chloride. The wash liquors and the main filtrate were combined and their iodine content was determined as follows. After addition of 30 ml (i.e., $\frac{1}{4}$ of the volume of the solution) of concentrated hydrochloric acid and 10 ml of 0.1 N hydrogen peroxide solution, the liquid was stirred and then left to stand for 30 minutes in a stoppered vessel; the liberated iodine was titrated with sodium thiosulfate, starch being added at the end of the titration. After decantation of the liquid, the silver precipitate was collected

TABLE 3

Expt. No.	Taken silver iodide (g)	Found silver iodide after 1st decomposition		Found silver iodide after 2nd decomp.		Total silver iodide found	
		in g	in %	in g	in %	in g	in %
I	0.1080	0.1060	98.15	0.0014	1.30	0.1074	99.45
	0.1269	0.1218	96.0	0.0022	1.72	0.1240	97.71
II	0.1080	0.1060	98.15	0.0009	0.83	0.1069	98.98
	0.1269	0.1244	98.03	0.0014	1.10	0.1258	99.13
III	0.1080	0.1066	98.70	0.0013	1.20	0.1079	99.90
	0.1269	0.1231	97.0	0.0029	2.29	0.1260	99.29
IV	0.1080	0.1056	97.78	0.0012	1.11	0.1068	98.89
	0.1269	0.1246	98.19	0.0015	1.19	0.1261	99.38
V	0.1080	0.1062	98.33	0.0013	1.20	0.1075	99.53
	0.1269	0.1236	97.40	0.0026	2.04	0.1262	99.44
Average		0.1061	98.22	0.0012	1.11	0.1073	99.33
		0.1235	97.32	0.0021	1.65	0.1256	99.99

on a filter, washed with water to a negative reaction for alkali, dried, carefully separated from the filter walls by means of a fine brush, transferred to a test tube, and there dissolved in 1 ml of moderately concentrated nitric acid with gentle heating (the filter was retained for further use). The cooled nitric acid solution was diluted with 5 ml of water, when a slight precipitate of silver iodide was formed. The solution with the precipitate was heated to boiling, cooled, the precipitate was collected on the bottom of the test tube by centrifugation, and the clear liquid was then carefully decanted through a small funnel, the narrow opening of which was plugged fairly tightly with cotton wool or paper. At the end of the filtration, the filter was washed with water.

The clear filtrate and wash liquors were collected in a 250 ml conical flask.

In view of the fact that silver nitrate solution reacts rather violently with the above-mentioned mixture of alkaline hydrogen peroxide, and the reduced silver is formed predominantly in a finely-divided state (this is often accompanied by some loss of silver), the silver nitrate solution contained in the flask was first treated with the necessary quantity of 0.1 N sodium chloride solution, and the precipitate was dissolved in excess ammonia. A clear mixture consisting of 2.5 ml of caustic soda and 5 ml of hydrogen peroxide, of the concentration indicated above, was added to the solution. The liquid was warmed and then boiled until ammonia was completely removed; 200 ml of water was then added and the liquid was brought to the boil. When cool, the silver was collected on a filter, washed to a negative reaction for alkali, ashed together with the filter, heated until fusion started, cooled and weighed.

The silver iodide collected on the surface of the filter plug was washed with water and returned to the tube containing the main mass of this precipitate. 10 drops of alkali and, in portions, an equal volume of hydrogen peroxide, both of the above-mentioned concentrations, were added to the precipitate. When the liquid was boiled, the silver was reduced to the metal; the methods described above were used to separate and determine this metal and to determine iodide in the filtrate.

The results of silver (upper line) and iodide (lower line) determinations are given in Table 3.

LITERATURE CITED

- [1] T. Fairley, Chem. News 33, 273 (1876).
- [2] M. Kleinstück, Ber. 51, 108 (1918); J. W. Mellor, Comprehensive Treatise on Inorganic and Theoretical Chemistry 1 (London, 1922) p. 940.
- [3] Yu. V. Karyakin, Pure Chemical Reagents [in Russian] (Goskhimizdat, Moscow-Leningrad, 1947) p. 940.
- [4] M. B. Shchigol', J. Gen. Chem. 3, 540 (1933); Industrial Lab. 9, No. 3, 310 (1940).
- [5] P. P. Shat'ko, Industrial Lab. 21, No. 8, 921 (1955).
- [6] V. L. Zolotavin and T. B. Troitskaya, in the book: Methods of Analysis for Ferrous and Nonferrous Metals [in Russian] (Sverdlovsk-Moscow, 1953) p. 125.
- [7] E. Nikitina, Industrial Lab. 19, No. 9, 1040 (1953).
- [8] L. Erdey and L. Buzas, Referat. Zhur. Khim. 14, 29133 (1955).
- [9] K. S. Lyalikov and V. N. Piskunova, J. Phys. Chem. 28, No. 4, 595 (1954).
- [10] C. R. Johnson, J. Chem. Educ. 31, No. 4, 205 (1954).

Received January 15, 1958

ELUTION OF NOBLE METALS FROM ANION EXCHANGERS AFTER ADSORPTION

A. B. Davankov and V. M. Laufer

Methods for extraction, concentration, and accumulation of considerable amounts of valuable substances on ion exchangers are becoming of great significance in modern sorption technology. Development of rational methods for displacement of adsorbed substances from resins is no less important.

Various chemical reagents are used for regeneration of ion-exchange resins to allow of their repeated use. Aqueous solutions of salts, acids, and bases are the reagents most commonly used; the use of organic solvents with or without added acids or bases has been less well studied.

Most modern ion exchangers have relatively low dynamic exchange capacities: they usually do not exceed 2-4 meq per g of resin, and reach 8-10 meq for only a few. Accordingly, increase of the dynamic exchange capacity of ion exchangers, and searches for new methods for concentration and accumulation of considerable amounts of adsorbed substances on ion exchangers, are of great practical importance, as successful solution of this problem would greatly increase the operating intervals between regenerations and reduce sharply the number of regeneration cycles necessary.

Since considerable increases of the dynamic exchange capacity of ion exchangers by increases of the total contents of functional (ionogenic) groups in the molecular network of the resins are difficult to achieve because of the excessive solubility or swelling of such resins in water, in our opinion a definite practical interest attaches to the use of secondary reactions, either accompanying ion exchange or induced artificially on the resins, for this purpose.

We have already reported [1] that by alternation of ion exchange with reduction or precipitation reactions, which convert adsorbed substances into a nonionic (insoluble form) it is possible to concentrate an amount of adsorbate which is 4-5 times the total exchange capacity of the resin. This procedure is particularly effective for concentration of noble metals on ion exchangers, as the ions of these metals are readily reduced to the metals and are deposited in that form on the resins in amounts exceeding 100% the adsorbent weight.

Since isolation of noble metals from resin adsorbents, after combustion of the latter, is a relatively simple process, which has been described fully in the literature [2], in this paper we shall deal mainly with questions of the elution of complex ions of certain noble metals [AuCl_4^- , $\text{Au}(\text{CN})_2^-$] adsorbed on anion exchangers, and the stability of these ions to the action of certain reducing agents.

Experiments showed that chloraurate ions AuCl_4^- , adsorbed on "N-O" anion exchanger are readily reduced by hydroquinone to the metal, and accumulate in that form on the resin during several sorption cycles, over 5 meq per gram of adsorbent being accumulated (Table 1).

The behaviour of cyanoaurate ions $\text{Au}(\text{CN})_2^-$ under the same conditions is entirely different. Under the experimental conditions they were not reduced to any appreciable extent, and were easily displaced from the resin not only by caustic alkalis and carbonates in solution, but even by solutions of the reducing agents themselves - sodium hydrosulfite, sulfide, and hydrosulfide. The exchange capacity of the resin then returned to its initial value. Thus, there was no "accumulation" of considerable amounts of gold on the anion exchangers by reduction of adsorbed $\text{Au}(\text{CN})_2^-$ ions, such as was found for AuCl_4^- anions, under the experimental conditions used.

TABLE 1

Concentration of Gold by Adsorption and Reduction of AuCl_4^- Ions on "N-O" Ion-Exchange Resin in the Chloride Form. (5 g of resin in column; moisture content of resin 66%; height of resin layer in column 18.5 cm; initial gold content of solution 200 mg/liter; pH of original solution 3.5)

Expt. No.	Cycle No.	Volume of solution passed through resin to breakthrough of AuCl_4^- ions (liters)	Total volume of solution passed through resin (liters)	Total gold content of solution passed through column (mg)	Gold extracted from resin			
					after combustion (g)	% of the amount entering column	% on weight of dry resin	in meq/g
1	1	2.917	3.236	647.2	1.8752	86.50	110.30	5.59
	2	2.600	2.810	562.0				
	3	1.800	2.011	402.2				
	4	1.000	1.410	282.0				
	5	0.840	0.840	168.0				
2**	6	0.600	0.631	126.2	1.9494	91.61	114.67	5.81
	1	2.800	2.900	580.0				
	2	1.500	1.710	342.0				
	3	1.600	1.682	336.4				
	4	1.800	2.053	410.6				
	5	2.100	2.294	458.8				

* After each sorption cycle 200 ml of 5% Na_2S solution was passed through the column, the resin was washed with distilled water and then with 5% HCl solution.

** The AuCl_4^- anions on the resin were reduced by the action of hydroquinone solution (5.5 g/liter).

The sorption of $\text{Au}(\text{CN})_2^-$ ions and their desorption from "N-O" resin by solutions of caustic alkali or sodium sulfides was effected in a glass adsorption column 8 mm in diameter, containing 5 g of "N-O" anion-exchange resin with grains 0.8-2 mm in size; the chloride form of the resin was used. A solution of potassium cyanoaurate acidified with hydrochloric acid was passed at a rate of 6-8 ml/minute through a layer of resin 18 cm high. Filtrate samples were taken at 100-ml intervals. When gold ions appeared in the filtrate, percolation of the gold solution through the column was stopped. Breakthrough of gold ions into the filtrate was detected by means of the color reaction with benzidine acetate solution.

After the adsorption, the column was rinsed through with distilled water, and a definite amount of 0.1 N sodium sulfide, hydrosulfide, or hydrosulfite solution was passed through. The resins was then again rinsed with water. The percolated solution together with the wash waters was evaporated to dryness on the water bath, and the residue was treated in the usual manner for isolation of gold.

After desorption the washed adsorbent was treated with 5% hydrochloric acid solution to "charge" it with Cl^- ions, and then used again for further extraction of $\text{Au}(\text{CN})_2^-$ anions under the conditions described for the first experiment. In this way four consecutive cycles of sorption of these anions by "N-O" resin were performed, alternating with desorption from the resin by means of 0.1 N sodium sulfide or hydrosulfide solution.

The results of these experiments are given in Table 2. It follows from the data in Table 2 that $\text{Au}(\text{CN})_2^-$ ions are completely displaced from the resin by sodium sulfide, hydrosulfide, and hydrosulfite solutions in the same way as by caustic alkalis, without undergoing any significant changes (such as reduction to the metal).

TABLE 2

Extraction of Gold from Potassium Cyanoaurate Solution by "N-O" Anion-Exchange Resin in the Chloride Form with Subsequent Desorption of Sodium Sulfides and Hydrosulfite. (Amount of resin in the column 5 g; moisture content of resin in Experiment No. 1 68%, in Experiment No. 2 60%; height of resin layer in column 18 cm in Experiment No. 1 and 17.5 cm in Experiment No. 2; initial gold concentration in solution 200 mg/liter in Experiment No. 1 and 24.5 mg/liter in Experiment No. 2; pH of initial solution 3.5 in Experiment No. 1 and 6 in Experiment No. 2; filtration rate of solution through resin 6-8 ml/minute)

Expt. No.	Cycle No.	Volume of solution passed through resin to breakthrough of $\text{Au}(\text{CN})_2^-$ ions (ml)	Total volume of solution passed through resin (ml)	Total gold content of solution (mg)	Volume of 0.1 N solution passed through resin after adsorption (ml)			Gold isolated			
					Na_2S	NaHS	Na hydro-sulfite	from solution after desorption		from resin after combustion	
								in mg	% of original content in solution	in mg	% of original content in solution
1	1	1700	1705	341	100	—	—	340.0	99.7	—	—
	2	1605	1605	321	150	—	—	314.8	98.0	—	—
	3	1400	1500	300	—	200	—	284.0	94.7	—	—
	4	1100	1100	220	—	250	—	236.2	107.3	Traces	
2	1	3500	6000	147	—	—	250	75.6	51.4	—	—
	2	4000	6000	147	—	—	150	30.4	20.7	—	—
	3	3000	5000	122.5	—	—	150	45.1	36.8	82	66.9

All this shows that the cyanoaurate anions are very stable to the reducing or precipitating action of these reagents, both in the adsorbed and in the free state. Similar results were obtained with the use of such an active reducing agent as hydroquinone. When the "N-O" resin was treated with 5% NaOH solution in order to convert it from the chloride to the hydroxyl form after adsorption of $\text{Au}(\text{CN})_2^-$ anions on it, most of these ions were displaced by the alkali solution after a small amount (11-12 ml) had been passed; the rest of the ions were eluted by means of 0.55% hydroquinone solution, which was passed through the resin in order to reduce the $\text{Au}(\text{CN})_2^-$ anions and to convert them into a nonionic form (insoluble in caustic alkalies).

The results of a series of consecutive experiments on the sorption of these ions by "N-O", "TN", and "TN-1" resins with the use of hydroquinone as reducing agent, and solutions of caustic soda, thiourea, and hydrochloric acids in acetone as eluants are given in Table 3.

It follows from Table 3 that hydroquinone solution and sodium sulfide, hydrosulfide, and hydrosulfite do not reduce $\text{Au}(\text{CN})_2^-$ anions to the metal under the experimental conditions used, either on the resin or in alkaline or acid solution during elution; all the gold passed from the resin into solution.

However, all the foregoing data on the stability of complex gold anions to the action of various reducing agents relate to pure, artificially prepared solutions of potassium cyanoaurate, and the cyanoaurate ions were displaced from the resin soon after completion of the sorption process.

The results were different in experiments performed under industrial conditions, when alkaline contaminated liquors, containing residual potassium cyanoaurate from the wash bath of the electroplating section of the Moscow Jewelry Factory, were passed for 2-3 months through "N-O" resin. In this case when "N-O" resin was regenerated by 5% caustic soda solution only 4.8-8.9% of the original gold content was extracted from the resin. There was no significant improvement when the resin was left twice overnight in contact with excess 5% caustic alkali, followed by additional washing of the resin by fresh alkali solution in the adsorption column. The extraction of gold could be raised to 29.4-41.6% of the original content in the resin only as the result of successive treatment of small quantities (5 g) of adsorbent, taken from column No. 3, with 5-10% NaOH solution in the cold or heated to 70-75°, followed by washing of the gold-containing resins with 5% HCl solution. Partial hydrolysis of the resin took place in this process.

TABLE 3

Extraction of Gold from Potassium Cyanoaurate Solutions by "N-O", "TN", and "TN-1" Resins with Subsequent Treatment by Hydroquinone Solution and Displacement of Gold Anions from the Adsorbents by Solutions of NaOH, Thiourea, or Acetone. (Amount of resin in column, 5 g; initial gold concentration in solution, 200 mg/liter; pH of original solution, 3.5; filtration rate of solution through resin 6-8 ml/min in Expt. No. 1; 5-6 ml/min in Expt. No. 2-5; flow rate of eluants through resin 5-6 ml/min)

Expt. No.	Adsorbent	Cycle No.	Total vol. of gold sol. passed through resin (ml)	Total amount of gold in solution (mg)	Vol. of gold sol. passed through resin to breakthrough of Au (CN) ₂ ions (ml)	Vol. 5% NaOH sol. passed through resin in regeneration (ml)	Vol. of mixt. of 10% thiourea and 5% HCl sol. (1:1) passed through resin (ml)	Vol. of mixt. acetone + 5% HCl and 5% H ₂ O passed through resin (ml)	Gold isolated								
									from alkaline solution		from thiourea solution		from acetone solution		from resin after combustion		
									in mg	% of orig. soln. in cont.	% amt. adsorbed by resin in mg	"N-O" anion exch. chlor. form	in mg	% amt. adsorbed by resin	in mg	% of orig. soln. content in	
1	"N-O" anion ex-changer in chloride form	1	800	160.0	800	44	—	—	155.8	97.3	—	—	—	—	—	—	—
		2	1231	246.2	1000	12	—	—	233.3**	90.7	—	—	—	—	—	—	—
		3	1219	243.8	800	25	—	—	170.6**	70.0	—	—	—	—	—	—	—
		4	1030	206.0	1030	50	—	—	264.8	128.5	—	—	—	—	—	—	—
		5	1205	241.0	1205	100	—	—	252.0	104.5	—	—	—	—	—	—	—
		6	1205	241.0	1200	100	—	—	228.4	94.7	—	—	—	—	—	15.4	6.3
2	"TN" anion exchanger in chloride form	1	11050	1349.4*	4000	100	—	150	857.6	63.5	—	—	765.4	—	—	—	—
		2	2406	481.2	2200	—	—	—	—	—	—	—	—	—	—	—	—
3	"TN-1" anion ex-changer in chloride form	1	10200	1084.3*	3200	—	250	—	—	—	868.3	80.1	—	—	—	—	—
		2	2208	441.6	1600	—	150	—	—	—	—	323.0	73.1	—	—	—	—
4	"N-O" anion exchanger in chloride form	1	6200	831.4*	2800	—	—	150	—	—	—	—	—	774.6	—	—	—
		4	1670	334.0	1670	—	—	100	—	—	—	—	—	316.2	94.6	23.8	7.1
5	"N-O" anion exchanger in chloride form	1	1670	334.0	1670	—	—	100	—	—	—	—	—	—	—	—	—

* Gold adsorbed by resin.

** Including gold from hydroquinone solution: 64 mg in Experiment No. 2, and 28 mg in Experiment No. 3.

TABLE 4

Extraction of Gold by Thiourea Solutions from Samples of "N-O" Resin. (Amount of air-dry resin in column, 3 g; volume of thiourea solution passed through column, 100 ml in Experiment No. 1 and 150 ml in Experiments No. 2-6; filtration rate of solution through resin 5-6 ml/minute)

Expt. No.	Temperature (°C)	Gold isolated (mg)	
		from thiourea solution	from ash after combustion of resin
1	70-75	89.8	1.4
2	30	82.8	not detected
3	30	85.6	not detected
4	20	82.4	2.2
5	20	81.8	not detected
6	20	74.8	not detected

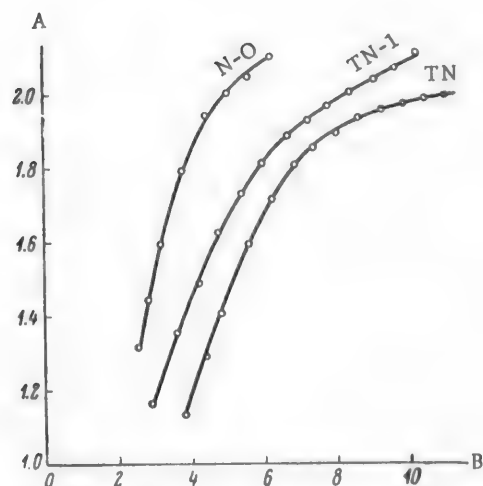
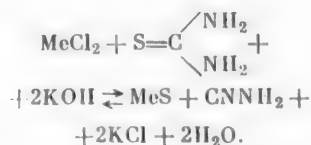
In regeneration of resins which had been in use for not more than one month, the caustic soda solution did not extract more than 16% of the original amount of gold. It is possible that this low yield in elution of gold adsorbed by the resin was caused by incorrect use of "N-O" resin under production conditions; in particular, by complete discharge of water from the resin at night, when the adsorbent remained in contact with air.

This suggestion was tested experimentally under laboratory conditions; the same jewelry factory effluents were used for adsorption, the resin was kept in the adsorption column for one month under a layer of water and then regenerated by 5% caustic soda solution, when 50-76% of the adsorbed gold was displaced from the column.

Possibly, when "N-O" resin is used at length (2-3 mo) industrially for extraction of $\text{Au}(\text{CN})_2^-$ anions from strongly contaminated and slightly alkaline liquors (especially with access of air), the gold and the resin form a stable complex which resists the action of dilute caustic alkalis (5% NaOH) and acids. However, this compound proved to be very sensitive to aqueous thiourea solution and to dilute solutions of HCl in organic solvents.

It is known that reagents containing thiono ($\text{C}=\text{S}$) and thiol ($\text{C}-\text{SH}$) groups are important among the reagents used in inorganic analysis. Compounds of this type include thiourea, which readily forms complexes, especially with cations of metals whose sulfides are insoluble in water. These metals include the noble metals.

Thiourea combines with the metal through the free pair of electrons in sulfur, despite the fact that the nitrogen also has unshared pairs of electrons in the amide groups, capable of complex formation. Thiourea complexes are readily decomposed in weakly alkaline solutions with formation of sulfides. Kurnakov considers that this occurs most readily in the presence of Me:S bonds, which are converted into ionic bonds in sulfide formation:



Sorption of gold by N-O, TN, and TN-1 anion exchangers: concentration of $\text{KAu}(\text{CN})_2$ solution 200 mg Au/liter, solution pH 3.5; A) amount of gold extracted (meq/g); B) amount of solution passed (liters).

It is known that silver and platinum form extremely stable complexes with thiourea. Saturated thiourea solutions dissolve all silver halides even in the cold. Metal-thiourea complexes are considerably less stable than metal sulfides. The instability constant of the silver-thiourea complex $9[\text{AgTM}_3]^+$ is $1.3 \cdot 10^{-14}$.

We used this property of thiourea in elution of gold and silver from anion-exchange resins after saturation with anions containing these metals.

The advantage of thiourea solutions over other eluants is that they ensure complete extraction of noble metals from resin adsorbents, especially when other eluants (acid and alkali solutions) do not give positive results.

The use of thiourea for elution of ions of noble metals from adsorbents is not mentioned in the literature. We were the first to use acid solutions of thiourea for this purpose.

Table 4 contains the results of experiments on the treatment of gold-containing "N-O" resin with thiourea solutions. The resin, which had been used for a long time for adsorption of $\text{Au}(\text{CN})_2^-$ anions from industrial wastes (wash liquors), was obtained from the Moscow Jewelry Factory. Samples of gold-containing resin were taken from different layers in the adsorption column.

It follows from the results in Table 4 that a mixture of equal volumes of 10% thiourea solution and 5% hydrochloric acid solution displaces gold from the adsorbent almost completely (100%), whereas treatment of the same gold-containing resin by 5% NaOH solution extracted not more than 5-10% of the original gold content.

Good results in elution of gold adsorbed by the resin were obtained by the use of organic solvents - acetone, ethyl alcohol, and ethyl acetate - with addition of hydrochloric acid (sp. gr. 1.19) and water (5% of each); this is clear from Tables 3 and 5 and the diagram. It also follows from these tables that after treatment of the gold-containing resin with organic solvents, containing 5% HCl (sp. gr. 1.19) and 5% water, the resin completely regains its power of adsorption and desorption; under the experimental conditions used, the first 50 ml of the mixture of acetone with hydrogen chloride and water in the above proportions extracted 97-99% of the gold (calculated as the metal) present in the resin.

SUMMARY

1. Acidified aqueous thiourea solution, and acetone, ethyl alcohol, and ethyl acetate with additions of 5% hydrochloric acid (sp. gr. 1.19) and 5% water, extract gold almost completely from

TABLE 5
Extraction of Gold from Industrial Samples of Gold-Containing "N-O" Ion-Exchange Resin by Organic Solvents, with Repeated Use of the Adsorbent

Expt. No.	"N-O" resin from production column	Cycle No.	Amount of air-dry resin in adsorption column (g)	Ht. of resin layer in column (cm)	Gold concentration in solution (mg/liter)	pH of original solution	Filtration rate of solution through resin (ml/minute)	Vol. of solution passed through resin to breakthrough (ml)	Total volume of solution passed through resin (ml)	Total gold content of solution (mg)	Vol. of eluant passed through resin (ml)	Filtration rate of eluant through resin (ml/minute)	Gold extracted (mg) •	From ash after combustion of resin
1	N ^o 1	1	3	34.9	—	—	—	—	—	—	100	5-6	44.2	7.0
2	N ^o 2	1	2	24.5	200	3.5	5-6	2600	2801	560.2	100	5-6	50.0	2.6
3	N ^o 3	1	2	28.2	200	3.5	5-6	2600	2802	560.4	100	5-6	570.1	11.7
4	N ^o 5	1	2	25.0	200	3.5	5-6	1306	1306	261.2	100	5-6	283.7	1.4

• Initial gold content of the resin was not determined.

anion-exchange resins after adsorption of $\text{Au}(\text{CN})_2^-$ anions, not only from pure solutions, but from strongly contaminated industrial waste liquors, containing potassium or sodium cyanoaurates (in the latter case good results are not always obtained by elution of gold ions by caustic alkali solutions).

2. The $\text{Au}(\text{CN})_2^-$ anions adsorbed by anion-exchange resins from pure solutions are highly resistant to the action of reducing agents and are completely displaced from the resins by aqueous solutions of strong or weak bases.

3. AuCl_4^- anions adsorbed by anion-exchangers are readily reduced to the metal. By alternate adsorption and reduction it is in this case possible to "accumulate" gold in the ion exchangers in quantities several times the dynamic exchange capacities of the resins.

LITERATURE CITED

- [1] A. B. Davankov, V. M. Laufer and L. A. Shits, J. Appl. Chem. 30, No. 6, 839 (1957).*
- [2] A. B. Davankov and V. M. Laufer, J. Appl. Chem. 29, No. 6, 952 (1956); 29, No. 7, 1029 (1956);* Industrial Lab. 7, 788 (1956).

Received September 19, 1957

* Original Russian pagination. See C. B. Translation.

COMPARATIVE STUDY OF THE THERMAL STABILITY OF SULFONATED CATION EXCHANGERS HEATED IN WATER

N. G. Polyanskii

Under industrial and laboratory conditions, resins are often subjected to heat treatments in air in water, and in aqueous solutions.

Ion exchangers are heated in air in determinations of their moisture contents [1], or for dehydration. Some stages in the synthesis of ion-exchange resins also take place at elevated temperatures [2].

Contact of ion-exchange resins with hot aqueous solutions is of frequent occurrence. For example, hot solutions are used for regeneration of ion exchangers used for separation of certain elements [3]. The favorable influence of temperature increase on the rate of ion exchange and the distribution coefficient has been successfully applied in separation of elements of the cerium and yttrium groups [4]. Quite recently the use of hot eluant solutions for separation of rare-earth elements [5-7] and transplutonium elements [8] has been described. In recent years the importance of ion exchangers for softening [9] and deactivation [10] of process waters has increased sharply.

The demands of industry and scientific research laboratories have placed the thermal stability of ion exchangers among the problems of great practical significance. There is no doubt that studies of the thermal stability of existing industrial ion exchangers will assist in the solution of more general problems raised by various authors in recent years. Foremost in this connection is the synthesis of thermostable cation and anion exchangers [11, 12].

All the ion exchangers so far synthesized are more or less unstable to the action of heat. A consequence of this instability is the decrease of capacity noted when resins are dried [13], used as catalysts in industrial synthesis [11, 14], or heated in autoclaves in presence of water [15]. The decrease in the capacity of the resins in all these cases is correctly attributed to loss of a significant proportion of sulfo groups — thermal desulfonation.

Saldadze [16] was the initiator of studies of thermal desulfonation of sulfonated cation exchangers in air. He used the thermographic method and concluded that SBS and Espatite 1 (KU-1) resins do not undergo changes in their physicochemical properties at high temperatures, and the sorption capacities of the cation-exchangers NFS and Wofatit P remain constant when they are heated to 150°. In studies of the Russian cation exchangers KU-1 and KU-2, the present author [17, 18] found a considerable decrease in their capacity as the result of heating in air. The capacity losses of KU-1 and KU-2 resins after 24 hours of heating at 186° were 42.4 and 14.5%, respectively.

An interesting study of the thermal stability of a number of sulfonated cation exchangers was carried out by Vasil'ev [1] in relation to drying conditions in moisture determinations. According to his results, prolonged heating of various cation exchangers produces an apparent increase of capacity, which is correctly attributed to liberation of sulfuric acid as the result of thermal hydrolysis of these resins. Vasil'ev found that volatile desulfonation products are formed at 170°; this is a very important fact which agrees with our own observations [19].

There have been no special studies of the thermal stability of ion-exchange resins in water.

The purpose of the present investigation was to fill this gap and to study the thermal stability of certain Russian sulfonated cation exchangers in contact with water at different temperatures. The most detailed studies were conducted with sulfonated phenol-formaldehyde cation exchanger KU-1, and sulfonated polystyrene cation

exchanger KU-2, which are used especially frequently in laboratory and industrial practice. For greater completeness, individual results of studies of the thermal stability of SBS, MSF, KU-1G (granulated sulfonated phenol-formaldehyde resin) and Wofatit R resins are also given in this paper.

EXPERIMENTAL

The resins used in the experiments were technical samples of grain size 0.5-1.0 mm, previously purified by repeated washing with 3 N HCl solution in order to remove inorganic impurities. The purified resins were taken to the air-dry state and then dried in a vacuum desiccator (at $p = 10$ mm) over P_2O_5 to constant weight. The cation exchangers in the hydrogen form had the following capacities (in meq/g) after this treatment: KU-1, 2.01; KU-1G, 2.99; MSF, 3.22; Wofatit R, 1.38; SBS, 2.65; KU-2, 4.67. The capacities of the Na forms of KU-2 and KU-1 resins were 4.20 and 1.92 meq/g, respectively.

The resins were subjected to heat treatment in stoppered weighing bottles or sealed tubes, placed in a thermostat with automatic temperature regulation (to the nearest $\pm 1^\circ$).

It was found in special experiments that ordinary chemical glass is not leached out to any appreciable extent below the boiling point of water. At higher temperatures (up to 175°) tubes made from ordinary glass are strongly corroded and therefore cannot be used for the heating tubes. Heat-resistant glass proved to be the most resistant to water and acid solutions in the temperature range studied (110 - 175°), and it was therefore used for making the tubes for heat treatment of the ion exchangers.

A resin sample weighing 0.2000 - 0.6000 g in a tube was covered with freshly boiled water (1.5 ml). The tubes were put in a vacuum desiccator, which was evacuated by means of a water-jet pump until evolution of air bubbles from the resin grains ceased. After this treatment, a further 2 ml of water was introduced into the tube and the evacuation was repeated. The tubes were then sealed and put in the thermostat for the required time. At the end of this time the tubes were removed, opened immediately, and the resin was filtered off and washed repeatedly with water on the filter.

Our selection of a method for analysis of the filtrates (which we shall term aqueous extracts for brevity) was based on the assumption that sulfonated cation exchangers, like monomeric sulfonic acids [20], are hydrolyzed on heating with formation of sulfuric acid. The aqueous extracts did in fact have an acid reaction in all cases, and gave a positive reaction for SO_4^{2-} ions with $BaCl_2$.

The total acidity of the aqueous extracts was determined by titration with caustic soda in presence of Thymol blue. For identification of the acid present in the aqueous extracts, the alkalimetric titration was augmented by quantitative determinations of sulfate. The volumetric method of Szekeres [21] was used with success for the analysis; this method is based on addition of a known volume of standard Na_2CO_3 solution to the sample and determination of the total contents of SO_4^{2-} and CO_3^{2-} ions by titration with 0.1000 N $BaCl_2$ solution. Various indicators of a suitable range can be used for determination of the end point; according to our observations Thymol blue gives the sharpest color change.

The content of SO_4^{2-} ions in the liquid phase after contact with the resin is the most definite measure of the intensity of the thermal desulfonation process, as the H^+ ion concentration may vary as the result of interaction with alkaline products formed by decomposition of the glass or (in the case of resins in the sodium form) as the result of exchange of Na^+ ions in the resin with H^+ ions in solution.

Removal of each sulfo group releases one SO_4^{2-} ion and one H^+ ion (in desulfonation of Na cation exchangers) or two H^+ ions (in desulfonation of H cation exchangers). Therefore, the decrease in the capacity of a resin in the hydrogen form must be equal to half the number of milliequivalents of H^+ or SO_4^{2-} ions in solution. If thermal desulfonation of the resins is not extensive, this indirect method for determination of capacity loss gives more accurate results than direct titration of the resin with alkali.

Considerable capacity losses can be determined with great accuracy by direct titration of the resins by the method of Vansheidt, Vasil'ev, and Okhrimenko [22]. For convenient comparison of the experimental data, the absolute capacity losses and contents of H^+ and SO_4^{2-} ions in the aqueous extracts are referred to 1 g of the original resin dried to constant weight over P_2O_5 . These results and the known original capacities of the resins (E_0) were used to calculate the relative capacity losses $R = \frac{E_0 - E_t}{E_0} \cdot 100$ (where E_t is the capacity of the resin after t hours of heat treatment).

TABLE 1

Effects of Temperature and Heating Time on the Capacity of Sulfonated Cation Exchangers

Resin	Tem- pera- ture (°C)	Resin capacity E_t and relative capacity loss R after the action of heat for							
		3 hours		6 hours		12 hours		24 hours	
		E_t	R	E_t	R	E_t	R	E_t	R
Resin in hydrogen form									
SBS	90	—	—	2.61	1.5	—	—	2.58	2.6
Wofatit R	90	—	—	1.30	5.8	1.28	7.2	1.27	8.0
MSF	90	—	—	3.14	2.5	—	—	3.05	5.3
KU-1G	90	—	—	2.94	1.7	2.92	2.3	2.89	3.3
KU-1	90	—	—	1.98	1.5	1.97	2.0	—	—
KU-1	110	1.91	5.0	1.84	8.5	1.80	10.4	1.72	14.4
KU-1	150	1.19	40.8	0.82	59.1	0.61	69.6	0.38	81.2
KU-1	175	0.26	87.2	0.17	91.5	0.13	93.5	0.08	96.1
KU-2	110	—	—	—	—	4.66	0.1	4.65	0.4
KU-2	150	4.55	2.6	4.49	3.9	4.47	4.3	4.37	6.5
KU-2	175	4.41	5.6	4.22	9.6	4.06	13.1	3.76	19.5
Resins in sodium form									
KU-1	150	1.90	1.0	1.85	3.6	1.59	17.2	1.35	29.6
KU-1	175	1.17	39.0	0.70	63.7	0.37	80.7	0.23	88.0
KU-2	175	—	—	—	—	—	—	4.12	1.9

To determine the mechanism of thermal desulfonation of resins in water, in some cases the contents of H^+ and SO_4^{2-} ions in the aqueous extracts were determined in addition to the absolute and relative capacity losses.

Special experiments were performed to study the effects of heat treatment on density and hydration (swelling) of the resins. The true density was determined by the usual pycnometric method after separation of free water by centrifugation at 2500 revolutions/minute [13] for 6 minutes.

After the density determination the resin sample was transferred quantitatively into a weighing bottle and dried at 130° to constant weight. The amount of bound water was found from the weight of the dried resin and the known weight of the hydrated resin.

DISCUSSION OF RESULTS

Under industrial conditions ion exchangers are in contact with water for various periods at different temperatures. Therefore studies of the effects of temperature and duration of heat treatment on resin capacity are of great importance.

The results of determinations of the capacities of sulfonated resins, after different times of contact with water at various temperatures, are given in Table 1.

It follows from Table 1 that all the sulfonated cation exchangers studied undergo thermal desulfonation when heated in water. The degree of desulfonation, quantitatively represented by the relative capacity loss, depends on the conditions of heat treatment and the nature of the resin. Of all the resins studied the highest resistance to the action of heat in water is shown by the polymeric sulfonated polystyrene cation exchanger KU-2; this resin is also the least susceptible to thermal desulfonation in air [1, 19]. This is the resin to be recommended for H or Na cation exchange under industrial conditions.

The sulfonated phenol-formaldehyde resins (KU-1, KU-1G, MSF, Wofatit R) are much less resistant. In this series of cation exchangers the relative capacity loss increases symbatically with the initial exchange capacity. The resin Wofatit R is an exception to this rule, possibly because it contains sulfo groups in the side chain as well as in the benzene nucleus [23].

In all experiments the capacity of KU-1 and KU-2 resins decreased continuously with increase of temperature and duration of heat treatment. A general feature of the desulfonation kinetics of these resins in air and in

TABLE 2

Results of Determinations of H^+ and SO_4^{2-} Ions in the Aqueous Extracts and Calculated Values of the Initial Capacity of the Resins in Hydrogen Form

Resin	Temperature (°C)	Contents of H^+ ions (A) and SO_4^{2-} ions (B) in aqueous extracts and calculated values of E_0 after thermal desulfonation lasting								
		6 hours			12 hours			24 hours		
		E_0	A	B	E_0	A	B	E_0	A	B
KU-1	150	2.04	2.35	2.44	2.03	2.73	2.85	2.03	3.26	3.30
KU-1	175	1.94	3.61	3.55	2.01	3.76	3.74	2.06	3.84	3.96
KU-2	150	4.59	0.25	0.21	4.65	0.32	0.35	4.60	0.50	0.47
KU-2	175	4.67	0.91	0.86	4.67	1.27	1.24	4.69	1.70	1.86

contact with water is a gradual slowing down of the rate of capacity decrease with increasing time of heat treatment. However, the almost complete cessation of desulfonation, which occurs after sufficiently long heat treatment in air, is not found at all in the removal of sulfo groups in presence of hot water. Therefore the capacity-time graph for desulfonation of resins in water is represented most correctly by a hyperbolic curve, or by a straight line in log-log coordinates. In our opinion, this difference in the desulfonation kinetics reflects the difference between the thermal desulfonation conditions in water and in air: in the former instance water is present in large excess throughout the process, and in the latter, is removed almost completely after several hours of heating.

The desulfonation rate in air [19] and in water increases sharply with rise of temperature. At 175° the sodium forms of the resins, which are usually more stable, show appreciable capacity losses; the loss is especially high in the case of KU-1 sulfonated phenol-formaldehyde resin, which loses up to 82% of its initial sulfo groups in 24 hours. In general, the sodium forms of the resins, containing Na^+ cations, which have a weaker polarizing effect than H^+ ions, are more stable than the resins in the hydrogen form. This superiority of resins in the Na form is very appreciable even at 150°, while at 110° KU-1 and KU-2 resins after 24 hours of contact with water show capacity losses of only about 0.004 (KU-1) and 0.003 (KU-2) meq/g.

For elucidation of the mechanism of thermal desulfonation, in some experiments the capacity determinations were supplemented by analysis of the aqueous extracts for their H^+ and SO_4^{2-} ion contents.

Analytical data for the aqueous extracts are given in Tables 2 and 3. The initial capacities E_0 of the resins in the hydrogen form were calculated from the results of quantitative determinations of SO_4^{2-} ions and the values found or their capacities after heat treatment (Table 1). The calculations were based on the assumption that, when 1 meq of sulfo groups is split off, 2 meq of SO_4^{2-} passes into solution. For resins in the Na form the contents of H^+ ions after heat treatment are also given. The analytical results, expressed in milliequivalents per gram of the original dehydrated resin, are average values for at least two parallel determinations.

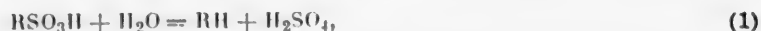
TABLE 3

Results of Determinations of H^+ and SO_4^{2-} Ions in the Aqueous Extracts and Contents of H^+ Ions in the Na Form of KU-1 Resin after Heat Treatment

Temperature (°C)	Contents of H^+ ions and SO_4^{2-} ions (D) in the aqueous extracts, contents of H^+ ions and the resin (B), and values of $A + B = C$ after heat treatment for											
	6 hours				12 hours				24 hours			
	A	B	C	D	A	B	C	D	A	B	C	D
150	0.03	0.05	0.08	0.14	0.20	0.10	0.30	0.66	0.41	0.16	0.57	1.14
175	1.04	0.20	1.24	2.44	1.56	0.05	1.61	3.10	1.60	0.05	1.65	3.39

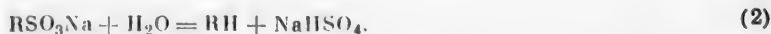
Comparison of the analytical results for the aqueous phases after contact with resins in the hydrogen form shows satisfactory agreement between the numbers of milliequivalents of H^+ and SO_4^{2-} ions. From this we may

conclude that the principal product of thermal desulfonation is sulfuric acid. The satisfactory agreement between the experimental and calculated capacities of both resins is consistent with the assumption that 2 meq of H_2SO_4 is formed per milliequivalent of sulfo groups split off. This corresponds to the reaction



which may be named the thermal hydrolysis reaction.

It is easy to see from Table 3 that desulfonation of the sodium forms of both resins in contact with water is also the result of thermal hydrolysis according to the equation



Consistently with this mechanism of thermal desulfonation, the aqueous extracts were found to contain about 2 meq of SO_4^{2-} ions per meq of H^+ ions in the liquid phase and in the resin. The presence of a certain amount of H^+ ions in the resin is not unexpected, and is caused by displacement of a part of the Na^+ ions by free H^+ ions formed in the liquid phase by Reaction (2).

TABLE 4

Density and Swelling of KU-1 and KU-2 Resins in the H, Na, and K Forms

Resin	Density of resin (g/cc)			Swelling of resin (in H_2O per g or original resin)		
	before heat treatment	after heat treatment		before heat treatment	after heat treatment	
		in air	in water		in air	in water
Ku-1, H-form	1.257	1.368	1.238	0.70	0.26	0.39
Ku-1, Na-form	1.295	1.336	1.236	0.63	0.46	0.48
Ku-1, K-form	1.331	1.331	1.239	0.51	0.49	0.53
Ku-2, H-form	1.151	1.215	1.143	1.78	1.01	1.55
Ku-2, Na-form	1.213	1.220	1.215	1.32	1.22	1.31
Ku-2, K-form	1.225	1.242	1.249	1.02	1.12	1.02

It is interesting to note that addition of sulfuric acid to the aqueous phase accelerates Reaction (1), and addition of alkali retards [24] Reaction 2.

Decrease of the active sulfo group content is the most important, but not the only consequence of heat treatment of ion-exchange resins.

It has already been shown by the author [17] that heat treatment of resins in air results in a considerable increase of their density in the swollen state and appreciable decrease of their swelling.

In the present investigation, determinations of swelling and density were extended to resins which had been heated in water.

Table 4 contains data on the density and swelling of the hydrogen, sodium, and potassium forms of KU-1 and KU-2 resins before and after heat treatment in air and in water. The duration of heat treatment was 24 hours in all cases. The resins were heated at 185° in air and at 175° in water. The densities refer to swollen resins.

In accordance with data published earlier [17], increases of density or decreases of hydration of sulfonated cation exchangers in different ionic forms are an objective measure of the degree of desulfonation of resins as the result of heat treatment in air.

There is no such definite relationship between the relative capacity loss and the density or swelling of resins in the hydrogen form after heat treatment in water. In these cases the densities of both resins decrease despite the

decrease of swelling. This is evidently the result of the tendency of substances with a mobile spatial structure to increase their degree of swelling with the temperature. In that case the swelling of a resin is determined by the action of two opposing effects: expansion of the spatial network of the resin, and decreased content of the strongly hydrated sulfo groups. Deformation of the spatial network accounts for the increase of the equivalent moisture capacity [15] of resins in the hydrogen form as the result of heating in water. This effect is especially pronounced in KU-1 resin, the swelling of which is decreased only by a factor of 1.8 for a loss of over 96% of its capacity. It may be noted here that in our interpretation of the causes of increase of the equivalent moisture capacity produced by the action of heat on the resins in water, we disagree with American workers [15, 25] who attribute this effect only to a decrease of the degree of cross linking of the resins.

In support of our viewpoint, it may be stated that deformation of the spatial network caused by the increase of its swelling, due to heating in water, is not completely irreversible. Thus, after the hydrogen forms of KU-1 and KU-2 resins, which had been subjected to thermal hydrolysis at 175° for 24 hours, had been dried, their swelling in cold water fell to 0.26 and 1.22, respectively. Similar results were found for resins in the potassium and sodium forms.

Consistently with the decreasing hydration of the ions themselves in the series $H > Na > K$, the swelling of resins in the H, Na, and K forms not subjected to heat treatment decreases in the same series, and the density correspondingly increases.

A definite relationship exists between the changes in the density and swelling of resins in the K and Na forms, caused by heating in air and their thermal stability. The Na and K forms of KU-2 resin and the K form of KU-1 resin, which are very resistant to thermal treatment in air, show relatively small density changes after being heated for 24 hours at 185°. The less stable Na form of KU-1 resin, which is appreciably desulfonated even when heated in air, shows a considerable density increase with a corresponding decrease in swelling.

When the K and Na forms of KU-1 resin are heated in water, their density decreased considerably despite the loss of most of the sulfo groups present in the original resins; the final densities of the Na and K resins are virtually the same as that of the resin in the H form. It is very probable that the densities of all these resins, desulfonated to a considerable extent, are determined by the properties of the phenol-formaldehyde polymer itself, and, especially, by its power to immobilize water at high temperatures.

The density and swelling of the sodium and potassium forms of KU-2 resin, which are only slightly susceptible to thermal hydrolysis, remain almost unchanged when these resins are heated in contact with water at 175° for 24 hours.

It follows that variations in the density and swelling of ion exchangers, under the influence of heat, are directly associated with desulfonation.

In conclusion, I thank K. M. Saldadze, A. B. Pashkov, and N. T. Romanchenko for providing samples of ion-exchange resins.

SUMMARY

1. It is shown that all the sulfonated cation exchangers studied, with different organic polymer radicals (KU-1, KU-2, SBS), undergo loss of capacity when heated in water, owing to loss of sulfo groups (thermal desulfonation).
2. The intensity of thermal desulfonation depends not only on the process conditions (temperature, heating time) but also on the structural characteristics of the organic framework of the resin macromolecule and the nature of its counter ions. The thermal stability of KU-2 cation exchanger is higher than that of the other resins. The sodium forms of all these cation exchangers are more stable than the hydrogen forms.
3. Kinetic studies of thermal desulfonation showed that there is a linear relationship between the logarithm of the capacity of KU-1 and KU-2 resins and the logarithm of the time of heat treatment in water.
4. It is shown that thermal desulfonation in presence of water is a hydrolysis reaction. It is therefore possible to determine indirectly the capacity losses of resins in the hydrogen form by titration of H^+ or SO_4^{2-} ions in the liquid phase, which had been in contact with the resins during heat treatment.

5. Capacity losses of cation exchangers as the result of thermal desulfonation are accompanied by changes in their true density and swelling. It is suggested that increase of the equivalent moisture capacity of resins is caused by increase of their swelling power on heating rather than by decreasing cross linking.

LITERATURE CITED

- [1] A. A. Vasil'ev, J. Appl. Chem. 30, No. 7, 1022 (1957).*
- [2] I. E. Apel'tsin, V. A. Klyachko, Yu. Yu. Lur'e, and A. S. Smirnov, Ion Exchangers and their Applications [in Russian] (Moscow, 1949).
- [3] Yu. I. Usatenko and L. I. Gureeva, Industrial Lab. 22, 781 (1956).
- [4] B. H. Ketelle and G. E. Boyd, in the book: Ion Exchange Chromatography (IL, 1949) p. 159 [Russian translation].
- [5] L. Wolf and J. Massone, J. prakt. Chem. 5, 21 (1957).
- [6] L. Wolf and J. Massone, J. prakt. Chem. 5, 288 (1958).
- [7] B. K. Preobrazhenskii, A. V. Kalyamin, and O. M. Lilova, J. Inorg. Chem. 2, 1164 (1957).
- [8] S. G. Thompson, B. C. Harvey, C. R. Choppin and G. T. Seaborg, J. Am. Chem. Soc. 76, 6229 (1954).
- [9] Bull. Am. Railway Assoc. 55, 511, 361 (1953).
- [10] F. C. Nachod and J. Schubert, Ion Exchange Technology, N. Y. (1956).
- [11] E. B. Trostyanskaya and A. B. Pashkov, Chem. Sci. and Ind. 11, 583 (1957).
- [12] J. A. Kitchener, Ion Exchange Resins, London (1957).
- [13] H. P. Gregor, K. M. Held, and J. Bellin, Anal. Chem. 23, 620 (1951).
- [14] I. P. Losev and E. B. Trostyanskaya, in the book: Investigations in the Field of Chromatography [in Russian] (Izd. AN SSSR, 1952) p. 188.
- [15] G. E. Boyd, B. A. Soldano and O. D. Bonner, J. Phys. Chem. 58, 456 (1954).
- [16] K. M. Saldadze, in the book: Investigations in the Field of Chromatography [in Russian] (Izd. AN SSSR, 1952) p. 114.
- [17] N. G. Polyanskii, Nature 9, 102 (1957).
- [18] N. G. Polyanskii, Summaries of Papers at the Conference on Chromatography [in Russian] (Izd. AN SSSR, 1958) p. 28.
- [19] N. G. Polyanskii, Bull. Acad. Sci. Latvian SSR 12, 163 (1957).
- [20] V. N. Ipatiev, Ber. 59, 1737 (1926).
- [21] L. Szekeres, Bacàcnée - Polgar E. Magyar kem. folyóirat, 61, 298 (1955).
- [22] A. A. Vansheidt, A. A. Vasil'ev, and O. I. Okhrimenko, Theory and Practice of the Use of Ion-Exchange Materials [in Russian] (Izd. AN SSSR, 1955) p. 110.
- [23] A. A. Vasil'ev, Technology of Synthetic Plastics [in Russian] (Leningrad, 1954).
- [24] N. G. Polyanskii, Bull. Higher Educ. Establishments, Min. of Higher Education USSR, Chem. and Chem. Technol. 1, 163 (1958).
- [25] B. Soldano, in the book: Ion Exchange Resins in Biology and Medicine (IL, 1956) p. 72 [Russian translation].

Received August 5, 1957

* Original Russian pagination. See C. B. Translation.

PHYSICOCHEMICAL PROPERTIES OF GLASSY LITHIUM SILICATES AND ALUMINOSILICATES

S. K. Dubrovo and Yu. A. Shmidt

In recent years there has been a considerable increase in the use of lithium compounds for the production of various silicate materials such as glazes, enamels, porcelain, special glasses, etc. However, they are not used nearly enough, especially in the glass industry. One reason for this is that the influence of lithium oxide on the physicochemical properties of glasses has been studied very little. The role of lithium oxide is seen most clearly in studies of the properties of simple systems in comparison with the properties of other alkali systems — potassium and sodium.

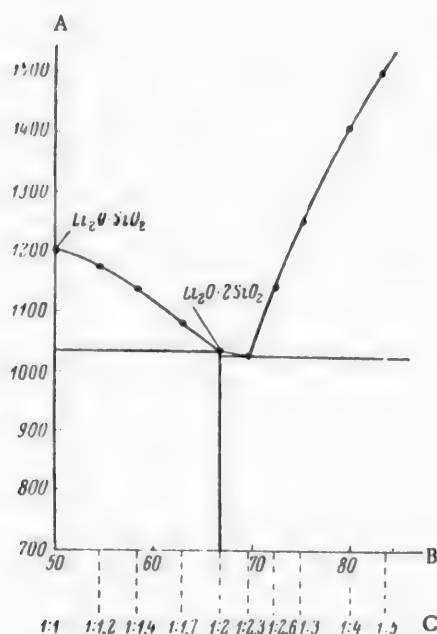


Fig. 1. Positions of the compositions studied on the phase diagram for the system $\text{Li}_2\text{O}-\text{SiO}_2$: A) temperature ($^{\circ}\text{C}$); B) SiO_2 content (molar %); C) $\text{Li}_2\text{O}:\text{SiO}_2$ ratio.

scanty. There are only occasional and incidental data, which are not the results of systematic investigations [9]. There is even less information on the physical properties of glassy lithium aluminosilicates. However, investigations of these properties are especially important at the present time, because glasses of the $\text{Li}_2\text{O}-\text{Al}_2\text{O}_3-\text{SiO}_2$ system form the basis of new silicate materials of especially high mechanical strength [10].

Our main object was to study the breakdown of glassy lithium silicates and aluminosilicates by the action of aqueous solutions. We also determined physical properties — density and refractive index — which were then

Simple lithium glasses have a higher tendency to crystallization than soda or potash glasses. Several workers have reported that it is impossible to obtain glassy materials, even with quenching, in the system $\text{Li}_2\text{O}-\text{SiO}_2$ with lithium oxide contents of 40 molar % and over [1, 2]. Lithium borate glasses have an even greater tendency to crystallization. Thus, according to Moore and McMillan, glasses of the $\text{Li}_2\text{O}-\text{B}_2\text{O}_3$ system containing over 25 molar % lithium oxide crystallize, whereas in sodium borate glasses of sodium oxide content can be raised to 33 molar %. The amount of alkali-metal oxides may be increased in presence of aluminum oxide [3]. It should be noted that these workers obtained glassy specimens of lithium silicates and aluminosilicates of a number of different compositions only in small amounts (0.5 g), and with the use of rapid cooling.

The literature contains few data on systematic studies of the physicochemical properties of glassy lithium silicates. The published data refer mainly to certain physical properties such as the coefficient of thermal expansion, viscosity, and density [3-7]. In recent years papers have also appeared on the electrical properties of simple and complex lithium borate and lithium borosilicate glasses [8]. The published results show that glassy lithium silicates have lower viscosities, coefficients of thermal expansion, and densities than potassium or sodium glasses of the same molecular composition. Published data on the chemical properties of simple lithium glasses, especially in relation to lithium silicates, are very

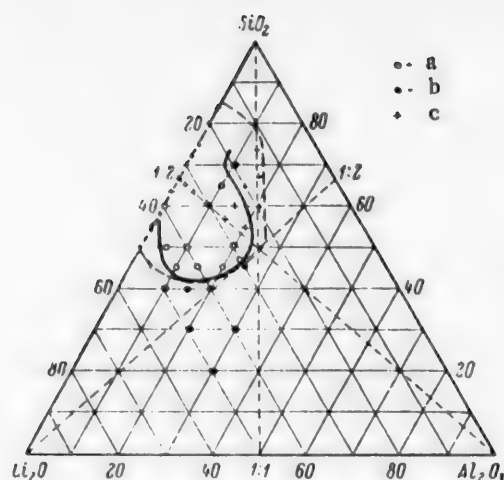


Fig. 2. Compositions in the system $\text{Li}_2\text{O}-\text{Al}_2\text{O}_3-\text{SiO}_2$. Region of glass formation in the system according to Moore and McMillan [3], continuous line: a) glassy composition; b) crystallized compositions; from our data, dash line: c) glassy compositions.

was sufficient. Certain difficulties arose in the preparation of glassy samples because of the high crystallization rate of simple lithium silicate glasses. The following method was used: a small portion of the melted glass was poured rapidly from the hot crucible into a flat steel mold in the form of a round depression (depth ~ 3 mm, diameter 45 mm) and pressed down at once with a massive steel block. The glass disk so formed was quickly transferred into the annealing muffle. Even with this rapid cooling, some of the glasses sometimes partly crystallized.

used for calculation of molar volumes and refractions of lithium glasses. The results were compared with data on soda and potash glasses. This combined investigation of physical and chemical properties provided a deeper insight into the behavior of simple silicates containing alkali-metal ions of different ionic radii.

EXPERIMENTAL

The glassy lithium silicates and aluminosilicates were made in a furnace with Siilt heaters. All the glasses were made in 50-100 g lots in platinum crucibles. The starting materials were lithium carbonate (analytical grade), aluminum hydroxide (pure grade), and ground rock crystal containing $\sim 0.07\%$ impurities. The thoroughly mixed batch was first heated in a muffle furnace at 500-600° to prevent powdering when it was put into the heated crucible. Lithium silicate glasses in the composition range ($\text{Li}_2\text{O}:\text{SiO}_2$) from 1:1 to 1:3 were melted at temperatures of about 1300°, and glasses of the composition 1:4 and 1:5 were melted at 1480-1500°. All these glasses were less viscous than the corresponding soda glasses, and were readily homogenized, so that hand stirring of the melt by means of a platinum stirrer

TABLE 1

Compositions of Glassy Lithium Silicates and Aluminosilicates

Composition by synthesis						Composition by analysis		
Oxide ratio			Molar percentages			Oxide ratio		
Li_2O	Al_2O_3	SiO_2	Li_2O	Al_2O_3	SiO_2	Li_2O	Al_2O_3	SiO_2
1	—	1	50.0	—	50.0	—	—	—
1	—	1.2	45.4	—	54.6	—	—	—
1	—	1.4	41.7	—	58.3	1	—	1.39
1	—	1.7	37.1	—	62.9	1	—	1.73
1	—	2.0	33.3	—	66.7	1	—	2.03
1	—	2.3	30.3	—	69.7	—	—	—
1	—	2.6	27.8	—	72.2	—	—	—
1	—	3.0	25.0	—	75.0	1	—	3.16
1	—	4.0	20.0	—	80.0	1	—	4.00
1	—	5.0	16.7	—	83.3	1	—	5.00
1	0.05	2.0	32.8	1.6	65.6	—	—	—
1	0.15	2.0	31.7	4.8	63.5	1	0.16	2.06
1	0.30	2.0	30.3	9.1	60.6	1	0.32	2.04
1	0.50	2.0	28.6	14.3	57.1	1	0.51	2.03
1	1.00	2.0	25.0	25.0	50.0	1	1.02	1.98
1	0.80	2.2	25.0	20.0	55.0	1	0.84	2.21
1	0.60	2.4	25.0	15.0	60.0	1	0.59	2.30
1	1.00	3.0	20.0	20.0	60.0	1	0.99	2.90
1	0.75	3.25	20.0	15.0	65.0	1	0.77	3.06
1	0.50	3.5	20.0	10.0	70.0	1	0.51	3.45
1	1.00	4.0	16.7	16.7	66.6	1	1.04	4.14
1	1.00	6.0	12.5	12.5	75.0	—	—	—

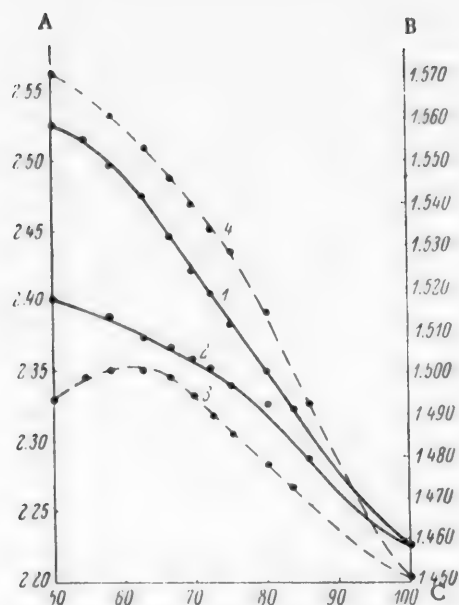


Fig. 3. Effect of composition on the densities and refractive indices of glassy lithium and sodium silicates: A) density; B) refractive index; C) SiO_2 content (molar %); refractive indices of glassy silicates: 1) lithium; 2) sodium; densities of glassy silicates: 3) lithium; 4) sodium.

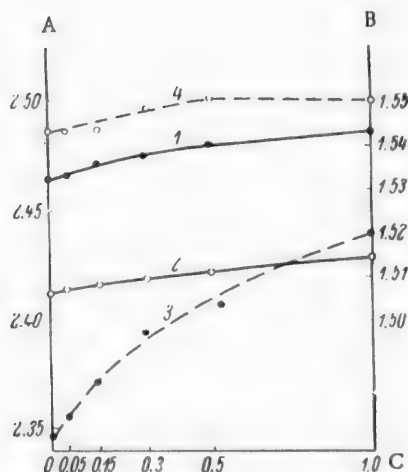


Fig. 4. Effect of composition on the densities and refractive indices of glassy lithium and sodium aluminosilicates: A) density; B) refractive index; C) addition (moles) of Al_2O_3 to glasses of the composition $\text{R}_2\text{O} \cdot 2\text{SiO}_2$; refractive indices: 1) lithium; 2) sodium; densities: 3) lithium; 4) sodium.

Glasses of the compositions 1:1 and 1:2 crystallized especially rapidly, with formation of large crystals of lithium metasilicate. These glasses were poured onto a flat plate and quickly flattened out. Some glass could be obtained even with these compositions, if the crystallized portions were then remelted. It must be pointed out that Kracek [11] was the only one to obtain glasses in this composition region, in the form of very small specimens. Plates of glasses of the compositions 1:4 and 1:5 were made similarly. Other workers could only obtain opaque glasses of these compositions [6, 7].

Lithium aluminosilicate glasses were made in two series. The first series of glasses consisted of lithium disilicate with 0.05 to 1 mole of aluminum added. The second series was based on glasses of lower alkali oxide content, of the composition $\text{Li}_2\text{O} \cdot \text{Al}_2\text{O}_3 \cdot a\text{SiO}_2$ ($a = 2, 3, 4$, and 6), and in some of them, part of the alumina was replaced by silica. The lithium aluminosilicate glasses were melted at 1450-1480°. They showed a lower tendency to crystallization than the lithium silicate glasses. All the samples were annealed in a muffle furnace, at temperatures from 450 to 500°, according to composition, and the quality of annealing was tested by means of the polariscope.

In this way we obtained glasses in the system $\text{Li}_2\text{O} - \text{SiO}_2$ containing from 16.7 to 50 molar % lithium oxide, and in the system $\text{Li}_2\text{O} - \text{Al}_2\text{O}_3 - \text{SiO}_2$ containing from 12.5 to 32.8 molar % lithium oxide and from 1.6 to 25 molar % aluminum oxide. Table 1 contains the compositions of these glasses, and Fig. 1 shows the position of the lithium silicate glass compositions on the phase diagram for the system $\text{Li}_2\text{O} - \text{SiO}_2$. Figure 2 shows the region of glass formation in the system $\text{Li}_2\text{O} - \text{Al}_2\text{O}_3 - \text{SiO}_2$, according to Moore and McMillan and to our data.

The refractive indices and densities of the glasses were determined. Refractive indices were determined by the immersion method to an accuracy of ± 0.003 , and densities were determined by hydrostatic weighing. Similar determinations were performed on sodium silicate and sodium aluminosilicate glasses. The results are given in Tables 2 and 3 and Figures 3 and 4. It is seen that glassy lithium silicates have higher refractive indices and lower densities than sodium silicates of the corresponding molecular composition. The density-composition curve for lithium silicate glasses takes an anomalous course, with a maximum at 58-63 molar % SiO_2 . The density and refractive index differences diminish with increasing silica contents in the glasses. Similar results are seen when the refractive indices and densities of glassy lithium and sodium aluminosilicates are compared. These values increase both for lithium and for sodium aluminosilicates with increasing alumina content, and decrease with increasing silica content.

The densities and refractive indices were used for calculation of the molar volumes and refractions of the glasses,

TABLE 2

Refractive Indices, Densities, and Molar Volumes of Glassy Lithium Silicates and Aluminosilicates, and the Ionic Refraction of Oxygen in Them

Oxide ratio			Refractive index	Density	Molar volume	Ionic refraction of oxygen
Li ₂ O	Al ₂ O ₃	SiO ₂				
1	—	1	1.559	2.330	19.29	4.08
1	—	1.2	1.555	2.346	19.76	4.00
1	—	1.4	1.549	2.351	20.18	3.99
1	—	1.7	1.542	2.350	20.78	3.94
1	—	2.0	1.532	2.347	20.29	3.94
1	—	2.3	1.524	2.332	21.81	3.86
1	—	2.6	1.518	2.319	22.29	3.85
1	—	3.0	1.511	2.307	22.74	3.83
1	—	4.0	1.500	2.283	23.64	3.80
1	—	5.0	1.491	2.267	24.24	3.80
1	0.05	2.0	1.533	2.355	21.57	3.95
1	0.15	2.0	1.536	2.372	22.12	4.09
1	0.30	2.0	1.538	2.395	22.84	4.25
1	0.50	2.0	1.540	2.407	23.85	4.49
1	1.00	2.0	1.543	2.440	25.19	4.97
1	0.80	2.2	1.538	2.419	25.17	4.69
1	0.60	2.4	1.535	2.406	24.43	4.13
1	1.00	3.0	1.525	2.409	25.90	4.59
1	0.75	3.25	1.519	2.392	25.20	4.37
1	0.50	3.50	1.516	2.297	25.30	4.30
1	1.00	4.0	1.516	2.374	26.08	4.42
1	1.00	6.0	1.509	2.360	26.05	4.02
α-Spodumene			1.657—	3.014	—	—
			1.674	—	—	—
β-Spodumene			1.517—	2.460	—	—
			1.523	—	—	—
Spodumene glass			1.515	2.327	—	—

TABLE 3

Refractive Indices, Densities, and Molar Volumes of Glassy Sodium Silicates and Aluminosilicates, and the Ionic Refraction of Oxygen in Them.

Oxide ratio			Refractive index	Density	Molar volume	Ionic refraction of oxygen
Na ₂ O	Al ₂ O ₃	SiO ₂				
1	—	1.0	1.517	2.562	23.81	4.60
1	—	1.4	1.513	2.533	24.02	4.37
1	—	1.7	1.508	2.508	24.22	4.27
1	—	2.0	1.506	2.486	24.40	4.20
1	—	2.3	1.503	2.470	24.54	4.14
1	—	2.6	1.501	2.451	24.71	4.10
1	—	3.0	1.497	2.435	24.80	4.00
1	—	4.0	1.492	2.391	25.26	3.96
1	—	6.0	1.479	2.328	25.85	3.84
1	0.05	2.0	1.507	2.487	24.66	4.27
1	0.15	2.0	1.508	2.487	25.19	4.36
1	0.30	2.0	1.509	2.497	25.80	4.52
1	0.50	2.0	1.510	2.501	26.62	4.72
1	1.00	2.0	1.514	2.500	28.39	5.14
1	1.00	3.0	1.505	2.463	27.93	4.75
1	1.00	4.0	1.498	2.420	27.77	4.55
1	1.00	6.0	1.491	2.368	26.69	4.17
Quartz glass			1.459	2.20	27.27	3.67

and also the average ionic refraction of oxygen in them. The molar refractions of the glasses were calculated from the Lorentz-Lorenz equation

$$R = \frac{n^2 - 1}{n^2 + 2} \cdot \frac{M}{d}$$

where n is the refractive index, M is the molecular weight, and d is the density of the glass. The molecular weight of each glass was calculated as the sum of the mole fraction of the oxides (xR_2O , yAl_2O_3 , $zSiO_2$), multiplied by their molecular weights (m_1 , m_2 , m_3):

$$M = x_{R_2O} \cdot m_1 + y_{Al_2O_3} \cdot m_2 + z_{SiO_2} \cdot m_3$$

The refraction of the oxygen ion in glass was calculated by subtraction of the ionic refractions of silicon, aluminum, and sodium or lithium from the molar refraction of the glass, by the formula

$$R_0 = \frac{R_g - xR_{Me} - yR_{Al} - zR_{Si}}{x + 1.5y + 2z}$$

The ionic refractions were taken from the literature sources [12]. The calculated molar volumes of the glasses ($v = \frac{M}{d}$) and the ionic refractions of oxygen in them are given in Table 2 for lithium glasses, and in Table 3 for sodium glasses. It is seen from these results that the molar volume increases and the ionic refraction of oxygen decreases with increasing silica contents in glassy lithium and sodium silicates. The molar volume and ionic refraction of oxygen increases with progressive replacement of silica by alumina in lithium and sodium glasses.

TABLE 4

Partial Refractive Indices, Molar Volumes, and Molar Refractions of Aluminum Oxide in Alkali Silicate Glasses

Oxide ratio			$\bar{n}_{Al_2O_3}$		$\bar{v}_{Al_2O_3}$		$R_{Al_2O_3}$	
R_2O	Al_2O_3	SiO_2	from lithium glasses	from sodium glasses	from lithium glasses	from sodium glasses	from lithium glasses	from sodium glasses
1	0.05	2.0	1.593	—	38.79	40.4	12.23	13.49
1	0.15	2.0	1.615	1.548	38.58	40.8	12.85	12.87
1	0.30	2.0	1.598	1.555	38.32	39.8	12.53	12.30
1	0.50	2.0	1.588	1.539	39.19	39.9	12.82	12.49
1	1.00	2.0	1.576	1.539	36.90	40.4	12.82	12.48
1	0.80	2.2	1.582	—	39.20	—	12.73	—
1	0.60	2.4	1.614	—	38.30	—	12.71	—
1	1.00	3.0	1.581	1.527	38.54	40.4	12.41	12.49
1	0.75	3.25	1.592	—	37.70	—	—	—
1	1.00	4.0	1.596	1.522	38.40	40.6	12.54	12.29
1	1.00	6.0	—	—	—	40.0	12.71	12.54
Mean			1.594	1.538	38.35	40.3	12.67	12.82
$Na_2O-CaO-bAl_2O_3-2SiO_2$			—	—	—	40.5	—	12.68
$Na_2O-CaO-bAl_2O_3-3SiO_2$			—	—	—	40.5	—	12.53
$Na_2O-CaO-bAl_2O_3-4SiO_2$			—	—	—	40.5	—	12.45
* $CaO-Al_2O_3-2SiO_2$ glassy			—	—	—	—	—	—
			1.620	—	—	—	—	—

• From Appen's data [7].

Comparison of the data in Tables 2 and 3 shows that the molar volume and ionic refraction of oxygen are lower for lithium than for sodium glasses. This shows that the structure of lithium glasses is more compact or denser than that of sodium glasses of the corresponding molecular compositions. Evstrop'ev found an empirical relationship between the average refraction of the oxygen ion and the energy of the structural network of the glass [13]. The two quantities are inversely proportional in the range of R_0 between 3.5 and 5. It follows that lithium silicate and lithium aluminosilicate glasses have greater energy of the structural network per mole of glass than the corresponding sodium glasses. It is to be expected that lithium glasses would be attacked more slowly than corresponding sodium glasses by chemical reagents.

The partial refractive indices, molar volumes, and molar refractions of aluminum oxide in glassy lithium and sodium aluminosilicates were then calculated. The calculations were based on the additivity principle: it was assumed that each glassy aluminosilicate consists of the corresponding silicate with an addition of a certain amount of alumina. Thus, calculations for compositions of the type $R_2O \cdot bAl_2O_3 \cdot 2SiO_2$ were based on the properties of $R_2O \cdot 2SiO_2$ glasses; for compositions of the type $R_2O \cdot Al_2O_3 \cdot aSiO_2$, on the properties of $R_2O \cdot 3SiO_2$, $R_2O \cdot 4SiO_2$ glasses, etc. The calculations were performed by means of Appen's formula [7]:

$$g = g_0 + (1 + \gamma_1) \frac{\Delta g}{\Delta \gamma_1},$$

where g is the measured property of an aluminosilicate glass, Δg is the difference between the values for the property of the given glass and of the corresponding glassy silicate, and γ_1 is the mole fraction of aluminum oxide.

The calculated results are given in Table 4. The results obtained by Safford and Silverman [14], who studied refraction in a series of soda-lime aluminosilicate glasses, are given in the same table. They compared their values with the partial molar refractions of aluminum oxide in crystalline aluminosilicates. The partial properties of aluminum oxide in the glasses were found to be very close to the values in albite, carnegieite, and anorthite, and different from the values in kyanite and corundum. Safford and Silverman therefore concluded that aluminum has coordination number four in the glasses studied. It follows from the data in Table 4 that the values of partial molar volume and partial molar refraction of aluminum oxide are very close to each other, and are within the range of values found for the glasses studied by Safford and Silverman.

Evidently aluminum must have coordination number four in glassy lithium aluminosilicates also. The acid resistance should therefore deteriorate with increase of the alumina content of lithium aluminosilicates above a certain limit; this was confirmed by subsequent investigation.

SUMMARY

1. Glasses were prepared in the system Li_2O-SiO_2 , containing from 16.7 to 50 molar % lithium oxide, and in the system $Li_2O-Al_2O_3-SiO_2$ containing from 12.5 to 32.8% lithium oxide and 1.6 to 25 molar % alumina. The crystallization rate of these glasses increases as the composition approaches that of lithium metasilicate (1:1.4, 1:1.2, 1:1). Lithium aluminosilicate glasses are less prone to crystallization.
2. Lithium silicate and aluminosilicate glasses have higher refractive indices but lower densities, molar volumes, and ionic refractions for oxygen than the corresponding sodium glasses.
3. Calculations of the partial properties of aluminum oxide in these glassy lithium and sodium silicates indicate that aluminum in them has coordination number four.

LITERATURE CITED

- [1] E. Preston, and W. E. S. Turner, *J. Soc. Glass Technol.* 18, 143 (1934).
- [2] A. Dietzel and H. A. Sheybany, *Verres et Refract* 2, 63 (1948).
- [3] H. Moore and P. W. McMillan, *J. Soc. Glass Technol.* 40, 193, 66T (1956).
- [4] L. Shartsis, S. Spinner and W. Capps, *J. Amer. Ceram. Soc.* 35, 6, 155 (1952).
- [5] K. Endell and H. Hellbrügge, *Glastechn. Ber.* 18, 12, 364 (1940).

- [6] D. Hubbard and G. W. Cleek, J. Res. N. B. S. 49, 4, 267 (1952).
- [7] A. A. Appen, Doctorate Dissertation [in Russian] (Leningrad, 1952).
- [8] A. E. Dale, E. F. Pegg and J. E. Stanworth, J. Soc. Glass Technol. 35, 164 (1951).
- [9] I. B. Lukach, Author's Summary of Dissertation [in Russian] (Leningrad Inst. Chem. Technology, 1953).
- [10] S. D. Stookey, Glass Ind. 38, 6, 331 (1957).
- [11] F. C. Kracek, J. Phys. Chem. 34, 12, 2641 (1930).
- [12] K. Fajans and N. J. Kreidl, J. Amer. Ceram. Soc. 31, 4, 105 (1948).
- [13] K. S. Evstrop'ev, J. Phys. Chem. 20, No. 6, 561 (1946).
- [14] H. W. Safford and A. Silverman, J. Amer. Ceram. Soc. 30, 7, 203 (1947).

Received April 28, 1958

PRODUCTION OF ACID-RESISTANT MATERIALS BASED ON CORUNDUM WITH ADDITIONS OF ORGANOSILICON POLYMERS

I. D. Abramson, V. A. Bork, and I. I. Kornblit

The D. I. Mendeleev Institute of Chemical Technology, Moscow

Acid-resistant materials used at present do not fully satisfy requirements. The present investigation was therefore undertaken in order to search for new ceramic materials, both of dense structure and with filtration properties, with high acid resistance.

The principal mineral material used was white synthetic corundum made in the electric furnace, which has high acid resistance. The sintering additive was an organosilicon polymer, ethyl silicate 40, hydrolyzed by aqueous alcohol to 21.9% SiO_2 content.

TABLE 1
Particle-Size Characteristics of Synthetic Corundum Powders

Granulation grade	Particle size of principal fractions (μ)
100	105 - 180
180	42 - 105
320	7 - 53
M-7	3.5 - 7.4

In pyrolysis of organosilicon compounds during firing of ceramics, the organic portion is volatilized and polymeric silica remains in the form of a coating on the grains of the main material [1, 2]. This should give an acid-resistant material, as SiO_2 is also resistant to acids. Moreover, if enough of the organosilicon compound is added, in some cases a porous material may be obtained as the result of evolution of gaseous pyrolysis products (CO , CO_2 , H_2O , etc.) during firing.

EXPERIMENTAL

Synthetic corundum of the following granulation grades was used for preparation of the samples: 100, 180, 320, and close to M-7 (a microgranular powder). The particle-size characteristics of these powders are given in Table 1.

For brevity, synthetic corundum is denoted here by the symbol "K". The number following the symbol represents the granulation grade of the original powder. Thus, "batch K-320" represents a batch based on synthetic corundum of granulation grade 320.

Cylinders of diameter and height 20 mm were made from the corundum powders with additions of hydrolyzed ethyl silicate 40 and technical paraffin wax as plasticizer, by the method used in the Sinoxal process [3]. The cylinders were fired at two different temperatures - 1250 and 1600° - and their acid resistance, mechanical (compressive) strength, and certain other characteristics were determined [4].

Acid resistance of the specimens was determined by alternate heating to 300° and cooling in sulfuric acid (sp.gr. 1.84), for 216 hours (three cycles each of 72 hours). After each cycle the weight loss of the specimen was determined (as % of the initial weight).

Four batches were prepared for each granulation grade of the corundum, with 1, 3, 5 and 7% binder calculated as SiO_2 . This gave 16 different batches, the composition of which are given in Table 2.

Examination of specimens fired at 1250° showed that many of them, especially those made from coarse-grained corundum, differed little or not at all in size from the unfired specimens, and therefore shrinkage (Δh)

was not determined for these. The mechanical strength of the specimens was low, but increased with decrease of particle size. The mechanical strength depends on the amount of organosilicon compound introduced into the batch; specimens containing 3% SiO_2 had the highest mechanical strength.

TABLE 2

Composition of Experimental Batches Made From Corundum and Hydrolyzed Ethyl Silicate

Batch No.	Granulation grade	Corundum content (wt. %)	Amount of binder calculated as SiO_2 (%)	Batch No.	Granulation grade	Corundum content (wt. %)	Amount of binder calculated as SiO_2 (%)
1	100	99	1	9	320	99	1
2	100	97	3	10	320	97	3
3	100	95	5	11	320	95	5
4	100	93	7	12	320	93	7
5	180	99	1	13	M-7	99	1
6	180	97	3	14	M-7	97	3
7	180	95	5	15	M-7	95	5
8	180	93	7	16	M-7	93	7

The contact area between the individual grains in the experimental batches and the density of the specimen, both increase with increased dispersity of the original powder. Naturally, the amount of binder also influences this property. Specimens containing 3% SiO_2 also had the highest density. The mechanical strength and density of the specimens are given in Table 3.

TABLE 3

Mechanical Strength σ_{comp} (in kg/cm^2) and Density γ (in g/cc) of Specimens Fired at 1250°

SiO_2 content (%)	Properties of specimens made from:							
	K-100		K-180		K-320		M-7	
	σ_{comp}	γ	σ_{comp}	γ	σ_{comp}	γ	σ_{comp}	γ
1	29	2.03	137	2.14	167	2.18	316	2.23
3	46	2.11	145	2.19	198	2.20	334	2.26
5	39	2.08	129	2.15	163	2.16	320	2.24
7	28	2.06	118	2.08	144	2.13	242	2.23

TABLE 4

Porosity B (%) and Water Absorption W (%) of Specimens Fired at 1250°

SiO_2 content (%)	Properties of specimens from:							
	K-100		K-180		K-320		M-7	
	B	W	B	W	B	W	B	W
1	45.8	22.4	45.4	22.9	45.6	22.5	44.9	22.4
3	45.3	22.1	45.1	22.2	45.0	22.3	44.3	22.0
5	45.7	22.2	45.2	22.5	45.3	22.4	44.7	22.1
7	45.3	22.2	45.2	22.3	45.7	22.6	44.8	22.2

The porosity and hence the water absorption of the specimens depended in the same manner on the grain size and SiO_2 content.

TABLE 5

Porosity, Water Absorption, and Shrinkage of Specimens Fired at 1600°

Granulation grade	Batch No.	SiO ₂ content (%)	Shrinkage (%)	Porosity (%)	Water absorption (%)	Granulation grade	Batch No.	SiO ₂ content (%)	Shrinkage (%)	Porosity (%)	Water absorption (%)
100	1	1	0.3	44.3	22.1	320	9	1	2.9	42.4	18.3
	2	3	0.6	42.1	19.0		10	3	4.7	41.3	18.0
	3	5	0.5	45.3	21.9		11	5	4.2	41.8	18.2
	4	7	0.4	44.8	21.7		12	7	3.1	42.2	18.5
180	5	1	0.9	43.8	19.9	M-7	13	1	8.0	29.3	10.7
	6	3	1.5	42.0	18.6		14	3	9.5	28.2	10.2
	7	5	1.4	43.4	19.8		15	5	7.5	28.4	10.4
	8	7	1.2	42.8	20.2		16	7	6.1	29.1	11.2

Nevertheless, the absolute values of all these parameters varied within narrow ranges for all the batches. The results of porosity and water absorption determinations are given in Table 4.

The data in Tables 3 and 4 confirm that 1250° is too low a temperature for the sintering of such a refractory material as corundum with such a high-melting binder as SiO₂. As a result, in a number of cases the specimens disintegrated during tests for acid resistance. No clear relationship between the batch composition and acid resistance could be found for specimens fired at the lower temperature.

A similar set of specimens was then fired at 1600°.

TABLE 6

Mechanical Strength of Specimens Fired at 1600°

SiO ₂ content (%)	σ_{comp} (kg/cm ²) of specimens made from			
	K-100	K-180	K-320	M-7
1	393	439	601	2268
3	453	468	964	2368
5	374	438	886	1655
7	320	376	648	854

TABLE 7

Solubility of Specimens, Fired at 1600°, in Concentrated H₂SO₄ by Cycles

Granulation grade	Batch No.	SiO ₂ content (%)	Solubility (% of original weight)			
			in 1st cycle	in 2nd cycle	in 3rd cycle	in all cycle
100	1	1	0.18	0.58	0.15	0.91
	2	3	0.09	0.33	0.09	0.51
	3	5	0.03	0.47	0.37	0.80
	4	7	0.27	0.45	0.15	0.87
180	5	1	0.32	2.12	—	2.44
	6	3	0.32	0.79	0.24	1.35
	7	5	0.14	0.53	0.08	0.75
	8	7	0.15	0.43	0.03	0.61
320	9	1	0.38	2.03	0.38	2.79
	10	3	0.20	1.33	0.16	1.69
	11	5	0.19	0.98	0.09	1.26
	12	7	0.11	1.08	0.07	1.26
M-7	13	1	0.31	2.90	1.11	4.32
	14	3	0.53	1.93	1.02	3.48
	15	5	0.53	1.64	0.63	2.80
	16	7	0.77	1.27	0.36	2.40

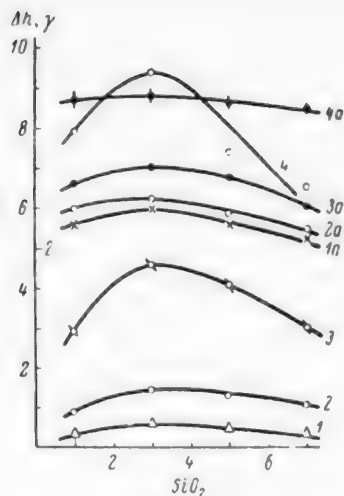


Fig. 1. Effects of different amounts of SiO_2 (in %) on the density (γ , curves 1a-4a) and shrinkage (Δh , curves 1-4); batches: 1 and 1a) K-100; 2 and 2a) K-180; 3 and 3a) K-320; 4 and 4a) KM-7.

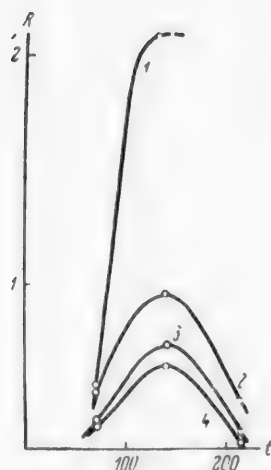


Fig. 2. Variations of solubility R (%) with treatment time t (hours) for K-180 batches. SiO_2 contents (%): 1) 1; 2) 3; 3) 5; 4) 7.

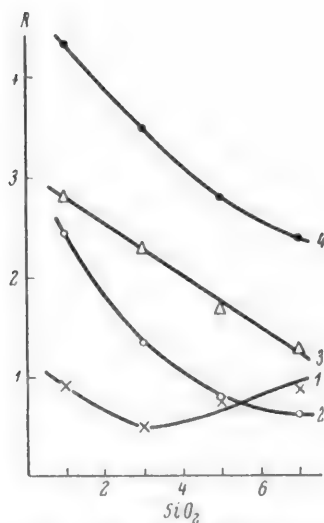


Fig. 3. Effects of different amounts of SiO_2 (%) on solubility R ; batches: 1) K-100; 2) K-180; 3) K-320; 4) KM-7.

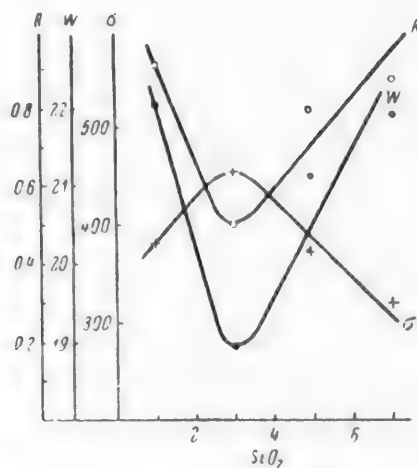


Fig. 4. Effects of different amounts of SiO_2 (%) on solubility R (%), water absorption W (%), and mechanical strength σ_{comp} (kg/cm²) of specimens from K-100 batches.

Measurements of specimens fired at 1600° showed that they all shrank, the shrinkage increasing with the dispersity of the original powder. Table 5 contains shrinkage, porosity, and water absorption data for the specimens. Batches made with the finest powder (M-7) had the lowest porosities and water absorption, and the greatest shrinkages.

The effects of different amounts of SiO_2 on density and shrinkage are shown in Fig. 1.

It follows that the density of the specimens increases with increasing dispersity of the original corundum, but the highest in all cases with 3% SiO_2 .

TABLE 8

Solubilities of Specimens with Different Binder Contents

Granulation grade	Batch No.	SiO ₂ content		Solubility (%)	Granulation grade	Batch No.	SiO ₂ content		Solubility (%)
		% by weight	in g/m ²				% by weight	in g/m ²	
100	1	1	0.777	0.91	320	9	1	0.062	2.79
	2	3	2.380	0.51		10	3	0.189	2.29
	3	5	4.050	0.80		11	5	0.323	1.69
	4	7	5.790	0.87		12	7	0.462	1.26
180	5	1	0.273	2.44	M-7	13	1	0.032	4.32
	6	3	0.837	1.35		14	3	0.097	3.48
	7	5	1.420	0.75		15	5	0.165	2.80
	8	7	2.040	0.61		16	7	0.235	2.40

These results are also consistent with the values of the mechanical strength of the specimens (Table 6).

The higher mechanical strength of specimens, containing 3% SiO₂ is apparently no accident: If the amount of organosilicon polymer introduced into the batch is above a certain optimum value, the batch has a high content of organic matter which is burned out during firing, so that the specimens have higher porosity, with lower density and mechanical strength.

The results of the tests for acid resistance are given in Table 7.

The data in Table 7 show that specimens fired at 1600° have high acid resistance.

During the first cycle, i.e., 72 hours, the solubility of the specimens is slight, varying between 0.03% and 0.77% for different batches. In the second cycle, i.e., during the following 72 hours, the solubility of all the specimens increases to between 0.33% and 2.9%. Finally, during the third cycle, the solubility decreases again and lies between 0.03% and 1.11%; thus, the solubility, after reaching a certain maximum, may fall to a negligible value (Fig. 2).

It follows from Fig. 3 that materials made from coarse-grained corundum have the lowest solubility.

Addition of SiO₂ decreases solubility, and thus the optimum SiO₂ content (3%) found earlier did not apply to acid resistance. The exception was the K-100 series, in which 3% SiO₂ gave the best values for all the characteristics (Fig. 4). One of us had shown earlier that the properties of ceramic materials, for a constant weight (%) content of binder, also depend on the amount of binder per unit surface (in g/cm²) of the original powder.

Examination of Table 8 shows that a similar relationship holds for acid resistance.

The amount of SiO₂ (in g/m²) in K-100 batch containing 1% SiO₂ by weight can be calculated as follows: if the specific surface of K-100 is 130 cm²/g, then the total surface of 99 g of K-100 is 1,288 m², and the amount of SiO₂ per square meter is 0.777 g/m².

The SiO₂ contents in g/m² can be found similarly for the other batches.

Calculated data on the distribution of SiO₂ in the experimental batches are given in Table 8.

It follows from these data that different amounts of binder are required to give an equal distribution of SiO₂ over all the grains for corundum powders of different grain sizes, conversely, if equal weights of SiO₂ are added to powders differing in grain size, the amount of binder per unit surface must be different.

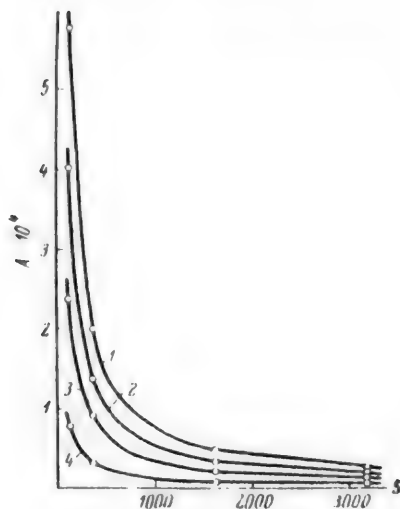


Fig. 5. Distribution of (SiO₂)_n binder A (g/m²) per unit surface S for different grain sizes; SiO₂ contents (%): 1) 7; 2) 5; 3) 3; 4) 1.

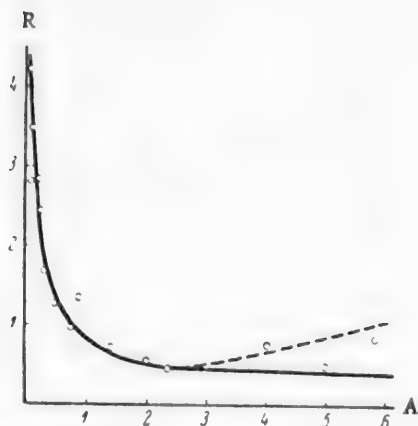


Fig. 6. Solubility $R(\%)$ as a function of the amount of binder $(\text{SiO}_2)_n$ per unit surface A of corundum powder (g/m^2).

structure, may be recommended for the production of highly acid-resistant filters. It must be remembered, however, that the mechanical properties may deteriorate if the amount of organosilicon polymer added to the batch is greatly increased. Moreover, the acid resistance increases only up to a definite limit. Therefore for production of dense (nonfiltering) acid-resistant materials, the amount of additive should range from 1.5 g SiO_2 per m^2 to 5-7 g SiO_2 per m^2 , as such additions give the highest densities and mechanical strengths together with maximum acid resistance. For further improvement of the properties of such materials, finer dispersion of the original powders or increase of the sintering temperature is needed rather than increase of the SiO_2 content in the batch.

SUMMARY

1. Materials made from synthetic corundum have the best physical and mechanical properties if ethyl silicate 40 (3% calculated as SiO_2) is added to the batches.
2. The effects of dispersity of synthetic corundum on the acid resistance, mechanical strength, and other properties of materials made from it have been studied. The acid resistance depends on the distribution of SiO_2 per unit surface of the original corundum powder. For high acid resistance, the amount of organosilicon polymer added should be the equivalent of between 1.5 and 5-7 g SiO_2 per m^2 .
3. High-quality acid-resistant filter materials can be made from synthetic corundum with addition of ethyl silicate 40; filters of different filtering powers can be made by variation of the grain size of the original powders and percentage contents of organosilicon polymer.

LITERATURE CITED

- [1] A. P. Kreshkov, *Organosilicon Polymers in Technology* [in Russian] (Industrial Construction Press, 1956).
- [2] A. P. Kreshkov and I. D. Abramson, *Trans. MKhTI* 13, 142 (1948).
- [3] I. D. Abramson, *Trans. All-Union Sci. Res. Inst. Aviation Materials* 2, 65 (1956).
- [4] K. K. Strelkov, *Technical Control in the Production of Refractories* [in Russian] (Metallurgy Press, 1952).

Received November 12, 1958

KINETICS OF FORMATION OF NICKEL CARBONYL FROM AMMINE SULFATE SOLUTIONS

G. N. Dobrokhotoy

Planning and Scientific Research Institute of the Nickel, Cobalt and
Tin Industry

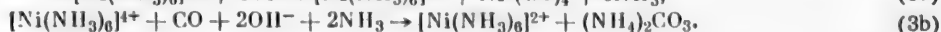
In the Weibel and Reppe process [1-4] nickel carbonyl is made by treatment of hexammine nickel chloride by carbon monoxide under pressure. The details of this process, which is represented by the over-all equation



were studied by Suzuki et al. [5]. They postulated the following reaction mechanism:



According to Hieber and Brück [6], the formation of nickel carbonyl from solution proceeds by way of a soluble and unstable Ni^{4+} complex with subsequent oxidation of CO in a secondary reaction

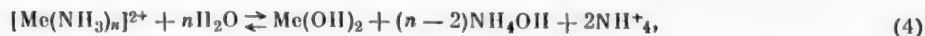


They confirmed this mechanism by the preparation of different stable organic Ni^{4+} derivatives, in the formation of which the carbonyl yield did not exceed 50%.

The present communication contains the results of kinetic studies of the formation of nickel carbonyl from solutions of nickel ammine sulfate complexes.

EXPERIMENTAL*

Experimental Procedure. It is known that solutions of ammine complexes of many metals [7] are liable to undergo hydrolysis:



which may be prevented by addition of ammonia or ammonium salts. Preliminary experiments, in which nickel ammine solutions were kept for prolonged periods at constant temperatures up to 200°, showed that, in the case of moderately concentrated solutions, hydrolysis may be completely prevented by additions of 1.0-1.5 moles of ammonium sulfate per liter. Accordingly, all the reduction experiments described below were performed with solutions containing not more than 0.5 mole of nickel per liter in the form of different ammine sulfates ($n = 2, 4$, and 6) and 1.5 moles of ammonium sulfate per liter.

*With the assistance of N. I. Onuchkina.

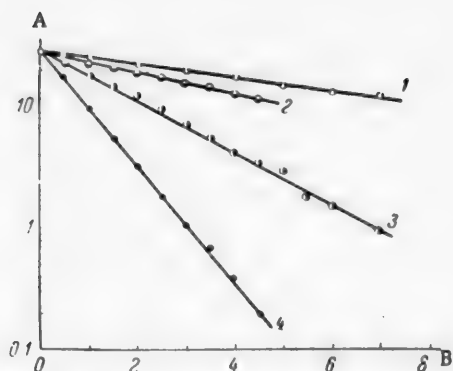


Fig. 1. Effect of temperature on the reduction rate of nickel in tetrammine solutions at 50 atmos carbon monoxide pressure: A) nickel content (g/ liter); B) time (hours); temperature ($^{\circ}\text{C}$): 1) 140; 2) 150; 3) 175; 4) 200; reaction rate constant (hours^{-1}): 1) 0.0543; 2) 0.0884; 3) 0.208; 4) 0.472

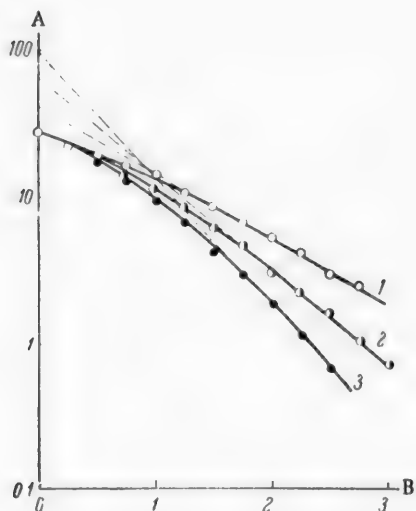


Fig. 2. Reduction rate of nickel in tetrammine solutions at a moderate rate of stirring at 200° : A) nickel content (g/ liter); B) time (hours); carbon monoxide pressure (atmos): 1) 46; 2) 66; 3) 86; reaction rate constant at the end of reduction (hours^{-1}): 1) 0.46; 2) 0.66; 3) 0.86.

The amine solutions were treated with carbon monoxide in autoclaves of the Vishnevskii [8] and Vasil'ev [9] types. The first of these, 3.0 liters in capacity, was fitted with a high-speed shaft stirrer which gave vigorous mixing of the liquid and gas at Reynolds number $\text{Re} = 23000$. A condenser for collection of liquid nickel carbonyl was attached to the autoclave. The second autoclave, 1.5 liters in capacity and without a condenser, had an ordinary propeller stirrer and its more moderate hydrodynamic regime [10] was characterized by the Reynolds number for mixers $\text{Re}_M = n d^2 = 2.1 \text{ rev} \cdot \text{m}^2 / \text{minute}$. The solution temperatures in the autoclave were measured by means of mercury thermometers and regulated to within $\pm 2^{\circ}$. The reduction rate of nickel was determined from analysis of solution samples taken from the autoclaves.

RESULTS AND DISCUSSION

In all cases when treatment of solutions by carbon monoxide was accompanied by vigorous agitation, the rate of reduction of nickel over a wide range of nickel and ammonia concentrations, pressures, and temperatures was represented by a kinetic equation of the first order

$$K \cdot \tau = \lg \frac{C_0}{C_{\tau}}, \quad (5)$$

where K is the reaction rate constant (in hours^{-1}), τ is the reduction time (hours), C_0 is the nickel concentration at the start of the experiment, and C_{τ} is the concentration after time τ .

Typical results of some reduction experiments are given in Fig. 1.

At a moderate stirring rate the experimental data were represented more satisfactorily by an equation for a fractional reaction order, always less than unity.

The results of some experiments of this series are plotted in $\tau - \log C$ coordinates in Fig. 2.

Here the reaction conformed to a first-order equation only at low nickel concentrations in solution, i.e., when the consumption of carbon monoxide in the reduction reaction was low even with moderate stirring. In absence of mechanical stirring the order of reaction was close to zero. All these observations are in good agreement with the theory of heterogeneous catalysis [11], according to which transition from the kinetic to the diffusion region should be accompanied by a decrease of one unit in the reaction order, while intermediate fractional values correspond to a mixed diffusional-kinetic regime.

Experimental data on the influence of temperature with vigorous stirring of the solution are given in Fig. 3.

The experimental rate constants give satisfactory Arrhenius plots. Calculation of the activation energy in experiments at carbon monoxide partial pressures of 50 and 75 atmos gives:

Data on the influence of pressure, determined under analogous conditions, are plotted in Fig. 4.

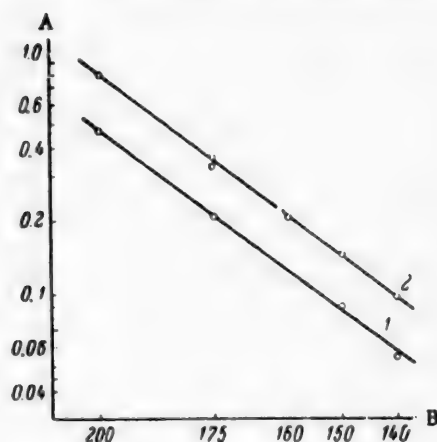


Fig. 3. Effect of temperature on the reduction rate of nickel in tetramine solutions: A) K (in hours^{-1}); B) $1/T$ ($^{\circ}\text{K}^{-1}$); carbon monoxide pressure (atmos): 1) 150; 2) 75.

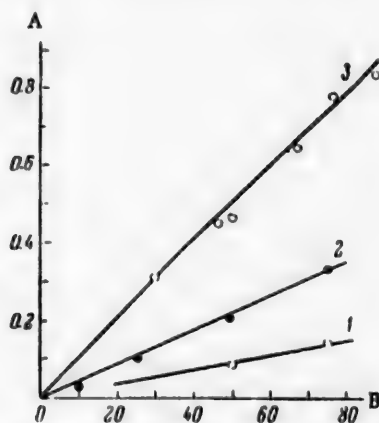


Fig. 4. Effect of carbon monoxide pressure on the reduction rate of nickel in tetramine solutions: A) reaction rate constant (hours^{-1}); B) partial pressure of carbon monoxide (atmos); temperature ($^{\circ}\text{C}$): 1) 150; 2) 175; 3) 200.

Rate Constants for Reduction of Nickel by Carbon Monoxide from Tetramine Solutions Containing 1.5 moles Ammonium Sulfate per Liter.

Temperature ($^{\circ}\text{C}$)	Carbon monoxide pressure (atmos)	Rate constant K_4 (hours^{-1})	Absolute rate constant $K_4^* \cdot 10^{-4}$ ($\text{hours}^{-1} \cdot \text{atmos}^{-1}$)
140	50	0.0543	1.93
140	75	0.0970	2.30
150	50	0.0884	1.94
150	75	0.143	2.28
160	75	0.205	2.74
175	10	0.028	1.35
175	25	0.102	1.92
175	50	0.208	2.01
175	75	0.398	2.56
175	75	0.335	2.15
200	30	0.315	2.24
200	30	0.572	2.02
200	75	0.800	2.28
Mean			2.13

In contrast to the results obtained in autoclave treatment with gaseous oxygen or hydrogen, described previously [12, 13], when the rate of the process is proportional to $\sqrt{P_{\text{O}_2}}$ or $\sqrt{P_{\text{H}_2}}$, a simple linear relationship holds for reduction by carbon monoxide. Carbon monoxide has the properties of a monomolecular gas. The linear relationship between the reaction rate and the pressure shows that at the determining stage carbon monoxide reacts with nickel in simple (1:1) stoichiometric proportions.

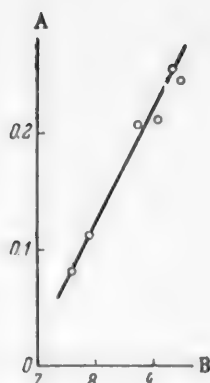


Fig. 5. Effect of pH on the reduction rate of nickel at 175° and 50 atmos CO pressure: A) reaction rate constant (hours⁻¹); B) pH.

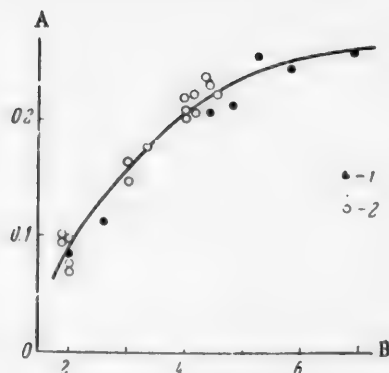


Fig. 6. Variation of the reduction rate of nickel with the NH₃ concentration at 175°, carbon monoxide pressure 50 atmos: A) reaction rate constant (hours⁻¹); B) number of moles of NH₃ per mole of NiSO₄; 1) direct determination; 2) calculated values.

Figure 5 shows data on the reduction rate as a function of pH. The results show that changes of the reduction rate constant are proportional to twice the corresponding changes of pH. It follows that the intermediate active complex must contain two OH⁻ groups for each nickel atom.

Applying the theory of rate processes [14] to these experimental data, we have

$$-\frac{dC_{Ni^{2+}}}{d\tau} = K^* \cdot C_{Ni^{2+}} \cdot C_{OH^-}^2 \cdot C_{CO} \cdot e^{-\frac{E}{RT}} \quad (7)$$

and for tetrammine solutions of the chosen composition

$$-\frac{dC_{Ni^{2+}}}{d\tau} = K_4^* \cdot C_{Ni^{2+}} \cdot C_{CO} \cdot e^{-\frac{E}{RT}}, \quad (8)$$

where $e = 2.7183$, $E = 13700$ cal/mole, and $R = 1.987$ cal/degree · mole.

Substitution of these values into Equation (8) and integration gives

$$\tau = 10^{2094/T} \cdot \frac{1}{P_{CO} \cdot K_4^*} \cdot \lg \frac{C_0}{C_\tau}, \quad (9)$$

where τ is the reduction time (hours), T is the temperature (deg K), P_{CO} is the CO partial pressure (atmos), K_4^* is the absolute rate of reduction in tetrammine solutions (hours⁻¹ · atmos⁻¹), and C_0 and C_τ are the initial and final concentrations of nickel.

Combining Equations (5) and (9) we have

$$K_4^* = \frac{K \cdot 10^{2094/T}}{P_{CO}}. \quad (10)$$

A summary of the experimental values of K_4 and calculated values of K_4^* is given in the table.

Substitution of the mean value of the absolute reaction rate $K_4^* = 2.13 \cdot 10^4$ Into Equation (9) gives

$$\tau = \frac{10^{\frac{2094}{T} - 4.328}}{P_{CO}} \cdot \lg \frac{C_0}{C_\tau}. \quad (11)$$



Fig. 7. Comparison of the reduction rates of nickel on addition of nickel powder at 200°, carbon monoxide pressure 26 atmos: A) nickel content (g/liter); B) time (hours); diammine solutions with additions of nickel powder (g/liter): 1) no addition; 2) 10; 3) 33.

ammonia concentrations in ammine form. It follows that the activation energy and the ammonia content in the intermediate active complex remain virtually constant. The nature of the curve in Fig. 6 suggests that the increase in the reduction rate of nickel, with increasing ammonia content in solution, is mainly attributable to increase of OH^- concentration, due to the general buffer properties of ammoniacal solutions.

The agreement between the experimental values of K found in experiments with condensation of nickel carbonyl vapor and the experimental values, determined in equipment in which the gas phase was not collected, shows that removal of the formed nickel carbonyl from the reaction zone is not a determining factor. The presence of $\text{Ni}(\text{CO})_4$ influences the process kinetics only in so far as the presence of the carbonyl in the gas phase lowers the partial pressure of carbon monoxide in the system as a whole.

Data on the effect of added nickel powder are presented in Fig. 7. The additive was prepared by treatment of pure nickel powder (99.99% Ni) with hydrogen at 300° for 8 hours. The particle size was 100–71 μ .

It is known that in the reduction of metals involving metallic surfaces, the magnitude of the latter has a decisive effect. This was not the case in the formation of nickel carbonyl. Thus, none of the stages in the mechanism postulated by Suzuki (Equations 2a–2c) in reality determines the rate of this process.

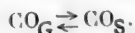
SUMMARY

1. Reduction of nickel from ammine sulfate solutions by carbon monoxide is a complex heterogeneous process in which the determining stage may be either the chemical reaction itself or the diffusion of carbon monoxide into the solution. With intensive mixing of the liquid and gas ($\text{Re} > 20000$) the system becomes kinetically homogeneous, and the reduction rate can be formally represented by a first-order equation. With moderate stirring the process is of a mixed diffusional-kinetic or diffusional character. The latter corresponds to a zero-order equation.

2. The reduction rate increases with increase of OH^- concentration in solution, the change of rate being proportional to double the change of pH. It follows that the intermediate active complex must contain two OH^- groups per nickel atom. Since the relationship between the rate and the partial pressure of CO is linear, it follows that a nickel atom reacts with only one carbon monoxide molecule. Removal of the nickel carbonyl formed from the reaction zone is not a determining factor.

3. The over-all reaction mechanism consistent with all the above facts can be represented by the following consecutive stages.

Stage I – solution of gaseous carbon monoxide in the aqueous medium (rapid):



Equation (11) unifies the experimental data. It gives the time required for reduction of nickel in tetrammine solutions under conditions of vigorous mixing of the liquid and gaseous phases.

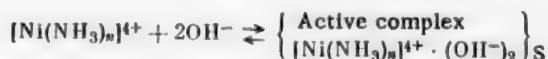
Various calculated and experimental values of K_N in a number of other experiments, performed with varying ammonia contents and at other temperatures, pressures, and stirring rates, are compared graphically in Fig. 6.

Direct experimental determinations of K_N were performed at 175°, at carbon monoxide partial pressure of 50 atmos in an autoclave with vigorous stirring, and with continuous condensation of the nickel carbonyl formed. The experimental values of K_N are represented in Fig. 6 by black circles. Calculated values of K_N were obtained with the aid of Equation (10) from experimental values of K_N under various reduction conditions. These are represented in Fig. 6 by white circles. It is seen that the calculated and experimental values of K_N coincide over a wide range of

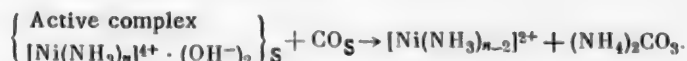
Stage II — formation of nickel carbonyl (rapid):



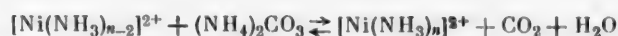
Stage III — formation of an intermediate active complex (rapid):



Stage IV — oxidation of carbon monoxide (slow):



Stage V — decomposition of ammonium carbonate (rapid):



LITERATURE CITED

- [1] W. Reppe, *Experientia* VI, (2), 68 (1950).
- [2] W. Reppe, *Lieb. Ann.* 582, 116 (1952).
- [3] W. Reppe, *Acetylene Chemistry*, N.Y. (1949).
- [4] *Acetylene Chemistry* (IL, Moscow, 1954) [Russian translation].
- [5] Shigenari Suzuki, Hiroo Ito, Hidemaro Tatemichi, and Sizuo Kimata, *J. Chem. Soc. Japan, Ind. Chem. Sect.*, 54, (7), 454 (1951); 54, (8), 511 (1951).
- [6] W. Hieber and R. Brück, *Z. Allg. anorg. Ch.* 289 (1-2), 28 (1952).
- [7] A. A. Grinberg, *Introduction to the Chemistry of Complex Compounds* [in Russian] (Moscow, 1951).
- [8] N. E. Vishnevskii, N. P. Glukhanov, and I. S. Kovalev, *High-Pressure Equipment with Shielded Electric Motors* [in Russian] (Mashgiz, 1956).
- [9] G. I. Blinov, G. N. Dobrokhoto, and P. V. Pevzner, *Coll. Tech. Inf. State Nickel Planning and Research Institute*, 12 (1955).
- [10] A. P. Planovskii, V. R. Ramm, and S. Z. Kagan, *Processes and Equipment of Chemical Technology* [in Russian] (Moscow, 1955).
- [11] A. I. Grodskii, *Physical Chemistry 2* [in Russian] (1948).
- [12] F. A. Forward and J. Halpern, *J. Appl. Chem.* 30, No. 1, 3 (1957).
- [13] S. I. Sobol' and V. I. Spiridonova, *Trans. Sci. Res. Inst. Nonferrous Metals*, No. 13, (1957).
- [14] S. Glasstone, K. Laidler, and H. Eyring, *Theory of Rate Processes* (Moscow, 1948) [Russian translation].

Received October 10, 1957

METHODS FOR PRODUCTION OF ALUMINUM HYDROXIDE AND THE DEFORMATION AND STRENGTH CHARACTERISTICS OF ITS PASTES IN PETROLATUM

A. A. Trapeznikov and A. M. Tolmachev

Institute of Physical Chemistry, Academy of Sciences, USSR

Aluminum hydroxide has a number of industrial uses; in particular it is one of the pigments used in printing inks.

The purpose of the present investigation was to determine the influence of precipitation conditions on the structural strength and transparency of aluminum hydroxide pastes in pure medicinal petrolatum, free from the polar impurities, which greatly influence particle interaction in pastes. Since in the industrial production of aluminum hydroxide solutions of potash alum and sodium carbonate are used, all the experiments were performed with 0.5 N solutions of these reagents.

Two methods were used for precipitation of the hydroxide. Method I consisted of gradual addition of soda solution to 2.0 liters of alum solution at a constant rate (20 ml/minute) to a definite pH value. The pH was determined continuously by the potentiometric method with a glass electrode. Aluminum hydroxide made by this method is not uniform in chemical composition, dispersity, and adsorption properties, as the solution pH and concentration change continuously during the precipitation. For preparation of the hydroxide under uniform conditions, our method for precipitation of the hydroxide at a constant pH throughout the process [1] was used; in this method the precipitation pH is kept constant by simultaneous addition of solutions of the reagents at constant rates into the reaction vessel; this was effected by the use of special "constant level" devices (Method II). The ratio of the rates varied in different experiments, but the total rate was 40-45 ml/minute. The precipitation lasted 90-100 minutes, and the pH was measured continuously throughout the process. The precipitation temperature was 18-21° in both methods.

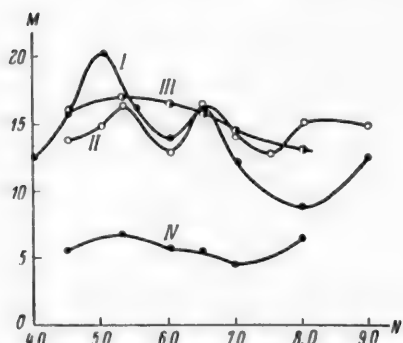


Fig. 1. Variations of the moisture content of aluminum hydroxide powders as a function of precipitation pH: M) moisture content (%), N) pH; precipitation series and temperature (°C): I) A and 105; II) B and 105; III) C and 105; IV) C and 61.

EXPERIMENTAL

Three series of aluminum hydroxide precipitates were prepared in the pH range of 4.0 to 9.0. In series A the hydroxide was prepared by Method II. The precipitate was filtered off at once on a Büchner funnel and washed on the funnel with distilled water. Series B differed from series A in that the precipitate was washed by decantation and filtered after that. In series C the hydroxide was prepared by Method I. The precipitates were washed by decantation as in series B. In all the series the precipitates after filtration were dried at 61° to constant weight, ground in a mortar, and conditioned to the air-dry state before use.

TABLE 1

Contents of SO_4 Groups in Samples of Series B and C (% by weight of precipitates dried at 105°)

	SO_4 group contents (wt %) at pH						
	4.5	5.3	6.0	6.5	7.0	7.5	8.0
Series B	29.42	22.17	12.70	6.01	—	0.85	0.64
Series C	30.11	22.02	21.88	18.92	16.12	—	10.91

The effects of precipitation pH on the moisture contents of the powders and the particle size of the precipitates are shown in Fig. 1 and Fig. 2, respectively. Particle size was determined by means of the Figurovskii sedimentation balance [1] directly after precipitates in series B had been washed by decantation. Such particles are aggregates, formed as the result of partial coagulation. The particle sizes found agree with literature data [3].

The results of determinations of SO_4 groups in the hydroxide precipitates are given in Table 1.

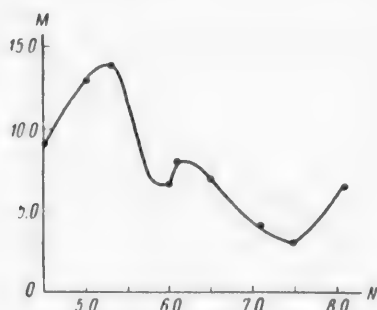


Fig. 2. Variation of particle size after coagulation by washing, as a function of precipitation pH: M) particle radius (μ); N) pH.

Pastes of aluminum hydroxide in petrolatum were prepared by rubbing on a glass plate by means of a special pestle (muller). The petrolatum-hydroxide ratio was varied from 2:1 to 3:1, according to the oil capacity of the precipitate, to give pastes of convenient consistency. The reproductibility of the properties of pastes made by different mixings was within $\pm 5\%$. Paste strength was determined by means of a tangentially moved riffled plate in a plane gap with riffled walls in a special cell, and by means of the instrument described earlier. The results are presented in graphical form in Fig. 3. The deformation of these pastes is almost independent of time, the pastes do not exhibit after-effects either during loading or during unloading, and do not undergo continuous plastic flow before the yield value is reached (Fig. 4); i.e., they behave as elasticobrittle bodies under these conditions. They are characterized by low breaking shear deformations $\epsilon_T = 5 - 35\%$, according to the concentration of the solid phase in the paste, and especially low elastic deformations

$\epsilon_{em} \approx 2.0\%$ (at $C = 33.3\%$) found by subtraction of residual from total deformations, $\epsilon_{em} = \epsilon_T - \epsilon_{res}$.

Curves showing variations of paste strength with concentration ($P_T - C$ curves) are given in Fig. 5.

Figure 6 shows variations of P_T with pH of hydroxide precipitation for series A, B, and C, with $C = 28.7\%$. The data for series A were obtained by the method of stepwise loading, and for series B and C by loading at constant rate ($25-27 \text{ g/cm}^2 \cdot \text{second}$). The former values are therefore somewhat higher than the latter. Special control experiments in which P_T was determined by the same method for samples of Series A and B gave roughly the same values of P_T in the region of precipitation pH where the course of the $P_T - \text{pH}$ curves is the same (at $\text{pH} < 6.5$). Since the only difference between series A and B was the method used for washing the precipitates, the influence of the following on the thickening properties was studied separately: a) the method used for washing the precipitate (Table 2), b) the settling time of the precipitate before separation, when washed by decantation (Table 3), and c) treatment of precipitates obtained at $\text{pH} \approx 5.75$ (series A) by solutions of different pH (Table 4). In cases "a" and "b" P_T was measured at constant rate of load, and in case "c" it was measured by stepwise loading.

The curves in Fig. 7 show variations of paste transparency ($D = \frac{I}{I_0}$) with the pH of hydroxide precipitation.

The transparency of the pastes, which were applied in layers 1 mm thick onto special glass plates, was measured relatively to a standard mat plate by means of the Pulfrich photometer.

DISCUSSION OF RESULTS

The conditions and methods used in preparation of aluminum hydroxide have a strong influence on the properties of its pastes in petrolatum. Both the precipitation pH and the subsequent treatment of the precipitate are

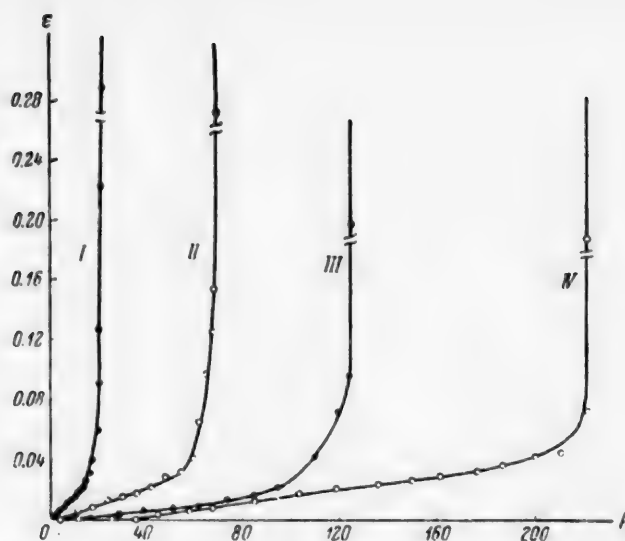


Fig. 3. Curves showing variations of the relative shear deformation ϵ with the shearing stress P for pastes of different concentrations made from aluminum hydroxide precipitated at pH = 5.0 in series A; paste concentrations (%): I) 23.6; II) 26.6; III) 28.7; IV) 33.3.

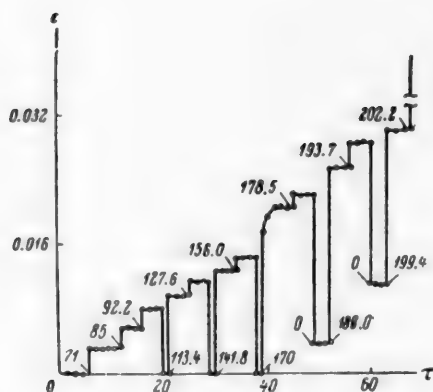


Fig. 4. Stepwise loading-unloading curve for a paste ($C = 33.3\%$) made from aluminum hydroxide precipitated at pH = 5.0 in series A.

in the formation of dense precipitates in which fine particles fill the interstices between coarse ones. As a result, when the precipitate is dried, it undergoes sintering, which is so extensive in precipitates formed in the acid region that a continuous monolithic structure is formed, which is very difficult to grind. A similar effect is found in the alkaline region. Apparently it is the presence of a stabilized fine fraction which determines the very strong influence of washing of the precipitate, when this fine fraction is washed out together with the electrolytes (Table 2). When the precipitate is washed on the filter, this fraction is washed out to a considerably smaller extent, and the paste strengths are therefore also much lower. The influence of the fine fraction is also confirmed by the fact that P_r depends strongly on the sedimentation time of the precipitate when it is washed by decantation (Table 3).

Particle coagulation, which leads to the formation of loose bulky precipitates, which consist of fine and relatively isolated particles and which can subsequently be easily crumbled, favors good thickening in the

important factors, which may lead to changes in the composition, degree of dispersion, and surface character of the particles, which determine their interaction in the oil medium and the mechanical properties of the pastes.

The curves in Fig. 6 show that with the two precipitation methods, the best thickening properties are found for aluminum hydroxide precipitated in the pH range between 5.0 and 8.0. In the former case (series C), there is a fairly sharp maximum at pH = 6.5, i.e., at the isoelectric point. For the method of precipitation at constant pH (series A and B), the curve has three maxima, at pH values of 5.3, 6.5, and 8.0. In this case the course of the curve greatly depends on the method used for washing the precipitate; with inadequate washing (in the filter) the curve (Fig. 5, curve 1) descends sharply at pH > 6.5, and therefore the maximum at pH = 8.0 is absent altogether. The weak thickening properties in the acid and alkaline regions (pH < 5.0 and > 8.0) are evidently associated with pronounced peptization and stabilization of the particles in the aqueous medium. This results

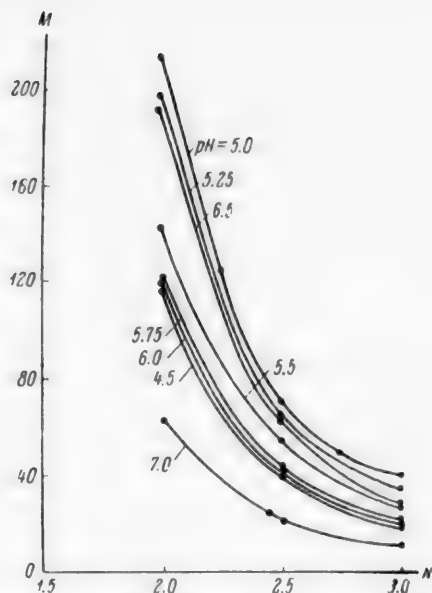


Fig. 5. Variation of strength of aluminum hydroxide pastes with concentration, series A: M) strength P_r (g/cm^2); N) wt. ratio of oil to hydroxide.

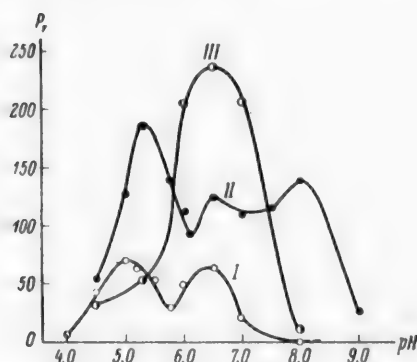


Fig. 6. Variation of paste strength with pH of hydroxide precipitation ($C = 28.7$): I) series A; II) series B; III) series C.

hydrocarbon medium. Therefore the surface properties of the particles which determine coagulation, also determine their thickening properties to a considerable degree. Moreover, the surface properties of the particles may also influence their interaction in the oil medium, either weakening or intensifying it. Thus, an excess of adsorbed ions may lead to particle repulsion. The role of surface properties of particles has been noted in relation to silica gel [4]. In additional treatment of aluminum hydroxide precipitates by solutions at pH values differing from the precipitation pH, it is seen (Table 4) that P_r can only decrease, whereas curve I in Fig. 6 suggests that P_r should increase in the transition from pH = 5.75 to pH = 5.0. This shows that the thickening properties of the hydroxide are determined not only by the surface properties of the particles, which should be the same with equal final pH values, but also by the original structure and composition of the particles.

The particle size, and the packing density of the particles in formation of the precipitate in an aqueous medium, which determine the active surface of the particles, also influence their moisture content. Possibly this accounts for the similar course of the curves for moisture contents of the powders (Fig. 2) and paste strength as functions of the hydroxide precipitation pH. The complex course of the P_r - pH curve for the hydroxide precipitated by Method II, is probably associated to a greater extent with the composition of the precipitate and changes in its structure than the course of the curve for the hydroxide precipitated by the "direct" method. Powder x-ray patterns of samples from series A and B show that at precipitation pH of 4.5 and 5.3, there are virtually no interference lines, whereas patterns of samples precipitated at pH 6.5 and 8.0 show quite distinct lines. These results are in agreement with Weiser's data [5]; Weiser also found that hydroxide precipitated by the "direct" method from AlCl_3 and $\text{Al}(\text{NO}_3)_3$ solutions have much more pronounced crystallinity than those precipitated from $\text{Al}_2(\text{SO}_4)_3$ solutions. It follows that crystallization of the precipitate is hindered by the presence of large amounts of sparingly soluble basic sulfates (Table 1, also [1]). The more distinct crystallinity of precipitates at higher values of precipitation pH are probably the consequence of decomposition of basic salts and formation of the hydroxide which can, moreover, undergo further hydrational and structural changes [5].

TABLE 2

Effect of Washing Method on Paste Strength

Precipitation method	Washing method	Paste strength (g/cm^2)		
		not washed	two washings	to negative reaction for SO_4
At constant pH = 8.0	by decantation	29.0	—	152.0
At constant pH = 8.0	on the funnel	29.0	—	87.8
At constant pH = 5.75	by decantation	96.0	127	140.0
At constant pH = 5.75	on the funnel	96.0	—	139.3

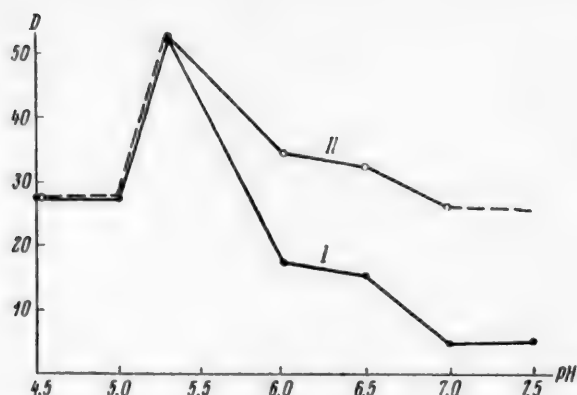


Fig. 7. Effect of pH of hydroxide precipitation ($C = 28.7\%$) on the relative paste transparency D : 1) series B; 2) series C.

The very fine particles precipitated at pH 5.3 coagulate during the washing process; this follows from the maximum particle radius found for this precipitate after it had been washed with water (Figs. 3 and 4). These two factors — the small particle size and the formation of loose coagulated precipitate from such particles — account for the greatest height of the maximum found for pH 5.3 (in the constant-pH method). The decrease of P_T with increase of pH may be attributed to decomposition of the basic salt and increasing crystallinity of the particles accompanied by a decrease of their dispersity. Near to pH = 6.5 coagulation begins to accelerate and the particle aggregates become larger again; this, in turn, favors the formation of a loose structure. A similar process occurs at pH = 8.0; the third maximum on the P_T — pH curve is due to this. However, the causes of three maxima

TABLE 3
Effect of Settling Time on Paste Strength

Settling time (minutes)	10	30	90
Strength P_T (g/cm ²)	85	104.4	57

of particle coagulation are not yet clear. Since these coagulation maxima are found only for washed precipitates and, as special experiments showed, do not occur with mother liquors, it seems likely that they depend on a complex and prolonged process of desorption of ions from the particles during the washing, and may also be caused by decomposition of basic salts in the particle surface layers. The difference between the course of the P_T — pH curves for the "direct" method and for the constant pH method may be attributed to differences in the precipitate composition.

It is clear from Table 1 that precipitates prepared by the "direct" method have much higher contents of basic salt than precipitates made at constant pH. Accordingly, the former are much more difficult to wash than the latter, and even washing of such precipitates by decantation is insufficient to cause coagulation and prevent their sintering when dried. This may be the explanation for the low values of P_T found for pastes made from precipitates prepared by the "direct" method at pH < 6.0 and pH > 7.0. Rapid coagulation occurs only in the pH region close to the isoelectric point (pH < 7.0 and > 6.0), and this leads to maximum values of P_T . In this case coagulation already occurs in the mother liquor (pH = 6.5) and is intensified during the washing.

An interesting fact is that paste transparency (Fig. 6) shows approximately parallel variations with the SO_4 group content of the precipitate and the paste strength (especially in the constant-pH method). At pH > 5.3 paste transparency is higher for precipitates made by the "direct" method; this corresponds to a higher SO_4 group content. However, there is no doubt that the SO_4 group content is not the sole significant factor, as the precipitate formed at pH 4.5 yields a less transparent paste than the precipitate formed at pH 5.3, despite the fact that the former has the higher SO_4 group content. It seems that the principal factors in paste transparency are the dispersity of the particles and their weak crystallinity, confirmed by the x-ray patterns.

TABLE 4

Effect of Solution pH on Paste Strength

Treatment pH	Strength (g/cm ²) after treatment time (hours)					
	0	0.5	1.5	3.0	4.0	22.0
4.60*	—	102	88	—	79	—
5.10*	—	136	—	94	—	81
5.75	200	—	—	—	—	—
7.0*	—	153	152	—	148	148
8.50*	—	121	120	—	119	—
8.50*	—	113	—	107	—	80

* These pH values were obtained by additions of appropriate amounts of soda or sulfuric acid to the mother liquor at the end of the precipitation.

SUMMARY

1. A new method is described for precipitation of aluminum hydroxide at constant pH throughout the process; this method gives aluminum hydroxide precipitates of uniform composition and properties.
2. The effects of the precipitation pH of aluminum hydroxide on the structural strength and transparency of its pastes in petroleum have been studied. It is shown that the thickening properties of aluminum hydroxide precipitates pass through a series of maxima with variation of the precipitation pH; these maxima are associated with particle coagulation and cohesion in the aqueous medium and during drying. For the same reasons the method used for washing the aluminum hydroxide precipitates has a strong influence on the thickening properties. It was found that pastes made from precipitates prepared in the acid region (pH = 5.3) have the highest transparency.
3. Aluminum hydroxide pastes in petrolatum do not exhibit after-effects or flow up to the yield value, and behave like elasticobrittle bodies in this region.

LITERATURE CITED

- [1] A. A. Trapeznikov and A. M. Tolmachev, J. Phys. Chem. 22, No. 3, 725 (1958).
- [2] N. A. Figurovskii, Sedimentation Analysis [in Russian] (1948).
- [3] S. A. Levina and N. F. Ermolenko, Colloid J. 17, 287 (1955).*
- [4] A. F. Siriani and I. E. Puddington, Canad. J. Chem. 33, 2, 391 (1955).
- [5] H. B. Weiser and W. O. Milligan, Advances in Colloid Sci. 1, 227 (1942).

Received January 27, 1958

EFFECTS OF HYDRODYNAMIC FACTORS ON THE CARBONATION OF AMMONIACAL BRINES IN GAS LIFT EQUIPMENT*

G. N. Gasyuk, A. G. Bol'shakov, A. V. Kortnev, and
P. Ya. Krainii

The previous communication [1] contained results of a study of the dependence of the carbonation process on the concentration of carbon dioxide in the incoming gas and on the temperature. It was found that the over-all mass-transfer coefficient is independent of the carbon dioxide concentration in the incoming gas, while the conversion rate is directly proportional to the carbon dioxide concentration.

The relationship between the over-all absorption coefficient and the temperature is represented by an exponential equation of the form

$$K_G a = I' e^{0.0288 t},$$

where t is the temperature.

The relationship between the conversion rate and temperature is represented by the power expression

$$U = I e^{0.40}.$$

The present communication contains the results of a study of the influence of the liquid and gas rates on the carbonation process. The experiments were performed in an experimental gas-lift unit described previously [2]. The liquid and gas rates and immersion depth in gas lifts (without account being taken of the physical properties of the liquid and gas) are interconnected, i.e.,

$$L = f(V, h), V = \varphi(L, h), h = \xi(L, V),$$

where L is the liquid rate, V is the gas rate, and h is the immersion depth.

Therefore, investigations of the effects of any one of these factors on mass transfer in gas lifts must be conducted in such a manner as to allow appropriate substitution of the variables. Otherwise the influence of these factors on mass transfer cannot be conclusively established.

Effect of the Liquid Rate On the Carbonation Process

The liquid rate in a gas lift can be varied in two ways: 1) by variation of the immersion depth at constant gas rate, 2) by variation of the gas rate at constant immersion depth.

In this investigation we consider the influence of liquid rate on the over-all absorption coefficient and conversion rate for these two cases.

* Communication 2.

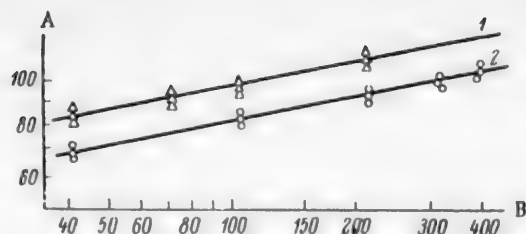


Fig. 1. Effect of volumetric liquid rate at constant gas rate on the over-all coefficient of absorption of carbon dioxide in ammoniacal chloride brine:

A) over-all absorption coefficient $\left(\frac{\text{kg} \cdot 10^{-2}}{\text{m}^3 \cdot \text{atmos} \cdot \text{hour}}\right)$

B) volumetric liquid rate $\left(\frac{\text{m}^3}{\text{m}^2 \cdot \text{hour}}\right)$; brines: 1) No.

2; 2) No. 6.

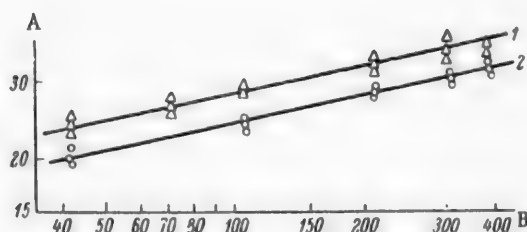


Fig. 2. Effect of volumetric liquid rate at constant gas rate on the conversion rate of carbon dioxide in ammoniacal chloride brine: A) conversion rate

$\left(\frac{\text{kg} \cdot 10^{-2}}{\text{m}^3 \cdot \text{hour}}\right)$; B) volumetric liquid rate $\left(\frac{\text{m}^3}{\text{m}^2 \cdot \text{hour}}\right)$;

brines: 1) No. 2; 2) No. 6.

Two series of experiments were performed at variable liquid rate with variations of immersion depth at constant gas rate. The experimental temperature was 30°, and in investigations of the absorption of carbon dioxide in No. 2 brine (the brine compositions are given in the preceding paper [1]) the gas rate was maintained constant at about 5650 m³/m²·hour, and the carbon dioxide concentration in the incoming gas was 36-37%; for brine No. 6 the corresponding values were 5800 m³/m²·hour and 37-38%, respectively. The liquid rate was varied over approximately a 9.5-fold range (from 42 to 397 m³/m²·hour), and the immersion depth was accordingly varied from 7 to 30%.

In Fig. 1 the values found for the over-all absorption coefficients are plotted against the liquid rate in logarithmic coordinates.

The experimental points fit on straight lines, which can be represented by the following power equation:

$$K_G a = F L^{0.18} \quad (1)$$

The effect of liquid rate on conversion rate is plotted in Fig. 2. The straight lines drawn through the points can be represented by the equation:

$$U = F L^{0.186} \quad (2)$$

The small difference between the power in Equations (1) and (2) is caused by the fact that the total pressure of the carbonation gas at entry increases with increase of the liquid rate and therefore the partial pressure of carbon dioxide, at constant concentration in the incoming gas, increases; as was shown earlier [1], the over-all absorption coefficient is independent of the carbon dioxide concentration and hence of the partial pressure. The conversion rate, however, is proportional to the partial pressure, i.e., the relationship found for the conversion rate in a sense takes into account the increase of the total pressure of the carbonation gas with increase of liquid rate, and is valid

for absorption of carbon dioxide from a gas with constant concentration of the absorbed component.

It follows from Equations (1) and (2) that increase of the liquid rate results in small increases of the over-all absorption coefficient and conversion rate (with a 9.5-fold increase of the liquid rate the absorption coefficient is increased only 1.5-fold). The explanation is that the immersion depth increases with increase of liquid rate at constant gas rate. The diffusional resistance of the liquid phase increases with depth of immersion [2], and it has been shown [1] that in the carbonation process the main resistance to absorption is concentrated in the liquid phase. Therefore the negative influence of changes in the immersion depth is superposed on the positive influence of changes in the liquid rate.

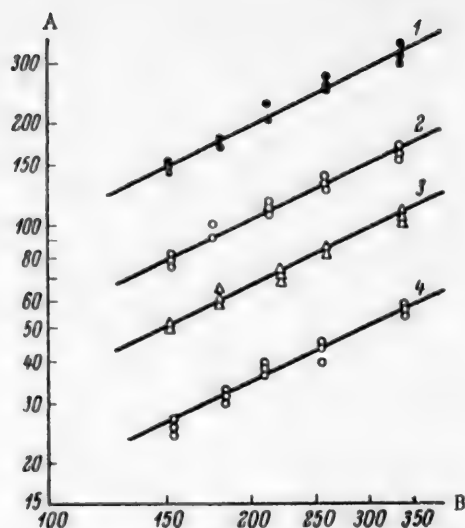


Fig. 3. Effect of volumetric liquid rate at constant immersion depth on the over-all coefficient of absorption of carbon dioxide by ammoniacal chloride brines of different ammonia contents: A) over-all absorption coefficient ($\frac{\text{kg} \cdot 10^{-2}}{\text{m}^3 \cdot \text{atmos} \cdot \text{hour}}$); B) volumetric liquid rate ($\frac{\text{m}^3}{\text{m}^2 \cdot \text{hour}}$); brines: 1) No. 1; 2) No. 2; 3) No. 3; 4) No. 4.

In studies with variations of the liquid rate at constant immersion depth, 8 series of experiments were performed in order to eliminate possible experimental errors and to elucidate the influence of the initial ammonia concentration in the brine and of the degree of carbonation on the over-all absorption coefficient and conversion rate. Four of the series were with brines of different initial ammonia contents (brines Nos. 1-4), and four were brines of different degrees of carbonation (Nos. 5-8).

All the experiments were performed at 30°, 20% immersion depth, with 37-38% carbon dioxide in the incoming gas. The gas and liquid rates were varied over wide ranges.

The variations of the over-all absorption coefficient with the liquid rate are plotted in logarithmic coordinates in Figs. 3 and 4. Figure 3 shows variations of the over-all absorption coefficient with the liquid rate for brines of different ammonia contents (brines Nos. 1-4), and Fig. 4, for brines of different degrees of carbonation (brines Nos. 5-7).

It is clear from Figs. 3 and 4 that the points, representing the over-all absorption coefficients for all the brines studied, fit on straight lines, which can be described by the following power equation:

$$K_G a = EL^{0.93}. \quad (3)$$

The value found for the exponent (0.93) in the relationship between the over-all coefficient of absorption of CO_2 .

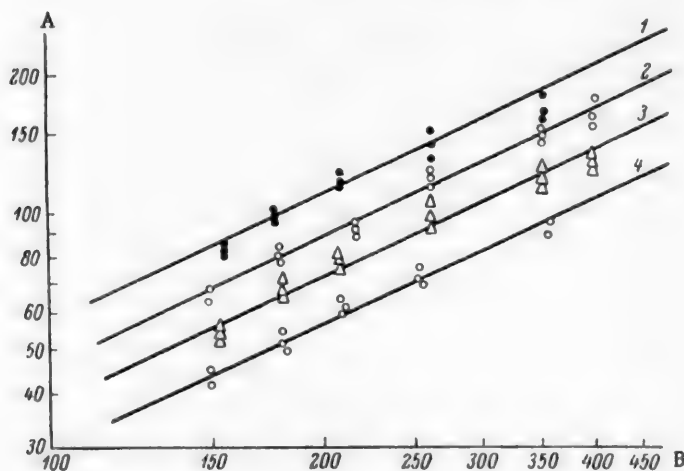


Fig. 4. Effect of volumetric liquid rate at constant immersion depth on the coefficient of absorption of carbon dioxide by ammoniacal chloride brines of different degrees of carbonation:

A) over-all absorption coefficient ($\frac{\text{kg} \cdot 10^{-1}}{\text{m}^3 \cdot \text{atmos} \cdot \text{hour}}$); B) volumetric liquid rate ($\frac{\text{m}^3}{\text{m}^2 \cdot \text{hour}}$); brines: 1) No. 5; 2) No. 6; 3) No. 7; 4) No. 8.

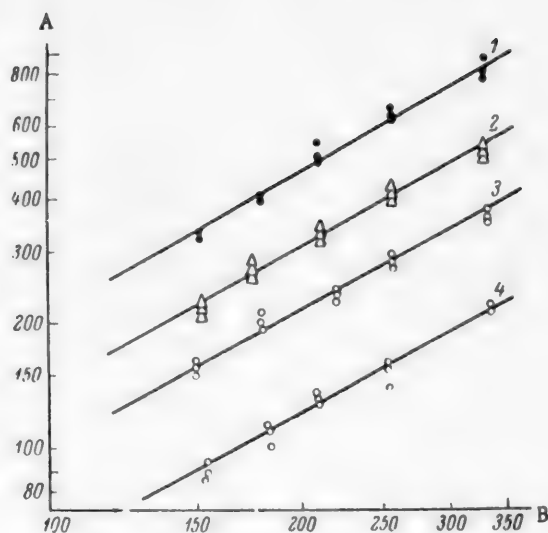


Fig. 5. Effect of volumetric liquid rate at constant immersion depth on the conversion rate of carbon dioxide in brines of different ammonia contents:

A) conversion rate $\left(\frac{\text{kg} \cdot 10^{-3}}{\text{m}^3 \cdot \text{hour}}\right)$; B) volumetric liquid rate $\left(\frac{\text{m}^3}{\text{m}^3 \cdot \text{hour}}\right)$; brines: 1) No. 1; 2) No. 2; 3) No. 3; 4) No. 4.

at variable liquid rate and constant immersion depth, 2) variation of gas rate at constant liquid rate and variable immersion depth.

by ammoniacal chloride brines and the liquid rate at constant immersion depth is very close to the value found for the exponent (0.91) in the relationship between the liquid-phase mass-transfer coefficient and the liquid rate [2]. Since the same apparatus and the same hydrodynamic conditions were used in determinations of the over-all coefficients of absorption of carbon dioxide by ammoniacal chloride brines and in determinations of the liquid-phase transfer coefficients, the fact that the exponents are almost equal is convincing proof that the liquid phase has the main influence in carbonation of ammoniacal brines.

The effects of liquid rate on the conversion rate are plotted in Figs. 5 and 6. The straight lines drawn through the points for the conversion rate can be represented by the equation

$$U = E' L^{1.07}. \quad (4)$$

Effect of Gas Rate on the Carbonation Process.

As in studies of the effect of the liquid rate, in studies of the effects of the gas rate on the over-all absorption coefficient and conversion rate, two cases must be considered: 1) variation of gas rate

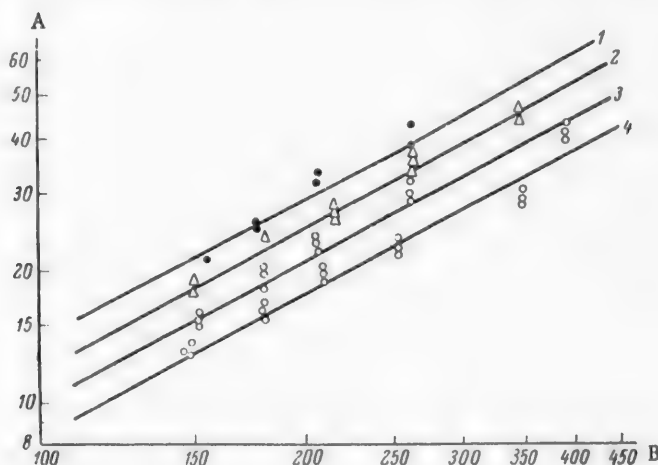


Fig. 6. Effect of volumetric liquid rate at constant immersion depth on the conversion rate of carbon dioxide in brines of different degrees of carbonation: A) conversion rate $\left(\frac{\text{kg} \cdot 10^{-3}}{\text{m}^3 \cdot \text{hour}}\right)$;

B) volumetric liquid rate $\left(\frac{\text{m}^3}{\text{m}^3 \cdot \text{hour}}\right)$; brines: 1) No. 5; 2) No. 6; 3) No. 7; 4) No. 8.

The relationship between the over-all absorption coefficient and the gas rate at variable liquid rate and constant immersion depth for brines with different initial ammonia contents (brines Nos. 1-4) is plotted in Fig. 7, and for brines of different degrees of carbonation, in Fig. 8.

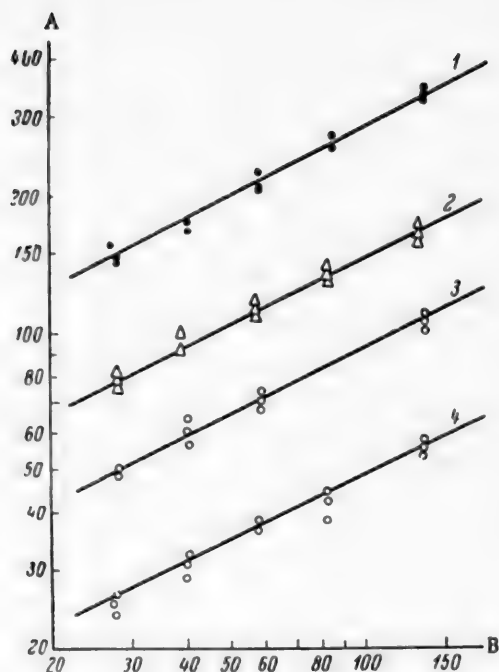


Fig. 7. Effect of volumetric gas rate at constant immersion depth on the coefficient of absorption of carbon dioxide by brines of different ammonia contents: A) over-all absorption coefficient ($\frac{\text{kg} \cdot 10^{-2}}{\text{m}^3 \cdot \text{atmos} \cdot \text{hour}}$); B) volumetric gas rate ($\frac{\text{m}^3 \cdot 10^{-2}}{\text{m}^2 \cdot \text{hour}}$); brines: 1) No. 1; 2) No. 2; 3) No. 3; 4) No. 4.

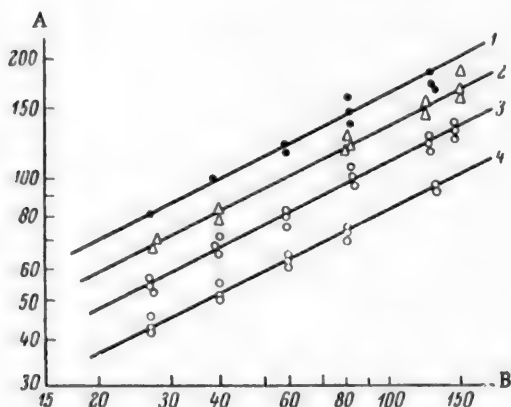


Fig. 8. Effect of volumetric gas rate at constant immersion depth on the over-all coefficient of absorption of carbon dioxide by brines of different degrees of carbonation: A) over-all absorption coefficient ($\frac{\text{kg} \cdot 10^{-2}}{\text{m}^3 \cdot \text{atmos} \cdot \text{hour}}$); B) volumetric gas rate ($\frac{\text{m}^3 \cdot 10^{-2}}{\text{m}^2 \cdot \text{hour}}$); brines: 1) No. 5; 2) No. 6; 3) No. 7; 4) No. 8.

The relationship between the over-all absorption coefficient and the gas rate (Figs. 7 and 8) can be represented by the equation:

$$K_G a = DV^{0.488} \quad (5)$$

This relationship may seem paradoxical, as it was noted earlier [1] that in carbonation processes (at least within the ranges studied) the diffusional resistance to absorption is mainly concentrated in the liquid phase (numerous investigators have shown that the liquid-phase partial coefficient of absorption is independent of the gas rate). In the present instance the liquid rate in the gas lift changes with variations of the gas rate at constant immersion depth. This variation of the liquid rate is what influences the over-all absorption coefficient, i.e., in this case the gas rate influences the over-all absorption coefficient because the liquid rate at a given immersion depth depends on the gas rate.

Figure 9 shows the effect of the gas rate on the conversion rate for brines with different initial ammonia contents (brines Nos. 1-4), and Fig. 10, for brines of different degrees of carbonation (brines Nos. 5-8).

This relationship can be represented by the equation:

$$U = D'V^{0.521} \quad (6)$$

In studies of the variations of gas rate at constant liquid rate and variable immersion depth, a series of experiments was carried out with brine No. 2. The experiments were performed at 30°, a liquid rate of about 183 m³/m²·hour, and with 37-38% carbon dioxide in the incoming gas. The gas rate was varied between 2720 and 12510 m³/m²·hour, and the immersion depth roughly between 10-13 and 22-25%.

The relationship between the absorption coefficient and the gas rate at constant liquid rate is represented in logarithmic coordinates by line 2 in Fig. 11. This relationship can be written as

$$K_G a = MV^{0.33}$$

For comparison, line 1 in Fig. 11, represents the relationship between the absorption coefficient and the gas rate at constant immersion depth.

It follows from Fig. 11 and Equations (5) and (7) that the exponent is lower at constant liquid rate and variable immersion depth than at constant immersion depth and variable liquid rate. This is because

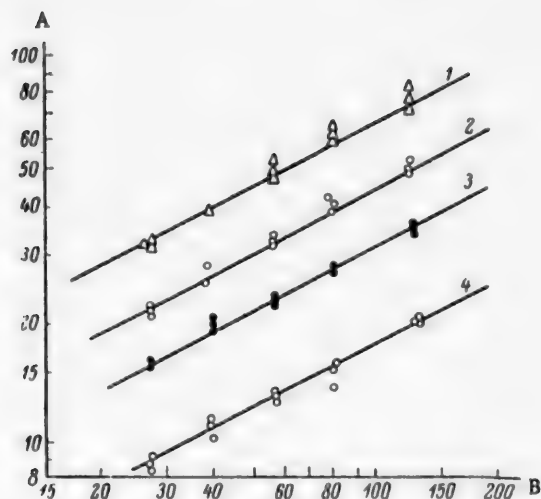


Fig. 9. Effect of volumetric gas rate at constant immersion depth on the conversion rate of carbon dioxide by brines of different ammonia contents: A) conversion rate $\left(\frac{\text{kg} \cdot 10^{-2}}{\text{m}^3 \cdot \text{hour}}\right)$; B) volumetric gas rate $\left(\frac{\text{m}^3 \cdot 10^{-3}}{\text{m}^2 \cdot \text{hour}}\right)$ brines: 1) No. 1; 2) No. 2; 3) No. 3; 4) No. 4.

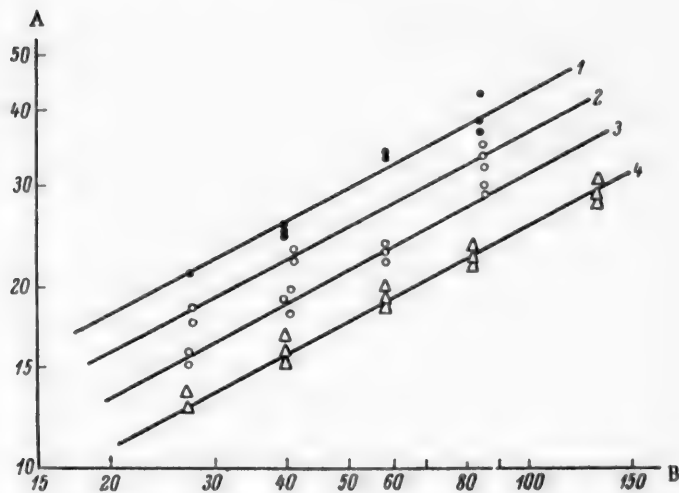


Fig. 10. Effect of volumetric gas rate at constant immersion depth on the conversion rate of carbon dioxide by brines of different degrees of carbonation: A) conversion rate $\left(\frac{\text{kg} \cdot 10^{-2}}{\text{m}^3 \cdot \text{hour}}\right)$; B) volumetric gas rate $\left(\frac{\text{m}^3 \cdot 10^{-3}}{\text{m}^2 \cdot \text{hour}}\right)$; brines: 1) No. 5; 2) No. 6; 3) No. 7; 4) No. 8.

in this instance the immersion depth varies with the gas rate at constant liquid rate. However, it has been found [2] that the immersion depth has less effect than the liquid rate on the liquid-phase mass-transfer coefficient, and therefore on the over-all coefficient of absorption of carbon dioxide by ammoniacal chloride brines. Thus, in this instance also the influence of gas rate on the over-all absorption coefficient must be regarded as a factor which determines the immersion depth at a given liquid rate.

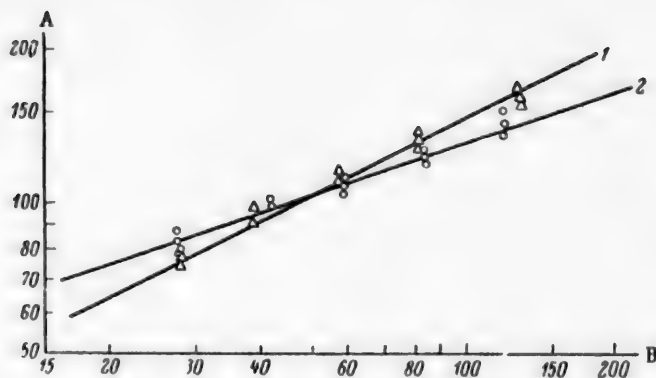


Fig. 11. Effect of volumetric gas rate on the coefficient of absorption of carbon dioxide by ammoniacal brine: A) over-all absorption coefficient ($\frac{\text{kg} \cdot 10^{-2}}{\text{m}^3 \cdot \text{atmos} \cdot \text{hour}}$); B) gas rate ($\frac{\text{m}^3 \cdot 10^{-2}}{\text{m}^2 \cdot \text{hour}}$)
1) at constant immersion depth; 2) at constant liquid rate.

SUMMARY

1. The experimental results show that the main diffusional resistance is concentrated in the liquid phase.
2. The influence of gas rate on the carbonation process must be regarded as a factor which influences either the liquid rate or the immersion depth.

LITERATURE CITED

- [1] G. N. Gasyuk, P. Ya. Krainli, A. G. Bol'shakov, and A. V. Kortnev, *J. Appl. Chem.* 31, No. 12, 1787 (1958).*
- [2] G. N. Gasyuk, A. G. Bol'shakov, A. V. Kortnev, and P. Ya. Krainli, *J. Appl. Chem.* 31, No. 7, 1019 (1958).*

Received October 8, 1957

* Original Russian pagination. See C. B. Translation.

THE PHYSICAL CHEMISTRY OF FOAMS

V. G. Gleim and I. K. Shelomov

Department of Chemistry, Rostov Institute of Railroad Transport Engineers

In series of earlier papers from our Department [1-4] we considered the influence of foam formation during boiling and bubbling on carry-over of the liquid phase with the vapor (or gas) into the space above the interphase boundary.

The present paper contains the results of a study of the influence of a number of factors — temperature, pressure, the physicochemical properties of the system — on the strength and average life of foam films.

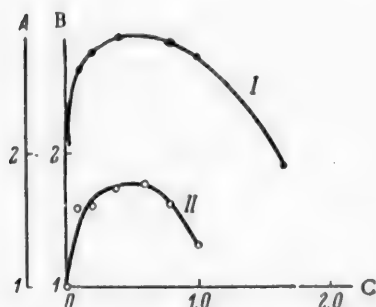


Fig. 1. Film strength and foam stability for aqueous solutions of n-propyl alcohol: A) logarithm of foam life ($\log \tau$); B) film strength ($\frac{W_{cr}^S}{W_{H_2O}^{cr}}$); C) alcohol concentration (moles/liter); D) $\log \tau$; II) film strength.

The data presented below constitute a kind of continuation and extension of the known work of Rebinder [5, 6], Trapeznikov [7, 8] and Bartsch [9]. It should be noted here that the influence of dynamic factors (gas or vapor velocity) on foaming intensity has been considered by Pozin [10] and D'yakonov [11].

The first part of the present paper deals with the rupture of bubble films, and considers the factors determining bubble stability on pure liquid surfaces.

In the second part these questions are considered in relation to true solutions of surface-active substances.

Finally, the third part contains the results of an experimental verification of the principal theoretical propositions.

Pure Liquids

Two types of force operate in a liquid film at equilibrium. The first type is determined by surface tension, and creates stresses which tend to rupture the film. The second type consists of forces of intermolecular cohesion, which tend to maintain the film intact. The relationship between these types of force evidently determines the average film life.

In order to obtain a quantitative expression of this relationship, we apply the general theory of liquid rupture, developed by Zel'dovich [12] and Kornfel'd [13], to the case in question — a thin liquid film.

By this theory, a vapor or gas bubble is formed in a liquid column under the influence of negative pressure as the result of thermal fluctuation; under certain conditions this bubble begins to grow, and this naturally leads to rupture of the liquid column. In the case of thin films, it is necessary to take into account a number of additional factors, which are insignificant in relation to a liquid column. These include the stress set up by surface tension, external pressure, and a number of others.

The energy of formation of a fluctuation bubble in a film can be expressed as follows:

$$W = \int_V \sum P_i dV, \quad (1)$$

where $\sum P_i$ is the resultant pressure in the film and V is the bubble volume.

Since V represents a sphere, then $dV = 4\pi R^2 dR$ and

$$W = 4\pi \int_0^R \sum P_i R^2 dR. \quad (2)$$

It is easy to see that

$$\sum P_i = P_1 + P_2 - P_3 - \lambda, \quad (3)$$

where P_1 is the external pressure; $P_2 = \frac{2\sigma}{R}$ is the Laplace pressure; P_3 is the pressure of a saturated vapor or dissolved gas; λ is the stress caused in the walls by surface tension.

If the liquid and gas phases are in equilibrium

$$P_1 = P_3. \quad (4)$$

The usual methods of the elasticity theory can be used to calculate λ , if we take into account that the excess bubble pressure is

$$P = \frac{4\sigma}{\rho}, \quad (5)$$

where ρ is the radius of curvature of the film.

Then

$$\lambda = \frac{2\sigma}{\delta}, \quad (6)$$

where δ is the film thickness.

From Equations (2)-(6) we find the energy of formation of a fluctuation bubble:

$$W = 4\pi\sigma R^3 \left(1 - \frac{2}{3} \frac{R}{\delta}\right) \quad (7)$$

We now consider the conditions for spontaneous growth of the fluctuation bubble, which leads, as was stated earlier, to rupture of the film. It is easy to see that the condition for spontaneous growth of a fluctuation bubble is represented by the inequality

$$P_3 > P_1 + P_2 - \lambda_1, \quad (8)$$

where λ_1 is the stress in the film after formation of a bubble of radius R in it.

It is obvious that

$$\lambda_1 = \frac{2\sigma}{\delta - 2R} \quad (9)$$

Inequality (8) in conjunction with Equations (4) and (9) takes the form

$$\frac{2\sigma}{R} < \frac{2\sigma}{\delta - 2R}, \quad (10)$$

or, after simplification

$$R > \frac{1}{3} \delta. \quad (11)$$

Hence

$$R_{cr} = \frac{1}{3} \delta \quad (12)$$

is a critical value, which determines the minimum energy required to rupture the film.

From Equations (7) and (12) we have

$$W_{cr}^L = 0.346\pi\delta^2\sigma, \quad (13)$$

where W_{cr}^L is the minimum energy required to rupture a film of the given liquid.

Thus, the strength of a film is determined by its thickness and the surface tension of the liquid.

The viscosity of the liquid has an influence only insofar as it determines the rate at which the film thickness changes. Such factors as temperature variations, evaporation rate of the liquid, etc., operate indirectly in a similar way.

The relationship between W_{cr}^L (the film strength) and its average life can be established with the aid of the expression [13]

$$U = AV e^{-\frac{W_{cr}^L}{KT}}, \quad (14)$$

where U is the rate of spontaneous bubble formation in the film, and A is a proportionality factor.

Since the formation of only one bubble of radius in excess of the critical value is enough to rupture the film, we can replace U in Equation (14) by $\frac{1}{\tau_{av}}$, where τ_{av} is the average film life.

Since $V = S\delta$, where S is the film area, Equation (14) becomes

$$\tau_{av} = \frac{1}{AS\delta} e^{\frac{0.346\pi\delta^2\sigma}{KT}} \quad (15)$$

Thus, the average film life increases exponentially with the film strength.

Solutions

In the case of solutions • the rupture mechanism of thin film is entirely identical with that described above. However, in such systems the relationship between the equilibrium values of the coefficient of surface tension and the intermolecular cohesion forces is much more complex.

The obvious cause of this is the existence of a whole series of factors which arise as the result of adsorption processes.

- Solutions of surface-active substances are considered.

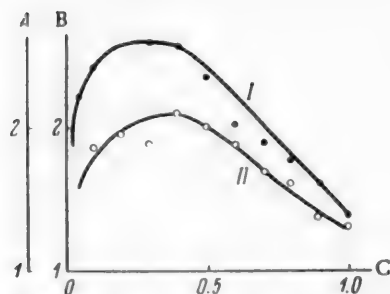


Fig. 2. Film strength and foam stability for aqueous solutions of n-butyl alcohol: A) logarithm of foam life ($\log \tau$); B) film strength ($\frac{W_{Cr}^S}{W_{H_2O}^{Cr}}$); C) alcohol concentration (moles/liter); I) $\log \tau$; II) film strength.

Indeed, since adsorption equilibrium cannot be established instantaneously, the energy of formation of a fluctuation bubble must depend on a certain nonequilibrium value σ_n of the surface tension, which must be always greater than the equilibrium value of σ .

$$\sigma_n \geq \sigma \quad (16)$$

At the instant when the surface is formed, the volume and the surface concentrations (C) must be equal. Subsequently, as adsorption equilibrium is reached, the concentration in the surface layer becomes

$$C_s = \frac{\Gamma \cdot 1000}{\beta}, \quad (17)$$

where β is the thickness of the surface layer.

The volume concentration can be disregarded without undue error for solutions with low solute contents. The concentration change took place, obviously, as the result of transfer of Γ moles of solute (per unit surface) from within the solution to the surface layer.

If the adsorption process is regarded as isothermal, we have for the energy of adsorption

$$\varphi = \Gamma RT \ln \frac{C_{cr}}{C}, \quad (18)$$

but the energy of adsorption is equal to the change of surface tension, and it follows from Equations (18) and (17) that

$$\sigma_n = \sigma + \Gamma RT \ln \frac{\Gamma \cdot 1000}{C\beta}. \quad (19)$$

Assuming as an approximation that $\Gamma = \frac{CG}{RT}$, where G is the surface activity, we have

$$\sigma_n = \sigma + CG \ln \frac{G \cdot 1000}{RT\beta}. \quad (20)$$

Putting $\varphi = CG \ln \frac{G \cdot 1000}{RT\beta}$, we have

$$\sigma_n = \sigma + \varphi \quad (21)$$

It is easy to see that the critical condition (10) for solutions takes form

$$\frac{2(\sigma + \varphi)}{R_{cr}} - \frac{2\sigma}{\delta - 2R_{cr}} = 0, \quad (22)$$

as the Laplace pressure is determined by the value of σ_n , and the stress in the film, by the value of σ .

It follows from Equation (22) that

$$R_{cr} = \delta \frac{\sigma + \varphi}{3\sigma + 2\varphi} = \delta\psi, \quad (23)$$

where

$$\psi = \frac{\sigma + \varphi}{3\sigma + 2\varphi}. \quad (24)$$

The critical energy of film rupture for a solution, with all the foregoing taken into account, is found to be analogous to that for pure liquids:

$$W_{cr}^s = \frac{4}{3} \pi \delta^2 \psi^3 (7\sigma + 6\tau). \quad (25)$$

If we assume approximately that the film thickness is independent of concentration, we have after suitable rearrangements:

$$\frac{W_{cr}^s}{W_{cr}^{H_2O}} = 11.57 \psi^2 \left(1 - \frac{2}{3} \psi + \frac{\varphi}{\sigma} \right) \frac{\sigma}{\sigma_{H_2O}}. \quad (26)$$

Thus, the film strength is higher in solutions than in pure liquids.

It must be noted that these considerations are valid also for solutions of surface-inactive substances, where water is the surface-active substance, and for colloidal systems, which are not considered here.

Experimental Verification of the Principal Theoretical Propositions

To verify the validity and degree of accuracy of the above theoretical considerations, calculated data on film strength for solutions of a number of surface-active substances were compared with data obtained by various workers on foam stability.

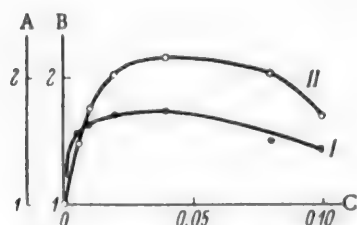


Fig. 3. Film strength and foam stability for aqueous solutions of isoamyl alcohol: A) logarithm of foam life ($\log \tau$); B) film strength ($\frac{W_{cr}^s}{W_{H_2O}^s}$); C) alcohol concentration (moles/liter); I) $\log \tau$; II) film strength.

The results of this comparison are presented in Tables 1-3 and Figs. 1-3.

Table 1 and Fig. 1 contain data on n-propyl alcohol. The foam stabilities are based on Erchikovskii's data [14].

In this case it was assumed that $\beta \approx 10A$, and hence $RT\beta \approx 2.4 \cdot 10^3 \frac{\text{erg} \cdot \text{cm}}{\text{mole}}$

In Table 2 and Fig. 2 the values of $\left(\frac{W_{cr}^s}{W_{H_2O}^s} \right)$ and of the logarithm of the foam stability in solutions of n-butyl alcohol are compared.

Erchikovskii's data on foam stability are again used.

In Table 3 and Fig. 3 the values of $\left(\frac{W_{cr}^s}{W_{H_2O}^s} \right)$ for isoamyl alcohol are compared with the average bubble life in the same solution, from Venstrem and Rebinder's data [5].

TABLE 1

Film Strength and Foam Stability in Aqueous Solutions of n-Propyl Alcohol

C, moles/liter	$\sigma \frac{\text{ergs}}{\text{cm}^2}$	G	φ	ψ	$\frac{W_{cr}^s}{W_{H_2O}^s}$	τ , sec	$\lg \tau$
0.1	66.0	70	23.6	0.369	1.58	450	2.65
0.2	61.4	46	27.1	0.371	1.60	580	2.76
0.4	54.6	34	36.0	0.386	1.73	752	2.88
0.6	50.0	26	37.0	0.388	1.75	760	2.88
0.8	46.0	20	33.9	0.388	1.61	688	2.84
1.0	43.4	14	24.7	0.379	1.30	540	2.73
1.67	—	—	—	—	—	80	1.90

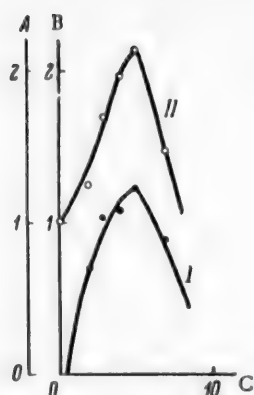


Fig. 4. Film strength and maximum foam stability for solutions of homologous alcohols: A) logarithm of foam life ($\log \tau$); B) film strength ($\frac{W_{cr}^s}{W_{H_2O}} \cdot \frac{1}{C}$); C) number of carbon atoms (n) in the alcohol molecule; D) $\log \tau$; II) film strength.

It is seen that experimental values of foam stability (or bubble life) and film strengths calculated on the basis of theoretical considerations are in good agreement for different concentrations of the solutions in question.

The maximum foam stability corresponds to the maximum value of the film strength calculated from Equation (26).

Therefore, the above analytical expressions and the underlying theoretical principles may be regarded as justified.

Further, it is not without interest to consider yet another aspect of the theory and practice of foam formation in solutions — the influence of the length of the hydrocarbon radical in the foaming agent on the foaming power of its solutions.

Solutions of certain homologous monohydric alcohols and fatty acids were taken at concentrations corresponding to the maxima of foam formation as given by Bartsch [7]. Film strengths for these solutions were calculated from Equation (26).

These data are compared graphically in Figs. 4 and 5.

The results show that the film strengths and foam stabilities pass through maximum values with increase in the length of the hydrocarbon chain, and then decrease rapidly.

The surface activity in the same series of homologs increases continuously.

TABLE 2

Film Strength and Foam Stability in Aqueous Solutions of n-Butyl Alcohol

C moles liter	σ $\frac{\text{ergs}}{\text{cm}^2}$	G	φ	ψ	$\frac{W_{cr}^s}{W_{H_2O}} \cdot \frac{1}{C}$	τ , sec	$\lg \tau$
0.1	56.2	100	37.3	0.384	1.86	280	2.45
0.2	48.6	66	43.7	0.396	1.96	380	2.58
0.3	44.4	48	43.0	0.398	1.89	398	2.60
0.4	41.2	43	49.6	0.410	2.10	390	2.59
0.5	38.0	36	48.5	0.410	2.02	230	2.36
0.6	35.0	30	45.4	0.410	1.88	108	2.03
0.7	32.4	25	41.0	0.408	1.69	82	1.91
0.8	29.6	22	38.8	0.410	1.60	62	1.79
0.9	27.8	18	32.6	0.406	1.37	42	1.62
1.0	26.2	16	30.4	0.406	1.29	24	1.38

TABLE 3

Film Strength and Foam Stability in Aqueous Solutions of Isoamyl Alcohol

C moles liter	σ $\frac{\text{ergs}}{\text{cm}^2}$	G	φ	ψ	$\frac{W_{cr}^s}{W_{H_2O}} \cdot \frac{1}{C}$	τ , sec	$\lg \tau$
0.005	69.8	670	18.9	0.358	1.48	36	1.56
0.010	66.2	550	30.0	0.372	1.74	41	1.61
0.020	61.0	396	40.2	0.385	2.01	47	1.67
0.040	53.3	250	47	0.394	2.17	52	1.72
0.080	46.0	140	45.5	0.399	2.01	31	1.49
0.100	43.2	100	37.3	0.394	1.69	28	1.45

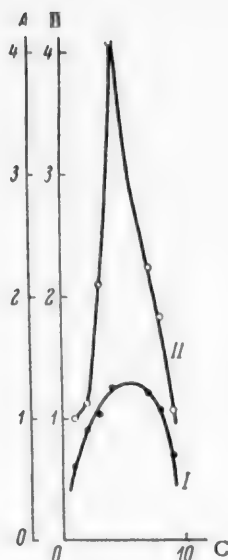


Fig. 5. Film strength and maximum foam stability for solutions of homologous fatty acids: A) logarithm of foam life ($\log \tau$); B) film strength $\left(\frac{W_{Cr}}{W_{H_2O}}\right)_{Cr}$; C) number of carbon atoms (n) in the acid molecule; I) $\log \tau$; II) film strength.

It follows that higher fatty acids and monohydric alcohols, which are preferentially adsorbed at interfaces because of their high surface activities, lower film strength, i.e., exert a foam-breaking effect.

Therefore, substances which have high adsorption potentials and at the same time do not confer any significant strength to the surface films may act as foam breakers.

It follows that foam breakers should be sought and studied with the aid of σ -C diagram for the corresponding aqueous solutions.

SUMMARY

1. The rupture of a film of a gas (or vapor) bubble at a liquid-gas interface can be considered in the light of the general theory of the strength of liquids (on the basis of formation of a fluctuation bubble in a thin film). The expressions derived show that the energy of film rupture is directly proportional to the surface tension and to the square of the film thickness.

2. For solutions of surface-active substances, the increase of the energy of film rupture is determined by the ratio of the adsorption (Gibbs) to the surface tension.

3. The action of the so-called foam breakers depends on their high adsorption potential and low energies of foam film rupture.

4. Comparison of foam stabilities (or bubble lives) determined by different workers with theoretical values for energy of film rupture gives good agreement; this confirms the concept on which the calculations are based.

LITERATURE CITED

- [1] V. G. Gleim, *J. Appl. Chem.* 26, No. 11 (1953). *
- [2] V. G. Gleim, *J. Appl. Chem.* 28, No. 1 (1955). *
- [3] V. G. Gleim and I. K. Shelomov, *J. Appl. Chem.* 30, No. 1 (1957). *
- [4] M. S. Ostrikov and V. G. Gleim, *Sci. Mem. Rostov State Univ.* 26, 5 (1951).
- [5] E. K. Venstrem and P. A. Rebinder, *J. Phys. Chem.* 2, No. 6 (1931).
- [6] P. A. Rebinder and A. A. Trapeznikov, *J. Phys. Chem.* 12, No. 5-6 (1938).
- [7] A. A. Trapeznikov, *J. Phys. Chem.* 12, No. 5-6 (1938).
- [8] A. A. Trapeznikov, *J. Phys. Chem.* 14, No. 5-6 (1940).
- [9] O. Bartsch, *Kolloid Chem. Bein.* 20, 1 (1925).
- [10] M. E. Pozin, I. P. Mukhlenov, et al., *The Foam Method for Treatment of Liquids and Gases* [in Russian] (Goskhimizdat, 1955).
- [11] G. D. D'yakov, *Questions of the Similarity Theory in the Field of Physicochemical Processes* [in Russian] (Izd. AN SSSR, 1956).
- [12] Ya. B. Zel'dovich, *J. Exptl. Theoret. Phys.* 12, 525 (1942).
- [13] M. Kornfel'd, *Elasticity and Strength of Liquids* [in Russian] (GITTL, Moscow-Leningrad, 1951).
- [14] G. A. Erchikovskii, *Formation of Flotation Foam* [in Russian] (GONTI, 1931).

Received September 20, 1957

*Original Russian pagination. See C.B. Translation.

CALCULATION OF THE HEIGHT OF EQUIPMENT FOR CHEMICAL INTERACTION OF GASES WITH LIQUIDS

L. A. Mochalova and M. Kh. Kishinevskii

Laboratory of Physical Chemistry, University of Kishinev

Although processes involving chemical interaction between gases and liquids are being used extensively in chemical technology, there are still no rational methods for calculations relating to the design of industrial equipment used for such processes.

The commonest types of absorption equipment are packed and bubble towers. The principal problem in the design of such equipment is determination of the height required for a given degree of extraction of the absorbed component from a gaseous mixture, and for a given degree of chemical conversion of the liquid phase. In a number of cases only one of the problems needs to be solved.

Neither methods for calculation of the height of equipment for chemical interaction of gases with liquids, nor methods for modeling such processes are described in the literature. This situation may lead to considerable errors in the construction of new industrial units, and retards improvements in the output of existing equipment.

In this paper an attempt is made to indicate the directions in which efforts must be made to eliminate this gap between the demands of industrial practice and the level of our knowledge of absorption equipment design and calculation methods.

The height of a packed or bubble tower required to give a specified degree of conversion can be calculated if the following are known: the liquid-phase and gas-phase mass-transfer coefficients, referred to unit volume of the equipment (for packed towers) or per m^2 of plate area (in bubble towers), the renewal time of the surface layer and certain physicochemical factors (rate constant of the slowest reaction, solubility of the absorbed component in the liquid phase, chemical equilibrium constant, etc.). The mass-transfer coefficients are determined by hydrodynamic factors: the geometry of the equipment, flow rates, the viscosities and densities of the liquid and gas phases, and the properties of the surface layers; and by a physicochemical factor — the coefficient of molecular diffusion. The renewal time of the surface layer is determined by hydrodynamical factors only.

In cases, when the literature does not contain reliable data on mass-transfer coefficients for a given type of equipment and a given hydrodynamical regime, model experiments are necessary.

Data on the renewal times of the surface layers under various conditions are immeasurably more scanty, because of the relative novelty of this concept and also because determinations of these values involve more laborious experiments on chemical systems, and more difficult calculations [1]. Nevertheless, without such data it is hardly possible to develop rational methods relating to the calculation and design of equipment for chemical reactions between gases and liquids.

The derivation of calculation formulas for determination of the height of absorption towers for chemical interaction of gases with liquids, presented in this paper, is based on the equation for the kinetics of absorption accompanied by chemical reaction. The form of this equation depends primarily on the mechanism and kinetics of the reactions in the liquid phase, and also on the hydrodynamical conditions.

Let us consider one of the commonest cases, when the absorption process is accompanied by an irreversible reaction of the second order. The equation for the absorption rate in this case is of the form [2]

$$q = \frac{\frac{C}{m}(1-A) + HP}{\frac{1}{k_L a} + \frac{H}{k_G a}}, \quad (1)$$

where q is the absorption rate (in kg-moles/hour \cdot m³ for packed towers and kg-moles/hour \cdot cm² for plate towers); C is the concentration of the active component of the absorbent (in kg-moles/m³); H is the solubility coefficient (in kg-moles/m³ \cdot atmos); P is the partial pressure of the absorbed component (atmos); $k_L a$ is the liquid-phase mass-transfer coefficient (in 1/hour or m/hour); $k_G a$ is the gas-phase mass-transfer coefficient (in kg-moles/hour \cdot atmos \cdot m³ or kg-moles/hour \cdot atmos \cdot m²); m is the number of molecules of the active component of the absorbent combining with one molecule of gas.

$$A = \frac{e^{-mHP^*K_C\Delta\tau}}{\sqrt{mHP^*K_C\Delta\tau}} \int_0^{\sqrt{mHP^*K_C\Delta\tau}} e^{y^2} dy,$$

where P^* is the partial pressure of the absorbed gas at the interface (in atmos); K_C is the rate constant for a second-order reaction (in m³/kg-mole \cdot hour); $\Delta\tau$ is the renewal time of the surface layer (hours).

In developed turbulence, since $\Delta\tau$ is very small, the exponential expressions may be resolved into series and the nonlinear terms omitted. Equation (1) becomes

$$q = \frac{HP}{\frac{1}{k_L a(KC + 1)} + \frac{H}{k_G a}}, \quad (2)$$

where $K = K_C\Delta\tau$

When $C = 0$, Equation (2) becomes the equation for the rate of absorption unaccompanied by chemical reaction. At high values of C the liquid-phase resistance becomes very low and the absorption rate is

$$q = k_G a P. \quad (3)$$

It must be pointed out that in physicochemical investigations and in determinations of numerical values of $\Delta\tau$ under various hydrodynamical conditions (Equation 1) should be used, as it is more accurate. In certain technical calculations, such as determinations of tower height, Equation (2) may be used, especially as industrial processes are commonly conducted under conditions of high turbulence.

In packed towers the gas and liquid streams are in countercurrent motion, while in plate towers they are in cross flow. This gives rise to different mathematical problems. We consider the former one first.

In earlier paper [3] we considered the case of constant concentration of the absorbent along the height of the tower. Now we examine the more general case, when the composition of both the gas and the liquid phase vary along the column. This problem involves solution of the system of equations

$$-Gdy = \frac{L}{m} dC = \frac{PH}{\frac{1}{k_L a(KC + 1)} + \frac{H}{k_G a}} dh, \quad (4)$$

where G is the flow rate of the inert gas (in kg-moles/hour \cdot m³), L is the liquid rate (in m³/m³ \cdot hour), y is the concentration of the absorbed component (in kg-moles/kg-mole of inert gas); h is the packing height.

With the aid of the expression

$$P = \frac{P_{\text{tot}} y}{1 + y}, \quad (5)$$

where P_{tot} is the total pressure (in atmos), after integration of Equation (4) we obtain the calculation formula

$$\begin{aligned} h \frac{P_{\text{tot}} k_G A}{G} = & \left(\frac{k_G a}{C_{\text{in}} + B y_{\text{ex}} + \frac{1}{K}} + \frac{k_G a}{B} \right) \ln \frac{C_{\text{in}} + \frac{1}{K}}{C_{\text{in}} + \frac{1}{K} - B(y_{\text{in}} - y_{\text{ex}})} + \\ & + \left(\frac{k_G a}{C_{\text{in}} + B y_{\text{ex}} + \frac{1}{K}} + A \right) \ln \frac{y_{\text{in}}}{y_{\text{ex}}} + A(y_{\text{in}} - y_{\text{ex}}), \end{aligned} \quad (6)$$

where $A = k_L a H K$, $B = \frac{G m}{L}$, y_{in} is the gas composition at entry into the tower, y_{ex} is the gas composition at the tower exit, and C_{in} is the absorbent concentration at entry.

Although Equation (6) is somewhat cumbersome, it can be used for easy calculation of the packing height corresponding to a given degree of extraction of the gas, provided, of course, that the mass-transfer coefficients and the renewal time of the surface layer are known. It must be emphasized that the derivation is based on the assumption that $k_L a$ and $k_G a$ are independent of the tower height. This assumption was verified experimentally. The main factors determining the values of these coefficients and the renewal time of the surface layer are: spray density; gas rate; dimensions, shape, and configuration of the packing; viscosity and density of the absorbent; state of the interphase layers, temperature.

In the case of cross flow, the following equations must be solved:

$$-\frac{L'z}{m} dC = G(y_{\text{in}} - y_{\text{ex}}) dh = \frac{\bar{P} H}{\frac{1}{k_L a z (K C + 1)} + \frac{H}{k_G a}} dh, \quad (7)$$

where L' is the linear velocity of the liquid in a horizontal direction on the plate (in m/hour); z is the height of the gas-liquid stream on the plate (m); dh is an element of the liquid path on the plate; $k_L a$ and $k_G a$ are the mass-transfer coefficients per unit volume of the gas-liquid stream; \bar{P} is the vertical mean partial pressure of the gas.

Equations (7) are valid if C is constant over a vertical plane at right angles to the direction of flow of the liquid on the plate. The composition of the gas phase is variable not only in the vertical direction, but also along the liquid path on the plate. For simplicity in calculation, the vertical mean value of the partial pressure of the absorbed gas is considered in Equation (7). This approach was used by Pozin [4].

Replacing \bar{P} in Equation (7) by

$$\bar{P} = \frac{P_{\text{tot}} y}{1 + y}, \quad (8)$$

when

$$y = \frac{y_{\text{in}} + y_{\text{ex}}}{2} \quad (9)$$

we find an expression for y_{ex} in terms of C

$$\frac{H P_{\text{tot}} k_L a k_G a (K C + 1) (y_{\text{in}} + y_{\text{ex}})}{(2 + y_{\text{in}} + y_{\text{ex}}) [k_G a + H k_L a (K C + 1)]} = G(y_{\text{in}} - y_{\text{ex}}). \quad (10)$$

Here we consider only the case when the concentration of the absorbed gas is relatively low; this is the simplest case, and is often met in practice. We disregard the numerator in comparison with the denominator in Equation (9) and solve Equation (10) for y_{ex} ; substitution of the result into the equation

$$-\frac{L'z}{m} dC = G(y_{\text{in}} - y_{\text{ex}}) dh$$

and integration gives the first variant of the calculation formula

$$\frac{2mGy_{in}}{L'z} h = \frac{2G}{P_{tot} H k_{Laz} K} \ln \frac{KC_{in} + 1}{KC_{ex} + 1} + (C_{in} - C_{ex}) \left(1 + \frac{2G}{P_{tot} k_{Gaz}} \right). \quad (11)$$

For use of Equation (11) it is necessary to know the liquid-phase and gas-phase mass-transfer coefficients referred to 1 m² of plate area, i.e., the products k_{Laz} and k_{Gaz} , and also the height of the gas-liquid stream z on the plate. This last condition makes it somewhat difficult to use the equation. However, the formula can be transformed, because

$$L'z = Lh \quad (12)$$

where L is the liquid flow rate per unit cross-sectional area of tower (in m³/m²·hour).

Substitution of Equation (12) into (11) gives the second variant of the calculation formula.

$$\frac{2mGy_{in}}{L} = \frac{2G}{P_{tot} H k_{Laz} K} \ln \frac{KC_{in} + 1}{KC_{ex} + 1} + (C_{in} - C_{ex}) \left(1 + \frac{2G}{P_{tot} k_{Gaz}} \right). \quad (13)$$

Formula (13) can be used for calculation of the flow rate of the liquid per m² of column cross section, required to give the required degree of chemical conversion of the absorbent on the plate at given gas rate per m², total pressure, and compositions of the gas and absorbent at entry to the plate. This is equivalent to determination of the plate length, as h can be found for a known total liquid rate, if the plate width is chosen and the liquid flow rate per m² of plate is calculated. After determination of the plate length it is easy to calculate the total number of plates in the tower.

Equations (6) and (13) were verified experimentally under laboratory conditions for the systems CO₂-aqueous ammonia solutions and CO₂-aqueous NaOH solutions, and satisfactory results were obtained.

SUMMARY

Equations have been derived for calculations of packed-tower height and plate length in absorption with chemical interaction of gas with liquid; they can be used in practice if the mass-transfer coefficients in the liquid and gas phases, referred to unit volume of the apparatus in the first case and to 1 m² of plate area in the second, and the renewal time of the surface layer are known.

LITERATURE CITED

- [1] L. A. Mochalova and M. Kh. Kishinevskii, J. Appl. Chem. 31, No. 4, 533 (1958). *
- [2] M. Kh. Kishinevskii, J. Appl. Chem. 27, No. 3, 450 (1954). *
- [3] M. Kh. Kishinevskii and L. A. Mochalova, J. Appl. Chem. 30, No. 9, 1386 (1957). *
- [4] M. E. Pozin, J. Appl. Chem. 25, No. 10, 1032 (1952). *

Received April 21, 1958

* Original Russian pagination. See C. B. Translation.

PHASE-CONTACT AREA OF IMMISCIBLE LIQUIDS DURING AGITATION BY MECHANICAL STIRRERS

V. V. Kafarov and B. M. Babanov

The stirring of immiscible liquids in order to produce emulsions or to effect extraction is a common industrial process [1].

The purpose of the present investigation was to determine the phase-contact area formed during agitation by mechanical stirrers. A sedimentometer of special design [2] was used for measurements of dispersity and surface area; the sedimentometer results were compared with the results of photoelectric determinations [3-6].

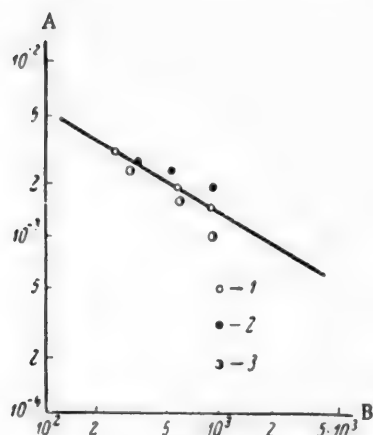


Fig. 1. Comparison of experimental data with the data of Vermeulen, Williams, and Langlois [3]: A) ratio of average drop diameter d_{av} to stirrer diameter d_s ; B) Weber number ($We = \frac{\rho_{mx} \cdot n^2 \cdot d_s^3}{\sigma}$); 1) toluene-water; 2) spindle oil-water; 3) kerosene-water. The results of Vermeulen et al. are represented by the straight line.

The following approach may be used for determination of the relationship between the surface area formed and the factors determining the stirring process.

It must be assumed that the phase-contact area per unit volume of the stirred mixture, or the specific phase-contact surface A (m^2/m^3), depends on the design of the mixer used, the angular velocity of the stirrer n (1/second), the stirrer diameter d_s , the interfacial tension σ (kg/m), the viscosity of the mixture μ_{mx} ($kg \cdot sec/m^2$), and the density of the mixture ρ_{mx} ($kg \cdot sec^2/m^4$), i. e.,

$$A = f(n, d_s, \sigma, \mu_{mx}, \rho_{mx}). \quad (1)$$

The viscosity of the mixture can be expressed as follows in terms of the viscosity of the disperse phase μ_d and the viscosity of the dispersion medium μ_m [3]:

$$\mu_{mx} = \frac{\mu_m}{1 - \alpha} \left(1 + 1.5\alpha \frac{\mu_d}{\mu_d + \mu_m} \right), \quad (2)$$

where α is the fraction of the disperse phase in the system.

The density of the mixture is given by the expression [7]:

$$\rho_{mx} = \rho_d \cdot \alpha + \rho_m \cdot (1 - \alpha), \quad (3)$$

where ρ_d and ρ_m are the densities of the disperse phase and the dispersion medium respectively.

Dimensional analysis of the functional relationship (1) yields the following relationship between three dimensionless groups:

$$A \cdot d_s = C \left(\frac{\mu_{mx} \cdot n^2 \cdot d_s^3}{\sigma} \right)^m \cdot \left(\frac{n \cdot d_s \cdot \mu_{mx}}{\sigma} \right)^l \quad (4)$$

Examination of the groups in the right-hand side of Equation (4) readily shows that one of them is the well-known Weber number, (We), and the other is the ratio of the Weber number to the Reynolds number (Re), as

$$\frac{We}{Re} = \frac{\left(\frac{\rho_{mx} \cdot n^2 \cdot d_s^3}{\sigma} \right)}{\left(\frac{\rho_{mx} \cdot n \cdot d_s^4}{\mu_{mx}} \right)} = \frac{n \cdot d_s \cdot \mu_{mx}}{\sigma},$$

then

$$A \cdot d_s = C_0 \cdot We^m \cdot \left(\frac{We}{Re} \right)^l = C_0 \cdot We^{m+l} \cdot Re^{-l}. \quad (5)$$

Expansion of this relationship gives

$$A = C_0 \cdot \rho_{mx}^m \cdot n^{2m+l} \cdot d_s^{3m+l-1} \cdot \sigma^{-m-l} \cdot \mu_{mx}^l \quad (6)$$

The constants C_0 , m , and l can be found only by experiment. We therefore carried out mixing experiments in geometrically similar vessels of two different sizes, with four types of stirrers and four liquid systems.

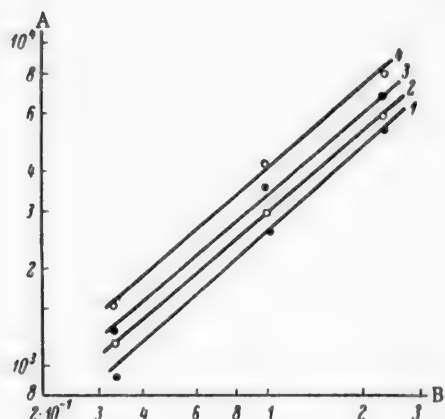


Fig. 2. Variation of phase-contact area with concentration of the disperse phase in the system spindle oil-water (stirrer Model No. 3): A) phase-contact area (m^2/m^3);

B) concentration of disperse phase $\left(\frac{\alpha}{0.15} \right)$;

1) $n = 600$ rpm; 2) $n = 700$ rpm; 3) $n = 800$ rpm; 4) $n = 1000$ rpm.

One of the vessels, 200 mm in diameter, was made of glass to allow visual observations of the mixing process; the other, 400 mm in diameter, was of stainless steel. In order to have conditions for hydrodynamic modeling [8], each vessel was fitted with four baffles. To avoid errors by entry of air into the agitated systems, both vessels were covered by lids and filled with the liquids under test. The characteristic dimensional ratios for the two vessels were:

$$H = D, \quad d_s = \frac{1}{3} D, \quad h = \frac{1}{3} H,$$

$$a = \frac{1}{12} D, \quad b = \frac{1}{60} D, \quad b = H,$$

where D is the internal diameter of the vessel; H is the filled height of the vessel, equal to the distance from the bottom of the vessel to the lid; d_s is the stirrer diameter; h is the distance from the bottom of the vessel to the stirrer; a is the baffle width; b is the baffle height; δ is the distance between the baffle and the vessel wall; (all dimensions in meters).

The following types of stirrers were used: a turbine 6-blade stirrer with flat vertical blades [9] (Model No. 1), a 2-blade stirrer with flat vertical blades (Model No. 2) and a 2-blade stirrer with flat blades set at a downward angle of 45°

(Model No. 3), with blade widths equal to $0.25 d_s$ in both cases; and a 3-blade propeller stirrer [10] (Model No. 4). The stirrer speeds were measured by means of an electrical tachometer, and the power was determined with the aid of a dynamometer device [11, 12]. The dispersion medium was water in all cases. The disperse phases used were toluene, kerosene, spindle oil, and petrolatum. As these liquids were of a technical purity grade, their densities (ρ_d) and viscosities (μ_d) were determined before each experiment, and the surface tensions at the water interface (σ) before and after each experiment; if the difference between the values of σ before and after an experiment exceeded 5%, the experimental results were rejected. The value of σ found after the experiment was used in calculation. The densities of the individual liquids were determined pycnometrically, viscosities by means of the Ostwald viscosimeter, and surface tensions by means of the stalagmometer [13].

In these experiments the surface tension was varied between 0.0023 and 0.0058 kg/m, viscosity from 0.00006 to 0.0196 kg·sec/m², and density from 79.5 to 102 kg/sec²/m⁴. For determination of the effect of the

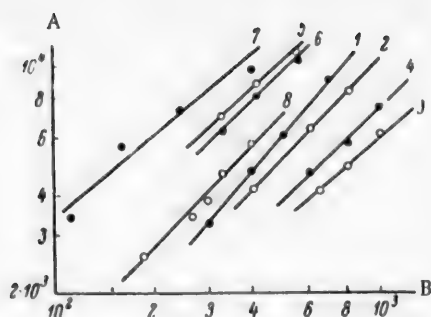


Fig. 3. Effect of stirrer speed on the phase-contact area for different stirrers and systems: A) phase-contact area (m^2/m^3); B) stirrer speed n (rpm); 1) toluene-water, stirrer Model No. 1, $d_s = 0.066$ m; 2) toluene-water, Model No. 2, $d_s = 0.066$ m; 3) toluene-water, Model No. 3, $d_s = 0.066$ m; 4) toluene-water, Model No. 4, $d_s = 0.066$ m; 5) kerosene-water, Model No. 1, $d_s = 0.13$ m; 6) toluene-water, Model No. 1, $d_s = 0.13$ m; 7) carbon tetrachloride-water, 4-blade stirrer, $d_s = 0.172$ m; 8) water-isooctane, 4-blade stirrer, $d_s = 0.172$ m.

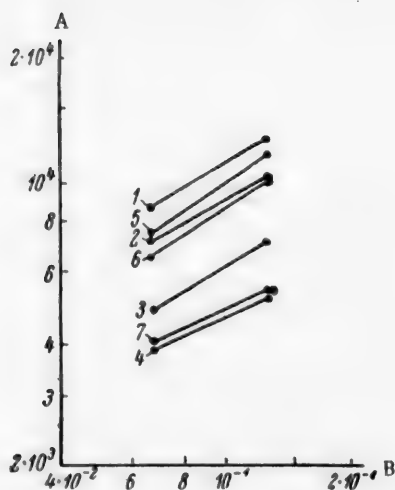


Fig. 4. Effect of stirrer diameter on phase-contact area for different systems at $n = 600$ rpm: A) phase-contact area (m^2/m^3); B) stirrer diameter (m); kerosene-water; 1) Model No. 1; 2) Model No. 2; 3) Model No. 3; 4) Model No. 4; toluene-water; 5) Model No. 1; 6) Model No. 2; 7) Model No. 3.

viscosity of the disperse phase on the contact area, a number of experiments with the system spindle oil-water were carried out under constant-temperature conditions, the mixers being placed in a water bath at 10, 20, and 30°. The effect of the amount of disperse phase was studied in the same system (with 5, 15, and 35% of disperse phase by volume in the system). All the other experiments were carried out at temperatures between 20 and 26°, with 15% of the disperse phase in the system.

For comparison of the results obtained with the sedimentometer [2] with the results obtained by the photoelectric method, several experiments were carried out with an apparatus similar to that described by Vermeulen Williams, and Langlois [3]. The systems taken for these experiments were toluene-water, spindle oil-water, and kerosene-water. The stirrer speeds were between 100 and 200 rpm, as at lower speeds the disperse phase was not distributed uniformly in the stirred system, while at higher speeds air was drawn from the atmosphere into the stirred system; therefore the systems were studied at 110, 152 and 197 rpm.

The average droplet size (d_{av} in m) was found from the equation

$$d_{av} = \frac{6V}{A}, \quad (9)$$

where V is the volume fraction of the disperse phase in the system. The results were in good agreement with the results obtained by the earlier workers; this follows from the graph (Fig. 1) plotted by Vermeulen et al., where the ratio of the average droplet size (d_{av}) to the stirrer diameter (d_s) is plotted against the Weber number ($We = \frac{\rho_{mx} \cdot n^2 \cdot d_s^3}{\sigma}$). It is seen from the graph that the average deviation of our experimental points from the linear Vermeulen plot does not exceed 12%.

It follows that the sedimentometric method for determination of the dispersity of emulsions is not inferior to the photoelectric method in accuracy and reliability, and has the advantage over the latter in that it is independent of the purity and properties of the liquids studied. The only exception is the system spindle oil-water; when this system is stirred the phase-contact area may be somewhat low, owing to penetration of minute water droplets into the oil droplets, as was observed in some experiments. Moreover, the sedimentometric method can be used for determinations of the fractional composition of emulsions, which is impossible with the photoelectric method.

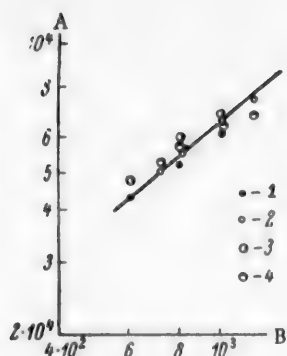


Fig. 5. Effect of the viscosity of the disperse phase at different stirrer speeds on the phase-contact area (stirrer Model No. 3): A) phase-contact area (m^2/m^3); B) stirrer speed n (rpm); spindle oil - water: 1) $\mu_d = 0.0196 \text{ kg} \cdot \text{sec}/\text{m}^2$; 2) $\mu_d = 0.0090 \text{ kg} \cdot \text{sec}/\text{m}^2$; 3) $\mu_d = 0.00415 \text{ kg} \cdot \text{sec}/\text{m}^2$; toluene - water; 4) $\mu_d = 0.000056 \text{ kg} \cdot \text{sec}/\text{m}^2$.

Concentration of the Disperse Phase. The volume concentration of the disperse phase was varied from 5 to 35%. The results of these experiments are plotted in Fig. 2. The concentrations of the disperse phase are expressed relative to 0.15, which represents the concentration of disperse phase (15%) taken as standard. The diagram shows that the slope of the lines remains almost constant irrespectively of the stirrer speed; the tangent of the angle of inclination (slope) is 0.84, i.e.,

$$A = K_1 \cdot \left(\frac{\alpha}{0.15} \right)^{0.84} \quad \text{or} \quad A = K_2 \cdot \alpha^{0.84}$$

Stirrer Speed. Figure 3 shows variations of the phase-contact area with stirrer speed for different stirrers and systems. To compare our experimental results with earlier data [3], the graph contains the lines 7 and 8, which represent the analogous relationship between the phase-contact area and stirrer speed for the systems carbon tetrachloride - water and water - isooctane stirred by means of a 4-blade stirrer with flat vertical blades, 0.172 m in diameter, in a vessel 0.25 m in diameter. The lines are nearly parallel; this shows that the area varies with stirrer speed in a similar manner, irrespectively of the properties of the mixed liquids or of the design and dimensions of the stirrer. Consideration of similar graphs for the systems spindle oil - water and petrolatum - water leads to the same conclusion. The slope was found to vary between 0.88 and 1.21. In generalization of the experimental data we took the average value of the slope as 1.11, i.e., $A = K_3 \cdot n^{1.11}$.

Stirrer Diameter. Experiments on the effect of stirrer diameter were carried out in vessels 200 and 400 mm in diameter, with all the types of stirrers, for the systems kerosene - water and toluene - water. Variations of surface tension found among systems mixed by means of stirrers of the same form in vessels of different size, did not exceed 5%. The results of these experiments are plotted in Fig. 4. It follows from the graph that the slope varies between 0.63 and 0.76, with an average value of 0.7, i.e., $A = K_4 \cdot d_s^{0.7}$.

Viscosity. The influence of viscosity was studied with the system spindle oil - water stirred at 10, 20, and 30°, and the system toluene - water at 23°, with similar values of surface tension, 0.00314, 0.00297, 0.00286 and 0.00297 kg/m, respectively. The respective densities of toluene (866) and oil (916, 910, and 904 kg/m³) also differed little, but the viscosity of the oil at 10°, 0.0196 kg·sec/m², was 350 times the viscosity of toluene, 0.000056 kg·sec/m². The systems were stirred by means of stirrer Model No. 3 in a vessel of $d = 200 \text{ mm}$. The results of these experiments are plotted in Fig. 5; they show that there were no appreciable differences between the phase-contact areas. It will be shown later by dimensional analysis that the power of the viscosity in the relationship in question is low (0.1); this is consistent with the experimental observations.

Surface Tension. Three compositions were chosen in the system toluene - water, with different values of $\sigma = 0.00232, 0.00310, \text{ and } 0.00405 \text{ kg/m}$ - chemically pure and technical toluene being mixed in different proportions. Under these conditions the other properties of the system, such as density and viscosity, remained virtually unchanged. The liquids were mixed in a vessel 200 mm in diameter by means of stirrer Model No. 3. The results of these experiments are plotted in Fig. 6. It follows from these results that the slope of lines remains almost constant at different stirrer speeds; the tangent of the angle of inclination is 0.50, i.e., $A = K_5 \cdot \sigma^{-0.5}$.

Density. It has been shown by previous investigators [3] that the phase-contact area is proportional to the density to the power 0.6. A similar power of ρ_{mix} is found from our experimental data on the influence of stirrer speed, stirrer diameter, and surface tension, with the aid of Equation (6).

If we equate the exponents of n , d_s , and σ in Equation (6) to the respective experimental values, we obtain three equations: $2m + l = 1.11$; $3m + l - 1 = 0.7$; $-m - l = -0.50$.

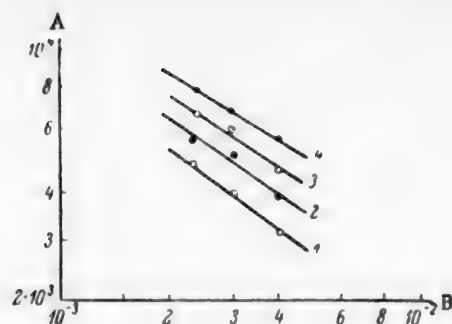


Fig. 6. Effect of surface tension on the phase-contact area with stirrer Model No. 3: A) phase-contact area (m^2/m^3); B) surface tension (kg/m) toluene - water: 1) $n = 700$ rpm; 2) $n = 800$ rpm; 3) $n = 1000$ rpm; 4) $n = 1200$ rpm.

Solving these equations in pairs, we obtain the following values: for m , 0.59, 0.61, and 0.6, average 0.6; for l , -0.07, -0.11, and -0.10, average -0.1. Therefore Equation (5) can be written as

$$A \cdot d_s = C_0 \cdot We^{0.5} \cdot Re^{0.1} \quad (8)$$

Generalization of the Experimental Results. The experimental data for each stirrer were plotted in the coordinates:

$$A \cdot d_s \cdot Re^{-0.1} \cdot \left(\frac{\alpha}{0.15} \right)^{-0.84} = f(We).$$

One such plot, for stirrer Model No. 3, is shown in Fig. 7. It can be seen that the experimental points are grouped

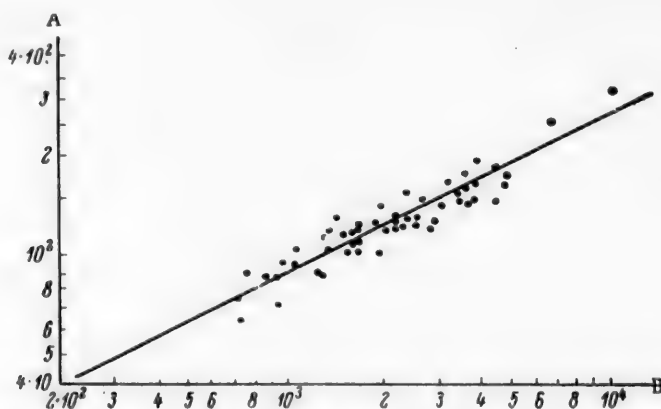


Fig. 7. Plot of $Ad_s Re^{-0.1} \left(\frac{\alpha}{0.15} \right)^{-0.84}$ against the Weber number for stirrer Model No. 3: A) values of $Ad_s Re^{-0.1} \left(\frac{\alpha}{0.15} \right)^{-0.84}$; B) Weber number.

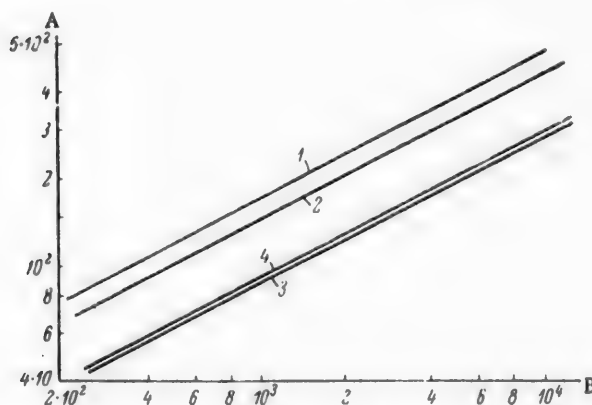


Fig. 8. Variations of $Ad_s \cdot Re^{-0.1} \cdot \left(\frac{\alpha}{0.15} \right)^{-0.84}$ with the Weber number for different stirrers: A) values of $Ad_s Re^{-0.1} \left(\frac{\alpha}{0.15} \right)^{-0.84}$; B) Weber number; models: 1) No. 1; 2) No. 2; 3) No. 3; 4) No. 4.

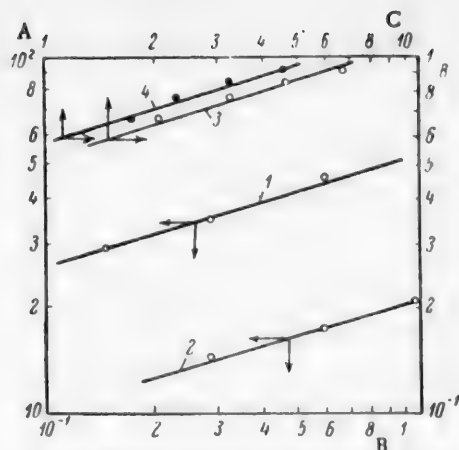


Fig. 9. Effect of power consumption of a 3-blade propeller stirrer on extractor efficiency and phase-contact area: A) phase-contact area (m^2/m^3); B) power consumption (in kg-m/sec); C) extractor efficiency; 1) toluene-water, $d_s = 0.066 \text{ m}$; 2) petrolatum-water, $d_s = 0.066 \text{ m}$; 3) water-n-butylamine-kerosene, $d_s = 0.01 \text{ m}$; 4) water-n-butylamine-kerosene, $d_s = 0.15 \text{ m}$.

satisfactorily around a straight line of slope 0.5, which satisfies the equation

$$A \cdot d_s \cdot Re^{-0.1} \cdot \left(\frac{\alpha}{0.15}\right)^{-0.84} = C_1 \cdot W_e^{0.5} \quad (9)$$

The average deviations of the points from the straight line does not exceed $\pm 13\%$. Similar relationships with the same slope were obtained for the 6-blade turbine stirrer, the 2-blade stirrer with vertical blades, and the 3-blade propeller stirrer (Fig. 8), leading to the general equation.

$$A \cdot d_s = C \cdot W_e^{0.5} \cdot Re^{0.1} \cdot \alpha^{0.84} \quad (10)$$

Values of the constant C, which characterizes the form of the stirrer, in Equation (10) are given below.

The relationship between the phase-contact area and the mixing conditions can be used in studies of mass-transfer processes. Overcashier, Kingsley, and Olney [14] studied the efficiency of extractors with mechanical stirrers, and determined the relationship between extractor efficiency ϵ (as a fraction of the theoretical step) and power consumption. To compare this relationship with the relationship between

Stirrer Model No.	Stirrer type	Number of blades	Values of constant C in Equation (10)
1	Turbine	6	25.9
2	With vertical blades	2	18.65
3	With blades set at 45° downward	2	13.65
4	Propeller	3	13.85

the phase-contact area and the power consumption, the data of Overcashier et al. [14] and our results were plotted in appropriate coordinates (Fig. 9); straight lines of equal slopes were obtained, showing that the phase-contact area has a determining influence on the extraction process, and that ϵ and A depend in the same manner on the power consumption.

LITERATURE CITED

- [1] V. V. Kafarov and S. A. Zhukovskaya, *J. Chem. Ind.* 2, 43 (1956).
- [2] B. M. Babanov and V. V. Kafarov, *Colloid J.* 20, No. 1, 121 (1958).*
- [3] T. Vermeulen, G. M. Williams, and G. E. Langlois, *Ch. Eng. Progr.* 51, 2, 85 (1955).
- [4] W. A. Rodger, V. G. Trice, and J. H. Rushton, *Ch. Eng. Progr.* 52, 12, 515 (1956).
- [5] G. E. Langlois, J. E. Gullberg, and T. Vermeulen, *Rev. Sci. Instr.* 25, 4, 360 (1954).
- [6] V. G. Trice and W. A. Rodger, *A. I. Ch. E. J.* 2, 2, 205 (1956).
- [7] R. B. Olney and G. J. Carlson, *Ch. Eng. Progr.* 43, 9, 473 (1947).

* Original Russian pagination. See C. B. Translation.

- [8] D. E. Mack and A. E. Kroll, Ch. Eng. Progr. 44, 189 (1948).
- [9] J. H. Rushton, E. W. Costich, and H. J. Everett, Ch. Eng. Progr. 46, 8, 395 (1950).
- [10] Standards in Chemical Equipment Construction [In Russian], 1 (Sci. Res. Inst. Chem. Equipment Construction, Mashgiz, 1950).
- [11] H. C. Foust, D. E. Mack, and J. H. Rushton, Ind. Eng. Chem. 36, 6, 517 (1944).
- [12] V. V. Kafarov, M. I. Gol'dfarb, and N. G. Ivanova, J. Chem. Ind. 7, 423 (1954).
- [13] A. Weissberger, Physical Methods of Organic Chemistry, 1 (IL, 1950) [Russian Translation].
- [14] R. Overcashier, H. A. Kingsley, and R. B. Olney, A. I. Ch. E. J. 2, 4, 529 (1956).

Received December 31, 1957

INVESTIGATION OF THE DUST-ABSORBING PROPERTIES OF SOLUTIONS OF WETTING AGENTS IN A DUST CHAMBER

S. Kh. Zakieva and A. B. Taubman

Institute of Physical Chemistry, Academy of Sciences, USSR

For removal of dusts liable to cause silicosis (quartz) or anthracosis (coal) in the course of mining operations, water is generally used in large quantities (by means of irrigated drilling, spaying, the use of water curtains, etc.). The dust-absorbing properties are improved by addition of wetting agents, which improve wetting and trapping of the solid particles by water. These agents include surface-active substances such as Sulfonol, OP-7, OP-10, DB, and others [1]. Practical experience with the use of such additives shows that the residual dust content of the shaft air can be reduced 2 to 3-fold and can often be brought to the permissible level [2].

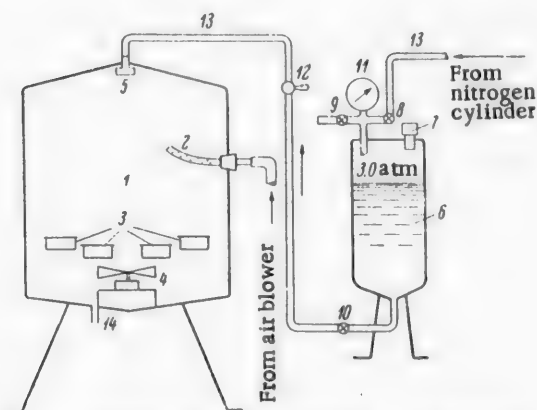


Fig. 1. Apparatus for determination of the dust-absorbing capacity of solutions of wetting agents in a dust chamber: 1) dust chamber; 2) sprayer; 3) receivers; 4) fan; 5) water jet; 6) tank with water or solution; 7) filling hole for tank; 8, 9, 10) valves; 11) monometer; 12) tap; 13) tube; 14) overflow.

It was shown earlier [5] that when solutions of wetting agents are used instead of water, organic particles of the wetting agent, which do not cause silicosis, are formed in the sprayed volume as the result of evaporation of the droplets; in consequence, counting methods give erroneous results in determinations of dust content and the dust-absorbing action of the solutions.

Moreover, gravimetric methods cannot be used in chamber tests, as the removal of air samples containing sufficient dust causes a considerable decrease of the dust concentration in the chamber.

We therefore developed a special method in which the dust-absorbing power of water and solutions of wetting agents is estimated from the turbidity of the suspensions formed by the dust trapped by the sprayed liquid.

Physicochemical studies and comparative evaluation of the dust-absorbing action of different wetting agents are of great importance in this connection.

Several wetting agents have been studied in detail by means of a dropping apparatus [3], in which floating dust particles are trapped by single drops of liquids falling through a dusty space; this study revealed the general laws governing the influence of wetting agents, in relation to their chemical composition and structure, the molecular nature and dispersity of the dust, and other factors, on the dust-absorbing properties of water.

In the present investigation we tested wetting agents in a laboratory dust chamber 1 m³ in capacity (Fig. 1); this investigation was of special interest because results obtained under conditions similar to the industrial conditions of dust removal by means of sprays in shafts are of greater practical significance than results obtained with the laboratory dropping apparatus.

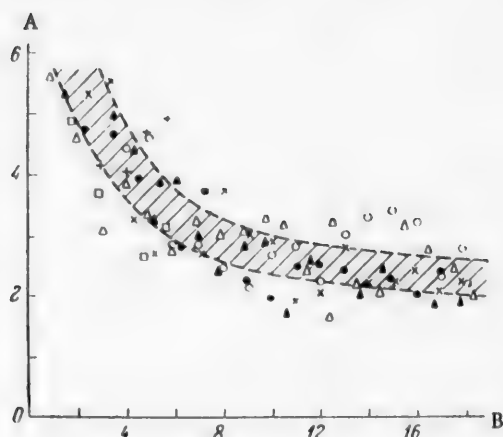


Fig. 2. Sedimentation curves of quartz dust in the dust chamber: A) dust content (in $n \cdot 10^{-4}$ particles/cm³); B) time τ (minutes).

The relative efficiency of dust removal (E) was defined as the ratio of the turbidity T_s of the suspension of dust in a solution of the wetting agent to the turbidity T_w of a suspension of dust in water [3]:

$$E = \frac{T_s}{T_w}$$

Since the dust concentration changes continuously during the experiment as the result of sedimentation of the largest fractions, the determinations were started after 7-8 minutes, when the initial concentration could be regarded as almost unchanged. The sedimentation curves for quartz dust (Fig. 2) show that the initial dust content under these conditions was $2.5-3.0 \cdot 10^4$ particles per cm³. These determinations of the initial dust content of the chamber space were performed by the counting method with the aid of the VDK flow ultramicroscope [6]. Samples were taken from approximately half way up the chamber.

Effect of Concentration of RAS-Na Solution on its Dust-Absorbing Power

Concentration of wetting agent, C (%)	$E = \frac{T_s}{T_w}$	Dust
0 (water)	1.0	Quartz
0.25	1.37	Quartz
0.5	1.67	Quartz
1.0	1.85	Quartz
1.0	2.22	Coal

The chamber was sprayed by means of water jet under an excess pressure of 3.0 atmos; the water droplet diameter distribution was as follows: 30-50 μ 67.3%, 50-100 μ 12.1%, 100-200 μ 10.7% and > 200 μ 9.9%.

The materials used for the study were dust of Baleisk origin, containing about 60% SiO₂, and coal dust (from the "Yasinovka" pit of the Donets field) of a degree of dispersity corresponding to floating dust (10 μ and finer).

A weighed sample of dust (1.0 g in the case of quartz dust, and 3.0 g in the case of coal dust) was placed in the sprayer, which consists of a glass tube with internal projections and a porous filter plate sealed in at the base (to prevent ejection of dust in a continuous mass). About one minute before the start of the experiment, the fan was switched on; this caused vigorous turbulent motion of the air in the chamber, so that the dust was distributed uniformly throughout the chamber. The dust sample was then gradually blown out of the sprayer by means of an air stream from the air blower. When the process was complete, the sprayer was removed from the chamber, the opening was closed by means of a plug, and the fan was switched off.

After the dust had been allowed to settle quietly for 7 minutes, the spraying was started; for this, water (or a solution of wetting agent) was fed into the jet from the tank at 3 atmos excess pressure. As the jet was turned on, the lids of the receivers were opened (by means of a device outside the chamber) and a sample was taken during one minute. The suspension, collected from four receivers, was transferred to a measuring flask. In experiments on spraying with pure water, the wetting agent was added to the suspension to act as a stabilizer. A blank experiment for determination of the correction for free-settling dust was performed in parallel with the main experiment. The turbidity of the suspensions was determined by means of the "NMF" nephelometer.

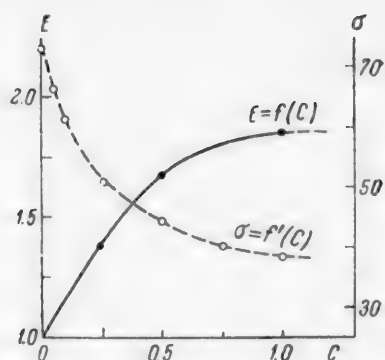


Fig. 3. Effect of concentration of RAS-Na solution on its dust-absorbing power: E) dust-absorbing power; C) concentration of wetting agent (%); σ) surface tension (ergs/cm²).

surface-active substances used as wetting additives in water, used for removal of dusts liable to cause silicosis or anthracosis in mining operations and coal winning.

2. The new synthetic wetting agent RAS-Na is an effective additive, which increases the dust-absorbing power of water.

LITERATURE CITED

- [1] L. I. Baron, Prevention of Silicosis and Anthracosis in Mining Operations [in Russian] (Coal Technology Press, 1954).
- [2] L. I. Baron, Control of Silicosis, 2 [in Russian] (Izd. AN SSSR, 1955), p. 71.
- [3] A. B. Taubman and S. A. Nikitina, Control of Silicosis, 2 [in Russian] (Izd. AN SSSR, 1955).
- [4] A. B. Taubman and S. A. Nikitina, Proc. Acad. Sci. USSR 110, 600, 816 (1956). **
- [5] S. A. Nikitina, A. B. Taubman and S. Kh. Zakieva, Control of Silicosis 3, [in Russian] (Izd. AN SSSR, 1957).
- [6] B. V. Deryagin and G. Ya. Vlasenko, Control of Silicosis, 2 [in Russian] (Izd. AN SSSR, 1955), p. 223.
- [7] A. Ya. Larin, Technological Cooperation 1, 25 (1957); M. A. Geiman, A. Ya. Larin, V. B. Shneerson, and R. A. Fridman, Trans. Inst. Petroleum Acad. Sci. USSR 6, 159 (1954).
- [8] S. A. Nikitina and A. B. Taubman, Proc. Acad. Sci. USSR 116, 113 (1957). **

Received December 31, 1957

* We thank A. Ya. Larin for kindly providing the wetting agent.

** Original Russian pagination. See C. B. Translation.

METHODS FOR CALCULATION OF MASS TRANSFER IN EQUIPMENT WITH CONTINUOUS VARIATION OF DRIVING FORCE IN APPARATUS OF THE STEPWISE TYPE

V. M. Govorkov and Ya. D. Averbukh

In the paper by Planovskii and Kasatkin, entitled "Methods for expressing the driving force of diffusional processes" [1], the minimum distinction is made between the calculation methods for the above-named types of equipment.

As we consider it necessary and useful to distinguish between these respective calculation methods, we share the views of Stabnikov [2] put forward in his comments on the cited paper [1], concerning the suitability of the concepts of "theoretical plate" and "plate efficiency", i.e., the view that concepts characteristic of the operation of apparatus of the stepwise type should be retained. Disregard of the distinction between calculation procedures for apparatus of the stepwise type and apparatus with continuous variation of the driving force, and, even more, formal application of the calculation methods used for one type to the other, is unrealistic and unproductive.

In equipment of the packed or spray (nonsectional) type, such as the absorber shown in Fig. 1, the difference between the concentrations of the absorbed substance in the gas and the liquid, i.e., the driving force of absorption, varies continuously and steadily during the process and conforms to a general law at any region of the packing, however small its height and however small its absorption area. It is because of this condition that the dimensions of the apparatus can be determined by integration of the original equation for mass-transfer rate

$$-Gdy = Ldx = K_F dF(y - y^*) \quad (1)$$

between y_i and y_f .

In Equation (1) Gdy represents the amount of substance absorbed by the liquid from the gas in unit time over area dF ; K_F is the absorption rate coefficient per unit area of packing, and $(y - y^*)$ is the driving force of the process, which varies from $(y - y^*)_i$ to $(y - y^*)_f$, where y is the existing concentration of the absorbed substance in the gas, and $y^* = f(x)$ is the concentration of this substance over the surface of the liquid, in equilibrium with the concentration of the latter.

If the relationship between y^* and x is linear, integration of Equation (1) yields the formula for calculation of the packing area

$$F = \frac{G(y_i - y_f)}{K_F \Delta y_{av}}, \quad (2)$$

where Δy_{av} is the average driving force for the process as a whole, given by the expression

$$\Delta y_{av} = \frac{(y - y^*)_i - (y - y^*)_f}{\ln \frac{(y - y^*)_i}{(y - y^*)_f}}.$$

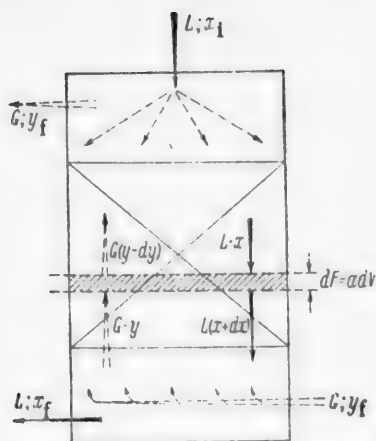


Fig. 1. Diagram of packed absorber.

course of the process, is met in equipment of the plate or sectional type.

Here the physical separation of the equipment into plates or sections results in movements of the gas and liquid which, although similar and repeated at each plate or in each section, do not ultimately combine into a single, monotonic, and internally entirely continuous motion. Accordingly, the concentration variations, which conform to similar laws within each stage of the apparatus (plate or section), do not as a whole constitute a truly continuous variation along the entire apparatus, which conforms within the apparatus as a whole to laws operative within each stage. The sum of such consecutive concentrational changes cannot be expressed by integration for the whole volume or the whole surface of the apparatus, as is done for internally continuous steady processes in packed or sprayed scrubbers. Other methods for calculation of the equipment dimensions should be and are applied in this case.

Calculations relating to equipment of the stepwise type are based on the number of required sections or plates. The method of "theoretical contacts" is widely used. This is based on the concept of a "theoretical contact" (theoretical plate), corresponding to contact between the gas and liquid such that a state of equilibrium is reached at the exit between the concentrations of the mass-transfer phases.

The number of contact units (plates or sections) actually required is determined as follows: the required number of theoretical contact units is found by well-known methods, and divided by the experimental value for the efficiency of the contact unit*.

This calculation method for equipment of the stepwise type takes into account the specific stepwise variations of the driving force in the process, but it cannot be regarded as fully satisfactory. The main defect of this method is that the value of the efficiency, common for all the contact units, used in this instance, i.e., the ratio of the number of theoretical contact units to the number required in practice:

$$\eta_0 = \frac{n_{\text{theor}}}{n_{\text{pract}}},$$

is a formal concept which does not reflect the nature of the mass-transfer processes in the contact stage.

If the relationship is nonlinear

$$y^* = f(x) \dots$$

* In our opinion, the "over-all efficiency" of the apparatus is a better term here than the efficiency of the contact unit.

** In rectification equipment there is always a curvilinear relationship between the equilibrium concentration y^* and the liquid concentration x , as they are taken at varying boiling points.

the over-all efficiency of the contact unit also depends on the concentrations of the absorbed component over given sections of the process. In consequence the over-all efficiency must differ for different contact units at different heights of the apparatus, and also for the experimental and planned apparatus when used in different ranges of concentration.

A more rational method for calculation of stepwise equipment is based on the concept of local plate efficiency, introduced by Murphree in 1925.

The local efficiency represents the actual approach of the mass-transfer phases to a state of equilibrium, resulting in the given contact unit, and is therefore a distinctive measure of the contact efficiency.

In contrast to over-all efficiency, the local contact efficiency is, under certain conditions, independent of the concentration of the transferred substance and under given hydrodynamic conditions it is constant for all the contacts of the apparatus [3]. For example, in rectification columns under the condition that the vapor and liquid are completely mixed within the contact unit, which is very nearly true in a number of cases (Fig. 2), we have

$$\frac{y_{n+1} - y_n}{y_n^* - y_n} = \eta_{loc} = 1 - e^{\frac{-K_F F}{G}} = \text{const}, \quad (3)$$

where F is the phase-contact area on the plate, and K_F is the mass-transfer coefficient per unit of this area.

Despite the difficulty of determining $K_F F$ under bubbling conditions, Equation (3) is valuable in that it provides a connection between local efficiency and the fundamental mass-transfer Equation (1), and therefore gives a definite relationship between local efficiency and actual operating conditions.

Constancy of η_{loc} is the basis of the method used for determination of the actual number of contact units necessary. In this case (Fig. 2) curve III, the line for the actual vapor composition, corresponding to the expression

$$y' = \varphi(x) = y + (y^* - y) \eta_{loc}$$

is drawn between the operating line I and the equilibrium curve II.

The graphical construction for determination of the number of contact steps from the operating line I and the actual vapor composition curve III is analogous to that used for determination of the number of theoretical plates, but this construction gives the number of actual contact units necessary.

Thus, because of the difference between the course of processes in packed equipment (with continuous variation of the driving force, both over the apparatus as a whole and over any part of the packing) and in apparatus of the stepwise type (with stepwise variations of the driving force), the calculation methods used differ in principle.

Both these methods involve certain difficulties in design calculations, primarily because it is necessary to use values determined experimentally, but each one is a correct reflection of the specific character of the process in the particular kind of apparatus to which it is applied, and therefore these methods have a real basis for further improvement and extension. Procedures in which these calculation methods are mixed, and in which calculation techniques for equipment of the one group are applied to equipment of the other groups, must be regarded as purely formal and unproductive.

Procedures for combining (or, more correctly, mixing) calculation methods suitable for equipment of the packed and stepwise types respectively, with the aid of the concept of the transfer unit, are now being widely advocated.

The packing area of the apparatus can be written as $F = aSH^2$, where a is the specific surface of the packing (in m^2/m^3), S is the cross-sectional area of the apparatus (in m^2) and H is the packing height (in m).

With the aid of Equation (1) the packing height can be expressed as follows:

$$H = \frac{G}{aSK} \int_{y_i}^{y_f} \frac{dy}{y - y^*}. \quad (4)$$

In this last expression

$$\int_{y_1}^{y_f} \frac{dy}{y - y^*} = \frac{y_1 - y_f}{(y - y^*)_{av}} = m \quad (5)$$

\underline{m} is known as the total number of transfer units, and represents the change of the actual concentration of the transferred substance per unit average driving force of the process. Introduction of \underline{m} into Equation (4) gives

$$H = \frac{G}{aSK_F} m,$$

where the term $\frac{G}{aSK_F}$ represents the section of the packing height \underline{h} , over which the change of the active concentration of the transferred substance is equal to the driving force of the process; this is termed the height of a transfer unit.

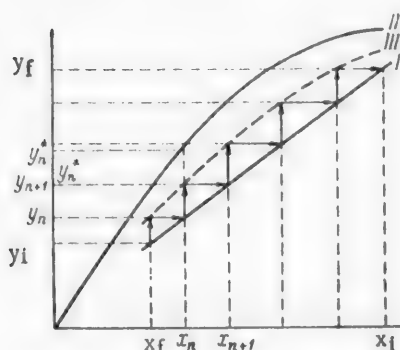


Fig. 2. Calculation of the number of contacts actually necessary: I) operating line: $y = ax + b$; II) equilibrium curve: $y^* = f(x)$; III) curve for the actual vapor composition: $y' = \varphi(x)$.

Since the height of a transfer unit is constant over any section of the packing for an apparatus of given design operating under given hydrodynamic conditions, i.e., at constant mass-transfer coefficient K_F and constant \underline{a} and G , determination of the height of a transfer unit is very simple. The total packing height is

$$H = \underline{h} m \quad (6)$$

where \underline{h} , the height of a transfer unit, can be found experimentally, and \underline{m} , the number of transfer units, can be calculated by different methods.

As is known, if the relationship $y^* = f(x)$ is linear, \underline{m} can be calculated directly by integration of Equation (5), and if the equilibrium relationship is nonlinear, it can be found by graphical integration or by special construction (graphical solution) with the aid of the equilibrium and operating lines [4].

Continuous variation of the driving force of the process is assumed in Equation (1) and in Equation (4) and (5), derived from it. Therefore, whatever the method used for determining the number of transfer units, it must be remembered that the real basis of the method is continuous variation of the driving force, conforming to a common law along the entire apparatus, and this is only true for apparatus of the packed or spray types.

Therefore, the method of transfer units is in principle applicable to apparatus of these types.

As already stated, stepwise equipment (of the bubbling and mechanical types) is characterized by peculiar discontinuous variations of the driving force, radically different from variations of the driving force in packed apparatus. Although the graphical representation of the driving force of the process has the same external appearance for both types of apparatus, the meaning of the respective diagrams is entirely different. Whereas the operating line for a packed apparatus can be regarded as a graphical representation of the continuous variation of the concentrations of the mass-transfer phases along the entire path of their contact, i.e., at any region of the packing surface, the operating line for a stepwise apparatus represents only the relationship between the concentrations in the spaces between the contact units, and does not reflect this relationship within the contact unit (Fig. 3), since here the phases are not truly countercurrent. Therefore integration of the expression $\frac{dy}{y - y^*}$ [Equation (5)], which is the basis of the concept of a transfer unit, in the limits representing the driving force in the inter-contact spaces, is a purely formal operation in which the real process conditions are disregarded. This applies equally to integration in the limits $(y - y^*)_1 - (y - y^*)_n$, when the number of transfer units of the whole apparatus is determined, and to integration in the limits $(y - y^*)_{n+1} - (y - y^*)_n$, when the number of transfer units corresponding to one contact unit is determined.

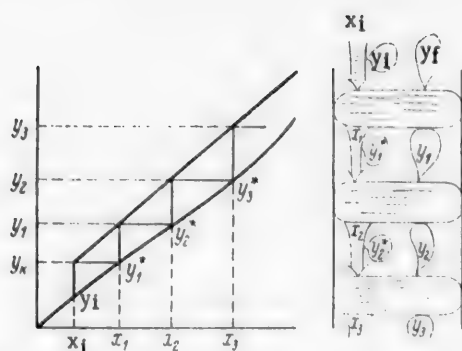


Fig. 3. Schematic diagram of stepwise apparatus and section of the diagram for graphical determination of the number of theoretical plates.

recommended by Kasatkin [5] for calculations relating to packed towers when the equilibrium relationship is nonlinear is very doubtful. It is recommended to find the number of theoretical plates ("concentration steps") by the usual graphical method with the aid of the operating and equilibrium lines, and then to find the corresponding number of transfer units for each theoretical plate. The packing height is then given as the product of the sum of the transfer units for all the theoretical plates and the height of a transfer unit.

It is easy to see that this method has the same disadvantages as the method of the equivalent packing height, and is hardly more convenient to use than direct graphical integration of Equation (1).

The graphical method proposed by Kasatkin [5] for determination of the number of plates in a rectification column, based on the concept of transfer numbers, is applicable in principle to stepwise equipment, since its basis is analysis of mass-transfer conditions on the plate itself.

However, even in this case the use of the transfer-unit concept has not made the calculations more precise than calculations with the aid of the local plate efficiency. It is easy to see that the same result is obtained in calculations based on transfer units and on local efficiency, as Cy^{**} is a transformed expression of the latter.

Thus, use of the transfer-unit concept introduces nothing new into calculations relating to equipment of the sectional type, either with regard to accuracy or with regard to correspondence of the calculation method to the true course of the process.

We must point out that the long-established method for calculations of packed towers in terms of the number of theoretical plates ("concentration steps") is equally erroneous in this respect.

In this case the number of theoretical plates is determined by graphical construction. An experimental value — the equivalent packing height — is then introduced; this is multiplied by the number of plates found, to give the total packing height in the apparatus.

This method for calculating the height of packed equipment is very simple, but the results are often insufficiently accurate, and therefore it should be abandoned.

This calculation method will always give equal numbers of theoretical plates for packed towers operating under the most diverse conditions, but with particular substances within given concentration ranges. Neither the packing characteristics nor the hydrodynamic regime in the apparatus are reflected in the number of theoretical plates; they must be taken into account by means of the experimental value for the equivalent packing height.

Thus, with this method for calculation of packed towers we not only arbitrarily distort the course of the process, but also lose touch to a considerable extent with the actual operating conditions, and lose the possibility of determining clearly the influence of different operating conditions on the efficiency of the apparatus.

* The fact that n_0 is not constant when the equilibrium relationship is nonlinear is also evident from Equation (18-36) recommended [4] for determination of n_0 .

** See Equation (3-153a) in A. G. Kasatkin's book [5].

It is evident that successful calculations of packed towers, based on the number of theoretical plates require extensive investigations of the relationship between the equivalent packing height and the actual operating conditions. However, even if such investigations are carefully performed, the calculation method will be inaccurate in the majority of cases, namely, when the equilibrium relationship $y^* = f(x)$ (Fig. 2) is represented by a curve.

By using the equivalent packing height in the calculation, we assume that the same packing area is equivalent to each theoretical plate (step). However, packing areas equivalent to individual theoretical plates will be equal only if the equilibrium relationship is linear, as can be easily shown if Equation (1) is applied to each plate separately. If the relationship $y^* = f(x)$ is nonlinear, the packing areas equivalent to individual theoretical plates will not be equal to each other, so that it is obviously impossible to estimate the latter in terms of the same equivalent packing height. When $y^* = f(x)$ is nonlinear, each theoretical plate is equivalent to a different packing height, dependent on the phase concentration at the given step, and the substitution of equal packing regions for all the theoretical plates in calculations relating to packed towers, i.e., introduction of a certain constant equivalent packing height, is incorrect, to say nothing of the crude formality of this procedure.

Therefore the concept of the equivalent packing height should be rejected in calculations relating to packed towers; it is valid only if the equilibrium relationship is linear, and does not make the calculations any simpler than the direct use of Equations (1) and (2).

Since the physical nature of the process should be reflected in the calculations, the following conclusions may be drawn.

1. Calculations relating to mass-transfer equipment with continuous variations of the driving force should be based on the fundamental mass-transfer Equation (1). If the equilibrium relationship is linear, the value of the average driving force may be used in the calculations; if it is nonlinear, graphical integration of Equation (1) is necessary. In this case the transfer-unit method is a variant of the fundamental method, and is suitable whenever the process conditions make clear definition of the phase-contact area difficult.
2. Calculations relating to equipment of the stepwise type, with peculiar stepwise variations of the driving force, should be performed graphically, with the aid of the concept of local plate efficiency.
3. Mixing of these two methods is a formal device, which does not represent the nature of the processes and is therefore unproductive.

LITERATURE CITED

- [1] A. N. Planovskii and A. G. Kasatkin, *Chem. Ind.*, 9 (1953).
- [2] V. N. Stabnikov, *Chem. Ind.*, 7 (1955).
- [3] W. K. Lewis, *Ind. Eng. Chem.*, 2, 4 (1936).
- [4] A. N. Planovskii, V. M. Ramm, and S. Z. Kagan, *Processes and Equipment of Chemical Technology* [in Russian] (Goskhimizdat, 1955).
- [5] A. G. Kasatkin, *Principal Processes and Equipment of Chemical Technology* [in Russian] (Goskhimizdat, 1955).

Received November 10, 1957

GENERAL FORM OF CRITERIAL EQUATIONS FOR MASS TRANSFER IN EQUIPMENT WITH FIXED INTERFACIAL AREA

L. D. Berman

In a recent paper Kafarov [1] stressed the great practical importance of the similarity principle for investigations of processes and equipment in chemical technology.

At the same time, attention should be drawn to the tendency to overestimate its role and potentialities which is apparent in a number of publications. The similarity theory, which provides a strict scientific basis for analysis of experimental data and which in that sense is a powerful research tool, can only yield generalized expressions of the relationships between the quantities chosen as measures of a given process. The range of applicability of the quantitative expressions so obtained proves to be much wider than the applicability ranges of purely empirical formulas. However, the similarity theory is applicable only when a correct model of the given process has been constructed, and when the principal parameters required for definition of the given class of phenomena have been determined [2]. Studies of the mechanism and general laws governing the phenomena in question are within the scope of special theoretical and experimental investigations.

If a system of similarity criteria, adopted without adequate analysis of the mechanism of the effect under consideration, is used for analysis of experimental data, the consequence is, as has been pointed out earlier [3-5], that the experimental relationships so obtained do not in reality have the advantages characteristic of criterial equations. Moreover, a quantitative relationship which is in essence purely empirical, but which is presented in the form of an equation, involving criteria which do not reflect sufficiently fully the characteristics of the given phenomenon, gives rise to the wrong idea that it can be extended to conditions other than those under which the experiments were carried out. This leads to improper practical use of such an empirical relationship, which has only a very limited range of applicability.

Such errors stem, in particular, from the widely held but incorrect concept that the equation connecting the criteria from mass transfer in conditions of a fixed interphase area (surface absorbers, wetted-wall equipment, surface rectification and condensation equipment, etc.) have the general form for a given phase (liquid or gas)

$$Nu_D = A \cdot Re^m \cdot Pr^n_D, \quad (1)$$

analogous to the heat-transfer equation:

$$Nu = A \cdot Re^m \cdot Pr^n, \quad (2)$$

where $Nu_D = \frac{Bl}{D}$ is the Nusselt diffusion criterion * (or the Sherwood criterion Sh), $Re = \frac{wl}{\nu}$ is the Reynolds criterion

* We cannot agree with the interpretation of the physical meaning of the Nusselt and Reynolds criteria given in the review in question [1]. The author considers that the Nusselt criterion is "a quantitative measure of the increase of mass (or heat) transfer due to turbulence, relative to purely molecular transfer" and that the Reynolds criterion is "a quantitative measure of the ratio between turbulent and molecular friction forces." If this were true, these criteria could not have finite values and they could not be used under conditions of purely laminar liquid flow, in absence of turbulent transfer (of momentum, mass, or heat). In reality, Re is a measure of the ratio of the inertia forces in the stream to the forces of internal friction. With regard to Nu_D (or Nu), this criterion follows from a purely formal definition of the coefficient of mass transfer (or heat transfer) which does not reflect the true nature of the relationship between the flow rate of mass (or heat) and the process conditions [2].

$Pr_D = \frac{\nu}{D}$ is the Prandtl diffusion criterion (or the Schmidt criterion Sc); $Nu = \frac{\alpha l}{\lambda}$ is the Nusselt thermal criterion, $Pr = \frac{\nu}{a}$ is the Prandtl thermal criterion, β is the mass-transfer coefficient, D is the diffusion coefficient, ν is the coefficient of kinematic viscosity, α is the heat-transfer coefficient, λ is the coefficient of thermal conductivity, l is the determining linear dimension, and a is the coefficient of temperature conductivity.

In reality, although Equation (1) can be applied in many cases of practical importance, it refers only to certain definite conditions. Its unjustified extension to other conditions sometimes leads to the result that relationships of this type derived by different authors differ substantially from each other, or even that the experimental results cannot be interpreted at all with the aid of such equations.

In the general case, the criterial equation for mass transfer for a fixed interfacial area should include, in addition to Re and Pr_D , other determining criteria, the role of which under certain conditions may be very considerable. This will be demonstrated below for mass transfer in a gas phase, which constitutes a mixture of several components in the case under consideration; we shall postulate a binary mixture.

It must be pointed out in this connection that we cannot agree with the approach, which is sometimes used, whereby separate consideration of mass-transfer in two interacting phases is identified with utilization of the so-called film theory [6]. The film theory of Lewis and Whitman [7, 8], which has for a long time been meeting with valid objections [6, 9], some of which have been put forward by the present author [5, 10, 11], is based on an oversimplified model of the phenomenon. According to this theory, on each side of the interface, there is a diffusion layer or "film" which separates the main mass of each phase from the interface, and it is assumed that the concentration of the active component of the mixture changes only within the limits of the "film" and that only molecular diffusion of the active component occurs in the film. Rejection of this model, which does not reflect the whole complexity of the phenomenon, especially with turbulent flow of the mixture, does not, however, necessarily mean that separation of the total resistance to mass transfer into its components corresponding to the liquid and gas phases should be abandoned, as this has been adequately justified on physical grounds for many types of equipment. The transfer resistance at the interface is usually slight and, as has been confirmed experimentally [12, 13], it may be disregarded in such cases. The same applied in many cases to the influence of mechanical interaction between the phases [3, 14]. In cases when the influence of the pressure drop at the interface, which depends on the magnitude of the accommodation coefficient, is considerable, as in instances when the absolute pressures are low, the resultant additional resistance must be taken into account and added to the other partial resistance. This additivity of partial resistances to transfer in presence of considerable resistance at the interface has been confirmed by recent experiments [15].

In returning to the question of similarity criteria for mass transfer in the gas phase, attention must be drawn to the following characteristics of the mechanism of this process in presence of a fixed interfacial area which are not taken into account in Equation (1).

1. Transverse flow of the substance (active component of the mixture) i.e., flow directed normally toward the interface, influences the fields of longitudinal velocities and partial pressures or concentrations of the mixture; if the direction of transverse flow of the substance is away from the surface (as in desorption, evaporation, etc.) and the concentration of the active component of the mixture remains unchanged at the interface, increase of the mass-transfer rate leads, as a rule, to increases in the thickness of the hydrodynamic and diffusional boundary layers and to decreases of the velocity and partial-pressure (concentration) gradients at the interface; the reverse is the case if the transverse flow of the substance is directed toward the interface (as in absorption, condensation, etc.)

2. In view of the fact that the interface is usually impermeable to the inert component of the mixture, additional molecular flow of the substance, of the so-called Stefan type, takes place.

3. If the total rate of transverse flow of the substance is sufficiently high, superposed on the main flow of the mixture along the interface, the transfer mechanism may itself remain unchanged mainly because free turbulence arises in the layer of mixture immediately adjacent to the interface.

Because of these features of the mass-transfer process under the conditions in question, the analogy breaks down between it and pure heat transfer to which Equation (2) relates; the more intensive the mass transfer, i.e.,

the greater the density of transverse flow of the substance, the less does the analogy apply. If these features are taken into account in the derivation of the original differential equations (equations of motion*, continuity, and diffusion) and in determination of the boundary conditions, then the criterial equation for steady mass transfer in forced motion assumes the form [3, 16, 17]

$$Nu_n^* = Nu_D \cdot \epsilon_{cr} = \Phi \left(Re, Pr_D, \Pi_n, \frac{R_t}{R} \right) \quad (3)$$

or, if the criteria are so transformed that the criterion to be determined does not contain independent variables, while the determining criteria, on the contrary, contain only such variables following from the conditions:

$$Nu_n = \Phi \left(Re, Pr_D, \Pi_n, \epsilon_G, \frac{R_t}{R_G} \right), \quad (4)$$

where

$$\Pi_n = \frac{g_t l}{\nu \gamma}; \quad \Pi_n = \frac{\Delta p_t}{p}$$

and R , R_t and R_G are the gas constants for the mixture and its active and inert components respectively; $\epsilon_G = \frac{p_G}{p}$ is the volume (molar) content of the inert component of the mixture; g_t is the density (gravimetric) of the transverse flow of the substance; ν and γ are the coefficients of kinematic viscosity and density of the mixture; Δp_t is the difference between the partial pressures of the active component of the mixture in the main mass and at the interface; p is the total pressure of the mixture.

If the process is anisothermal, i.e., mass transfer occurs simultaneously with the heat transfer, but the conditions are such that the additional effects caused by superposition of molecular phenomena (thermal diffusion, heat transfer by diffusion, and barodiffusion) and variability of the physical constants may be disregarded, which is permissible in many practical cases, then Equations (3) and (4) remain valid. However, Equation (2) cannot be applied to the accompanying heat transfer, as the transverse flow of the substance changes the hydrodynamic conditions and the temperature field, and thereby evidently affects not only the mass-transfer rate but also the heat-transfer rate. If the transverse flow is directed away from the interface, increase of its density decreases the heat-transfer coefficient, while if it is directed toward the interface increase of its density increases the heat-transfer coefficient. The criterial equation for heat transfer accompanying mass transfer differs from Equation (2) and is of the form [3, 16, 17]

$$Nu = \Phi \left(Re, Pr, \Pi_n, \frac{c_{pt}}{c_p} \right), \quad (5)$$

where c_p and c_{pt} are the heat capacities of the mixture and of its active component.

* In the case of transverse flow of the substance, the equation of motion may be written in a form in which at first sight it does not differ from the usual Navier-Stokes equation, and which would not seem to yield an additional similarity criterion characterizing the hydrodynamic conditions (the Π_w criterion). For example, in the case of steady flow of a binary mixture along a plane surface, we can write the following equation, even in presence of mass transfer (the x axis is the direction of flow and the y axis is normal to the surface):

$$w_x \frac{\partial w_x}{\partial x} + w_y \frac{\partial w_x}{\partial y} = X - \frac{1}{\rho} \frac{\partial p}{\partial x} + \nu \left(\frac{\partial^2 w_x}{\partial x^2} + \frac{\partial^2 w_x}{\partial y^2} \right).$$

However, in the case under consideration this equation differs from the Navier-Stokes equation in that here w_y is not the true velocity of the medium (mixture) in the y direction, but the velocity of Stefan flow, connected with the velocity of the actual transverse flow w_t of the active component of the mixture by the relationship

$w_y = w_t \frac{\rho_t}{\rho}$ where ρ and ρ_t are the densities of the mixture and its active component, respectively. The apparent velocity of the inert component in the y direction, normal to the interface impermeable to it, is zero.

It was noted earlier that free turbulence may arise if the transverse flow rate of the substance in the layer of mixture adjacent to the interface is high enough [18]. As the corresponding turbulent-exchange coefficient should then depend on Π_w and Re , the influence of turbulence of the layer of mixture adjacent to the interface on the rates of heat and mass transfer may be taken into account with the use of Equations (3)-(5) without introduction of additional determining criteria [4, 19].

Only with very dilute mixtures, in which the concentration of the inert component ϵ_G is close to unity, or at small differences Δp_t of partial pressure, when the density of transverse flow of the substance is also small, it is possible to disregard the additional criteria in Equations (3)-(5) and to use expressions of the type (1) for isothermal mass transfer, and of types (1) and (2) for simultaneous mass-transfer and heat-transfer processes.

Analysis of experimental data on the condensation of water vapor containing an admixture of air ($\epsilon_G = 0.01$ and over) on horizontal pipes [20, 21] confirmed that such mass-transfer data are satisfactorily represented for the Re region between 350 and 11000 by the equation

$$Nu_D = C \cdot Re^{0.5} \cdot \Pi_g^{-1/3} \cdot \epsilon_G^{-0.6}, \quad (6)$$

where $C = 0.47$ for a single pipe.

The Prandtl diffusion criterion and the ratio $\frac{R_t}{R_G}$ were almost constant under these experimental conditions, and had the values $Pr_D \approx 0.55$ and $\frac{R_t}{R_G} = 1.61$. If on the basis of other experimental results we introduce $Pr_D^{0.4}$ into the equation, we have

$$Nu_D = C_1 \cdot Re^{0.5} \cdot Pr_D^{0.4} \cdot \Pi_g^{-1/3} \cdot \epsilon_G^{-0.6}, \quad (6a)$$

where $C_1 = 0.60$ (for a single pipe).

These experimental data demonstrate the erroneous character of a recently published and inadequately thought out assertion [22] that in systems in which viscosity depends little on ϵ_G , which include the system water vapor-air, the concentration of the active component of the mixture should have little influence on the mass-transfer rate. These results also explain why in some instances experimental data on mass transfer can be represented by means of Colburn's formula [23] although, as has been pointed out [24], there are several errors in its derivation.

Colburn concluded on the basis of the film theory that the influence of transverse flow of the substance can be taken into account merely by introduction of the term $\left(\frac{p_{ga}}{p}\right)^{-1}$ into Equation (1), i.e.,

$$Nu_D = \left(\frac{p_{ga}}{p}\right)^{-1} \cdot \Phi(Re, Pr_D), \quad (7)$$

where p_{ga} is the mean logarithmic value of the partial pressure of the inert component of the binary mixture in the gas film.

When $Pr_D \approx \text{const}$, Equations (6) and (7) can be reduced to the form

$$Nu_D = C \cdot Re^{0.5} \cdot \Pi_g^{-0.933} \left(\frac{\Pi_g}{\epsilon_G}\right)^{0.6}, \quad (6b)$$

$$Nu_D = B \cdot Re^{0.5} \cdot \Pi_g^{-1} \cdot \ln \left(1 + \frac{\Pi_g}{\epsilon_G}\right). \quad (7a)$$

It follows that if the experiments are so conducted that the ratio $\frac{\Pi_g}{\epsilon_G}$ remains constant or varies within a relatively narrow range, i.e., when $\frac{\Pi_g}{\epsilon_G} \approx \text{const}$ and $\ln \left(1 + \frac{\Pi_g}{\epsilon_G}\right) \approx \text{const}$, the difference between the two equations

is slight. Such conditions applied, for example, to the experiments of Cairns and Roper [4, 25] who studied evaporation with low contents of the inert components in the vapor-gas mixture, so that their results could be represented by an equation of type (7), with only a modification of the exponent of $\frac{p_{ga}}{p}$. But the relationship so obtained cannot be extended to conditions characterized by substantially different values of $\frac{\pi_g}{\epsilon_G}$. In the general case, the introduction of only one additional argument $\frac{p_{ga}}{p}$ into the criterial equation is insufficient. The same may be said of attempts to use, as the sole additional argument, the ratio and even more so, a temperature criterion of the parametric type $\frac{T-T_w}{T}$ (where T and T_w are the absolute temperatures of the vapor-gas mixture and the wet-bulb thermometer respectively).

LITERATURE CITED

- [1] V. V. Kafarov, *J. Appl. Chem.* 30, 1449 (1957). *
- [2] A. A. Gukhman, *Physical Principles of Heat Transfer* [in Russian] (ONTI, 1934).
- [3] L. D. Berman, *Heat and Power Engineering* 5, 25 (1954).
- [4] L. D. Berman, *Heat and Power Engineering* 5, 30 (1956).
- [5] L. D. Berman, *J. Appl. Chem.* 28, 138 (1956). *
- [6] *Questions of Mass Transfer* [in Russian] (Goskhimizdat, 1957).
- [7] W. G. Whitman, *Chem. and Met. Eng.* 29, 146 (1923).
- [8] W. K. Lewis and W. G. Whitman, *Ind. Eng. Chem.* 16, 1215 (1924).
- [9] V. G. Lertsovich, *Physicochemical Hydrodynamics* [in Russian] (Izd. AN SSSR, 1952).
- [10] L. D. Berman, *Oxygen* 3, 34 (1948).
- [11] L. D. Berman, *Bull. VTI* 1, 18 (1948).
- [12] Ya. D. Zel'venskii, *J. Chem. Ind.* 14, 292 (1937).
- [13] T. G. Goodgame and T. K. Sherwood, *Chem. Eng. Sci.* 3, 37 (1954).
- [14] L. D. Berman, *Heat and Power Engineering* 6, 3 (1954).
- [15] T. K. Sherwood and N. E. Cooke, *A. I. Ch. E. J.* 3, 37 (1957).
- [16] L. D. Berman, *Heat and Power Engineering* 8, 10 (1955).
- [17] L. D. Berman, *Evaporative Cooling on Circulation Water* [in Russian] (Gosenergoizdat, 1957).
- [18] L. E. Kalikhman, *J. Tech. Phys.* 25, 1957 (1955).
- [19] L. D. Berman, *J. Tech. Phys.* 26, 2604 (1956).
- [20] L. D. Berman and S. N. Fuks, *Bull. VTI* 11, 11 (1952).
- [21] L. D. Berman, *Heat and Power Engineering* 6, 43 (1957).
- [22] L. E. Westkaemper and R. R. White, *A. I. Ch. E. J.* 3, 69 (1957).
- [23] A. P. Colburn, *Trans. Am. Inst. Chem. Eng.* 2, 174 (1933).
- [24] L. D. Berman, *Bull. VTI* 8, 11 (1947).
- [25] R. S. Cairns, and C. H. Roper, *Chem. Eng. Sci.* 3, 97 (1954).

Received December 14, 1957

* Original Russian pagination. See C. B. Translation.

APPARATUS FOR DETERMINATION OF LIQUID-VAPOR EQUILIBRIA •

I. N. Bushmakín

The Leningrad (Order of Lenin) State University

The most accurate liquid-vapor equilibria data possible were required in connection with our studies of rectification processes.

The literature contains very many descriptions of single-evaporation apparatus for determination of such data. We have studied the operation of a number of the most typical of these instruments. It was found that in many types of apparatus it is possible to obtain accurate data on liquid-vapor equilibria, but the apparatus must be used within a narrow range of conditions characteristic for its design and dimensions. The optimum conditions may vary from one system to another. Searches for the optimum conditions involve the performance of numerous experiments and the consumption of large amounts of materials.

The Scatchard apparatus [1] stands out among the others. With it searches for optimum conditions are not needed. The only necessary conditions are good heat insulation, and boiling at not excessively low rates (when the Cottrell pump does not work) nor at very high rates (when distillate spray is carried over into the trap). The main disadvantage of the Scatchard apparatus is that the boiling rate must remain strictly constant during an experiment (with solutions boiling at high temperatures). With the slightest fluctuation of the boiling rate, the complex equilibrium between the two liquids and the vapor breaks down, and the results given by the apparatus are not quite correct. Therefore the results of equilibrium determinations with this apparatus are not quite the same in duplicate experiments. The Scatchard apparatus may be described as reliable (the results obtained with it are free from gross errors), but not absolutely accurate.

Since the different types of apparatus described in the literature did not satisfy our requirements, we designed two pieces of apparatus ourselves.

All the determinations of liquid-vapor equilibrium described in this series of papers were performed with the apparatus which we shall refer to as the "old" apparatus. The design of this apparatus is briefly described in Communication I [2].

Since the publication of that communication we had gained experience in the use of the apparatus and certain modifications had been introduced into the procedure; for that reason, and also to demonstrate the advantages of the new apparatus over the old, we shall briefly discuss some characteristics of the old apparatus. A diagram of the apparatus is given in Fig. 1. Its advantage over similar apparatus, described in the literature (by Othmer [3], Kireev [4], and Lang [5]), is that during its operation the space A along which the vapor passes to the condenser is separated from the vapor jacket B by a liquid seal (the liquid level in A is 4-5 cm higher than in B). Because of this the vapor from the vapor jacket does not pass directly into the condenser, but first bubbles through the liquid seal into A and reaches equilibrium with this liquid. The steam jacket is externally insulated by means of asbestos which contains a Nichrome heating coil and a thermometer. Experience shows that external heating is not essential in experiments with solutions boiling below 80°. If the solutions boil above 80° the vapor jacket should be heated, otherwise the difference between the compositions of liquid and vapor exceeds the equilibrium value.

• Communication IX.

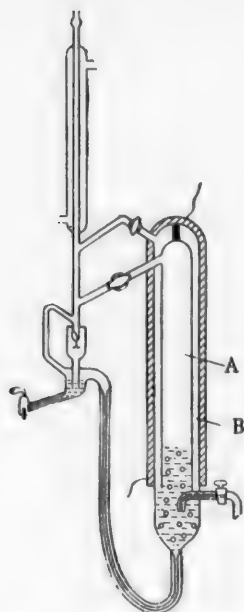


Fig. 1. Apparatus of the old design.

The thermometer mounted in the asbestos insulation of the jacket does not give the true vapor temperature in the jacket; it serves merely for comparative estimation of the heating of the jacket walls. Therefore, the vapor space is always either underheated or overheated.

With this disadvantage, the apparatus is used as follows. The first equilibrium determination (for example, with 10-15 molar % of the more volatile component) consists of 3-4 experiments. These experiments are performed at the same rate of boiling, but with differences in the degree of heating of the vapor jacket, for example: 1) without heating, 2) with the thermometer of the vapor jacket reading 30° below the boiling point of the solution, 3) with the vapor jacket at the boiling point of the solution, and 4) with the vapor jacket at a temperature 10° above the boiling point.

As the experiments are repeated the composition of the solution in the still changes a little. It is therefore sometimes difficult to use the liquid and vapor composition for determining whether the equilibrium values are the same. For convenience, these data are used to calculate the relative volatilities α , which are compared. Usually the first value of α (without heating) is higher than the others, but all the other values of α agree within the limits of experimental error, or the last two values coincide. Agreement between the values of α , found with different degrees of heating of the vapor jacket shows that the apparatus is working correctly at these degrees of heating.*

The subsequent determinations should be conducted within this heating range. The equilibrium is determined at the next concentration with the vapor jacket heated to some temperature intermediate between the permissible values; at the next concentration after that, at some other intermediate temperature, etc. At the middle and the last concentrations 2-3 experiments are performed, as at the first (the degrees of heating may be different). If the values of α lie on a smooth plot of $\alpha = f(x)$, where x is the content of the volatile component in the liquid (in molar %), this shows that there are no errors due to incorrect operation of the apparatus (there may be systematic errors due to a systematic analytical error or to inadequate purity of the materials). Our method for checking the absence of systematic errors is described in Communications II and V [6, 7]. If the value of α does not fit on the curve, this indicates an incidental analytical error, and the experiment is repeated. All the results are additionally checked by means of control experiments at several concentrations, in which the degree of heating of the vapor jacket remains constant, but the rate of boiling is varied. The number of experiments depends on the results obtained and on the form of the $\alpha = f(x)$ curve.

In this manner exact and reliable liquid-vapor equilibrium data are obtained.

With the use of this apparatus (Fig. 1) the number of experiments needed for a complete investigation of equilibria in a given system is less than with the other types of apparatus described in the literature, because of the wider range of permissible degrees of heating of the vapor space in our apparatus. However, the number of experiments required is excessive even with our apparatus. The reason is that there is no theoretical basis for the accuracy of the experimental data obtainable with our old apparatus. Everything depends on whether the nonequilibrium vapor from the vapor jacket has time to reach equilibrium with the liquid when it bubbles through the latter, and whether the vapor condenses on the internal walls of the inner tube. This cannot be established theoretically; it can only be shown by experiment that under certain operating conditions the apparatus gives correct results. Numerous experiments are needed to find these conditions and especially to verify that correct results are in fact obtained under such conditions.

This disadvantage is eliminated with the new apparatus (Fig. 2). Its characteristic feature is that the equilibrium temperature within its vacuum jacket is easily checked. The amount of liquid put in the apparatus is

* Our experience over many years shows that the apparatus may give incorrect results if the vapor space is underheated, but incorrect data were never obtained if it was overheated, and the rate of boiling was not too high. Therefore, a certain degree of overheating might have been adopted as a regular procedure. However, this is not done because of the risk that a new system may behave differently from those investigated previously.

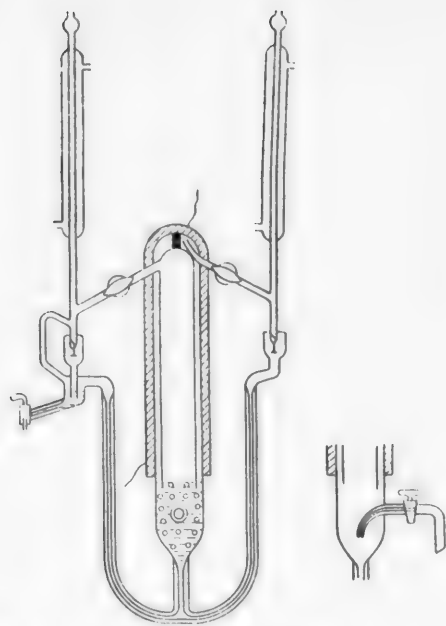


Fig. 2. Apparatus of new design.

the dropping rate is reduced to half the maximum value, the vapor composition remains exactly the same as at the maximum dropping rate.

Thus, in contrast to the old apparatus, there is full theoretical justification for the possibility of exact results with the new apparatus. The conditions under which the apparatus conforms to the theoretical requirements can be easily found by means of one experiment, without numerous exploratory and control experiments. Moreover, as has been pointed out above, fairly considerable deviations from the optimum operating conditions do not affect the accuracy of the results. This simplifies the experimental procedure and makes the work easier, as control of the constancy of the degree of heating of the vapor jacket during the experiment need not be as strict.

Experimental Procedure with the Apparatus

Liquid is sucked into the dry and clean apparatus through the siphon tube of the still to a level 1-2 cm above the lower end of the inner tube, with twice the amount of liquid necessary to fill the distillate trap up to the overflow tube. The top stopcocks are open. The liquid can be boiled at any desired rate. As soon as the liquid in the distillate receiver reaches the overflow tube, it is all discarded. This rejected liquid contains water and other impurities adsorbed on the walls of the apparatus. The boiling rate is then lowered to 100-150 drops per minute (1-3 ml/minute) in the left-hand dropper (with an inner tube 28 mm in diameter). At higher boiling rates there is a risk that liquid droplets may be formed and carried over into the distillate trap. The apparatus is connected to a manostat. The heater of the vapor jacket is switched on. The maximum dropping rate in the right-hand dropper is determined. The heating of the vapor jacket is then reduced so that the dropping rate in the right-hand dropper is approximately 10% below the maximum (to avoid overheating), and a reading is taken of the thermometer mounted in the asbestos insulation of the vapor jacket ("the working temperature"). When work on a new system is started, the working temperature is determined only once (if the difference between the boiling points of the components does not exceed a few degrees). In subsequent experiments with the same system, the dropping rate in the left-hand dropper and the working temperature are kept constant.

The use of the working temperature for maintenance of the required degree of heating of the vapor-jacket walls is more advantageous than regulation of the degree of heating by the dropping rate in the right-hand dropper, for the following reasons. When the apparatus is assembled for the next experiment, it is difficult to mount the still heater exactly in the same way as in the previous experiment. If the position of the heater in relation to the apparatus is changed, the origin and direction of the stream of vapor bubbles in the liquid change, with

such that its level during the experiment is 1-2 cm above the lower end of the inner tube. When the solution in the still is boiled, part of the vapor rises up the inner tube, condenses in the left-hand condenser, and the distillate flows down into the trap and returns to the still; another part of the vapor goes to the vapor jacket and condenses there, and the condensate flows back into the still. As the walls of the vapor jacket become heated through, vapor condensation in it decreases; the vapor begins to pass into the right-hand condenser and condenses there, and the condensate flows down the drainage tube into the still. To accelerate the heating of the vapor jacket, it is heated externally by means of an electric current passed through the Nichrome coil in the asbestos insulation. As the vapor jacket becomes heated, condensation within it decreases and the dropping rate in the right-hand dropper increases. At a certain degree of heating the dropping rate reaches a maximum; with further heating it remains unchanged for some time, and then begins to increase slowly again. This is the result of additional boiling of the liquid at its points of surface contact with the walls of the vapor jacket. At the instant when the maximum dropping rate is reached, the temperature of the vapor-jacket walls is exactly equal to the boiling point of the liquid. This represents the optimum operating conditions. It has been found by experiment that if

corresponding changes in the dropping rates in the left-hand and right-hand droppers. Therefore, with a constant dropping rate in the left-hand dropper (fixed by regulation of the rheostat of the still heater) the maximum dropping rate in the right-hand dropper may vary in different experiments, and it must be found for each experiment; the working temperature, however, remains constant with any position of the still heater.

It is desirable that the areas of the liquid surfaces in the inner tube and the vapor jacket should be equal. Then, if the heater is positioned correctly, the maximum dropping rate is close to the dropping rate in the left-hand dropper. If the apparatus is so constructed that with 100 drops per minute in the left-hand dropper the maximum dropping rate in the right-hand dropper is too high to count (over 200 drops per minute), the maximum dropping rate is determined at a very low rate in the left-hand dropper and the temperature reading is taken; in subsequent experiments (with 100-150 drops per minute in the left-hand dropper) a temperature 1-2° below this is used. Since in the new apparatus vapor from the vapor jacket does not enter the distillate trap, another experimental procedure is possible. It is possible to dispense with external heating of the vapor jacket, neither the dropping rate in the right-hand dropper nor the working temperature being regulated. For this procedure the mass of vapor passing through the vapor jacket must be several times greater than the mass of vapor passing through the inner tube. This can be achieved if the apparatus is so designed that the surface of the liquid in the inner tube is considerably less than the surface, if the liquid in the vapor jacket, and if the heater is appropriately positioned. With this procedure the asbestos insulation should be replaced by another material of lower heat capacity and conductivity (cotton wool, eiderdown). Moreover, the insulation should be extended (the liquid surface must be above the lower end of the insulation). The dropping rate in the left-hand dropper is maintained at 100-150 per minute as before, while in the right-hand dropper it becomes established independently (it may be very high, or there may be a stream of liquid. In this way it is also possible to work with liquids boiling at high temperatures; the results are accurate, but since they are not fully justified theoretically, they should be verified at 2-3 concentrations with another apparatus by the first experimental procedure.

The speed at which equilibrium becomes established between the distillate in the trap and the liquid in the still depends on their relative amounts. At a ratio of 6/60 ml and a boiling rate of 1 ml/minute (in the left-hand dropper) equilibrium is fully established 1-1.5 hours after the working temperature has been reached. The speed at which equilibrium is established also seems to depend upon the nature of the system. Therefore in investigations of each system we increase this time to 2-3 hours in several experiments.

Liquid samples from the trap and still are taken from the cooled apparatus. In view of the fact that on cooling the vapor above, the liquid in the still condenses and changes the liquid composition somewhat, a correction is applied to the composition of the liquid. This correction is not large. If the ratio of the liquid volume to the volume of the vapor space is 60:380 and $\alpha = 1.070$, the correction increases the value of α by $2 \cdot 10^{-3}$.

In the old apparatus the upper stopcocks are required for filling of the vapor jacket with vapor at the start of an experiment. The stopcock leading from the vapor jacket to the condenser is opened and the other stopcock is closed. In the new apparatus the upper stopcocks are not needed at all during the experiments; they are used when the apparatus is dried, which is done by alternate evacuation and blowing of air.

The still heater is a truncated cone with a longitudinal cut. Nichrome wire is wound around the cone. The inverted cone is fitted over the bottom of the apparatus.

The new apparatus gives accurate results over wide ranges of the degree of heating of the vapor jacket and of the boiling rate. Therefore the operating conditions described above (for the first variant) serve merely as an illustration, and they may be varied. We usually keep to these conditions, but experiments are performed at higher boiling rates for 2-3 concentrations.

In order to obtain completely reliable data, liquid-vapor equilibrium studies should be conducted with two different pieces of apparatus (of the same or of different design), which must be of different sizes, and with liquids of different origins. The use of different apparatus eliminates errors caused by possible imperceptible imperfections and incorrect proportions; moreover, this provides a check of the correction applied to the liquid composition.

Our thorough investigations of the performance of the apparatus have shown that errors do not occur as the result of incorrect operation; there are errors caused by errors in determinations of the liquid composition, but these are minimized by duplicate analyses of samples from the same experiment.

LITERATURE CITED

- [1] G. Scatchard, C. L. Raymond and H. H. Gilman, *J. Am. Chem. Soc.* 60, 1275 (1938).
- [2] I. N. Bushmakín and E. D. Voelkova, *J. Gen. Chem.* 19, 1615 (1949). *
- [3] D. F. Othmer, *Ind. Eng. Chem.* 35, 614 (1943).
- [4] V. A. Kireev, *J. Phys. Chem.* 15, 492 (1941).
- [5] H. Lang, *Z. phys. Chem.* 196, 278 (1950).
- [6] I. N. Bushmakín, *J. Gen. Chem.* 21, 1197 (1951). *
- [7] I. N. Bushmakín, R. V. Lyzlova, and P. Ya. Molodenco, *J. Appl. Chem.* 26, 1258 (1953).*

Received February 17, 1958

* Original Russian pagination. See C. B. Translation

EFFECTS OF FUSED LITHIUM, SODIUM, AND POTASSIUM HYDROXIDES ON NICKEL, COPPER, IRON, AND STAINLESS STEEL

E. I. Gurovich

Investigations of the corrosive action of fused alkalis, especially of alkali-metal hydroxides, are of very great theoretical and practical interest.

There has been a fairly large number of investigations in this field, mainly in relation to the choice of metallic materials of construction for the production of alkalis (evaporation, concentration, drying, etc.). For example, Pershke and Popova [1] studied metal corrosion in concentrated alkali solutions for selection of constructional materials used in alkali production. They studied the action of alkalis containing water and carbonates on ordinary cast irons, nickel, copper, cast iron containing nickel and chromium, Monel, and certain brasses and bronzes. However, in these investigations the maximum temperature was 260°, and the tests were 15 hours in duration and were started at room temperature, i.e., the tests were performed under conditions of alkali evaporation.

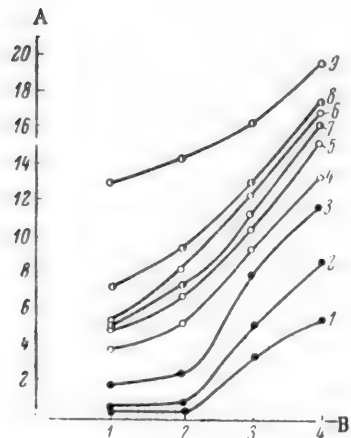


Fig. 1. Isotherms for corrosion in fused NaOH: A) corrosion (g/m^2); B) duration of experiment (hours). Nickel: 1) 350°; 2) 400°; 3) 450°; "Armco" iron: 4) 350°; 5) 400°; Kh18N9T steel: 7) 350°; 8) 400°; 9) 450°.

extensive: it includes nickel-chromium alloys [17], molybdenum [18], tungsten [19, 20], beryllium [21], zirconium, indium, niobium, tantalum, titanium etc. [22].

Despite the relative abundance of papers dealing with the action of alkalis on metals, there have not been any systematic investigation from the kinetic standpoint. Moreover, nearly all the investigations were largely

Schmitz [2] studied the behavior of certain steels in fused alkalis and other reagents, in relation to their carbon, nickel, and chromium contents.

Berl and Taack [3] studied the action of alkalis and salt solutions on iron at high temperatures (up to 310°), and selected corrosion inhibitors for these cases. They found, in particular, that sodium sulfate is especially useful as a corrosion inhibitor.

The corrosion of iron in fused alkalis has also been studied by many workers [4-7].

Publications on the behavior of nickel and its alloys in fused alkalis are especially numerous, but they are nearly all concerned with the evaporation of alkalis [8-10].

Copper and its alloys have also been studied as materials which are fairly resistant to the action of alkali solutions at high temperatures [11-13].

The resistance of silver to fused alkalis has long been known, but even now publications dealing with the corrosion resistance of silver to fused alkalis can be found [14-16].

The list of materials which have been studied in relation to the effects of fused substances, including alkalis, on them is very

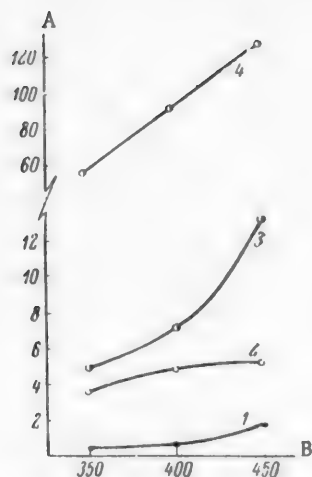


Fig. 2. Polytherms for corrosion in fused NaOH: A) corrosion (in g/m²·hour); B) temperature (°C); 1) nickel; 2) "Armco" iron; 3) Kh18N9T steel; 4) copper.

Tests in Caustic Soda. Figure 1 shows corrosion isotherms for nickel, "Armco" iron, and Kh18N9T steel at all the experimental temperatures.

It follows from Fig. 1 that nickel had the highest resistance to fused NaOH at all the test temperatures; this is also clear from the polytherm (Fig. 2).

The behavior of "Armco" iron and Kh18N9T steel is roughly the same. Films differing in thickness and density are formed on the metal specimens, with the exception of copper. For example, films from 0.3 to $2.9 \cdot 10^{-4}$ cm thick are formed on the surface of "Armco" iron. These results were found by calculation from the film weights, determined as the differences between the weight of each specimen with and without the film. The films were removed from the specimens either by the action of hot concentrated ammonium oxalate solutions, or by dilute hydrochloric acid containing gelatin as an inhibitor. The films on Kh18N9T steel were considerably thinner, but their densities were higher.

As caustic alkalis usually contain carbonates, the carbonate contents of the alkalis were determined each time. In the case of NaOH the Na₂CO₃ content before the experiment was about 4%, and after the experiment the carbonate content was about 5.5%.

Caustic alkalis also usually contain moisture. The moisture content of NaOH was not determined, because it is usually relatively low, and because the moisture was removed almost completely from the melts during the tests.

It follows from Figs. 1 and 2 that corrosion losses increase with temperature and exposure time.

The corrosion behavior of copper is shown separately in Fig. 5.

The corrosion loss for copper is very much greater than the losses for the other metals tested; this is also clear from Fig. 2, where the corrosion polytherm for copper is given together with the corrosion polytherms for the other metals tested.

Tests in Caustic Potash. Figures 2, 4 and 5 show isotherms and polytherms for the corrosion of the metals tested in fused KOH.

In this case also the highest corrosion losses are found with the copper specimens. When copper is tested in fused alkalis, protective films are not formed on the specimens, such as are formed on the other metals tested. This fact is probably reflected in the relatively lower corrosion resistance of copper to fused alkalis.

concerned with selection of metallic materials for evaporation and concentration equipment, and therefore the majority were performed at temperatures not exceeding 350-400°.

These gaps are filled to some extent by the present investigation. The corresponding corrosion isotherms and polytherms for metals in fused alkalis have been determined.

EXPERIMENTAL

The method of investigation and the conditions used for testing metals in fused alkalis (NaOH, KOH, and LiOH) showed few essential differences from the methods and conditions used in our earlier investigations, which were concerned with the effects of chlorides [23] and nitrates [24] on metals. In the present instance it was merely necessary to change the quartz vessels more often, as they became unserviceable earlier, despite the published reports concerning the relatively high resistance of quartz to fused alkalis [25]

The metals tested were nickel, copper, "Armco" iron, and Kh18N9T stainless steel, at 350, 400 and 450° in NaOH melts, and at 400, 450, and 500° in KOH melts; the tests in LiOH melts were conducted at 500, 550, and 600°. The exposure times of the metals in the melts were 1, 2, 3, and 4 hours in each case.

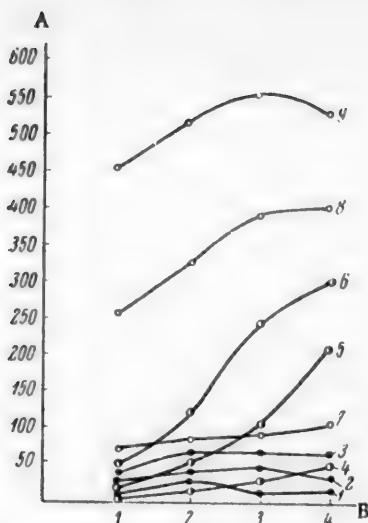


Fig. 3. Isotherms for corrosion in fused KOH: A) corrosion (in g/m^2); B) duration of experiment (hours); nickel: 1) 500° ; 2) 450° ; 3) 400° ; Kh18N9T steel: 4) 400° ; 5) 450° ; 6) 500° ; "Armco" iron: 7) 500° ; 8) 400° ; 9) 450° .

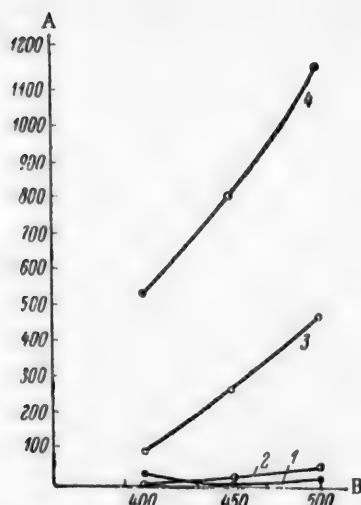


Fig. 4. Polytherms for corrosion in fused KOH: A) corrosion (in $\text{g}/\text{m}^2 \cdot \text{hour}$); B) temperature ($^\circ\text{C}$); 1) nickel; 2) Kh18N9T steel; 3) "Armco" iron; 4) copper.

As in the case of caustic soda, all the metals tested except copper form surface films differing in thickness when exposed to fused caustic potash. For example, the thickness of the films formed on "Armco" iron is in the $1.2-21.5 \cdot 10^{-4}$ cm range. The film thickness decreases with increase of temperature. Moreover, the films formed on "Armco" iron specimens are looser than those formed in caustic soda melts. Nickel and Kh18N9T steel specimens showed the least corrosion, but the corrosion was considerably greater in fused KOH than in caustic soda. In this case also the corrosion losses of all the metals tested increase with temperature and with the exposure time (Figs. 3, 4, 5).

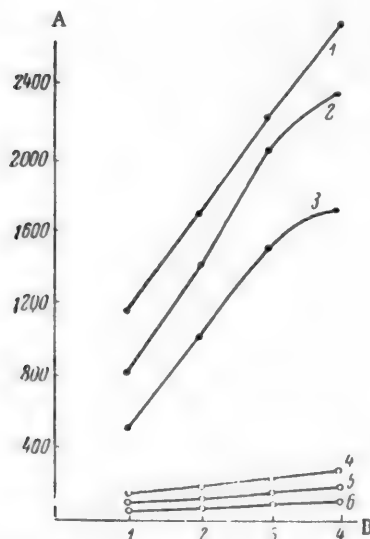


Fig. 5. Isotherms for corrosion of copper in fused NaOH and KOH: A) corrosion (in g/m^2); B) duration of experiment (hrs); in KOH: 1) 500° ; 2) 450° ; 3) 400° ; in NaOH: 4) 450° ; 5) 400° ; 6) 350° .

The average contents of K_2CO_3 in KOH before the experiments was 9%, and at the end the carbonate content fell to about 7% (it was virtually unchanged).

The moisture content of KOH varied from 12 to 18% at the start of the experiments; i.e., it was considerably higher than in caustic soda. This moisture content fell considerably when KOH was held at the experimental temperatures; for example, the moisture was lost almost completely when KOH was kept in the fused state for 2 hours at 500° . At lower temperatures traces of moisture remained; this is also clear from the isotherms in Fig. 4. It follows from Fig. 3 that corrosion losses are considerably less at 500° than at lower temperatures, because the moisture was removed almost completely from the melt.

Of course, this influenced the growth and nature of the films formed on the metal surfaces, and also introduced certain difficulties in comparisons of the results of corrosion tests in NaOH and KOH melts, although an attempt was made to make comparison of this kind for all the caustic alkalies tested.

Figure 5 shows isotherms for corrosion of copper in fused NaOH and KOH.

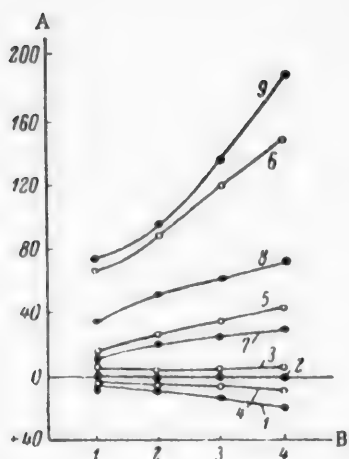


Fig. 6. Isotherms for corrosion in fused LiOH: A) corrosion in g/m^2 (upward from 0—weight increase; downward—loss); B) duration of experiment (hours); Kh18N9T steel: 1) 500°; 2) 550°; 3) 600°; "Armco" iron: 4) 500°; 5) 550°; 6) 600°; copper: 7) 500°; 8) 550°; 9) 600°. The curves for nickel are close to the abscissa axis.

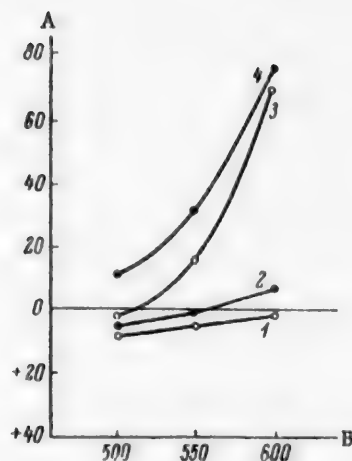


Fig. 7. Polytherms for corrosion in fused LiOH: A) corrosion in $\text{g/m}^2 \cdot \text{hour}$ (upward from zero—weight increase; downward—loss); B) temperature ($^{\circ}\text{C}$); 1) nickel; 2) Kh18N9T steel; 3) "Armco" iron; 4) copper.

In this case corrosion losses also increase with temperature and the time of exposure of the specimens to the alkali melts. It is clear from Fig. 5 that corrosion losses are considerably higher in fused caustic potash than in caustic soda; apart from the higher corrosiveness of KOH as compared with NaOH, this result also depends on the moisture content of the alkali.

Tests in Lithium Hydroxide. Isotherms and polytherms for corrosion of metals in fused lithium hydroxide presented in Figs. 6 and 7.

Here again the highest corrosion losses are found for copper, followed by "Armco" iron. Kh18N9T steel shows a slight weight increase at 500 and 550°, and a small loss in weight at 600°.

Nickel is corroded with a very slight increase in weight.

"Armco" iron also forms a surface film at 500°. The thickness of this film varies in the range of $0.05\text{--}1.2 \cdot 10^{-4}$ cm. The method used for determination of film thickness was described earlier.

This alkali, LiOH, had an average carbonate content of 3% before the experiments, while after the experiments the Li_2CO_3 content was about 3.5%.

The moisture content of LiOH was not determined in every case, as it was removed almost completely when LiOH was heated to 500° (the weight of a LiOH sample remained constant).

It is clear from Fig. 6 and Fig. 7 that the corrosion losses of the tested metals increase with temperature and exposure time.

SUMMARY

It is quite obvious from a comparison of the test results for all the alkalis that corrosiveness of caustic alkalis decreases in the series $\text{K} > \text{Na} > \text{Li}$, i.e., caustic potash is more corrosive than caustic soda, and the latter is more corrosive than lithium hydroxide. Thus, lithium hydroxide is the least corrosive in this series.

In the paper by Pershke and Popova [1] cited earlier, the corrosion activities of caustic alkalis under somewhat different conditions were compared. It was found that the corrosiveness of KOH is 2.5-3 times as high as that of NaOH. We found that KOH is considerably more corrosive than NaOH, which may be attributed to the higher moisture content of KOH.

It has been observed earlier in studies of the corrosion behavior of metals in certain fused salts [23, 24] that the radius of the cation in a particular salt influences the corrosiveness of the salt in the fused state. A comparison between these salts and the alkalies studied in the present investigation reveals the same relationship; i.e., corrosion activity of a particular alkali depends on the position of its cation in D. I. Mendeleev's periodic table.

LITERATURE CITED

- [1] V. K. Pershke and L. I. Popova, *J. Chem. Ind.* 7, 1, 16 (1930).
- [2] F. Schmitz, *Z. Metallkunde* 21, 64 (1929).
- [3] E. Berl and F. van Taack, *Forschungsarbeiten aus dem Gebiete des Ingenieur Wesens*, Berlin, 330 (1930).
- [4] U. Perret, *Chim. e. ind. Italy*, 20, 133 (1938).
- [5] K. Taussig, *Arch. Wärmewirt.* 8, 337-340 (1927).
- [6] H. Iodko and M. Wiekiera, *Przem. chem.* 10, 12, 593 (1954).
- [7] P. G. Rudenskii, *Soviet Patent* 42043, March 31, 1935.
- [8] R. I. McKay, *Ind. Eng. Chem.* 21, 1283 (1929).
- [9] H. E. Searle and R. Worthington, *International Nickel Co., Techn. Bull.* T-6 (1933).
- [10] R. A. Lad, S. L. Simon, *Corrosion* 10, 12, 435 (1954).
- [11] T. Wallace and A. Fleck, *J. Chem. Soc.* 119, 1839 (1921).
- [12] A. S. Perry, *Ind. Eng. Chem.* 29, 677 (1937).
- [13] O. L. Kowalke, *Chem. Met. Eng.* 22, 37 (1920).
- [14] I. G. Farbenindustrie AG, *German Patent* 53799, March 1, 1928.
- [15] D. Martin and E. Parker, *Trans. Am. Inst. Min. Met. Eng.* 152, 269 (1943).
- [16] I. C. Chaston, *J. Inst. Met.* 71, 23 (1945).
- [17] E. H. Schultz, and W. Jenge, *Z. Metallkunde* 18, 377 (1926).
- [18] J. A. van Liempt, *Rec. trav. chim.* 45, 508 (1926); 46, 11 (1927).
- [19] S. L. Malowan, *Z. Metallkunde* 23, 69 (1931).
- [20] H. Wartenberg and H. Moehl, *Z. phys. Chem.* 128, 439 (1927).
- [21] L. Gmelin, *Handbuch anorg. Chem.* 26 (1930).
- [22] *Metal Corrosion*, 1 (1952) p. 380 [Russian translation from English, by E. I. Gurovich, edited by V. V. Skorcheletti].
- [23] E. I. Gurovich, *J. Appl. Chem.* 27, No. 4, 425 (1954). *
- [24] E. I. Gurovich, *J. Appl. Chem.* 29, 1358 (1956).*
- [25] Z. von Hirschberg, *Korrosion* 4, 25 (1929).

Received January 28, 1958

* Original Russian pagination. See C. B. Translation.

CATHODIC LIBERATION OF ZINC FROM ZINC SULFATE SOLUTIONS WITH HIGH CONTENTS OF IRON IONS

O. A. Khan and L. S. Dukhankina

The Altai Mining and Metallurgical Scientific Research Institute of the Academy of Sciences Kazakh SSR

In modern hydrometallurgical practice monometallic solutions are generally used for electrolytic separation of metals [1, 2]. Other metals (impurities) are present in very low concentrations in such solutions.

The extent and nature of the influence of impurity cations on the kinetics of cathodic liberation of the principal metal must depend on the nature of these cations and the electrolysis conditions [1, 3, 4].

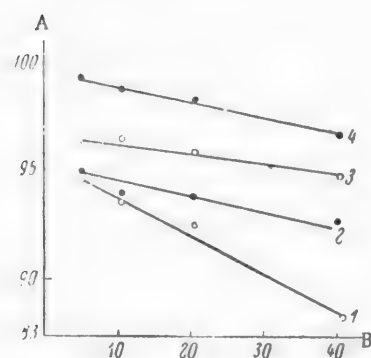


Fig. 1. Partial current efficiency for zinc as a function of the ferrous ion concentration at different temperatures: A) current efficiency for zinc (%); B) ferrous ion concentration (g/liter); temperature (°C): 1) 20; 2) 40; 3) 60; 4) 80.

Because of their low concentrations, the "limiting current densities" (D_{lim}) for the discharge of the impurity cations are very low. Therefore the rates of deposition of some of the impurities on the cathode should be independent on the current density (D_c) at which the principal metal is deposited, as in practice D_c will always be greater than D_{lim} . It follows that in electrolysis of solutions containing impurities in low concentrations, the purity of the deposit or, in other words, the selectivity of the deposition of the metal on the cathode, may be increased by increase of current density [5, 6].

If the concentration of extraneous metals in the electrolytes is high, strictly selective deposition of the metal on the cathode is impossible in practice. However, under definite electrolysis conditions and with the aid of special measures (introduction of complex formers into the electrolyte, etc.) it is possible to isolate one of the metals preferentially on the cathode from such multicomponent solutions.

The present investigation was concerned with zinc electrolytes containing iron. Such solutions may be formed in hydrometallurgical processes in which ferric sulfate or ferric chloride solutions are used as leaching agents [7, 8], in anodic dissolution of multimetallic mattes [9], and in other processes. Because of the high iron contents

of these solutions, their conversion by methods such as those used in the hydrometallurgy of zinc is difficult.

The electrolytic method seems appropriate for this purpose.

The literature contains only brief information on the electrolysis of solutions containing zinc and iron. The few investigations were performed a relatively long time ago, and they were not concerned with the same aims as the present work [10, 11]. The kinetics and mechanism of cathodic liberation of metals from zinc-iron solutions have been studied very little. At the same time, it should be noted that electrolysis of zinc solutions with high contents of iron ions is now beginning to attract attention also in relation to the cathodic formation of iron-zinc alloys, which have a number of specific properties distinctive from those of the pure metals [12].

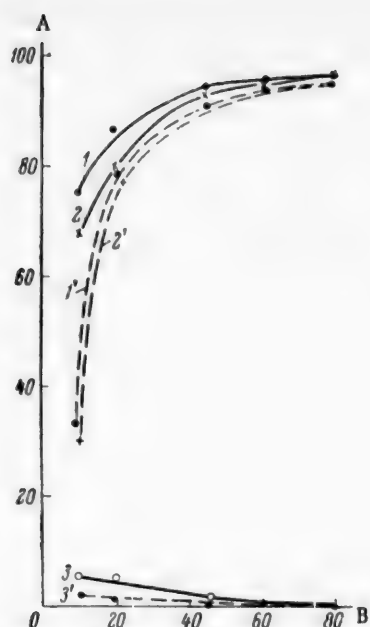


Fig. 2. Effects of zinc ion concentration in solution on cathodic current efficiencies and iron contents of the cathode deposit: A) current efficiencies for metals (%); B) concentration of zinc ions in solution (g/liter). Sulfuric acid contents (g/liter): 1, 2, 3) 2; 1', 2', 3') 20; current efficiencies (%): 1, 1') alloy; 2, 2') zinc; 3, 3') iron.

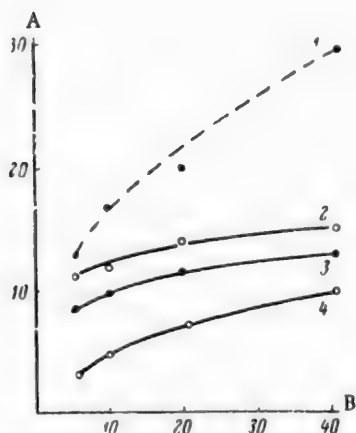
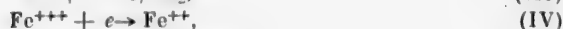
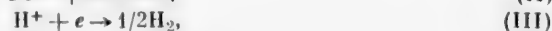
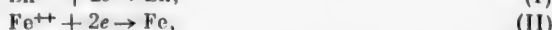
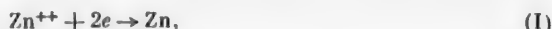


Fig. 3. Effects of ferrous ion concentration at different temperatures on the volume of hydrogen liberated at the cathode: A) volume of hydrogen (in cc); B) concentration of ferrous iron (g/liter). Temperature (°C): 1) 20 (20 g H_2SO_4 /liter); 2) 20; 3) 40; 4) 60.

In electrolysis of a zinc-iron solution in a cell with insoluble anodes the following reactions are possible at the cathode:



The reduction of Fe^{+++} ions to Fe^{++} at the cathode is undesirable, as it lowers current efficiency for zinc [13, 15]; it can be avoided if the cell is divided by a diaphragm and a stream of electrolyte is caused to flow from the cathode to the anode compartment. The cathod process in the electrolysis of Zn-Fe solution is then determined by the polarization for each of the first three reactions (I)-(III).

The present communication contains the results of experiments on the influence of cathodic current density, concentrations of iron and zinc ions, and other factors on the current efficiencies and the iron content of the cathodic deposit.

EXPERIMENTAL

The solutions were electrolyzed in a cell (300 ml in capacity) divided by a porous partition. One cathode and one anode was placed in the cell. The cathodes were aluminum plates, and the anodes were plates of lead-silver alloy (1% Ag).

The electrolyte was fed into the cathode compartment and flowed out of the anode compartment of the cell. The electrolyte temperature was kept constant to within $\pm 0.5^\circ$.

Cathodic polarization was measured by the compensation method with the PPTV-1 potentiometer and a null galvanometer of sensitivity $1 \cdot 10^{-5}$ amp.

The experimental results and conditions are given in the table (0.3 amp-hr was passed at each current density).

It follows from the tabulated data that the total current efficiency for the alloy decreases slightly with increase of current density. The iron contents of the deposits increase both with increase of ferrous ion concentration and with increase of current density. The same table also contains values of the partial current efficiency for zinc, calculated from the electrochemical equivalents of the metals and analytical data for the deposits. These results show that cathodic depositions of zinc from Zn-Fe solution in a divided cell proceeds at a relatively high current efficiency. The partial current efficiency for zinc falls with increase of current density and iron concentration in the electrolyte, and the metals are deposited on the cathode at higher negative potentials (see table).

The results of experiments on the effects of ferrous ion concentration on the partial current efficiency for zinc at different temperatures are presented in Fig. 1. In all the experiments the zinc and sulfuric acid contents of the electrolyte were constant at 45 and 2.2 g/liter, respectively. Figure 1 shows that the partial

Cathodic Current Efficiencies and Iron Contents of Cathodic Deposits at Different Current Densities and Ferrous Ion Concentrations in the Solutions. Composition of solution (g/liter): Zn 40,5-41, H₂SO₄ 2; temperature 20°

Current density (amp/ m ²)	Iron content of solution (g/liter)						
	3.9				8.3		
	Cathode potential (v)	Current efficiency (%)		Iron content of deposit (%)	Cathode potential (v)	Current efficiency (%)	
		total	for zinc			total	for zinc
100	-0.763	96.5	96.36	0.09	-0.778	94.64	94.52
200	-0.777	95.95	95.68	0.12	-0.790	94.30	93.99
400	-0.785	95.64	95.43	0.18	-0.800	94.0	93.30
600	-0.802	95.45	94.90	0.50	-0.811	92.77	91.63
800	-0.813	93.0	89.5	0.76	-0.829	90.41	88.74
							1.80

current efficiency for zinc increases with temperature and decreases with increase of the Fe : Zn ratio in the electrolyte. At a higher content of sulfuric acid in the electrolyte (20 g/liter) the current efficiency for zinc falls more steeply with increase of the ferrous iron concentration than it does in the less acid electrolyte.

The effects of the zinc ion concentration on the cathode process ($D_c = 400$ amp/m²) are shown graphically in Fig. 2. The course of the curves in Fig. 2 indicates that the increase of the current efficiency for the alloy with increase of the zinc concentration in the electrolyte is the consequence of an increase of the partial current efficiency for zinc, as the partial current efficiency for iron decreases in this case.

The cathodic current efficiency for the alloy and the partial current efficiency for zinc are much lower in electrolysis in a cell without a diaphragm (stationary electrolyte). For example, in a solution containing 45-46 g/liter of zinc*, 42 g/liter of iron, and 20 g/liter of sulfuric acid, the current efficiency for zinc (for the same time of electrolysis as in the diaphragm cell) was 65% at $D_c = 200$ amp/m², and only 5% at $D_c = 800$ amp/m². In the latter case the cathodic deposit was periodically redissolved. With increase of the sulfuric acid content of this electrolyte to 100 g/liter, there was virtually no deposit formed on the cathode.

The above experimental data show that the mechanism of cathodic liberation of zinc from sulfate solutions in presence of iron ions is very complex. However, it is clear that zinc is deposited preferentially at the cathode in all cases. This may be attributed to the higher overvoltage for the discharge of ferrous ions at the cathode as compared with zinc ions.

The increase of the partial current efficiency for zinc with increase of the electrolyte temperature is also consistent with the results of our experiments (Fig. 3) in which the volume of hydrogen liberated at the cathode was determined. Figure 3 shows that in electrolysis of a solution containing 46 g of Zn and 2 g of H₂SO₄ per liter at $D_c = 400$ amp/m² the volume of hydrogen liberated decreases with increase of temperature. However, at higher concentrations of iron and sulfuric acid in the solution the volume of liberated hydrogen increases.

The partial current efficiency for zinc may decrease in presence of ferric ions in solution as the result of cathodic reactions (IV) and (V). Further investigations are needed to determine which of these reactions is the more probable and what is the influence of each on the cathode process.

SUMMARY

The electrolysis of zinc-iron sulfate solutions has been studied at different concentrations of zinc and ferrous ions in relation to cathodic current density and temperature; it was found that in a diaphragm cell the cathodic deposits have a relatively low iron content, and the cathodic current efficiency for zinc is high.

LITERATURE CITED

- [1] Yu. V. Baimakov, *Electrolysis in Metallurgy*, I [in Russian] (Metallurgy Press, 1939).

*The zinc concentration in the solution was kept constant during electrolysis by periodic additions of zinc sulfate or hydroxide to the electrolyte.

- [2] P. N. Plaksin and D. M. Yukhtanov, Hydrometallurgy [in Russian] (Metallurgy Press, 1949).
- [3] A. N. Frumkin, V. S. Bagotskii, Z. A. Iofa, and B. N. Kabanov, Kinetics of Electrode Processes [in Russian] (Izd. MGU, 1952).
- [4] A. T. Vagramyan, Electrodeposition of Metals [in Russian] (Izd. AN SSSR, 1950).
- [5] V. L. Kheifets and A. L. Rotinyan, Proc. Acad. Sci. USSR 3 (1952).
- [6] O. A. Khan, É. I. Urubkova and V. A. Kuznetsova, Trans. Altai Mining Met. Sci. Res. Inst. Acad. Sci. Kazakh SSR 5 (1956).
- [7] I. N. Kuz'minykh and E. L. Yakhontova, J. Appl. Chem. 23, 1142 (1950); *24, 449 (1951).*
- [8] T. P. Campbell, Hydroelectrometallurgy (ONTI, 1953) [Russian translation].
- [9] D. M. Chizhikov and V. N. Kovylna, Trans. Inst. Metallurgy Acad. Sci. USSR, 1 (Moscow, 1957).
- [10] F. Küster, Z. Electroch. 7, 257, 668 (1900 and 1901).
- [11] F. Forster, Z. Electroch. 2, 96 (1916).
- [12] S. Jepson, S. Meecham and F. Salt, Trans. Inst. Metal Finish. XXXII, 160 (1954-1955).
- [13] A. G. Pecherskaya and V. V. Stender, J. Appl. Chem. 23, No. 9, 920 (1950).*
- [14] U. F. Turomshina and V. V. Stender, J. Appl. Chem. 28, No. 4, 372 (1955).*
- [15] A. I. Levin, A. V. Pomosov, V. S. Kolevatova, N. E. Gurevich, E. A. Gukshe, and N. T. Rogatkina, Coll. Trans. Urals Polytechnic Inst. 43 (1953).

Received September 4, 1957

* Original Russian pagination. See C. B. Translation.

HYDROGEN OVERVOLTAGE AT A POROUS IRON-NICKEL CATHODE

I. B. Barmashenko and V. I. Shapoval

The Kiev Polytechnic Institute

One unproductive form of power consumption in industrial electrolysis of aqueous solutions is due to overvoltage. Several methods exist for decreasing overvoltage, based on the use of new electrode material and on special surface treatments.

For example, Voronin, Barmashenko, and Nadezhdin [1] have shown that hydrogen overvoltage may be diminished at porous iron cathodes containing small additions of cobalt, nickel, tungsten, or molybdenum.

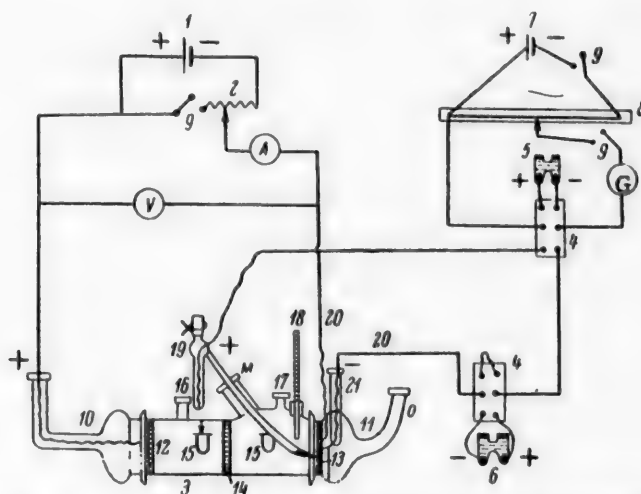


Fig. 1. Circuit of apparatus used for determination of hydrogen overvoltage: 1) current source; 2) rheostat; 3) electrolytic cell; 4) changeover switch; 5) Weston cell; 6) Weston counter-cell; 7) battery; 8) slide wire; 9) switches; 10) cover of anode section; 11) cover of cathode section; 12) steel anode; 13) iron-nickel cathode; 14) diaphragm; 15) hydrogen tubes; 16) O_2 outlet tubes; 17) H_2 outlet tubes; 18) thermometer; 19) reference half-cell; 20) leads; 21) side tube.

The aim of the present investigation was to find a cathode material which gives the maximum decrease of overvoltage and which economically is the most suitable for electrolysis of aqueous salts, alkalies, etc.

EXPERIMENTAL

The cathodes used were made by the sintering process from iron and nickel powders with grains 0.059-0.149 mm in size. 20 g of the thoroughly mixed powder was pressed in a cylindrical metal die at 1400 kg/cm². The electrode was then sintered in a tubular furnace in hydrogen at 750° for 1.5-2 hours.

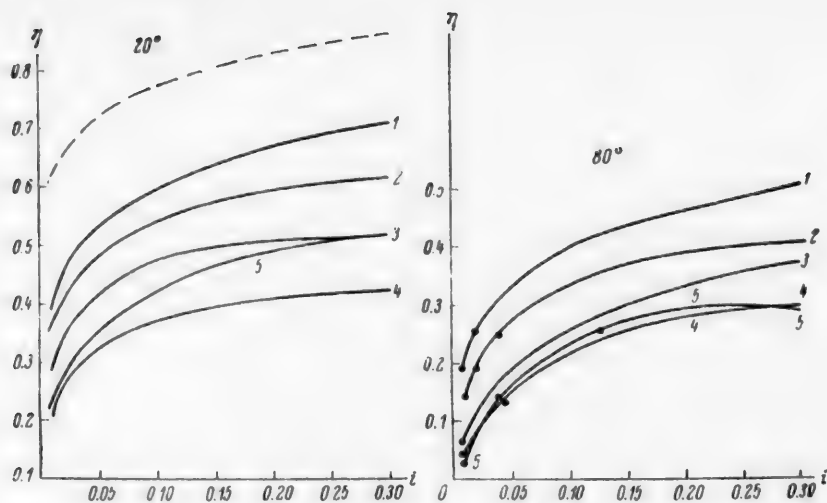


Fig. 2. Variations of hydrogen overvoltage η (in v) with current density i (in amp/cm²) at 20 and 80°; explanation in text.

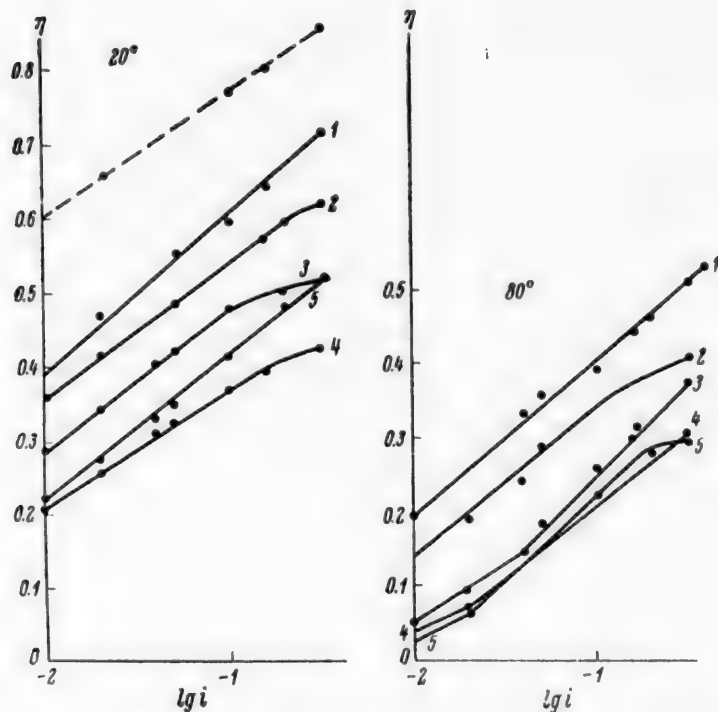


Fig. 3. Variations of hydrogen overvoltage η (in v) with $\lg i$ (in amp/cm²) at 20 and 80°; curve numbers as in Fig. 2.

The electrodes, of 7 cm² working area, had high strength and a silvery grayish surface without iridescence (the latter indicates surface oxidation).

The anode was a circular steel plate.

The potentials of the iron-nickel porous cathodes were measured during electrolysis by the direct method, with the usual compensation circuit containing a standard Weston cell, shown in Fig. 1. The method of determination

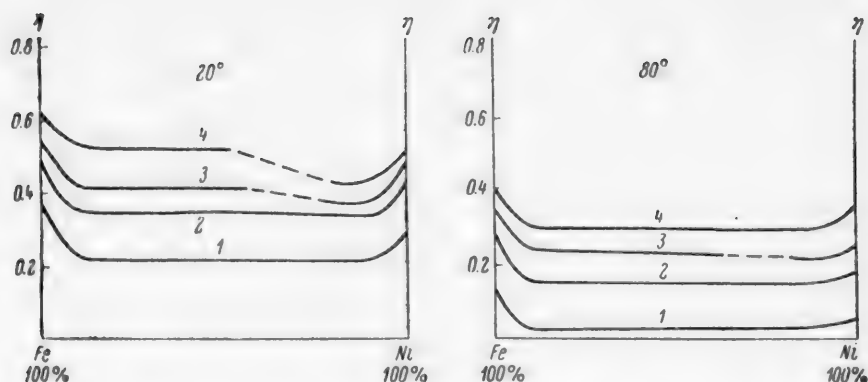


Fig. 4. Variations of hydrogen overvoltage with the nickel content in iron at 20 and 80°; current density (amp/m^2): 1) 100; 2) 500; 3) 1000; 4) 3000.

was the same as before [1], except that the cylindrical glass cell was widened at the cathode end to prevent the formation of a hydrogen pocket; this avoided any possible decrease of the effective cathode surface, especially at high current densities.

The electrolyte was a 15% solution of chemically pure caustic soda. The reference electrode was a mercury-mercury oxide half-cell containing 15% caustic soda solution; this eliminated the liquid-junction potential.

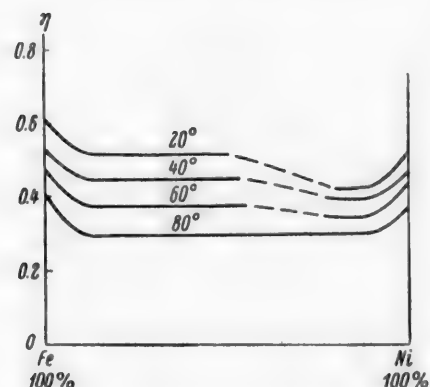


Fig. 5. Variations of hydrogen overvoltage η (in v) with the nickel content of iron at $i = 3000 \text{ amp}/\text{m}^2$ and different temperatures.

Variations of hydrogen overvoltage with current density in the 100-3000 amp/m^2 range were studied at 20-80°. The results of the experiments are plotted in Fig. 2. The dash line, based on Nadezhdin's data, represents hydrogen overvoltage at a smooth (cast) iron cathode. Curve 1 corresponds to an iron electrode treated with No. 2 emery. Curve 2 corresponds to a porous 100% Fe electrode; curve 3, 100% Ni; curve 4, 50% Fe, 50% Ni and 90% Fe, 10% Ni; curve 5, 20% Fe, 80% Ni and 10% Fe, 90% Ni.

Curves 4 and 5 were plotted because the overvoltages for the electrodes of these compositions differ by 12 mv. Curve 4, and especially curve 5, show considerable decreases not only relative to the smooth electrode but also relative to curve 2; by 0.2-0.3 at 20° and by 0.26 at 80°.

The curves in Fig. 3 show variations of hydrogen overvoltage at a porous cathode in $\eta_{\text{H}_2} - \lg i^*$ coordinates.

The curves in Figs. 4 and 5, plotted for different ranges of temperature and current density, present a full picture of the variations of hydrogen overvoltage with percentage contents of iron and nickel in porous electrodes.

It is clear from Fig. 4 that the overvoltage is effectively influenced not only by the first additions, as stated earlier [1], but also by nickel contents of 80-90%, which result in further decreases of overvoltage. A significant feature is that the decrease is greater than that found for a pure nickel electrode. This effect is more pronounced with increase of current density (Fig. 4). At low current densities (100-500 amp/m^2) the first additions of nickel of the order of 10%, may be regarded as effective. The curves in Fig. 4 ($t = 80^\circ$) show that the effect of nickel is less pronounced at higher temperatures. Temperature has a kind of eliminating action on the effect of large amounts of nickel over the entire current density range.

Figure 6 shows variations of hydrogen overvoltage with temperature for porous electrodes at current densities from 100 to 3000 amp/m^2 . Curves 1-4 correspond to different electrode compositions.

Figure 6 shows that the overvoltage is a linear function of temperature in the 20-80° range. However, the temperature gradient is not constant for electrodes of different composition. Figure 7 shows variations of the hydrogen overvoltage with current density for a porous cathode of the composition Fe 20%, Ni 80%. It is seen that the slope of the curves decreases with increase of current density. The temperature gradient decreases at current densities of 1000 amp/m² and over. The temperature gradient in the 20-80° range at current density 3000 amp/m² for cathodes of different composition are given below.

Cathode composition (%) . . .	100 Fe	100 Ni	90 Fe + + 10 Ni	50 Fe + + 50 Ni	20 Fe + + 80 Ni	10 Fe + + 90 Ni
Temperature gradient	3.5	2.4	3.6	3.6	2.0	2.0

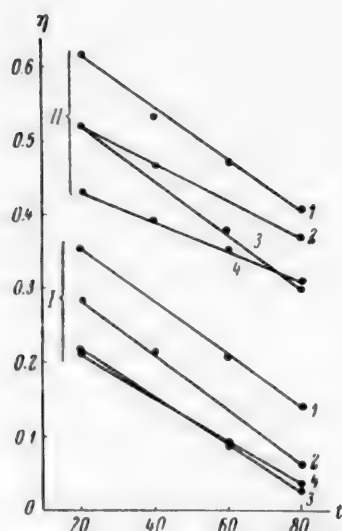


Fig. 6. Variations of hydrogen overvoltage η (in v) with temperature t (°C) for different cathode compositions; current density (amp/m²): I) 100; II) 3000; cathode composition (%): 1) Fe 100; 2) Ni 100; 3) Fe 90, Ni 10, Fe 50, Ni 50; 4) Fe 20, Ni 80, Fe 10, Ni 10.

It is seen that at current densities above 1000 amp/cm² the mechanism of the process changes; the discharge of hydrogen ion is accelerated, and this coincides with a change in the slope of the curves plotted in semilogarithmic coordinates (Fig. 3). This caused by formation of very thin oxide films on the cathode surfaces; these films can be reduced at current densities of 1000 amp/m² and over. This is confirmed by the high values of the constant \underline{b} in the Tafel equation, which depend on the temperature and the electrode composition, as the data in the table show.

It is seen that the values are high owing to the presence of oxide films. The value of \underline{b} increases with temperature. Except for the nickel cathode, the value of the constant \underline{b} changes by 3.5-5 mv for a temperature change of 10°.

DISCUSSION OF RESULTS

It follows from Figs. 2, 4, and 5 that the lowest hydrogen overvoltage is obtained at porous cathodes containing 10 or 20% Fe and 90 or 80% Ni. Similar results were obtained [1] with porous iron cathodes with layers (1 mm thick) of cobalt, tungsten, or molybdenum pressed onto them. In view of the scarcity of these metals and the considerably more complex sintering process required with their use, as compared with nickel, porous iron cathodes with pressed surface layers of the compositions indicated above are to be recommended.

The decrease of hydrogen overvoltage at cathodes made by the powder method may be due to porosity, which increases the true

Values of Constant \underline{b} in the Tafel Equation

Temperature	Constant \underline{b} for electrode of the composition %					
	100 Fe	100 Ni	90 Fe + 10 Ni	50 Fe + 50 Ni	20 Fe + 80 Ni	10 Fe + 90 Ni
20°	0.183	0.194	0.178	0.175	0.164	0.160
80°	0.207	0.200	0.210	0.213	0.185	0.180

effective surface of the cathode, and to the influence of additives. However, there is another important factor, which influences overvoltage. On the surface of a porous electrode made from one component, and more especially from two powdered metal components, active regions appear at which discharge of hydrogen ions requires less energy than at an ordinary smooth metallic electrode; this may influence the overvoltage.

Kobozev [2] postulated the existence of regions at which the quantities of energy required for liberation of hydrogen atoms are different. Frumkin et al. [3] state that if a surface is heterogeneous, the mechanism of the

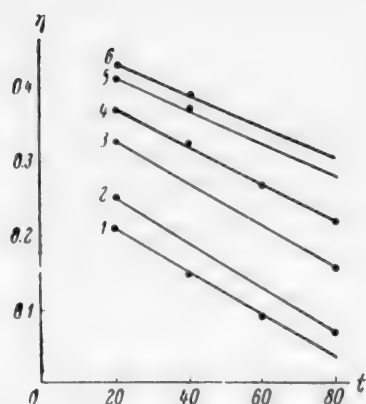


Fig. 7. Variations of hydrogen overvoltage η (in v) with temperature t ($^{\circ}\text{C}$) at a porous cathode (Fe - 20%, Ni - 80%); current density (amp/m^2): 1) 100; 2) 200; 3) 500; 4) 1000; 5) 2000; 6) 3000.

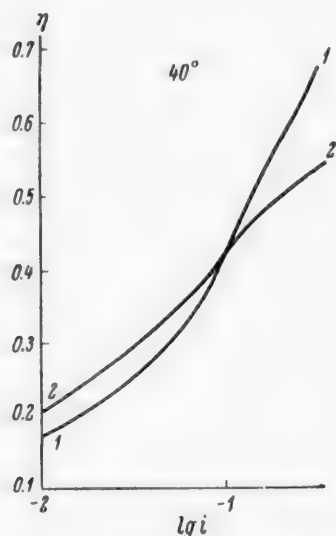


Fig. 8. Variations of hydrogen overvoltage η (in v) with i (amp/cm^2) at 40° for porous cathodes oxidized to different extents.

electrochemical reaction may differ at different regions. Lukovtsev [4] considers that at regions with a large heat of adsorption discharge is rapid and desorption is slow; if the heat of adsorption is low, discharge is slow and desorption is rapid. Loshkarev and Ozerov [5] consider that overvoltage is decreased mainly not as the result of an increase in the true surface area, but by increase of the discharge constant, i.e., owing to the presence of active regions on the electrode surface. On the porous cathodes studied in our investigation, which have a heterogeneous surface, discharge of hydrogen ions may occur at individual regions at a considerably higher rate and with less expenditure of energy than at smooth cathodes.

Our experiments showed that hydrogen overvoltage at these porous cathodes also depends on the degree of oxidation of the electrode surface. Curves 1 and 2 in Fig. 8 represent variations of overvoltage with log current density at 40° for two porous iron cathodes: one (curve 1) more highly oxidized, and the other (curve 2) with only traces of oxides. If even small amounts of oxygen are present in the electrolyte, the active regions are oxidized earlier and more easily. During electrolysis with a polarized cathode surface the current penetrates within the pores [6], where the amounts of oxides are undoubtedly very small. This leads to an increase of the effective acting surface, and at lower current densities ($100\text{--}1000 \text{ amp}/\text{m}^2$) curve 1 may even lie below curve 2. Further increase of current density results in much evolution of gas and displacement of the electrolyte from the pores; the acting surface then diminishes, as shown by the upward turn of curve 1. If only traces of oxides are present on the cathode (curve 2), the characteristic bend is less steep, and the overvoltage is less than in curve 1. In this case, as the current density increases, the reducing action of hydrogen on the traces of oxide films is intensified, with formation of additional new active regions, formerly oxidized. This results in a decrease of true current density, with a downward bend (curve 2). The influence of the oxide films indicates that porosity is a definite factor in decreasing hydrogen overvoltage, and its action depends on the current density range. Further studies of the effects of current density on overvoltage should be carried out at current densities between 6000 and $10000 \text{ amp}/\text{m}^2$.

SUMMARY

1. The decrease of hydrogen overvoltage at a porous cathode at $D_c = 1000\text{--}3000 \text{ amp}/\text{m}^2$ and $t = 20^{\circ}$ is 0.45 v (below the value for a smooth iron cathode), and 0.3 v at 20° and 0.2 v at 80° (below the value for a sand-rubbed smooth iron electrode).
2. The overvoltage is decreased sharply with increased contents of nickel in iron at 20 and 40° . This effect is diminished at 80° .
3. The temperature gradient of overvoltage decreases with increase of current density above $1000 \text{ amp}/\text{m}^2$. Increase of temperature by one degree produces an average decrease of 2.5–3.0 mv in the overvoltage.
4. It is suggested that the decrease of overvoltage at a porous iron-nickel cathode is due to the increased surface area and formation of active regions on the heterogeneous surface; less energy is required for liberation of hydrogen during electrolysis at these regions than at a smooth electrode.

5. The hydrogen overvoltage at an electrode made from a powder mixture may be lower than at either of the components taken separately.

6. The deviation of the $\eta_{H_2} - \log i$ curves from linearity are explained.

7. Porous iron electrodes with pressed surface layers (about 1 mm thick), containing 20% Fe and 80% Ni are recommended for tests on the semilarge scale. The cathodes are made from iron and nickel powders by pressing at 1400 kg/cm², followed by sintering in hydrogen at 750°. The dimensions of the porous cathode depend on the design and size of the cell and the nature of the electrolytic process.

LITERATURE CITED

- [1] N. N. Voronin, I. B. Barmashenko, and D. S. Nadezhdin, *Ukrain. Chem. J.* 20, 2 (1954).
- [2] B. N. Kobozev, *J. Phys. Chem.* 22, 1 (1952).
- [3] A. N. Frumkin, V. S. Bagotskii, Z. A. Iofa, and T. N. Kabanov, *Kinetics of Electrode Processes* [in Russian] (Izd. MGU, 1952) p. 186.
- [4] P. Lukovtsev and S. Levina, *J. Phys. Chem.* 21, 589 (1947).
- [5] M. A. Loshkarev and A. M. Ozerov, *J. Phys. Chem.* 24, 547 (1951).
- [6] Daniel'-Bek, *J. Phys. Chem.* 22, 697 (1946).

Received September 30, 1957

MECHANISM OF FORMATION OF BRIGHT NICKEL DEPOSITS IN BATHS WITH SULFUR-CONTAINING ADDITIVES

R. M. Morgart and O. É. Panchuk

Laboratory of Physical Chemistry, Chernovits University

The formation mechanism of bright nickel deposits from baths with various brightening agents is still very obscure.

The sulfur compounds which may be used as brightening agents in nickel plating include mono- and polysulfonated benzene and naphthalene and their homologs; aromatic sulfonamides and sulfonimides; also, as investigations in our laboratory have shown [1], a number of other inorganic and organic compounds containing bivalent sulfur.

Some authors [2-7] consider that the most likely effect is adsorption of the sulfur-containing additives in the molecular state over the whole cathode surface, or at individual regions - growing crystal faces. Raub and Wittum [8] suggested that aromatic sulfonic acids are decomposed at a nickel cathode with liberation of nonsulfonated compounds. Some authors believe that sulfonic acids may be decomposed at the cathode with formation of the corresponding mercaptans [9-10], which form adsorption layers on the cathode surface. It is postulated that this is followed by reduction and decomposition of the aromatic nucleus, while the sulfur is included in the deposit in the form of nickel sulfide. It is known, however, that reduction of, say, the naphthalene nucleus occurs at potentials [11] which are hardly attainable even at individual cathode regions. The reduction process of naphthalenesulfonic acids is itself obscure [12]. A polarographic wave for the reduction of naphthalenesulfonic acids on mercury cannot be obtained [11, 12]. However, it has been shown that this is possible with the use of a rotating nickel microcathode [13]. Reduction of sulfonic acids yields mercaptans - substances containing bivalent sulfur. The latter react readily with Raney nickel, nickel sulfide being formed [14-18]. The reaction proceeds in the cold, and in most instances quantitatively. There is no reason to doubt that a nickel cathode in the course of electrolysis is at least as powerful a reducing agent as Raney nickel. The nickel sulfide produced in the process is apparently in the colloidal state; this is analogous to the formation of colloidal nickel hydroxide in the reaction of Raney nickel with water [14]. Naphthalenesulfonic acids split off sulfur only after it has been reduced to S^{-2} , similarly to the reaction of Raney nickel with sodium sulfite solution with formation of nickel sulfide [15]. Our experiments showed that sodium sulfite can act as a brightener for nickel deposits. Sulfonic acids also differ from substances containing bivalent sulfur because their sulfur is in the anion. Since only molecules are reduced, only a small proportion of the added brightener takes part in this process. When the concentration of the brightener is increased above a certain optimum value, the number of molecules of the additive to undergo decomposition remains constant. This explains why it is possible to add very large amounts (up to 30-50 g/liter) of naphthalenesulfonic acids to electrolytes without large increases of cathodic polarization [12] or deterioration of the mechanical properties of the coating [3].

The question of the action of additives in nickel plating must be considered in close association with the causes of brightness of electrolytic deposits. It seems that neither the grain size [9, 19-21] nor crystal orientation [15, 22-24] is decisive in this respect. The most acceptable view is that the surface becomes leveled, i.e., angles and projections, etc., are usually smoothed out [20]. The question of leveling is closely related to the layer structure found in bright nickel deposits [10, 20, 21, 25a]. Several theories have been put forward to explain the formation mechanism of periodically recurring layers [9, 10], but, as was noted above, these are inadequately justified and contradict certain experimental data. Henricks [9, 26] obtained a multilayer nickel deposit from a

bath yielding dull deposits, by intermediate exposure of the deposit in 1% "rodin" (a thiourea derivative), 13 μ thick and with a high luster. We carried out similar experiments with intermediate exposure of the deposit in 1% thiourea solution and in a solution containing 0.065 g of gelatin per liter. The deposits were dull in the former case and bright in the latter. Semibright nickel deposits are obtained by exposure to acid solutions of thiourea. The same result can be obtained by periodic cathodic polarization of the specimens in a neutral thiourea solution containing potassium sulfate. It follows that in a neutral solution thiourea is not adsorbed on nickel to a sufficient extent to have a significant effect on its structure during subsequent electrodeposition. This effect is produced if hydrogen is liberated at the nickel electrode. Probably in this case nickel may react with the additive to yield nickel sulfide, which is adsorbed on the specimen and is not washed off it. Experiments with gelatin show that colloids are adsorbed well by nickel.

The sign of the charge on the colloidal nickel sulfide particles under the acid conditions which arise in the catholyte zone is significant in relation to the manner in which colloidal nickel sulfide influences the cathode process. It has been stated that the sign is negative [25b, 27]. However, other data [28] suggest that if the sulfide is formed in the catholyte zone, the charge is positive. Charge reversal in colloids with change of acidity is a well-known phenomenon. A colloidal solution of nickel sulfide was prepared by the mixing of very dilute solutions of nickel nitrate and sodium sulfide. Electrophoresis showed that the particles are negatively charged. The solution pH was a little above 7. The value of the electrokinetic potential (5.3 mv) indicated that the colloid was unstable and that the solution pH was close to the isoelectric point. Tests showed that the colloid did not coagulate for at least 1.5 hours after preparation. The colloidal solution was introduced into an electrolyte yielding dull deposits through a glass tube pressed against the cathode. During 51 minutes of electrolysis, which was enough to give a nickel layer 10 μ thick, about 2.5 ml of solution flowed out. The deposit was bright where the colloidal solution flowed over it. It seems that when the colloid is supplied directly to the cathode, its charge is changed to positive and it is adsorbed on the cathode. To confirm that the effect is not due to alkali, a similar experiment was performed with addition of caustic soda solution at pH = 10 to the electrolyte. The deposit remained dull over its entire surface.

Subsequent experiments showed that electrodeposition of nickel from electrolytes containing suspended nickel sulfide yields bright deposits despite the low solubility of this substance. Other sulfides, such as those of antimony, cobalt, etc., act analogously. Henricks' findings [9] that sodium sulfide acts as a brightener in the electrodeposition of nickel were also confirmed.

The instances of layer structure in bright nickel deposits which have been described in the literature refer to the deposits from baths of high pH values. To determine the effect of electrolyte acidity on deposit structure, an electrolyte containing 3 g of a technical mixture of 2,6- and 2,7-naphthalenesulfonic acid per liter was adjusted to pH 5.8, and a layer 50 μ thick was deposited from it. The solution was then acidified to pH 2.3, and a further 50 μ was deposited. A similar experiment was performed without brightener in the electrolyte. Photomicrographs of polished cross sections of the two deposits showed that the part of the deposit, formed at pH 2.3 from the electrolyte containing brightener, did not have a layer structure. To find at what pH layers can still be detected, specimens were obtained at six different pH values (2.3, 4, 5, 5.5, and 6) from an electrolyte containing the same brightener. The sections were all etched by the same solution for equal times. Examination of the sections showed that layers are found only in deposits formed at pH of 6 and 5.5, and in the latter case they are rather weak. A layer structure is also found in nickel deposits formed in presence of other sulfur compounds.

In the light of all the above data, the most probable mechanism of the action of sulfur-containing additives on the cathode process in the electrodeposition of nickel is the following.

When a molecule of a sulfur compound comes into contact with a projection on the cathode, it is reduced and decomposed with formation of positively charged colloidal nickel sulfide. The additive is decomposed at these points because they are the most advantageous from the energy aspect (the potential is highest). Any nickel sulfide accidentally formed in depressions or at flat regions migrates to regions of higher potential. As a result, most of the projections on the cathode eventually become insulated. Therefore, the deposit grows mainly at the unoccupied regions. The process continues in this manner until the surface has been leveled to some extent, and as a result the true total surface area of the cathode is decreased so much that reduction of nickel sulfide becomes possible [29]. This liberates the surface regions which had been occupied by nickel sulfide. However, a part of the colloid, adsorbed on regions of intermediate local current density, may escape reduction and remain in position being subsequently included in the deposit. It is possible that nickel layers containing unreduced sulfide are more

easily etched, so that a rhythmic structure is revealed in polished cross sections of the deposits. The liberated sulfide ions leave the cathode through a zone almost free from nickel ions. Beyond this zone nickel sulfide is formed, first as a true and then as a colloidal solution. During this period a polycrystalline deposit grows without hindrance. Individual projections again begin to appear on its surface. Colloidal nickel sulfide, newly formed in the cathode zone, is adsorbed on these, and the whole process is repeated. Consecutive growth of the layers formed in this manner leads to the formation of a level bright deposit. The individual metal layers may differ in thickness, as this depends on the microgeometry of the basis metal, variations of the electrolysis conditions, such as fluctuations of current strength during deposition of nickel, etc.

In the light of this mechanism it is easy to explain the observed dependence of the luster of nickel deposits formed from baths containing naphthalenesulfonic acids [12, 13, 30] and other sulfur compounds [1] on the cathodic current density, temperature, and acidity of the electrolyte.

It must be pointed out that the mechanism postulated for the action of sulfur-containing brighteners does not exclude possible stabilization of colloidal basic nickel compounds formed by the decomposition of these brighteners by colloidal nickel sulfide; such compounds were found by Gorbunova et al. [20, 21] in nickel deposits formed from electrolytes containing naphthalenesulfonic acids. They also found that the surface layer of the deposit contained a certain amorphous phase, the nature of which could not be established, although it was suggested that it consists of nickel hydroxide with the additive adsorbed on it. In the light of our suggested mechanism the presence of such an amorphous phase, consisting of nickel sulfide or a mixture of the latter with nickel hydroxide in the surface layer, is entirely probable, as the surface layer is in direct contact with the colloid which is continuously forming at the cathode.

SUMMARY

1. The possible conversions of sulfur-containing brighteners in the cathode region during electrodeposition of nickel were considered, and it is suggested that these conversions lead to the formation of the same final product from all sulfur-containing additives — colloidal nickel sulfide.
2. The mechanism postulated for the action of colloidal nickel sulfide in the formation of bright nickel deposits accounts for certain facts observed in the course of bright nickel plating.

LITERATURE CITED

- [1] A. V. Pamfilov and R. M. Morgart, *Ukrain. Chem. J.* 23, 684 (1957).
- [2] N. T. Kudryavtsev and V. V. Fedurkin, *Bright Nickel Plating* [in Russian] (Russian Local Industries State Press, Moscow, 1951).
- [3] G. E. Gardam, *Sheet Met. Ind.* 25, 743 (1948).
- [4] L. I. Antropov and S. Ya. Popov, *J. Appl. Chem.* 27, No. 2, 206 (1954). *
- [5] F. Denise and H. Leidheiser, *J. Electrochem. Soc.* 100, 490 (1953).
- [6] C. C. Roth and H. Leidheiser, *J. Electrochem. Soc.* 100, 553 (1953).
- [7] N. T. Kudryavtsev, O. M. Korol'kova, and V. V. Fedurkin, *J. Appl. Chem.* 22, No. 6, 586 (1949).
- [8] E. Raub and M. Wittum, *Z. Elektrochem.* 46, 71 (1940).
- [9] J. A. Henricks, *Trans. Am. Electrochem. Soc.* 82, 113 (1942).
- [10] A. F. Brockington, *Met. Ind.* 69, 468 (1946).
- [11] E. S. Levin and A. P. Shestov, *Proc. Acad. Sci. USSR* 96, 999 (1954).
- [12] A. V. Pamfilov and O. E. Panchuk, *Ukrain. Chem. J.* 23, 391 (1957).
- [13] A. V. Pamfilov and O. E. Panchuk, *Ukrain. Chem. J.* 24, 408 (1958).
- [14] J. Aubry, *Bull. Soc. Chim. France*, (5) 5, 1333 (1938).
- [15] J. Bougault, E. Cattelain, and P. Chabrier, *Bull. Soc. Chim. France* (5) 6, 34 (1939).

* Original Russian pagination. See C. B. Translation.

- [16] J. Bougault, E. Cattelain, and P. Chabrier, *Bull. Soc. Chim. France*, (5) 7, 781 (1940).
- [17] R. Mozingo, S. Harris, D. E. Wolf, and K. Folkers, *J. Am. Chem. Soc.* 65, 1013 (1943).
- [18] *Newer Methods of Preparative Organic Chemistry* (IL, Moscow, 1950) p. 215 [Russian translation edited by D. N. Kursanov].
- [19] H. J. Read and R. Weil, *MetaIoberfl.* A5, 97 (1951).
- [20] K. M. Gorbunova, T. V. Ivanovskaya, and N. A. Shishakov, *J. Phys. Chem.* 25, 981 (1951).
- [21] K. M. Gorbunova, T. V. Ivanovskaya, and O. S. Popova, *Proc. 1950 Conference on Electrochemistry* [in Russian] (Izd. AN SSSR, Moscow, 1953) p. 396.
- [22] G. L. Clark and S. H. Simonsen, *J. Electrochem. Soc.* 98, 110 (1951).
- [23] A. T. Vagramyan and Z. A. Solov'eva, *J. Phys. Chem.* 26, 981 (1952).
- [24] W. Smith, J. H. Keeler, and H. J. Read, *Plating* 36, 355 (1949).
- [25] H. Fischer, *Elektrolytische Abschneidung und Elektrokristallisation von Metallen*. Springer-Verlag: a) 514, b) 537 (1954).
- [26] J. A. Henricks, *Met. Ind.* 62, 26 (1943).
- [27] E. Raub and B. Wulhorst, *Arch. Metallkunde* 3, 323 (1949).
- [28] E. Beutel and A. Kutzelnigg, *Monatsh.* 58, 295 (1931).
- [29] K. Fischbeck, and E. Elnecke, *Z. anorg. allg. Chim.* 175, 341 (1928).
- [30] A. V. Pamfilov and O. É. Panchuk, *Ukrain. Chem. J.* 24, 266 (1958).

Received September 7, 1957

PRODUCTION OF BRIGHT COATING IN ELECTRODEPOSITION OF COPPER-GOLD ALLOYS

B. S. Krasikov and Yu. D. Grin

The need to replace gold plating by cheaper copper-gold coatings, retaining the same corrosion resistance and decorative properties, has led to a number of investigations [1-3], including a paper [4] by one of the present authors; this last paper contained details of electrolyte composition and operating conditions for production of gold-copper alloy coatings over a wide range of alloy compositions.

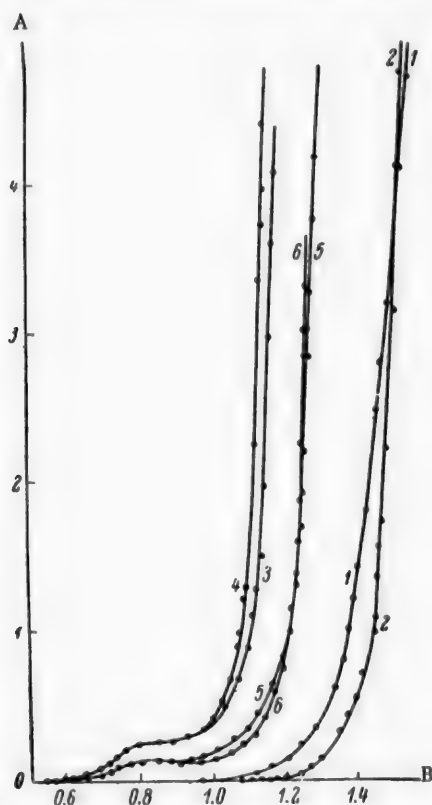


Fig. 1. Polarization curves for cyanide solutions containing copper and gold: A) current density (amp/dm²); B) negative potential (v); electrolyte composition (g/liter): 1) Cu 9.4, KCN_{free} 17.4, (NH₂)₂CS 0.7; 2) Cu 9.4, KCN_{free} 17.4, 3) Au 4, KCN_{free} 16.6, (NH₂)₂CS 0.7; 4) Au 4; KCN_{free} 16.6; 5) Au 2, Cu 9.6, KCN_{free} 19.2, (NH₂)₂CS 0.7; 6) Au 2, Cu 9.6, KCN_{free} 19.2

The present paper reports a continuation of the study of the electrodeposition of copper-gold alloys for production of bright coatings, which do not require subsequent polishing, from the electrolytes studied earlier [4], on jewelry (with gold content 70-80% by weight in the coating).

It is reported in the literature that bright copper deposits can be obtained from cyanide [5] and thiocyanate [6] electrolytes, and bright gold deposits [7-11] from cyanide electrolytes, in presence of various brighteners. In our opinion electrolytes with additions of thiourea are the most promising, since both copper and gold can be deposited separately in the form of bright coatings from cyanide electrolytes [5-7], or an electrolyte containing Trilon B as a brightener for copper [1]. We therefore concentrated mainly on electrolytes containing thiourea, and also tested the possible use of electrolytes containing Trilon B. The procedure consisted of determination of polarization curves, composition, and quality of the deposits formed. The cathodes were polished brass plates of total area 4.87 cm²; the anodes platinum-plated iron. The electrolyte composition was adjusted at intervals in accordance with analytical data for all the components.

In experiments with electrolyte containing Trilon B, layers up to 2 μ thick which did not require further polishing could be obtained from the freshly-prepared solution; however, the electrolyte is unstable and cannot be regenerated after use (the original electrolyte contained 2 g Au, 1.56 g Cu, and 2 g free KCN per liter).

Thiourea in amounts from 0.7 to 1.0 g/liter [6] was added to various electrolytes, containing 2-4 g gold and 1.5-20 g of copper (as the metals) and 8-18 g of free potassium cyanide per liter.

Some selected results are given in Figs. 1-3 and in the table.

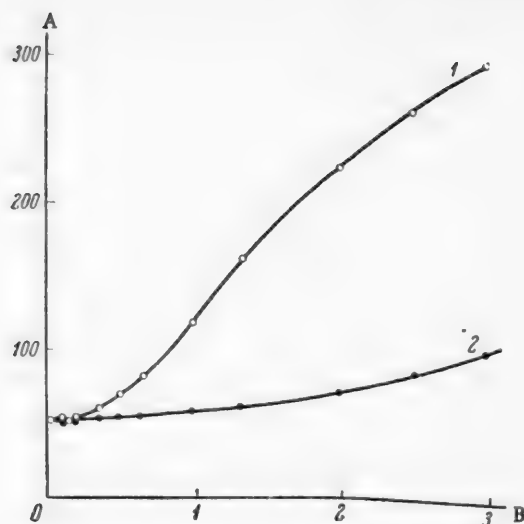


Fig. 2. Variations of the capacity of the double layer on gold electrodes with the current density used for electrodeposition: A) capacity ($\mu\text{F}/\text{cm}^2$); B) current density (amp/cm^2); electrolyte composition (g/liter): 1) Au 4, KCN_{free} 17.0; 2) Au 4, KCN_{free} 17.0, $(\text{NH}_2)_2\text{CS}$ 0.7.

It is clear from the polarization curves in Fig. 1 that addition of thiourea to copper cyanide electrolyte facilitates discharge of complex anions of type $[\text{Cu}(\text{CN})_2]^-$ and $[\text{Cu}(\text{CN})_3]^{--}$, in accordance with the retarded-discharge theory (in solutions of $\text{pH} > 7$ thiourea is a surface-active agent of the cationic type [6]). However, at very high current densities the current efficiency for copper is rather low, while discharge of water molecules is not retarded by surface-active agents, and the electrode potential - current density curves for solutions with and without the additive almost coincide (curves 1 and 2 in Fig. 1).

Discharge of the complex $[\text{Au}(\text{CN})_2]^-$ anions is retarded mainly as the result of concentrational polarization [3, 12] and addition of thiourea to the electrolyte does not influence the nature of the polarization curve at $D_c \leq i_{\text{lim}}$, but at current densities higher than the limiting current density for discharge of gold ions (i_{lim}) at a given concentration of these ions in the electrolyte the polarization curves diverge by 30-35 mv, when the curve for the solution with added thiourea (curve 3) lies at higher negative values of the potential. This result is easily explained in terms of the nature of the deposits formed. Specific adsorption of the

Composition of Quality of the Deposits Formed $D_c = 1 \text{ amp}/\text{dm}^2$, $t = 60 \pm 2^\circ$

Electrolyte composition (g/liter)	Thickness of deposit (μ)	Composition of deposit (%)	Nature of deposit
Au 2, Cu 19, KCN_{free} 16	2.4	Au-70.2 Cu-29.8	Compact, dull with slight luster, golden pink
Au 2, Cu 19, KCN_{free} 16 thiourea 0.7	2.3	Au-36.3 Cu-63.7	Compact, bright, pink with slight dull edges
	1.9	Au-34.0 Cu-66.0	Compact, bright, pink
Au 2, Cu 13.3, KCN_{free} 16 thiourea 0.7	1.6	Au-44.3 Cu-55.7	Compact, bright with dull edges, pink

cation-active additive does not influence the discharge potential of H_2O molecules, but the presence of the adsorption film leads to a sharp improvement in the quality of the deposits formed. If the dispersity of the gold deposits formed is estimated by measurements of the capacity of the double layer with the aid of alternating current and a compensation bridge [13, 14], it is found from the results of measurements in solutions of H_2SO_4 ($\text{pH} = 3$) + 0.5 N Na_2SO_4 that the capacity of gold electrodes formed from electrolytes without thiourea is 50-290 $\mu\text{F}/\text{cm}^2$ (according to the current density) whereas the capacity of gold deposits formed from electrolytes with additions of 0.7 g thiourea per liter is 50-97 $\mu\text{F}/\text{cm}^2$. These results are presented in Fig. 2. If the current densities are calculated per unit true surface area, the polarization curves for solutions with and without the additive almost coincide. It must be pointed out that capacity determinations for specimens obtained at current densities $D_c \leq i_{\text{lim}}$ give similar results (50-58 $\mu\text{F}/\text{cm}^2$) irrespectively of the type of electrolyte (with or without thiourea) from which the deposit was formed.

Polarization curves for gold-copper electrolytes are shown in Fig. 1 (curves 5 and 6). Depolarization of the copper-deposition process owing to formation of Cu-Au solid solution shifts the polarization curves in the

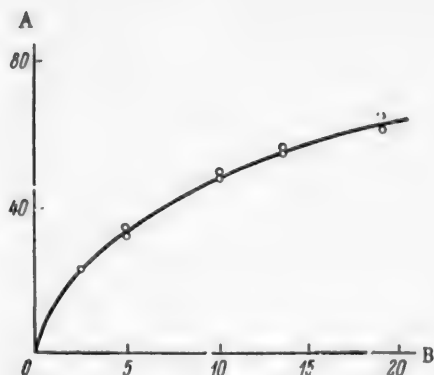


Fig. 3. Effect of the copper content of gold-copper electrolyte on the composition of the deposit: A) copper content of deposit (wt. %); B) copper content of solution (g/liter); composition of electrolyte (in addition to copper) in g/liters: Au 2, KCN_{free} 19, (NH₂)₂CS 0.7; temperature: $60 \pm 2^\circ$, $D_c = 1 \text{ amp/dm}^2$.

of these experiments are given in Fig. 3, which shows that in presence of 0.7 g thiourea per liter in the electrolyte bright deposits of gold-copper alloy, corresponding in color to gold 583 fine are obtained when the copper content of the electrolyte is 3-4 g/liter, whereas coatings of the same composition (but dull) are obtained under the same conditions from an electrolyte without the additive with a copper content of 7-8.5 g/liter.

The presence of some dull scale on coatings which in general have a fairly higher luster is due to irregular distribution of current over the specimen surface. This could be avoided by stirring. Agitation by means of air bubbles is unsuitable for cyanide electrolytes [12], and we therefore tried mechanical agitation of the electrolyte by means of stirring, and agitation by means of ultrasonics.

Stirring by means of ordinary blade stirrers at a very moderate rate gave the desired results - the deposits formed were mirror-bright and did not require any polishing.

Agitation increases the limiting current for discharge of gold ions, so that the current density was correspondingly increased and the KCN content was lowered somewhat in order to increase the total current efficiency; the best results were obtained with an electrolyte of the following composition (in g/liter): Au (as metal) 2, Cu (as metal) 9-10, KCN_{free} 10-12, thiourea 0.6-0.8; temperature $60 \pm 2^\circ$, $\eta = 63-69\%$, $D_c = 1.5 \text{ amp/dm}^2$.

Similar results (mirror-bright deposits) were obtained with ultrasonic agitation of the electrolyte. The ultrasonic source was generator with a piezoelectric quartz oscillator. It should be noted that the best agitation was obtained at an oscillator frequency of 650-680 kilocycles/second; increase of the frequency to 800 kilocycles at the same power gave deposits of much worse quality (dull, uneven, sometimes powdery). Such effects had been observed earlier by other workers [15, 16] and are not discussed here.

Further investigations were concerned with the stability of the electrolyte in use; several series of specimens were coated during 13 days of continuous operation of the bath, during which time 50 amp-hr was passed per liter of electrolyte, i.e., the metal content of the bath was renewed repeatedly. There was no changes in the quality or composition of the deposits, and therefore it may be assumed that the electrolyte is very stable in operation if the composition is correctly adjusted.

Tests of the quality of the coating on silver objects kindly provided by the 2nd Leningrad Jewelry Factory also demonstrated that our electrolyte is completely suitable for production of bright copper-gold alloy coatings 780-800 fine.

direction of higher positive potentials at $D_c > i_{lim}$. The copper content in deposits formed from solutions with added thiourea is considerably higher than in deposits from electrolytes without the additive (see table).

Data for the electrolyte without added thiourea are taken from the previous paper [4].

It follows from the table that addition of thiourea to the solution, apart from raising the copper content of the deposit, results in a considerable change in the external appearance of the deposits, which become bright, but are slightly dull at the edges at thickness greater than 2μ .

In view of the purpose of the investigation, it was necessary to raise the gold content of the deposit to 70-80 wt. %.

The character of the polarization curves for the mixed electrolyte suggested that increases of electrolyte temperature and current density would increase the copper content of the deposit, which is undesirable. In addition to increasing the copper content of the deposit, the use of higher current densities for electrolysis had an adverse effect on the deposit quality. Therefore, the most acceptable procedure was to decrease the copper content of the solution. The results of

SUMMARY

1. Studies of polarization curves and of the dependence of the deposit composition on current density and electrolyte composition have led to the development of a method for production of bright gold-copper alloy coating from cyanide electrolytes containing thiourea.

2. An electrolyte composition and electrolysis condition have been worked out for formation of gold-copper alloy coating 780-800 fine. The coating do not require subsequent polishing they are mirror-bright).

3. The electrolyte is stable in operation; tests showed that it is quite suitable for production of bright gold-copper coatings of jewelry.

LITERATURE CITED

- [1] British Patent 718574; Metal Ind. 86, 2, 30 (1955).
- [2] Electrolytic Gold Plating of Jewelry [in Russian] (Information leaflet, Russian Industrial Council, Moscow, 1955).
- [3] E. Raub and F. Sautter, Metaloberfl. 3, 65 (1956).
- [4] B. S. Krasikov, J. Appl. Chem. 30, 799 (1957). *
- [5] L. I. Kadaner, Latest Advances in Electroplating [in Russian] (Khar'kov State Univ. Press, 1951) p. 89.
- [6] B. S. Krasikov and A. M. Gvoz'd', J. Appl. Chem. 30, 954 (1957). *
- [7] B. Wulhorst, Metal Finishing 8, 30 (1954).
- [8] B. C. Rinker, Plating 40, 861 (1953).
- [9] E. A. Parker, Plating 38, 1154 (1951).
- [10] U. S. Patent 2660554 (1953).
- [11] German Patent 731043, Metaloberfl. 4 (1953).
- [12] V. I. Lainer and N. T. Kudryavtsev, Fundamentals of Electroplating, 1 [in Russian] (Metallurgy Press, Moscow, 1953).
- [13] P. I. Dolin and B. V. Ershler, J. Phys. Chem. 14, 886 (1940).
- [14] V. L. Kheifets and B. S. Krasikov, Proc. Acad. Sci. USSR 94, 101 (1954).
- [15] W. Winkler, Metaloberfl. 4 (1953).
- [16] G. S. Gardam, Metal Finish. 6, 105 (1954).

Received July 8, 1957

* Original Russian pagination. See C. B. Translation.

THE STATE OF NICKEL IN AMMONIACAL TARTRATE AND CITRATE SOLUTIONS

T. F. Frantsevich-Zabludovskaya, A. I. Zayats, and V. T. Barchuk

Rational control of electrolytic processes requires an understanding of electrode processes. In particular, in order to understand the mechanism of electrodeposition of alloys of tungsten and molybdenum with nickel from ammoniacal hydroxy-acid solutions it is necessary to know the state of the nickel ions in solution.

Several investigators have studied the interaction of metals of the iron group with tartaric and citric acids and their salts [1-6]. According to their results, bivalent metals of the iron group, including nickel, form complexes with metal-citrate ratios of 1:1 and 1:2 in acid and 1:1 in alkaline and neutral media. Excess of alkali or ammonia may break down the complex with formation of the metal hydroxide, which forms a complex ammine cation in presence of ammonia. It has also been shown that the citrate complex is more stable than the tartrate complex [1, 2].

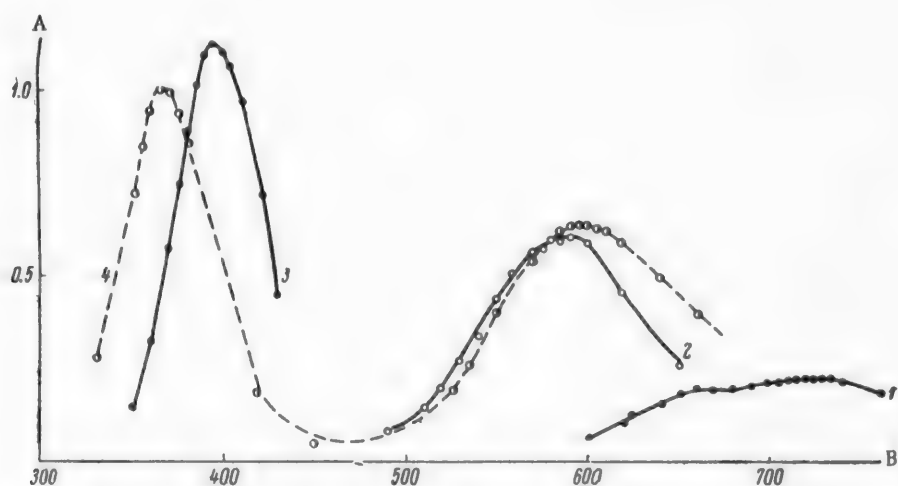


Fig. 1. Optical density of nickel solutions: A) wavelength ($m\mu$); B) optical density; concentrations (moles/liter): nickel sulfate 0.2, ammonium hydroxide 2, potassium-sodium tartrate 0.5, 1) Nickel sulfate; 2) the same, with ammonium hydroxide; 3) nickel sulfate with Rochelle salt; 4) the same with ammonia.

The view was put forward in our earlier papers [7, 8] that in ammoniacal citrate and tartrate electrolytes used for electrodeposition of alloys of molybdenum and tungsten with nickel, the latter is discharged from a complex hydroxy-acid anion. The basis for this hypothesis was the existence of only one maximum of light absorption for ammoniacal citrate electrolytes, and the considerable shift of the deposition potential of nickel in the negative direction as compared with ammoniacal electrolytes. To verify this hypothesis, we carried out additional investigations of the absorption spectra of nickel sulfate solutions in presence of citrates or tartrates, ammonia, and mixtures of these, and also determined the sign of the charge on the nickel-containing particles.

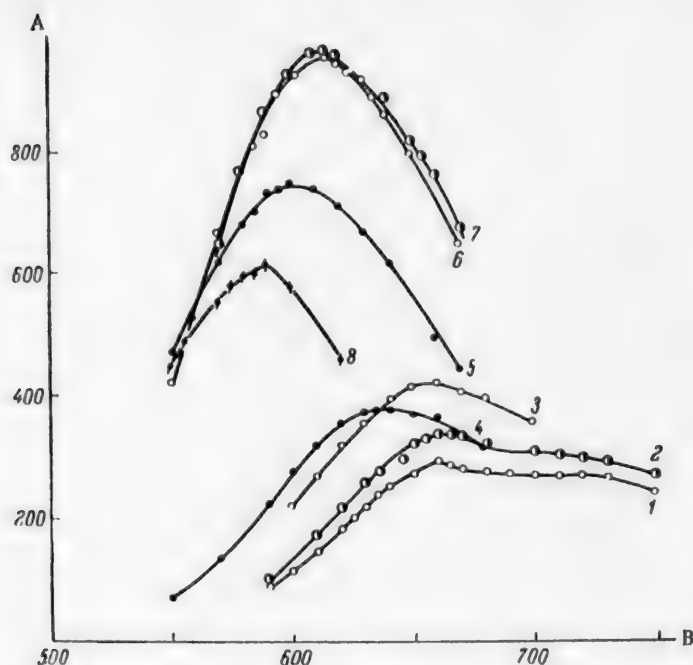


Fig. 2. Optical density of nickel solutions: A) wavelength; B) optical density; concentrations (moles/liter): nickel sulfate 0.2, ammonium hydroxide 2. 1) Nickel sulfate + 0.1 mole sodium citrate; 2) nickel sulfate + 0.2 mole sodium citrate; 3 and 4) nickel sulfate + 0.5 mole sodium citrate; 5) nickel sulfate + ammonium hydroxide + 0.1 mole sodium citrate; 6) nickel sulfate + ammonium hydroxide + 0.2 mole sodium citrate; 7) nickel sulfate + ammonium hydroxide + 0.5 mole sodium citrate; 8) nickel sulfate + ammonium hydroxide.

EXPERIMENTAL

Spectrophotometric Studies. The absorption spectra were determined by means of the SF-4 quartz spectrophotometer. The compositions of the solutions studied, given in Table 1, are close to the component concentrations in electrolytes used in production of alloys of molybdenum and tungsten with nickel.

The results are given in Fig. 1 and Fig. 2. Figure 1 (curve 1) shows the optical density of nickel sulfate solutions (Table 1, solution No. 1). The curve passes through a flat extended maximum corresponding to a wavelength of 725 m μ . Addition of two moles of ammonia to this solution produces an intense blue color characteristic of nickel ammine, and sharply increases the optical density, the maximum of which corresponds to 590 m μ (Fig. 1, curve 2). Nickel sulfate solution containing tartrate (Table 1, solution No. 3), of an emerald-green color, has a very high optical density, the maximum of which lies in a region of relatively short wavelengths at 395 m μ (Fig. 1, curve 3). In presence of both complex formers in solution (Fig. 1, curve 4), the latter maximum is shifted by 30 m μ in the direction of shorter wavelengths, with some decrease of intensity, whereas the intensity and position of the absorption maximum for the ammine complex remain unchanged.

The data in Table 1 for solutions Nos. 2 and 5-8 (Fig. 2) show that the optical density maxima for ammoniacal and citrate solutions of nickel sulfate are at similar wavelengths, especially for neutral and alkaline solutions. The maxima of curves 1, 2, and 3 in Fig. 2, which represent data for solutions Nos. 5, 6, and 7 of Table 1, correspond to a wavelength of 660 m μ ; with a deficiency of sodium citrate (Fig. 2, curve 1) an indistinct absorption maximum corresponding to nickel sulfate may be detected. When the solution acidity is decreased to pH = 7 and higher, the green solutions acquire a bluish tinge, and the absorption maximum is shifted (by 23 m μ) in the direction of shorter wavelengths (Fig. 2, curve 4). Addition of two moles of ammonia to these solutions

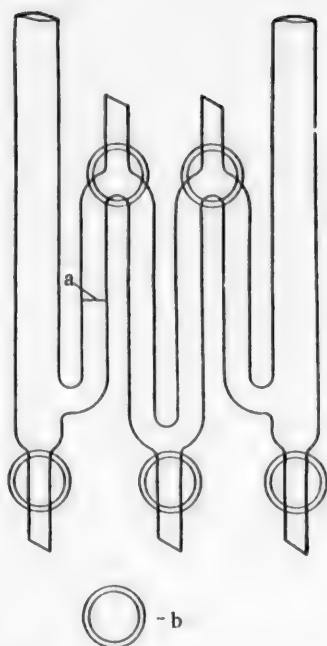


Fig. 3. Vessel for determination the sign of the charge: a) initial boundary between electrolyte and buffer; b) two-way cocks.

shifts the maximum still further in the direction of shorter wavelengths, and a second maximum is not observed (Fig. 2, curves 5, 6 and 7). The optical-density curve of an ammoniacal nickel sulfate solution is shown for comparison (Fig. 2, curve 8). Comparison of curves 5, 6, 7, and 8 shows that the maxima of curves 8 and 5, i.e., ammoniacal and citrate nickel sulfate solutions with a deficiency of sodium citrate, correspond to almost the same wavelength — 590 and 600 $m\mu$, respectively. With the molar concentrations of nickel sulfate and sodium citrate in 1:1 ratio, as with excess sodium citrate (Fig. 2, curves 6 and 7) the maximum lies between the maxima corresponding to the ammoniacal and the citrate nickel sulfate solutions, i.e., at 615 $m\mu$. It must be noted that the optical density of mixed citrate-ammoniacal solutions is much higher than that of each separately.

Determination of the Sign of the Charge of the Nickel-Containing Ions

The cell (Fig. 3) with nonpolarizing copper-coppersulfate electrodes was used for the determinations which were performed at 140 v and current strength ~ 20 ma. The composition of the solutions used are given in Table 2.

The conducting salt was ammonium sulfate in ammoniacal tartrate solutions, and sodium sulfate in ammoniacal citrate solutions. The density of the buffer solution was regulated by addition of the corresponding sulfate, and the pH was adjusted to 10-11 by addition of ammonia so that both the density and the pH corresponded to those

TABLE 1

Solution Compositions, Color, pH, and Wavelength of the Absorption Maxima

Solution No.	Concentration (moles/liter)				pH	Wave-length of adsorption maximum ($m\mu$)	Color
	nickel sulfate	ammonium hydroxide	potassium sodium tartrate	sodium citrate			
1	0.2	—	—	—	5.5	725	Pale green
2		2	—	—	11.0	590	Intense blue
3		—	0.5	—	6.0	395	Emerald green
4		2	0.5	—	10.0	367	Blue with greenish tinge
5		—	—	0.1	5.5	595	Green
6		—	—	0.2	5.5	660	
7		—	—	0.5	6.0	660	
8		—	—	0.5	7.0	637	Bluish green
9		2	—	0.1	and over	615	Blue with greenish tinge
10		2	—	0.2	10.5	615	
11		2	—	0.5	10.5	615	

of the test solution. Before each experiment, the first bend (Fig. 3) was filled with the test solution to the mark "a"; the rest of the volume was filled with the buffer. The electrode connected to the first bend was joined to one of the poles of a direct-current source. The movement of the boundary between the colored solution and the colorless buffer under the influence of the current was observed; after the experiment the presence of nickel was detected qualitatively in the middle bend of the vessel.

TABLE 2

Composition of Solutions Used for Determination of the Sign of the Charge on the Nickel-Containing Ions

Composition of solution (moles/liter)					Composition of buffer (moles/liter)			
nickel sulfate	sodium sulfate or ammonium sulfate	potassium sodium tartrate	sodium citrate	ammonium hydroxide	sodium sulfate or ammonium sulfate	potassium sodium tartrate	sodium citrate	ammonium hydroxide
0.2	0.1	0.5	—	2	0.1	0.5	—	2
0.2	0.1	—	0.5	2	0.1	—	0.5	2

The results are given in Table 3.

Our observations lead to the conclusion that whereas the nickel-containing ions in ammoniacal tartrate solutions are positively charged, ammoniacal citrate electrolytes contain both positive and negative ions containing nickel. Additions of 0.06 mole of molybdenum or up to 0.15 mole of tungsten per liter to these solutions do not affect the behaviour of the electrolyte in the electric field.

DISCUSSION OF RESULTS

The following conclusions may be drawn from our results in conjunction with data available in the literature.

In alkaline ammoniacal tartrate solutions nickel forms both an ammine complex and a tartrate compound; this is shown by the existence of two maxima in the spectrum, corresponding to the maximum optical density of each compound separately (Fig. 1, curve 4). According to the views of some authors [2, 3] complex anions, containing nickel should be formed under these conditions. However, this viewpoint is not confirmed by our determinations of the sign of the charge at the ratio of the component concentrations used. It seems that the existence of an undissociated and uncharged, or a very slightly dissociated, compound of nickel with the tartrate salt must be assumed in this case.

TABLE 3

Direction of Moving Boundary

Nickel electrolyte	Pole connected	Observed direction of moving boundary	Presence of nickel in middle bend
Ammoniacal citrate	Negative	Rapid movement toward anode Boundary moves toward anode. Solution above boundary up to the third stopcock (Fig. 3) becomes violet-bluish	Detected
	Positive		
Ammoniacal tartrate	Negative	Movement toward cathode Movement toward cathode	Not detected
	Positive		Detected

The situation is different in alkaline ammoniacal citrate solutions. Experiments on determination of the sign of the charge on the nickel-containing ions show that the solutions contain both positive and negative nickel-containing ions. Spectrophotometric investigations of these solutions revealed only one maximum.

Recently Sychev [6] studied citrate complexes of certain bivalent metals, including nickel in acid and alkaline media. According to his results, their structure, number of negative charges, and stability differ in these respective media. In agreement with this, we also found that the wavelength of the absorption maximum and the

color of citrate nickel solutions vary with pH (Fig. 2, curves 1-4). When excess ammonia is added to these solutions, two types of nickel complexes should be formed, the concentrations of which are determined by their stability constants and the concentrations of the components. Accordingly, there should be two absorption maxima on the spectrophotometric curves, provided that these complexes do not interact. However, we found only one maximum for the solution studied, of a much greater intensity, corresponding to a certain intermediate wavelength. This indicates interaction between the two types of complex with possible formation of a new complex compound, the composition of which may be, for example, $[\text{Ni}(\text{NH}_3)_6][\text{NiCit}]$. Such a compound can yield both types of nickel-containing ions in solution.

Thus, our earlier hypothesis that in the electrodeposition of alloys of nickel with tungsten or molybdenum, from such solutions, nickel is liberated at the cathode from a complex anion, does not quite correspond to reality. It may be asserted with confidence that in this instance cathodic reduction of nickel takes place predominantly from a complex ammine cation. It is also possible that complex nickel citrate anions or uncharged nickel tartrate compounds are partially involved in the electrode process; on entering the cathode field by diffusion, they may act as dipoles. The appreciable shift of the potential of nickel liberation in the negative direction observed when salts of hydroxy acids are added to ammoniacal nickel solutions [7, 9] is evidently due to a decrease in the concentration of the ammine cations.

SUMMARY

1. It was shown by determinations of ion transfer under the action of current that ammoniacal citrate solutions contain both positively and negatively charged nickel complexes, whereas anions were not detected in ammoniacal tartrate solutions.

2. Measurements of optical density in ammoniacal tartrate solutions revealed two absorption maxima, the wavelengths of which correspond to an ammine and a tartrate compound of nickel.

Ammoniacal citrate solutions give only one maximum, the nature of which indicates interaction between positively and negatively charged complexes.

3. Nickel is discharged predominantly from complex ammine cations in ammoniacal hydroxy-acid electrolytes.

LITERATURE CITED

- [1] P. N. Kovalenko and L. S. Nadezhdina, *J. Gen. Chem.* 22, 740 (1952). *
- [2] M. Bobtelsky and J. Jordan, *J. Am. Chem. Soc.* 67, 1824 (1945).
- [3] M. E. Tsimbler, *Ukrain. Chem. J.* 17, 587 (1951); M. E. Tsimbler and V. I. Derenovskii, *J. Gen. Chem.* 25, 671 (1955); * *Ukrain. Chem. J.* 23, 454 (1957).
- [4] I. V. Pyatnitskii, *J. Inorg. Chem.* 1, 2368 (1956).
- [5] C. Heitner-Wirgin and I. Eliezer, *Bull. Soc. Chim. France* 2, 149 (1957).
- [6] A. Ya. Sychev, Author's Summary of Candidate's Dissertation [in Russian] (Kishinev State University, 1957).
- [7] T. F. Frantsevich-Zabludovskaya, *J. Appl. Chem* 28, 700 (1955). *
- [8] T. F. Frantsevich-Zabludovskaya, and A. I. Zayats, *J. Appl. Chem.* 30, 723 (1957). *

Received November 14, 1957

* Original Russian pagination. See C. B. Translation.

SEPARATION OF MIXTURES OF ALCOHOLS AND HYDROCARBONS BY EXTRACTION

V. B. Kogan, V. M. Fridman, and T. G. Romanova

In some industrial processes, such as the production of aliphatic alcohols, mixtures of alcohols and hydrocarbons may be formed and have to be separated.

Our purpose in the present investigation was to study the possibility of separating mixtures of alcohols and hydrocarbons by extraction. Tests of various substances showed that effective solvents for this purpose are polyhydric alcohols, such as ethylene glycol which has sharply different miscibilities with aliphatic alcohols and hydrocarbons, respectively.

TABLE 1

Compositions and Densities of Saturated Solutions in the System
Heptane-Butanol-Ethylene Glycol

Solution composition (wt. %)			Density at 20°
heptane	butanol	ethylene glycol	
0.23	4.61	95.16	1.0934
0.38	9.02	90.60	1.0758
0.50	12.91	86.59	1.0606
1.17	18.92	79.91	1.0352
2.30	21.95	75.75	1.0203
3.73	29.75	66.52	0.9828
5.00	33.20	61.80	0.9652
6.07	35.01	58.92	0.9542
7.31	36.51	56.18	0.9440
9.41	39.26	51.33	0.9246
11.77	40.70	47.53	0.9091
16.25	42.28	41.47	0.8842
19.34	42.63	38.03	0.8701
27.56	41.96	30.48	0.8378
33.47	40.18	26.35	0.8190
40.59	37.29	22.12	0.7936
47.17	35.01	17.82	0.7818
51.18	33.10	15.72	0.7715
58.30	29.70	12.00	0.7544
63.47	26.88	9.65	0.7431
67.00	25.00	8.00	0.7353
73.05	21.14	5.81	0.7237
77.94	17.95	4.11	0.7149
84.78	12.90	2.32	0.7036
92.63	6.61	0.76	0.6928

Data on liquid-phase equilibria in the system alcohol-hydrocarbon-ethylene glycol are required for quantitative evaluation of the effectiveness of separation of alcohol-hydrocarbon mixtures. The system butyl alcohol-n-heptane-ethylene glycol was chosen as a typical system.

The physical constants of the butanol and heptane used are given in an earlier paper [1]. Ethylene glycol was of "analytical" grade, and had the following constants:

Constant	Experimental data	Literature data [2]
d_4^{20}	1.113	1.113
n_D^{20}	1.4316	1.4318
B.p. at 760 mm	197.2°	197.4°

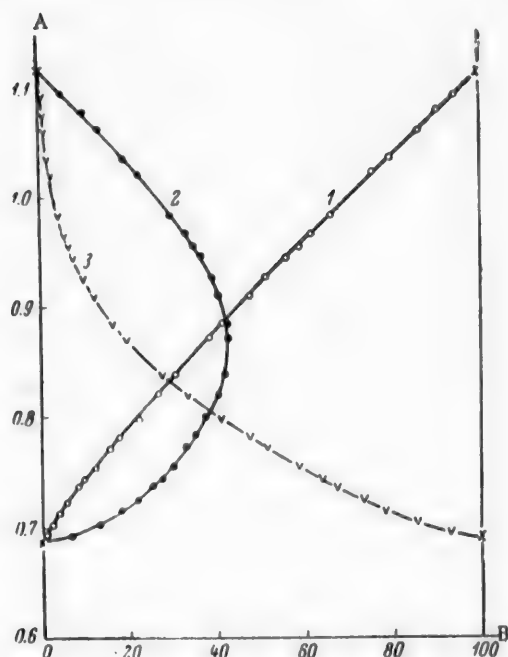


Fig. 1. Effect of composition on the density of saturated solutions in the system heptane-butyl alcohol-ethylene glycol: A) density; B) contents of components: 1) ethylene glycol; 2) butyl alcohol; 3) heptane (in wt. %).

The water contents of butanol and ethylene glycol, determined volumetrically by means of calcium hydride, were respectively 0.07 and 0.2% by weight. The solubility determinations in this system were carried out at 20°; the temperature was maintained constant within $\pm 0.05^\circ$ by means of a Höppler thermostat.

Compositions of the saturated mixtures lying on the binodal line were determined by titration to turbidity. These compositions were determined more accurately by weighing on an analytical balance to an accuracy of ± 0.0002 g. The densities of these mixtures, given in Table 1, were determined in pycnometers 25 ml in volume.

The data in Table 1 were used for determination of the compositions of the equilibrium phases as follows. Weighed quantities of the components were thoroughly mixed and allowed to separate out; the curves in Fig. 1 (based on the data in Table 1) were then used to find the composition of the equilibrium phases from the densities.

The compositions of the original heterogeneous system and the compositions found for the layers are represented in the triangular diagram in Fig. 2. Accuracy of the experimental data was confirmed by the fact that the points for the over-all composition of the original mixtures and for the compositions of the equilibrium phases fitted fairly accurately on the same straight line.

TABLE 2

Composition of Equilibrium Phases in the System Heptane-Butanol-Ethylene Glycol

Composition No.	Ethylene glycol layer			Hydrocarbon layer			Distribution coefficient of butanol
	heptane	butanol	ethylene glycol	heptane	butanol	ethylene glycol	
1	0.35	7.50	92.15	98.6	1.3	0.1	5.770
2	0.8	16.0	83.2	95.9	3.7	0.4	4.324
3	1.55	21.3	77.15	94.45	5.0	0.55	4.260
4	3.35	29.15	67.5	91.05	7.8	1.15	3.737
5	5.55	34.1	60.35	87.15	10.9	1.95	3.128
6	8.75	38.5	52.75	83.5	13.9	2.6	2.770
7	13.7	41.5	44.8	76.2	18.9	4.9	2.196
8	20.8	42.7	36.5	68.7	24.0	7.3	1.780
9	29.3	41.4	29.3	59.0	29.4	11.6	1.408
10	44.4	36.3	19.3	44.4	36.3	19.3	1

• Critical point.

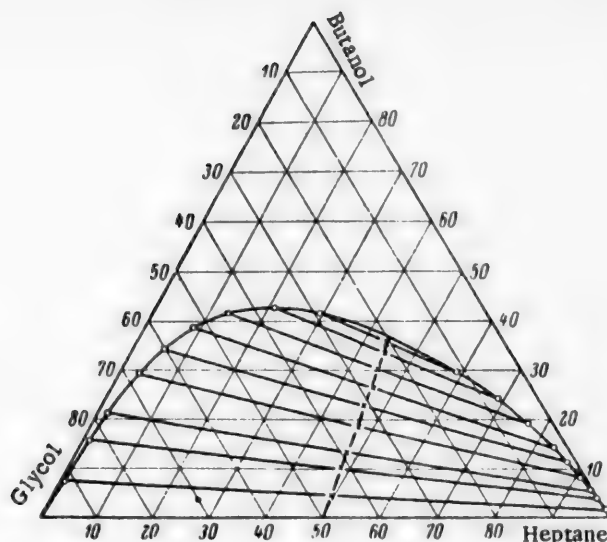


Fig. 2. Liquid-liquid equilibrium diagram for the system heptane-butyl alcohol-ethylene glycol.

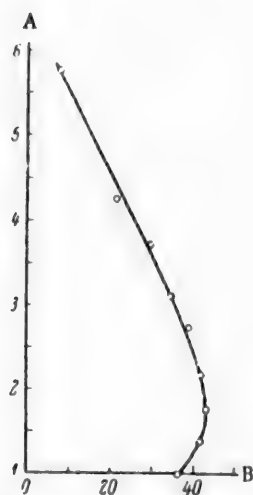


Fig. 3. Variation of the distribution coefficient of butanol in the system heptane-butanol-ethylene glycol with the butanol content of the glycol layer: A) distribution coefficient of butanol; B) butanol content (wt. %).

The compositions of the equilibrium phases and the composition of the mixture at the critical point (determined by Alekseev's method) are given in Table 2.

The same table also contains distribution coefficients of butanol, calculated from the equilibrium data.

Variation of the distribution coefficient with composition is plotted graphically in Fig. 3.

It is clear from these data that butanol passes into the lower (glycol) layer at all mixture compositions.

Fig. 3 shows that at mixture compositions fairly far from the critical point, the distribution coefficient of butanol is very high, of the order of 3-4;

These results show that ethylene glycol is a very effective solvent for separation of alcohol-hydrocarbon mixtures by extraction. The following experiments were performed to show that this process is feasible. A solution containing 40% butanol and 60% heptane by volume, was prepared and was subjected to single extractions with ethylene glycol in various proportions by volume. The experiments were carried out in a graduated vessel for direct determination of the layer volumes. The mixture was extracted for 0.5 hour, and then allowed to separate. Because of the large density difference between the mixture and the extractive solvent, the separation was very rapid and complete.

The following results were obtained:

Volume ratio of mixture to ethylene glycol 2:1 1:1 1:2 1:3 1:1*
Butanol content (wt. %) in heptane layer after extraction 12.8 5.0 1.8 0.97 0.22

It is clear from these results that a single extraction with a 2 to 3-fold quantity, or two extractions with an equal volume of ethylene glycol, are sufficient to isolate the almost pure hydrocarbon from mixtures with butanol.

* Twofold extraction.

It was of interest to compare ethylene glycol and glycerol as solvents, as these substances are the simplest representatives of the homologous series of di- and trihydric alcohols.

Because of the high viscosity of glycerol, aqueous solutions of glycerol and ethylene glycol were compared as extractive solvents. Their viscosities are sharply reduced on dilution even with small amounts of water, and they are much easier to use as solvents. The same graduated vessels were used for experiments on consecutive extractions of butanol-heptane mixture by aqueous solutions of ethylene glycol and glycerol. The results of these experiments are given in Table 3.

TABLE 3

Extraction of Butanol-Heptane Mixture by Aqueous Solutions of Ethylene Glycol and Glycerol.

Extraction No.	Solvent	
	80% glycerol and 20% water by volume	80% ethylene glycol and 20% water by volume
1	35	7.2
2	31	0.5
3	25	—
4	18	—
5	10	—

Table 3 gives the butanol contents (in volume %) in the upper hydrocarbon layer after each extraction. The results show that aqueous ethylene glycol is as effective as the anhydrous compound for separation; glycerol is a much less effective solvent than ethylene glycol.

The results of this investigation show that when a mixture of an alcohol and a hydrocarbon is extracted by ethylene glycol, the upper layer is the almost pure hydrocarbon which can easily be separated by decantation. The lower layer, which is a mixture of butanol with ethylene glycol or with ethylene glycol and water, can be separated by ordinary rectification without difficulty.

The results formed the basis of an industrial process for separation of mixtures of hydrocarbons and aliphatic alcohols [3].

SUMMARY

1. A method is proposed for separation of mixtures of aliphatic alcohols and hydrocarbons by solvent extraction with the aid of ethylene glycol.
2. The original mixtures can be separated completely by one or two extractions either with pure ethylene glycol or with its aqueous solutions.
3. The pure hydrocarbon is obtained directly by the extraction process, and the alcohol can be isolated from the lower layer by simple rectification.

LITERATURE CITED

- [1] V. B. Kogan, V. M. Fridman, and I. V. Deizenrot, *J. Appl. Chem.* 30, 1339 (1957). *
- [2] *Chemist's Reference Book*, 2 [in Russian] (State Chem. Press, 1951).
- [3] V. B. Kogan and V. M. Fridman, *Author's Certif. No. 107275* (June 3, 1957).

Received December 21, 1957

* Original Russian pagination. See C. B. Translation.

MAIN LAWS GOVERNING THE HYDROLYSIS OF POLYSACCHARIDES IN HOMOGENEOUS AND HETEROGENEOUS MEDIA*

A. A. Konkin and Z. A. Rogovin

All-Union Scientific Research Institute of Artificial Fibers

One of the crucial problems of modern physical chemistry of the polysaccharides is the influence of various factors in the stability of the acetal linkage in polysaccharide macromolecules to the action of various reagents. Investigation of this problem is not only of great theoretical interest, but is of no less important practical significance in relation to the development of rational technological processes for isolation and conversion of cellulose. The stability of the acetal linkage in polysaccharides is determined by characteristics of the composition and structure of the unit residues and of the macromolecular structure. Despite the great scientific and practical importance of this question, there have been no systematic investigations in this field.

The literature contains numerous data relating to studies of the influence of various factors on the stability of the acetal linkage, mainly in simple acetals and monosides, to the action of acids. However, such data are inadequate for establishing, with sufficient basis and detail, the principal laws governing the stability of the acetal linkage in monosides, disaccharides, and polysaccharides.

The main materials used up to now in studies of the hydrolysis process have been cellulose and starch. However, clarification of the problems associated with the mechanism and kinetics of hydrolysis requires detailed studies of the properties not only of cellulose but also of other polysaccharides, which differ from cellulose both in the composition and structure of the macromolecules and in physical structure. Only then is it possible to establish the general laws applicable to various extents to all polysaccharides, and to distinguish the specific properties characteristic of cellulose. We therefore selected a relatively large number of polysaccharides for investigation. Hydrolysis studies were carried out on polysaccharides, monosides and disaccharides in homogeneous media, and of polysaccharides in heterogeneous media. The hydrolysis rates of monosides, disaccharides, and polysaccharides in homogeneous media are determined by the composition and structure of the macromolecules, as the physical structure does not influence the kinetics in this case. Comparison of the results of homogeneous and heterogeneous hydrolysis of polysaccharides revealed the role and significance of structural characteristics in heterogeneous hydrolysis.

The results obtained in studies of the hydrolysis of amylose [1], mannan [2], galactan [3], laminarin [4], xylan [5] and chitin have been described in a number of papers.

In this paper we consider certain general laws governing the hydrolysis of polysaccharides and simple model compounds in homogeneous and heterogeneous media. Summarized data on the ratios of the hydrolysis rates of polysaccharides, disaccharides, and monosides under different reaction conditions are given in the table.

Principal Laws Governing Homogeneous Hydrolysis of Polysaccharides, Disaccharides, and Monosides

It follows from the table that cellulose and chitin are the most resistant to the action of hydrolytic agents. The hydrolysis rates of the other polysaccharides are on the average 3-5 times the hydrolysis rate of cellulose.

* Communication 73 in the series on the structure and properties of cellulose and its derivatives. Communication 12 in the series on the hydrolysis of polysaccharides.

Mannan, galactan, laminarin, and xylan are hydrolyzed at approximately the same rate in a homogeneous medium. The hydrolysis rate of amylose is approximately 1.5 times the hydrolysis rates of these polysaccharides. The polysaccharides form the following series in order of decreasing stability of the acetal linkage under the action of acids: chitin > cellulose > galactan > mannan > laminarin > xylan > amylose. These polysaccharides differ considerably from each other both in structure and composition of the unit residues and in macromolecular structure. Nevertheless, these differences do not cause any appreciable variations in the stability of the acetal linkage. Studies of the kinetics of hydrolysis of polysaccharides in a homogeneous medium lead to the conclusion that differences in the form of the acetal linkage (cellulose, amylose), spatial configuration of the acetal linkage (cellulose, galactan), spatial positions of the hydroxyl groups (cellulose, mannan), position of the linkage between the residues (cellulose, laminarin), and presence or absence of primary hydroxyl groups (xylan, cellulose) have relative little influence on the resistance of the acetal linkage to the action of hydrolytic agents. Moreover, the stability of the glycoside linkage changes little even if the hydroxyl group in the α -position in the glycoside linkage is replaced by a methylated amino group (chitin, cellulose). In monosides and polysaccharides the carbon atoms are linked by a single σ -bonds. In this case the mutual influence of atoms not directly linked, separated by single bonds, is due to the induction effect which dies down rapidly along the chain of atoms in the molecule. Even introduction of the strongly polar carboxyl group at the sixth carbon atom does not cause any significant change in the stability of the acetal linkage [6].

Ratios of Hydrolysis Rate Constants for Polysaccharides in Homogeneous and Heterogeneous Media, and Model Compounds in Homogeneous Media

Ratio of hydrolysis rate constants in a homogeneous medium		Ratio of hydrolysis rate constants for polysaccharides in a heterogeneous medium
glycosides and disaccharides	polysaccharides	
$\frac{K_{\text{maltose}}}{K_{\text{cellulose}}} = 2$	$\frac{K_{\text{amylose}}}{K_{\text{cellulose}}} = 5$	$\frac{K_{\text{amylose}}}{K_{\text{cellulose}}} = 61$
$\frac{K_{\text{lactose}}}{K_{\text{cellobiose}}} = 2.1$	$\frac{K_{\text{galactan}}}{K_{\text{cellulose}}} = 2.6$	$\frac{K_{\text{galactan}}}{K_{\text{cellulose}}} = 290$
$\frac{K_{\text{methymannoside}}}{K_{\text{methylglucoside}}} = 2$	$\frac{K_{\text{mannan}}}{K_{\text{cellulose}}} = 2.8$	$\frac{K_{\text{mannan}}}{K_{\text{cellulose}}} = 65$
—	$\frac{K_{\text{laminarin}}}{K_{\text{cellulose}}} = 3$	$\frac{K_{\text{laminarin}}}{K_{\text{cellulose}}} = 225$
$\frac{K_{\text{isopropylxyloside}}}{K_{\text{isopropylglucoside}}} = 4.2$	$\frac{K_{\text{xylan}}}{K_{\text{cellulose}}} = 3.8$	$\frac{K_{\text{xylan}}}{K_{\text{cellulose}}} = 7.5$
—	$\frac{K_{\text{chitin}}}{K_{\text{cellulose}}} = 0.6$	$\frac{K_{\text{chitin}}}{K_{\text{cellulose}}} = 0.4$
$\frac{K^*_{\text{sucrose}}}{K_{\text{cellobiose}}} = 10^4$	$\frac{K^*_{\text{inulin}}}{K_{\text{cellulose}}} = 10^6$	—

* Approximate data, found by calculation.

From the results of our studies of the breakdown rates of acetal linkages in a relatively large number of polysaccharides, in conjunction with certain literature data, the conclusion may be drawn that in most polysaccharides the acetal linkages differ little in their resistance to hydrolytic agents. It does not follow, of course, that it is in general impossible to alter the resistance of the acetal linkage in polysaccharides to the action of hydrolytic and other agents. This would be contrary to large amounts of experimental data existing in organic and carbohydrate chemistry on the mutual influence of atoms. It is known that the hydrolysis rate of the glycoside of a tertiary alcohol (trimethylcarbinol) is 470 times the hydrolysis rate of the glycoside of a primary alcohol

(methanol) [7]. The three methyl groups, which give a positive induction effect, displace the electron cloud of the covalent acetal linkage and thereby diminish its stability. Nitroethanol glycosides are extremely unstable compounds. The strongly polar NO_2 group induces electron asymmetry in the N-C bond, which is transmitted to the C-O acetal linkage and weakens it. Although substituents with positive and negative induction effects in aglycones displace the bonding electron pair in different directions, in both cases the acetal linkage is weakened.

The ketal linkage in disaccharides and polysaccharides differs sharply from the acetal linkage in its resistance to the action of acids. The relative stabilities of these two types of linkage can be estimated if the hydrolysis constants are reduced to similar experimental conditions. It is then found that the hydrolysis rate of the ketal linkage is approximately 10^5 - 10^6 times the hydrolysis rate of the acetal linkage.

According to numerous literature data, the composition and structure of monosides have little influence on the hydrolysis rate of monosides. Hydrolysis data for the eight compounds listed in the table lead to the same conclusion. The hydrolysis rates of these compounds vary by a factor of 4 at the most. It is significant that the acetal linkage in glycosides and cellobiose has the highest stability. As was to be expected, the stability of the acetal linkage in polysaccharides and disaccharides conforms to the same relationships.

Polysaccharides and their simple models (monosides, disaccharides) have similar ratios of hydrolysis rates (see table). According to our data, the hydrolysis of amylose and inulin, and of disaccharides of analogous structure (maltose, sucrose), proceeds at the same rate. For example, the hydrolysis rate constants of maltose and amylose in 58% H_2SO_4 at 30° are $4.3 \cdot 10^{-2} \text{ hour}^{-1}$ and $4.4 \cdot 10^{-2} \text{ hour}^{-1}$, respectively, and the constants for sucrose and inulin in 0.05 N HCl at 40° are $13.4 \cdot 10^{-2} \text{ hour}^{-1}$ and $10 \cdot 10^{-2} \text{ hour}^{-1}$, respectively. Thus, the general principle of polymer physical chemistry, that bond stability in compounds of a given polymeric homologous series is independent of the degree of polymerization, extends to polysaccharides. Cellulose is an exception to this general rule; its hydrolysis rate constant is approximately one half that of cellobiose. The cause of this is not clear.

The hydrolysis rate constants of the polysaccharides retain constant values up to a degree of conversion corresponding to breakdown of 30-40% of the total amount of acetal linkages. The following two conclusions may be drawn from this: 1) the use of a first-order equation for calculation of the hydrolysis rate constant is quite justified; 2) in the conditions of our experiments equivalent acetal linkages are broken down in all the polysaccharides studied.

These data provide additional confirmation that the results characterize the properties of the principal type of acetal linkage in polysaccharides, and therefore there is adequate experimental justification for the conclusion concerning the ratios of the hydrolysis rates.

Principal Laws Governing Heterogeneous Hydrolysis of Polysaccharides

The results obtained in studies of the hydrolysis rates of cellulose, amylose, galactan, mannan, laminarin, and xylan in heterogeneous conditions are given in the table. It is seen that the rates of heterogeneous hydrolysis differ considerably. Cellulose and chitin are the most difficult polysaccharides to hydrolyze. The other polysaccharides are hydrolyzed much more rapidly. The hydrolysis rates of amylose and xylan are approximately equal, and are 60-75 times the hydrolysis rate of cellulose. Mannan occupies an intermediate position between cellulose and amylose. The hydrolysis rate constants of galactan and laminarin are 220-290 times as high as the hydrolysis rate constant of cellulose, and approximately 4 times as high as the constants for amylose and xylan. The polysaccharides form the following series in order of their relative rates of hydrolysis in heterogeneous media: galactan > laminarin > xylan > amylose > mannan > cellulose > chitin.

Studies of homogeneous and heterogeneous hydrolysis of polysaccharides revealed the role and significance of physical structure in heterogeneous hydrolysis. Although the stability of the acetal linkage to the action of hydrolytic agents is approximately the same in different polysaccharides, if the process is carried out in a heterogeneous medium, there are sharp differences between the hydrolysis rates of the same polysaccharides. For example, the hydrolysis rate of amylose in a heterogeneous medium is 12 times that of cellulose, of mannan 15 times, of xylan 19 times, of laminarin 75 times, and of galactan 112 times. It is quite evident from these data that physical structure of the polysaccharides has the decisive influence on their hydrolysis rates in heterogeneous media. The high resistance of cellulose to hydrolysis, in comparison to other polysaccharides, is entirely due to the physical structure of cellulose. It follows that the structural characteristics of the macromolecules (form of the acetal linkage, spatial arrangement of the hydroxyl groups in the acetal linkage, position of the linkage between the residues,

composition of the unit residue), have slight direct influence on the stability of the acetal linkage, but in most cases give rise to different physical structures, which are decisive in relation to the mechanism and rate of the heterogeneous reaction. The influence of this factor is most prominent for cellulose and chitin. In the other polysaccharides the physical structure has less influence. Therefore the ratio of the reaction rates changes sharply as we pass from homogeneous to heterogeneous hydrolysis of polysaccharides.

The influence of the physical structure of cellulose on the rate of hydrolysis in the heterogeneous medium is confirmed by data for the reaction carried out in homogeneous and heterogeneous media under the same conditions [8]. The considerable influence of cellulose structure on its hydrolysis rate has been demonstrated in a series of investigations by Sharkov et al. [9], and by other workers.

Polysaccharide structure influences not only the rate of hydrolysis, but also the rates of other reactions in a heterogeneous medium, such as acetylation [10] and xanthation [11].

Numerous investigators have shown that hydrolysis of cellulose in a heterogeneous medium proceeds in two stages, at different hydrolysis rates.

Polysaccharides can be divided into two groups in accordance with the characteristics of their hydrolysis in a heterogeneous medium. The first group includes cellulose, mannan, laminarin, and xylan, which are hydrolyzed with a gradual decrease of the reaction rate, and the second group includes amylose and galactan, the hydrolysis rate constants of which remain unchanged throughout the reaction. Variations in the hydrolysis rates of polysaccharides in a heterogeneous medium as the reaction proceeds may be caused by structural heterogeneity and by the presence of nonequivalent linkages, and both these factors may operate simultaneously. At the present time there are no data available which would provide a solution of these problems for all polysaccharides. A fairly definite conclusion can be drawn only in the case of cellulose. It follows from literature data and our results that changes in the rate of heterogeneous hydrolysis of cellulose are due mainly to its structural heterogeneity. This effect is characteristic not only of native cellulose but also of various hydrate celluloses subjected to pre-treatments under harsh conditions, when any weak linkages which might have been present should be completely broken down.

SUMMARY

1. The stability of the acetal linkage to the action of hydrolytic agents differs little in different polysaccharides (cellulose, amylose, mannan, galactan, laminarin, xylan, chitin) and in corresponding disaccharides or monosides.
2. The stability of the acetal linkage to the action of hydrolytic agents is in general independent of the degree of polymerization of the polysaccharides.
3. The hydrolysis rates of polysaccharides in heterogeneous media are determined by their physical structure which in its turn depends on the structure and composition of the macromolecules.

LITERATURE CITED

- [1] A. A. Konkin and Z. A. Rogovin, *Hydrolysis Ind.* 6 (1950).
- [2] A. A. Konkin, A. G. Yashunskaya, and E. M. Bychkova, *Trans. All-Union Sci. Res. Inst. Artificial Fibers* 2, 3 (1955).
- [3] L. M. Vinogradova, A. A. Konkin and Z. A. Rogovin, *Trans. Moscow Text. Inst.* 13, 87 (1954).
- [4] A. A. Konkin and L. I. Novikova, *Trans. All-Union Sci. Res. Inst. Artificial Fibers* 3, 3 (1956).
- [5] A. A. Konkin, N. I. Kaplan, and Z. A. Rogovin, *J. Appl. Chem.* 28, 729 (1955).*
- [6] L. Morell and K. Link, *J. Biol. Chem.* 104, 183 (1934); A. A. Konkin, G. S. Smirnova, and Z. A. Rogovin, *Trans. Moscow Text. Inst.* 13, 99 (1954).
- [7] S. Veifel and E. Frederiksen, *Kgl. Danske Videnske Selsk. math. fysiske. Nedd.* 19, 1, 1 (1941).
- [8] A. A. Konkin, R. A. Krylova and Z. A. Rogovin, *Colloid J.* 15, 146 (1953).*

* Original Russian pagination. See C. B. Translation.

[9] V. I. Sharkov, in the book: Chemistry and Physical Chemistry of High Polymers [in Russian] (Izd. AN SSSR, 1952) p. 132.

[10] L. M. Vinogradova, A. A. Konkin, and Z. A. Rogovin, J. Appl. Chem. 27, 1302 (1954).*

[11] A. A. Konkin and Yu. A. Rymashevskaya, Trans. All-Union Sci. Res. Inst. Artificial Fibers 3 (1956).

Received December 27, 1957

* Original Russian pagination. See C.B. Translation.

POLYMERIZATION OF STYRENE IN PRESENCE OF
1-HYDROXY-1'-HYDROPEROXODICYCLOHEXYL PEROXIDE
AND COBALT NAPHTHENATE

R. K. Gavurina, P. A. Medvedeva, Sh. G. Yanovskaya
and Z. A. Granova

Polymerization of vinyl compounds in nonaqueous media in presence of catalysts has been studied in greatest detail with the system benzoyl peroxide-dimethylaniline. Horner [1], and later Imoto et al. [2-4] and Lal and Green [5] studied the influence of this system on the polymerization of vinyl chloride, styrene, methyl methacrylate, etc.

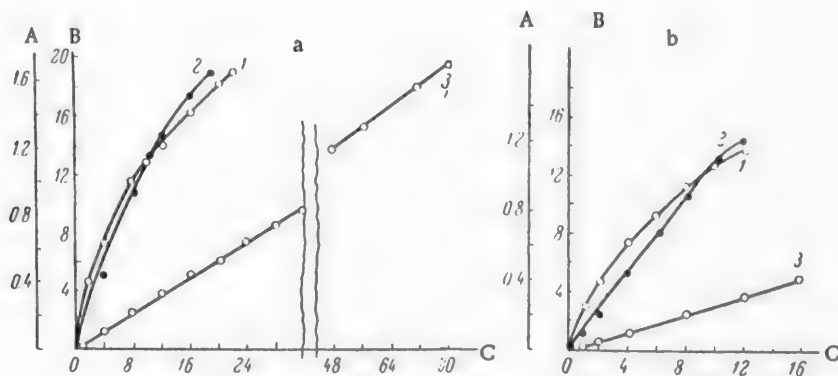


Fig. 1. Kinetic curves for polymerization of styrene at 25°: A) conversion (moles/liter); B) conversion (wt.%); C) time (hours); CN concentration (moles Co per liter): 1) $0.58 \cdot 10^{-3}$; 2) $0.058 \cdot 10^{-3}$; 3) 0.

Among other systems, most attention has been devoted to systems containing peroxides (or hydroperoxides) and salts of variable-valence metals. For example, Kern [6] polymerized styrene at 40° in presence of a reversible system consisting of benzoyl peroxide, iron naphthenate, and benzoin.

Dolgoplosk and Tinyakova [7] showed that a system consisting of isopropylbenzene hydroperoxide, iron naphthenate, and the diethyl ester of dihydroxymaleic acid is effective in the polymerization of styrene at 50°.

In a later paper Dolgoplosk et al. [8] showed that iron naphthenate itself, in absence of initiators, initiates homogeneous polymerization of isoprene at 100°, and Fe^{3+} is reduced to Fe^{2+} in the process.

The present paper describes results obtained in the polymerization of styrene in presence of 1-hydroxy-1'-hydroperoxodicyclohexyl peroxide (HPC-1) and cobalt naphthenate (CN).

According to the theory developed by Kern [9] and others [7, 10], such systems by themselves, without introduction of additional reducing agents, lead to reversible oxidation-reduction cycles as follows:



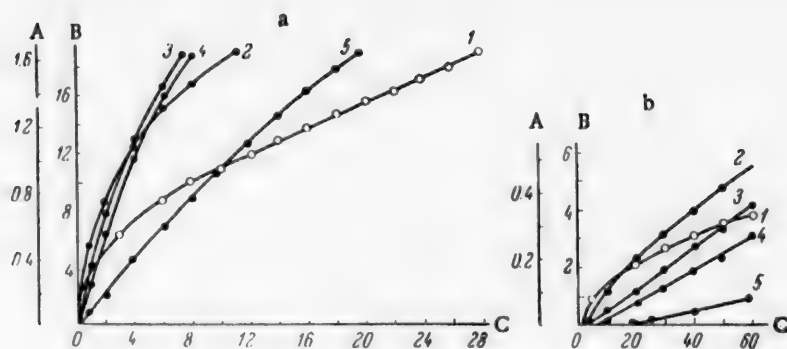


Fig. 2. Kinetic curves for polymerization of styrene at 38.4°: A) conversion (moles/liter); B) conversion (wt. %); C) time (hours); D) time (min); CN concentration (moles Co per liter): 1) $5.8 \cdot 10^{-3}$; 2) $0.58 \cdot 10^{-3}$; 3) $0.116 \cdot 10^{-3}$; 4) $0.058 \cdot 10^{-3}$; 5) 0.

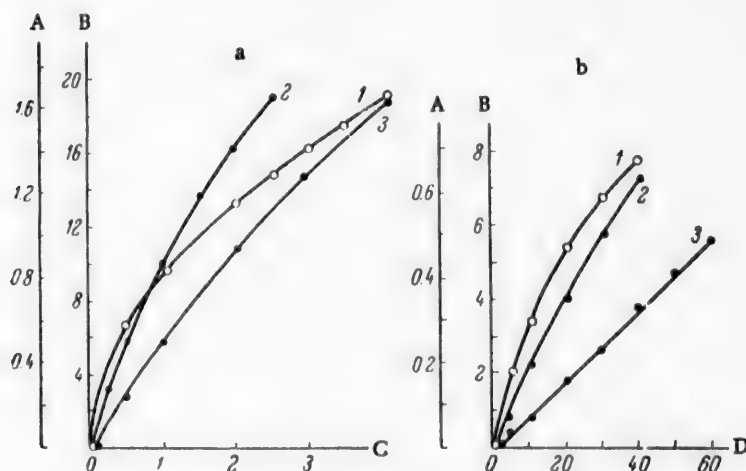


Fig. 3. Kinetic curves for polymerization of styrene at 56.4°: A) conversion (moles/liter); B) conversion (wt. %); C) time (hours); D) time (minutes); CN concentration (moles Co per liter): 1) $0.58 \cdot 10^{-3}$; 2) $0.058 \cdot 10^{-3}$; 3) 0.

Studies of polymerization in presence of HPC-1 and CN are of particular interest because this system is already extensively used in technological cold hardening (copolymerization) of unsaturated polyester resins.

RESULTS AND DISCUSSION

The polymerization kinetics of styrene in presence of HPC-1 and CN was studied by both the dilatometric method and by polymerization in ampoules (at high conversions). The polymerization was effected in oxygen-free nitrogen.

Polymerization in Dilatometers. Three series of experiments were performed, at 25, 38.4, and 56.4°.

Polymerization was effected with a constant content of HPC-1 (0.80 molar %) and variable concentrations of CN. The final conversion was 19% in all experiments. The kinetic curves for these experiments are given in Figs. 1-3.

The most interesting regions of the curves, corresponding to the initial stage of polymerization, are shown in Figs. 1-3, b, on a large scale.

TABLE 1

Polymerization Time for 19% Conversion

CN concentration ($\frac{\text{moles Co}}{\text{liter}} \cdot 10^3$)	Polymerization time (hours)		
	25°	38.4°	56.4°
0	79	20	4.25
0.058	18.5	8	2.5
0.116	—	7.5	—
0.58	22	11	4.25
5.8	—	28	—

TABLE 2

Effect of Accelerator Concentration on R_0

CN concentration ($\frac{\text{moles Co}}{\text{liter}} \cdot 10^3$)	R_0 ($\frac{\text{moles}}{\text{liter} \cdot \text{sec}} \cdot 10^3$)		
	25°	38.4°	56.4°
0	0.009	0.035	0.145
0.058	0.035	0.072	0.37
0.116	—	0.11	—
0.58	0.09	0.25	0.97
5.8	—	0.77	—

TABLE 3

Intrinsic Viscosity of Polymer Solutions (19% Conversion)

CN concentration ($\frac{\text{moles Co}}{\text{liter}} \cdot 10^3$)	[η]		
	25°	38.4°	56.4°
0	0.30	0.24	0.20
0.058	0.19	0.20	0.19
0.116	—	0.175	—
0.58	0.26	0.285	0.30
5.8	—	0.60	—

It is seen from these results that introduction of CN increases the initial rate of polymerization (R_0) in all cases, the increase being greater with higher concentrations of the accelerator. However, R_0 decreases subsequently and especially steeply if its initial value is high. Similar results were obtained by Imoto et al. in studies of the polymerization kinetics of various vinyl compounds in presence of benzoyl peroxide and dimethylaniline [2-4].

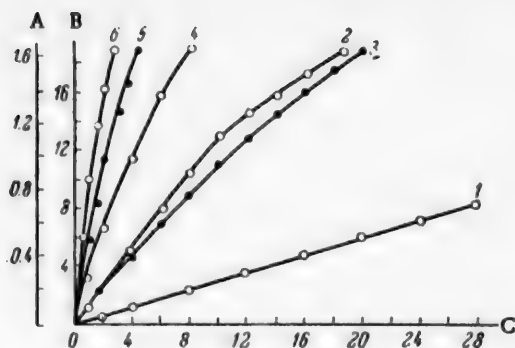


Fig. 4.

Fig. 4. Influence of temperature on polymerization rate: A) conversion (moles/liter); B) conversion (wt. %); C) time (hours); temperature ($^{\circ}\text{C}$) and CN concentration (in moles Co/liter): 1) 25 and 0; 2) 25 and $0.058 \cdot 10^{-3}$; 3) 38.4 and 0.4; 4) 38.4 and $0.058 \cdot 10^{-3}$; 5) 56.4 and 0; 6) 56.4 and $0.058 \cdot 10^{-3}$.

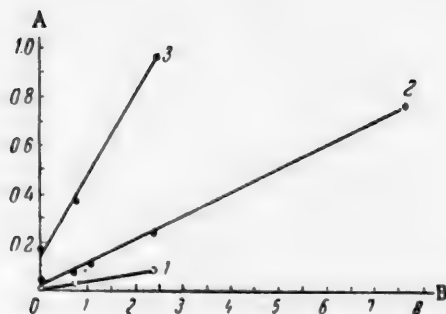


Fig. 5

Fig. 5. Effect of amount of accelerator on the initial rate of polymerization: A) initial rate of polymerization $R_0 \cdot 10^3$ (moles/liter \cdot sec); B) $[\text{Co}]^{1/2} \cdot 10^3$ where $[\text{Co}]$ is the CN concentration (in moles Co/liter); temperature ($^{\circ}\text{C}$): 1) 25; 2) 38.4; 3) 56.4.

The time needed to reach the final conversion (19%) varied with the accelerator concentration.

The relevant data are presented in Table 1.

The shortest polymerization time was observed in experiments with low accelerator concentration ($0.058 \cdot 10^{-3}$ mole Co/liter).

Increase of the CN concentration resulted in increases of the polymerization time at all three temperatures.

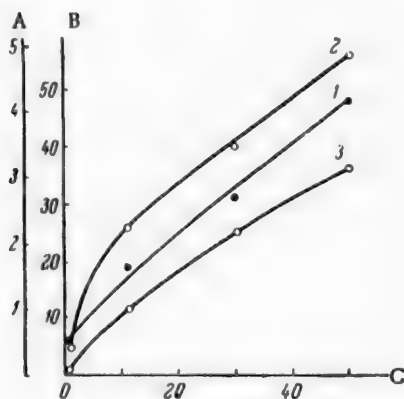


Fig. 6

Fig. 6. Kinetic curves for polymerization of styrene in ampoules: A) conversion (moles/liter); B) conversion (wt. %); C) time (hours); CN concentration (moles Co/liter): 1) $0.58 \cdot 10^{-3}$; 2) $0.058 \cdot 10^{-3}$; 3) 0.

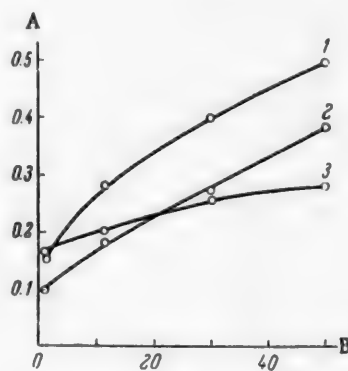


Fig. 7

Fig. 7. Variations of the viscosity of polymer solutions with time and amount of accelerator: A) intrinsic viscosity $[\eta]$; B) time (hours); CN concentration (moles Co/liter): 1) $0.58 \cdot 10^{-3}$; 2) $0.058 \cdot 10^{-3}$; 3) 0.

When the CN concentration was increased to $5.8 \cdot 10^{-3}$ mole Co/liter the polymerization time was even greater than in the control experiment without accelerator (28 and 20 hours respectively).

It is interesting to note that greater reductions of the polymerization time occur at lower temperatures; thus at 25° there was a 4-fold decrease of the time, and at 56.4° it was less than twofold.

The effects of temperature in experiments with equal accelerator concentrations are plotted in Fig. 4.

The distances between the curves for a given temperature with and without the accelerator decrease appreciably with increase of temperature. At 56.4° the accelerating effect is already very weak, and curves 5 and 6 lie close together.

The effects of accelerator content on R_0 are given in Table 2 and Fig. 5. The values of R_0 were found graphically from the kinetic curves in Figs. 1-3.

Fig. 5 shows that at all three temperatures R_0 is a linear function of the square root of the cobalt concentration.

The results of determinations of the intrinsic viscosity $[\eta]$ of solutions of the polymers formed are given in Table 3. The viscosity was determined in benzene solutions.

At all temperatures $[\eta]$ first decreases with introduction of the accelerator, and then increases appreciably at higher CN concentrations. The minimum value of $[\eta]$ for each temperature corresponds to experiments with the shortest polymerization times (compare Tables 1 and 3).

The decrease of $[\eta]$ at low CN concentrations is particularly pronounced at low temperatures; thus, at 25° $[\eta]$ changed from 0.30 to 0.19, and at 56.4°, only from 0.20 to 0.19.

Polymerization in Ampoules. The course of the kinetic curves at higher conversions was studied by means of experiments in ampoules. This series of experiments was conducted at one temperature, $38.4 \pm 0.05^\circ$. The amount of HPC-1 remained constant at 0.80 molar %, as in the dilatometer experiments.

The CN concentration was varied in the range $0-0.58 \cdot 10^{-3}$ mole Co/liter. The kinetic curves are shown in Fig. 6, and values of $[\eta]$ in Fig. 7.

The character of the kinetic curves confirms the results of the dilatometric determinations. After 1 hour the greater conversion (0.5 mole/liter) was found in the experiment with the higher CN concentration ($0.58 \cdot 10^{-3}$). However, after 50 hours the conversion was higher in the experiment with the lower CN concentration (4.9 and 4.2 moles/liter respectively).

Figure 7 shows that at lower degrees of conversion $[\eta]$ decreases on addition of accelerator. The extent of the decrease, and the region in which the decrease of $[\eta]$ occurs, depend on the accelerator concentration. Thus, when the CN concentration is $0.058 \cdot 10^{-3}$ mole Co/liter $[\eta]$ decreases up to 33% conversion, whereas at CN concentration of $0.58 \cdot 10^{-3}$ mole Co/liter it decreases only up to 8% conversion. As the polymerization process extends in experiments with the accelerator, (curves 1 and 2) $[\eta]$ increases rapidly. As a result, at the end of the process (after 50 hours) the samples polymerized in presence of the accelerator had much higher viscosities than the sample polymerized in its absence.

Comparison of curves 1 and 2 shows that increase of the accelerator concentration is associated with increase of $[\eta]$. Curve 1 lies above curve 2 throughout.

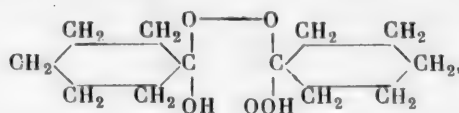
These results are in good agreement with the experimental data in Table 3. At constant conversion (19%) $[\eta]$ decreased only at low accelerator concentrations.

EXPERIMENTAL PROCEDURE

The starting substances were synthesized and prepared as follows.

Styrene. Before the experiments styrene was repeatedly washed with aqueous alkali and water to remove hydroquinone, dried, and distilled under vacuum in a current of oxygen-free nitrogen.

Synthesis of HPC-1, to which the following structure has been ascribed [11]



was effected by the method of Criegee and Schnorrenberg, by the action of 30% perhydrol on cyclohexanone [11, 12]. The components were taken in the ratio of 1 mole H_2O_2 to 1 mole of cyclohexanone. The reaction was effected at room temperature in a flask fitted with a stirrer. When the liquids were mixed, a homogeneous solution was first formed, and after 10-15 minutes a white precipitate began to form. After 2 hours the amount of precipitate was so large that stirring had to be discontinued. The mixture was held for 2-3 hours without stirring, and the crystalline precipitate was then separated on a Schott filter and dried at 50° . The dried substance was then recrystallized twice — first from ethanol (1 g of substance to 1 g of solvent, dissolved at 40°) and then from ligroine (68- 80° fraction, 1 g of substance to 5 g of solvent, dissolved at 60- 65°). The recrystallized substance was dried under vacuum at room temperature. The same batch of HPC-1 was used in all the polymerization experiments. The substance melted at 74- 76° and contained 12.75% active oxygen.

Cobalt Naphthenate. The usual precipitation method was used for preparation of CN. The same batch of CN was used for all the experiments.

Polymerization in Dilatometers. The dilatometers were cylindrical in shape, each with one graduated side tube with 0.01 ml divisions. Before use the dilatometers were treated for 24 hours with chromate mixture, washed repeatedly with distilled water, steamed with live steam for 2 hours, and then dried. Freshly distilled styrene was charged into the dilatometers. The following procedure was used for adding HPC-1 and CN to styrene. A weighed quantity of HPC-1 was dissolved in one portion of styrene, and a weighed quantity of CN in another; the two portions were then cooled to between -10 and -15° and mixed. The cooled mixture was transferred to the dilatometer, which was then cooled to the same temperature. Oxygen-free nitrogen was blown through the dilatometers while the mixture was cooled to between -50 and -60° ; the dilatometers were evacuated at 2-3 mm, and the mixture was then warmed to room temperature in a continuous stream of nitrogen. This procedure was repeated three times.

The prepared dilatometers were sealed in a current of nitrogen and placed in water thermostats. The thermostat temperature was maintained to an accuracy of $\pm 0.05^\circ$ by means of an electronic thermoregulator. Polymerization in dilatometers was terminated when 19% conversion was reached. To precipitate the polymer the mixture was poured into methanol with vigorous agitation by means of a stirrer. The polymer was washed with methanol and dried, and its intrinsic viscosity in benzene was then determined.

Conversion was calculated from the formula

$$U = \frac{K \Delta V \cdot 100}{V}$$

The following values were taken for K: $K_{38.4} = 0.1646$ and $K_{56.4} = 0.1711$ [13]. The value of K for 25° was found from the values of K for 38.4, 56.4, and 70.1° [14]; K_{25} had the value 0.1590.

Polymerization in Ampoules. The same preparation and charging procedure was used for the ampoules as for the dilatometers.

Several ampoules were filled with the same mixture, and they were all put simultaneously in a thermostat at $38.4 \pm 0.05^\circ$. The ampoules were removed successively after definite time intervals (1, 11, 30, and 50 hours), their contents were dissolved in benzene, and the polymer was precipitated by addition of methanol. The conversion was calculated from the polymer yield.

SUMMARY

1. The action of an oxidation-reduction system consisting of 1-hydroxy-1'-hydroperoxodicyclohexyl peroxide (HPC-1) and cobalt naphthenate (CN) in the bulk polymerization of styrene has been studied; it was found that the system is active at low temperatures (25- 56°).

2. Introduction of CN increases the initial rate of polymerization (R_0). Increase of the cobalt concentration $[Co]$ increases R_0 . The functional relationship between R_0 and $[Co]^{\frac{1}{2}}$ is linear. The polymerization rate decreases appreciably with increasing conversion; the decrease is greater at higher CN concentrations.

3. Under the influence of this oxidation-reduction system $[\eta]$ for the polymers formed changes significantly. When CN is added at low degrees of conversion $[\eta]$ decreases, while at high conversions it increases sharply. The value of $[\eta]$ also increases with CN concentration.

LITERATURE CITED

- [1] L. Horner, Lieb. Ann. Chem. 566, 69 (1950).
- [2] M. Imoto and C. Senckon, J. Inst. Polytechnic, Osaka City, University, 4, C, 1, 115 (1953).
- [3] M. Imoto, T. Otsu, and K. Kimura, J. Polym. Sci. XV, 80, 475 (1955).
- [4] M. Imoto, T. Otsu, and T. Ota, Makrom. Chem. XVI, 1, 10 (1955).
- [5] J. Lal and R. Green, Polym. Sci. XVII, 85, 403 (1955).
- [6] W. Kern, Makrom. Chem. I, 3, 249 (1948).
- [7] B. A. Dolgoplosk, E. I. Tinyakova and V. N. Reikh, Vulcanization of Rubbers [In Russian] (Goskhimizdat, 1954) p. 51.
- [8] B. A. Dolgoplosk and E. N. Kropocheva, J. Gen. Chem. 26, 2980 (1956). *
- [9] W. Kern and H. Willersinn, Makrom. Chem. XV, 1, 36 (1955).
- [10] C. E. H. Bawn, Discussion Faraday Soc. 14, 181 (1953).
- [11] R. Criegee, W. Schnorrenberg, and J. Becke, Lieb. Ann. Chem. 565, 7 (1949).
- [12] W. Cooper, J. Chem. Soc. 1340 (1951).
- [13] G. Goldfinger and K. E. Lauterbach, J. Polym. Sci. III, 2, 145 (1948).
- [14] G. V. Schulz and G. Harborth, Ang. Chem. A-59, 3, 90 (1947).

Received January 31, 1958

* Original Russian pagination. See C. B. Translation.

INVESTIGATION OF CERTAIN EPOXY STABILIZERS FOR POLYVINYL CHLORIDE •

A. A. Berlin, E. N. Zil'berman, N. A. Rybakova,
A. M. Sharetskii, and D. M. Yanovskii

One of the important disadvantages of chlorine-containing polymers is their relatively low stability under the influence of heat and light. Therefore conversion and utilization of polyvinyl chloride and other chlorine-containing polymers is accompanied by considerable dehydrochlorination and oxidative degradation, which have sharply adverse effects on the physical, mechanical, and dielectric properties of the materials. Various inorganic and organic stabilizers have been recommended for raising the thermal stability of polyvinyl chloride. Among the organic stabilizers, certain classes of compounds containing the epoxy ring in the molecule are of practical significance; the epoxy group reacts with the hydrogen chloride liberated in dehydrochlorination of polyvinyl chloride, with formation of the corresponding chlorohydrins [1-3].

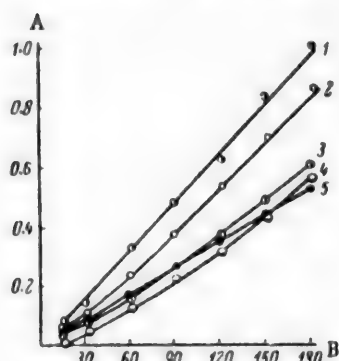


Fig. 1. Kinetics of liberation of hydrogen chloride from polyvinyl chloride resin at 175° in presence of epoxy stabilizers: A) amount of HCl (% of polymer weight); B) time (minutes). Stabilizers: 1) without stabilizers; 2) 2% of lead silicate; 3) E-40; 4) ED-6; 5) diglycidyl ether of 2,2-bis-(4-hydroxy-3-methylphenyl)propane.

The present paper contains comparative data on the stabilizing effects of certain commercial products and of compounds synthesized by us. The tested stabilizers for polyvinyl chloride were the commercial epoxy resins E-40 and ED-6, and low-molecular epoxy resins (not described previously) based on the diglycidyl ethers of 2,2-bis-(4-hydroxy-3-methylphenyl)propane (I), 1,1-bis-(4-hydroxyphenyl)cyclohexane (II), 1,1-bis(4-hydroxymethylphenyl)cyclohexane (III), and 2,2-bis-(4-hydroxy-3-nitrophenyl)propane (IV). The following were also synthesized and their thermal stabilizing effects studied: *cis* butyl 9,10-epoxystearate (V), and epoxidized castor oil (VI) and whale oil (VII).

Epoxy resins (I)-(IV) were synthesized by condensation of epichlorohydrin with diphenols. Stabilizer (V) and oxirane derivatives of triglycerides, (VI) and (VII), were prepared by direct epoxidation of the corresponding unsaturated compounds by the action of peracetic acid, by the method developed by Swern et al. [4].

The individual stabilizers were characterized by the temperature at which polyvinyl chloride dehydrochlorination commenced, by the thermal stability of the resin at 175° (Table 1), and by the kinetics of hydrogen chloride liberation at the same temperature (Figs. 1 and 2). The amounts of all the stabilizers added to polyvinyl chloride corresponded to the same content of oxirane oxygen (0.094 wt. %). In addition, the physical properties of plasticized polyvinyl chloride with these stabilizers or their mixtures with lead silicate were determined (Table 2).

It follows from the experimental data that if epoxy resins are added as stabilizers to polyvinyl chloride, the temperature of the start of dehydrochlorination is raised considerably, the time before liberation of hydrogen chloride begins is lengthened, and the rate of hydrogen chloride liberation is diminished. Resins E-40, ED-6, (I),

• Communication I in the series on intermediates and auxiliaries used in polymer technology.

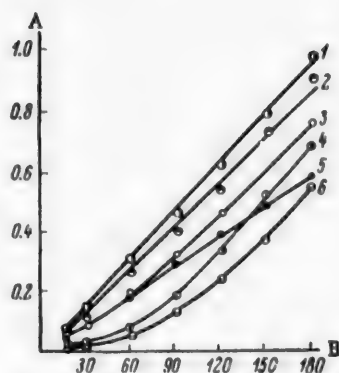


Fig. 2. Kinetics of liberation of hydrogen chloride from polyvinyl chloride resin at 175° in presence of epoxy stabilizers: A) amount of HCl (% of polymer weight); B) time (minutes). Stabilizers: 1) without stabilizer; 2) 1% of lead silicate; 3) epoxidized whale oil; 4) 1% epoxidized whale oil and 1% lead silicate; 5) butyl 9,10-epoxystearate; 6) 1% E-40 and 1% lead silicate.

(II), and (III) are approximately equal in their stabilizing action. Introduction of a nitro group into the aromatic ring of the diphenol (compound IV) lowers sharply the stabilizing power of the diglycidyl ether. When butyl epoxystearate or the epoxidized glycerides (VI) and (VII) are used as stabilizers, the temperature of the start of dehydrochlorination rises sharply and the time before liberation of hydrogen chloride begins is lengthened. However, these stabilizers are somewhat inferior to the epoxy resins in their influence on the kinetics of HCl liberation when polyvinyl chloride is heated, and on the electrical properties of plasticized resins. On the other hand, stabilizers (V)-(VII) are superior to the epoxy resins in their influence on frost resistance of the plasticized product. The best results in all respects were obtained with the use of mixed epoxy-lead stabilizers. These mixtures not only combine the favorable properties of each of the components, but give a synergetic effect [1].

EXPERIMENTAL

Synthesis of Diglycidyl Ethers of Diphenols, (I)-(IV)*. For preparation of 2,2-bis-(4-hydroxy-3-methylphenyl)propane, *o*-cresol was condensed with acetone in presence of hydrochloric acid [5]; yield 65%, m.p. 136° (from xylene). Phenol or *o*-cresol was condensed with cyclohexanone in presence of gaseous hydrogen chloride [4] to give, respectively, 1,1-bis-(4-hydroxyphenyl)cyclohexane (yield 84%, m.p. 183° from alcohol-benzene mixture) and 1,1-bis-(4-hydroxy-3-methylphenyl)cyclohexane (yield 59%, m.p. 186° from aqueous methanol). Nitration of diphenylolpropane by concentrated nitric acid [7] gave 2,2-bis-(4-hydroxy-3-nitrophenyl)propane, yield 75%, m.p. 130°.

TABLE 1

Stabilizing Action of Epoxy Compounds

Stabilizers	Temperature of start of dehydrochlorination (°C)	Time of heating at 175° to start of HCl liberation (minutes)
Without stabilizer	159	10
E-40	187	20
ED-6	178	26
Diglycidyl ether of 2,2-bis-(4-hydroxy-3-methylphenyl)propane	188	19
Diglycidyl ether of 1,1-bis-(4-hydroxyphenyl)cyclohexane	190	20
Diglycidyl ether of 1,1-bis-(4-hydroxy-3-methylphenyl)cyclohexane	186	19
Diglycidyl ether of 2,2-bis-(4-hydroxy-3-nitrophenyl)propane	167	Not determined
Butyl 9,10-epoxystearate	209	20
Epoxidized castor oil	195	26
Epoxidized whale oil	193	20
E-40 and 1% lead silicate	201	33
Epoxidized whale oil and 1% lead silicate	192	30
1% lead silicate	189	39

* The diglycidyl ethers were prepared with the assistance of I. F. Spasskaya.

TABLE 2

Physical and Mechanical Properties of Plasticized Resins Made with Epoxy Stabilizers

Stabilizer	Stabilizer content of resin parts by wt to 100 parts of polyvinyl chloride	Tensile strength (kg/cm ²)	Relative elongation at break (%)	Volume resistivity (ohm · cm)	Frost resistance (°C)
E-40	3	210	316	$5.3 \cdot 10^{12}$	-45
E-40	5	193	328	$1.2 \cdot 10^{13}$	-45
E-40 + lead silicate	5 + 6	200	344	$1.0 \cdot 10^{13}$	-40
ED-6	3	215	316	$1.5 \cdot 10^{13}$	-35
ED-6	5	220	328	$2.6 \cdot 10^{13}$	-40
ED-6 + lead silicate	3 + 6	175	356	$2.2 \cdot 10^{13}$	-40
Diglycidyl ether of 1,1-bis-(4-hydroxyphenyl)cyclohexane	3	206	348	$4.4 \cdot 10^{12}$	-50
Diglycidyl ether of 1,1-bis-(4-hydroxyphenyl)cyclohexane	5	197	320	$5.0 \cdot 10^{12}$	-45
Diglycidyl ether of 1,1-bis-(4-hydroxyphenyl)cyclohexane	6	191	344	$1.1 \cdot 10^{13}$	-40
Diglycidyl ether of 1,1-bis-(4-hydroxy-3-methylphenyl)cyclohexane	3	198	308	$1.1 \cdot 10^{13}$	-45
Diglycidyl ether of 1,1-bis-(4-hydroxy-3-methylphenyl)cyclohexane	5	201	356	$1.9 \cdot 10^{13}$	-45
Diglycidyl ether of 1,1-bis-(4-hydroxy-3-methylphenyl)cyclohexane + lead silicate	3 + 6	188	360	$4.5 \cdot 10^{13}$	-40
Butyl 9,10-epoxystearate	3	191	366	$0.1 \cdot 10^{13}$	-50
Butyl 9,10-epoxystearate	6	183	376	$0.46 \cdot 10^{12}$	-50
Epoxidized whale oil	3	208	330	$0.12 \cdot 10^{13}$	-50
Epoxidized whale oil	6	180	346	$0.54 \cdot 10^{12}$	-50
Epoxidized castor oil	3	234	304	$0.17 \cdot 10^{13}$	-50
Epoxidized castor oil	6	183	382	$0.85 \cdot 10^{12}$	-50
Control specimens with lead silicate	12	187	348	$1.1 \cdot 10^{13}$	-40

To a stirred mixture of 3.5 g of 1,1-bis-(4-hydroxyphenyl)cyclohexane and 6 g of 15% NaOH at 40° there was added 2.45 g of epichlorohydrin from a dropping funnel; the mixture was then slowly heated to 90° while a further 1.4 g of 15% NaOH was added. Extraction with dichloroethane, washing, and drying yielded 78% (on the diphenol) of a viscous oil (II), containing 3.8% oxirane oxygen. Analogous methods were used to prepare (I), a viscous oil, yield 55%, 4.5% oxirane oxygen, and (III), a fusible hygroscopic substance, yield 74%, 4.1% oxirane oxygen.

Ether (IV) was prepared by a modification of an earlier method [8]. 5 g of 2,2-bis-(4-hydroxy-3-nitrophenyl)propane was dissolved on warming in 53 ml of 3% NaOH. The solution was cooled and 2.9 g of epichlorohydrin was added at room temperature. The reaction was continued for 4 days at room temperature, with intermittent stirring by hand. The bright yellow solid product was washed with 2% NaOH and then with water until neutral to phenolphthalein; the yield of (IV) was 65%, m.p. 135°, 4.5% oxirane oxygen.

Preparation of Stabilizers by Epoxidation of Unsaturated Compounds. The peracetic acid required for epoxidation was prepared from acetic anhydride and 25-30% hydrogen peroxide [9].

For preparation of (V) 50 g of butyl oleate was mixed at room temperature with 207 ml of 1.10 N peracetic acid solution. After three hours 500 ml of water cooled to 2° was added to the reaction mixture in a separating funnel. The top oily layer was washed with water to remove acetic acid and dried at 60-70° under vacuum; the yield of cis butyl 9,10-epoxystearate (V) was 21 g, oxirane oxygen content 3.8% [10].

Epoxidized castor oil (VI) and whale oil (VII) were prepared similarly, except that the epoxidized product was extracted in ether in order to increase the yield. Castor oil (iodine number 83, $n_D^{25} = 1.4747$) gave (VI) with iodine number 22, containing 2.3% oxirane oxygen; whale oil (iodine number 128, acid number 17, $n_D^{25} = 1.4738$) gave (VII) with iodine number 30, containing 4.8% oxirane oxygen.

Determination of the Thermal Stability of Polyvinyl Chloride

Polyvinyl chloride of "PF-special" grade was used in the work. The resin used in studies of the kinetics of hydrogen chloride liberation was previously washed free from alkali. The resin used for production of plasticized material was not subjected to any pretreatment.

Addition of stabilizer to the resin was usually effected by the mixing of ether or methanol solutions of the substance with polyvinyl chloride, with subsequent thorough drying of the mixture. Peroxides were removed from the ether before use. In the case of the insoluble stabilizer (IV) it was mixed mechanically with polyvinyl chloride.

To determine the decomposition temperature of the resin it was heated until liberation of hydrogen chloride began (shown by turbidity of silver nitrate solution).

For studies of the kinetics of hydrogen chloride liberation, the HCl evolved when polyvinyl chloride was heated was absorbed in redistilled water, and the conductivity changes were measured. The dehydrochlorination rate was characterized by the slope of the curve plotted in time — amount of liberated HCl coordinates. The heat treatment of polyvinyl chloride was carried out at $175 \pm 0.2^\circ$, the samples were placed in a reaction vessel previously heated to this temperature. The liberated hydrogen chloride was removed in a current of air, heated to 175° , previously freed from traces of HCl, which passed through the reaction vessel at a constant rate. A Kohlrausch bridge was used for the conductivity determinations.

The thermal stability of the samples was characterized by the time from the moment when the polymer was put in the reaction vessel to the start of HCl liberation.

The physical and mechanical properties of plasticized resins containing the amounts of our stabilizers indicated in Table 2 were determined by the methods described in Departmental Technical Specifications 1535-47.

SUMMARY

1. The following substances were synthesized and tested as stabilizers for polyvinyl chloride: low-molecular epoxy resins based on epichlorohydrin and 2,2-bis-(4-hydroxy-3-methylphenyl)propane, 1,1-bis-(4-hydroxyphenyl)cyclohexane, 1,1-bis-(4-hydroxy-3-methylphenyl)cyclohexane, and 2,2-bis-(4-hydroxy-3-nitrophenyl)propane; cis butyl 9,10-epoxystearate and epoxidized castor oil and whale oil. It is shown that all these compounds, with the exception of the derivative of 2,2-bis-(4-hydroxy-3-nitrophenyl)propane, are effective thermal stabilizers for polyvinyl chloride, and they also improve the physical and mechanical properties of the plasticized resin.

2. If mixtures of low-molecular epoxy resins or epoxidized triglycerides with lead silicate are used, the thermal stability of polyvinyl chloride is higher and the quality of the resin is better than if these stabilizers are used separately.

LITERATURE CITED

- [1] H. V. Smith, Brit. Plastics, 307 (1954).
- [2] W. J. Marmion, Research 7, 351 (1954).
- [3] R. J. Gall and F. P. Greenspan, Ind. Eng. Chem. 45, 2722 (1953).
- [4] D. Swern, J. Am. Chem. Soc. 67, 412 (1945).
- [5] A. Zincke, Ann. 400, 33 (1913).


- [6] M. E. McGreal, V. Niederl, and J. B. Niederl, *J. Am. Chem. Soc.* 61, 345 (1939).
- [7] T. Szeky, *Zbl. II*, 1737 (1904).
- [8] E. K. Marele and D. R. Boyd, *J. Chem. Soc.* 101, 308 (1912).
- [9] D. Swern, in the book: *Organic Reactions*, 7 (IL, Moscow, 1956) p. 476 [Russian translation].
- [10] L. P. Witnauer, H. B. Knight, W. E. Palom, R. E. Koos, W. C. Ault, and D. Swern, *Ind. Eng. Chem.* 47, 2304 (1955).

Received September 20, 1957

POLYCONDENSATION OF PHENOXYACETIC ACID WITH FORMALDEHYDE AND SYNTHESIS OF A WEAKLY ACIDIC ION EXCHANGER FROM THEM

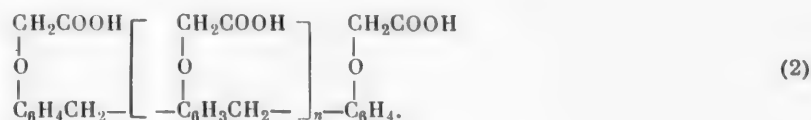
A. A. Vansheidt and N. N. Kuznetsova

Despite the enormous number of publications dealing with the polycondensation of phenols with formaldehyde and the structure of phenol-formaldehyde resins, the polycondensation of phenolic ethers with formaldehyde still remains to be studied, although there are indications that this reaction does occur, but under much harsher conditions than the reaction between formaldehyde and phenols [1]. Nevertheless, investigations of the reactions of formaldehyde with certain simple phenolic ethers are not only of theoretical interest, but could lead to valuable practical results. For example, polycondensation of formaldehyde with phenoxyacetic acid

 $-\text{CH}_2\text{COOH}$ in an acid medium, involving two or three H atoms of the phenol nucleus in the o-, o'-, and p-positions relative to the ether oxygen, should lead to the formation of both linear and space polymers. The former could be formed by condensation of the aldehyde with excess of phenoxyacetic acid, in the same way as has repeatedly been observed in the case of pheno-formaldehyde novolacs [2], according to the general equation (1)

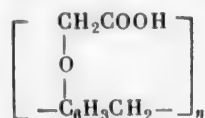


where $\text{R} = \text{CH}_2\text{COOH}$ or H (in the case of novolacs). These linear polymers should be polycarboxylic resins, fusible and soluble in organic solvents and aqueous alkalis, of the structure (2)



At the same time, because of the presence of a third active H atom in the phenol nucleus, the soluble polymers, like phenol-formaldehyde novolacs, should undergo hardening in presence of excess formaldehyde (owing to cross linking by CH_2 groups through these H atoms) with formation of insoluble space polymers of the resite or resitol types, in which the phenolic hydroxyls are replaced by $-\text{OCH}_2\text{COOH}$ groups. Thus, the products formed by the hardening of these soluble resins should be weakly acidic ion-exchange resins differing advantageously from cation exchangers made from aromatic hydroxy acids of the type of resorcylic acid (such as Wofatit C) by the absence of phenolic hydroxyls, which make the resins unstable to the action of alkalis and oxidizing agents. Moreover, it is to be expected that the presence in these resins of carboxyl groups linked to the aromatic nuclei through $-\text{O}-\text{CH}_2-$ groups rather than directly, confers considerable mobility to the carboxyls, and thereby favors their complete interaction with multivalent organic ions at all the active groups present in them, and increases the adsorption selectivity for these ions. These suppositions were fully confirmed by experiments, and it was found that although phenoxyacetic acid is much less reactive than phenol, nevertheless it readily entered into polycondensation with formaldehyde even at 100° when heated with the latter in presence of concentrated hydrochloric acid. As a result of these experiments, with the use of 0.7-1.0 mole of formaldehyde to 1 mole of phenoxy acid, fusible and soluble resins were obtained with molecular weights between 570 and 970. They were readily soluble in organic solvents and aqueous alkalis, and were similar in their composition and properties to linear polymers of structure [2], with average degree of polymerization (n) between 2 and 5.

Hardening of these soluble and fusible polymers was effected when they were heated to 100-140° with paraform in presence of sulfuric acid. The products were infusible resins, insoluble in organic solvents and aqueous alkalis, with swelling coefficients between 2 and 6 in accordance with the amount of paraform added for the hardening. They were weakly cross-linked polymers of the structure



and were typical weakly acidic cation-exchange resins (KFU); their total exchange capacity, in accordance with the composition shown above, was 5.8 meq/g. They have high resistance to the action of alkalis and oxidizing agents, and high mechanical strength; they have the power of adsorbing streptomycin selectively, and are being used in the production of antibiotics.

EXPERIMENTAL

Preparation of Phenoxyacetic Acid. Phenoxyacetic acid was prepared from phenol, monochloroacetic acid, and caustic soda by the Koelsch method [3]; in order to avoid the use of ether, which complicates the process, especially on the industrial scale, and to increase the yield, this method was modified as follows: 1.1 mole of monochloroacetic acid in the form of 50% aqueous solution was gradually neutralized at 30°, with stirring and cooling, by 35% caustic soda solution until the mixture was weakly alkaline to litmus. A solution of sodium phenolate, made from 1 mole of crystalline phenol and 1.05 mole of caustic soda in the form of 35% aqueous solution, was

TABLE 1

Composition and Properties of Soluble Polycondensation Products of Phenoxyacetic Acid and Formaldehyde

Characteristics of polycondensation products	Resin		
	I	II	III
PA/CH ₂ O ratio in original mixture	1.0	1.11	1.43
Melting point (°C)	103-107	90-94	69-72
Molecular weight	974	666	560
Degree of polymerization (n)	5.01	3.13	2.43
Ar/CH ₂ ratio in resin:			
Calculated	1.2	1.33	1.42
Found	1.15	1.22	1.39
Contents (%):			
C found	65.57	64.77	65.76
C calculated	65.40	65.17	65.00
H found	5.3	5.1	5.5
H calculated	4.9	4.9	4.9
COOH found	27.3	27.5	27.7
COOH calculated	27.7	27.9	27.6

added gradually at room temperature to the solution by the salt. The reaction mixture was heated at 100° for 1 hour, cooled to 60-70°, and dissolved in 3.5-4 liters of water with stirring. The clear solution of the sodium salt of phenoxyacetic acid was poured with stirring into 10-15% hydrochloric acid containing not less than 1.2 mole of HCl. The precipitated phenoxyacetic acid was filtered off, washed 4-5 times with distilled water, recrystallized twice from water, and dried in a thin layer at 30-40°. The yield of phenoxyacetic acid obtained by

this procedure was double the yield in the Koelsch method; it was about 70% of the theoretical yield calculated on the phenol taken. Titration showed that it contained about 99% phenoxyacetic acid, and only traces of phenol and chloride; the water content was 0.5-0.6%. After further recrystallization and washing with water to a negative reaction for chloride pure phenoxyacetic acid of m.p. 97-98° was obtained; this was used for preparation of the resins.

Synthesis of Fusible and Soluble Condensation Products of Phenoxyacetic Acid with Formaldehyde. In contrast to phenol, phenoxyacetic acid reacts with phenol only in the presence of considerable amounts of strong mineral acids. Thus, a solution of phenoxyacetic acid in formaldehyde solution, containing 1% sulfuric acid (on the weight of phenoxyacetic acid), did not show any layer separation or resin formation even after prolonged heating. In presence of 3% sulfuric acid a viscous resin was obtained after 12 hours of boiling, and a resin which hardened at room temperature could be obtained only with 5% sulfuric acid. In presence of phosphoric acid the reaction was even slow, and yielded only viscous resins. However, it was much more rapid with hydrochloric acid than with sulfuric acid, and therefore hydrochloric acid was used as catalyst in most of our experiments.

Fusible and soluble condensation products were prepared as follows.

Phenoxyacetic acid and formaldehyde (in the form of 35-40% aqueous solution) were put into a flask fitted with a reflux condenser, dropping funnel, stirrer, and thermometer; the mixture was heated to 80° on a glycerol bath until a clear solution was obtained. After this 25% hydrochloric acid (12% on the weight of phenoxyacetic acid) or 50% sulfuric acid (10% on the weight of phenoxyacetic acid) was added with stirring from the dropping funnel. The heating was stopped at the same time, as the temperature in the flask rose to the boiling point of the solution (98-100°C) owing to the exothermic reaction; the heating was then restarted and continued with the solution boiling gently. After 25-30 minutes from the start of boiling (with hydrochloric acid) or 2.5-3 hours (with sulfuric acid) the solution separated into two layers: an upper aqueous layer, and a lower layer consisting of the resinous condensation product.

The heating with stirring was continued until a sample of the resin hardened when cooled to room temperature. The heating was then stopped. The free formaldehyde content of the aqueous layer remained almost unchanged during any further heating. The resins were solid, colorless products, brittle at room temperature; they melted at 75-100° and were soluble in alcohol, ether, acetone, and aqueous caustic soda. They retained their fusibility and solubility if reheated.

In order to determine the effects of excess phenoxyacetic acid on the molecular weight and properties of the resins, they were prepared at three different molar ratios of phenoxyacetic acid (PA) to formaldehyde, from 1 to 1.43.

The molecular weights of the resins were determined cryoscopically in phenol after it had been shown that this method can be used with phenoxyacetic acid (found $M = 154$, calculated $M = 152$). The average degree of polymerization (n) of the resins was calculated from the formula

$$M = 164n + 152,$$

on the assumption that the resins are mixtures of polymer homologs of structure (2), and that their composition can be represented by the formula $(C_9H_8O_3)_n C_8H_8O_3$.

With the known values of M and n it was possible to calculate the carbon, hydrogen, and carboxyl contents of the resins from the equations:

$$\%C = \frac{(108 \cdot n + 96) \cdot 100}{M}, \quad \%H = \frac{8 \cdot (n + 1) \cdot 100}{M}, \quad \%COOH = \frac{45 \cdot (n + 1) \cdot 100}{M}$$

and to compare the results with data obtained by elementary analysis of the resins and titration in presence of phenolphthalein.

The results of these determinations are given in Table 1.

It follows from Table 1 that, as was to be expected, increase of the ratio of phenoxyacetic acid to formaldehyde in the original mixture from 1.0 to 1.43 resulted in decreases of the molecular weight and average degree

of polymerization of the resins, and also of their melting point. In all cases more than 1 mole of phenoxyacetic acid (between 1.2 and 1.4 moles) combined with 1 mole of converted formaldehyde. This was demonstrated by means of special experiments in which the unreacted substances were determined quantitatively; the structure (2) postulated for the soluble resins, according to which n CH_2 groups bind $(n + 1)$ aromatic nuclei, was thus confirmed. Moreover, it is seen in the table that the percentage contents of C, H, and COOH found are close to the values calculated from the same structural formula, with the molecular weight and average degree of polymerization taken into account.

Hardening of Fusible Resins. The hardening process, i.e., the conversion of fusible and soluble resins into infusible products insoluble in alkalis, was effected as follows. The resin was melted and heated to $100-110^\circ$, and the catalyst followed by formaldehyde (as paraform)* were added. After the paraform had dissolved, the resin was poured out into acid-resisting stainless steel trays (in layers 10-15 mm thick), and placed in a thermo-regulated closet, where it was kept first at 100° and then at $120-140^\circ$, until it was converted into an infusible and insoluble resin. The hardening rate depended on the temperature, amount of catalyst, component ratio, and other factors.

Different results were obtained in experiments on the hardening of resins with hydrochloric, phosphoric, and sulfuric acid catalysts, respectively. Thus, in presence of concentrated hydrochloric acid an insoluble product could not be obtained at all, probably because on account of its volatility the acid is lost from the reaction zone at the hardening temperatures before the formaldehyde has time to react. Hardening in presence of phosphoric acid proceeds at a very low rate even if 5% on the resin weight is used, and yields an only partially hardened product with a high content (over 50-60%) of soluble components. However, with sulfuric acid of 50% strength, added even in small quantities (about 0.3% on the resin weight) a hardened product containing 10% of alkali-soluble resin was obtained. The hardening rate rose rapidly with increase of the amount of sulfuric acid from 0.3 to 2%, and the time of hardening decreased from 7-8 to 3-4 hours. However, with more than 0.5% sulfuric acid the resin was strongly colored, first reddish brown and then black. This coloration appeared mainly on the surface of the resin, evidently as the result of oxidation by atmospheric oxygen.

The hardening process depends to a considerable extent on the temperature conditions. It was found that at the start of hardening the temperature must be maintained near 100° for about 4-5 hours. During this time the viscosity of the resins greatly increases, although the resin still remains soluble.

The temperature must then be raised to 120° and the product held at that temperature until it resinifies. At this stage the resin is only partially soluble in alkalis and does not melt but only softens when heated. The cooled resin was comminuted to a grain size of 4-5 mm and again heated at $120-140^\circ$ until its swelling coefficient stopped decreasing. If the hardening was effected at 120° rather than at 100° at the beginning of the process, the product was more porous and had a higher swelling coefficient, probably because of considerable evolution of formaldehyde vapor. To remove soluble organic and inorganic impurities, the hardened resin was comminuted to a grain size ≤ 1 mm, covered with a 10-fold volume of 1 N caustic soda solution, and left for 24 hours. The acid form of the hardened resin was thereby converted into the salt (sodium) form, retaining its insolubility, while the unhardened portion of the resin and the catalyst passed into solution. On the following day the alkali was decanted off and the product was again treated with caustic soda solution; this operation was repeated until the alkaline extracts no longer turned turbid when acidified. About 10-12% of insoluble organic impurities (on the weight of the original resin) could be extracted in this way from the hardened resin. The sodium salt of the ion exchanger was then converted into the original H form by treatment with hydrochloric acid; the product was washed with distilled water to a negative reaction to Methyl orange. The H form of KFU resin consists of yellow grains, with considerable mechanical strength and chemical resistance. The volume swelling of the H form in water is only 5-6%. However, in 1 N caustic soda solution the swelling coefficient of the resin is much higher, owing to its conversion into the sodium form. The swelling coefficient varied between 2 and 6, in accordance with the amount of paraform taken, and decreased with increased cross linking of the polymer. Thus, it is clear from Table 2 that with increase of the amount of paraform from 5 to 20% the swelling coefficient of the hardened resin fell from 4.4 to 2.6, with equal yields of insoluble resin. However, the exchange capacity of the resins varied little.

For determination of the exchange capacity a sample of resin was treated with excess 0.2-0.5 N caustic soda solution and the excess alkali was then titrated with 0.5 N hydrochloric acid solution in presence of

* Paraform was prepared from formalin solution by distillation of 2/3 (by weight) of the latter under vacuum (20-100 mm) at $50-60^\circ$.

phenolphthalein; alternatively, 0.5 N sodium acetate solution was added to the resin [4] and the liberated acetic acid was titrated; both methods gave the same results. The titration rate depends on the grain size of the sample and its swelling coefficient. Thus, samples of grain size 0.1 mm and swelling coefficient 2.5-4 could be titrated within 10-15 minutes. A coarser fraction (up to 0.5) with the same swelling coefficient was titrated much more slowly (24 hours and over).

The relatively high swelling coefficients of the resins listed in Table 2, and also of the products formed by the hardening of soluble resins (I)-(III), indicate that their degree of cross linking is low. This also confirmed by the results of elementary analysis, which indicate that resins (I)-(III) are close in composition to linear polymers of the composition $(C_9H_8O_3)_n$, but not to strongly cross-linked polymers with higher carbon contents.

TABLE 2

Yields and Characteristics of the Hardened Products

Characteristics of hardened products	Amount of paraform (% on weight of soluble resin)		
	5	10	20
Coefficient of swelling in 1 N NaOH	4.4	3.7	2.6
Capacity (in meq/g)	5.80	5.80	5.75
Yield of hardened product (% on weight of original resin)	90	88	90

The composition of the hardened resins obtained from the soluble products is given below.

Original resin	C	H
Found %		
I	65.50	5.04
II	66.00	5.14
III	65.65	5.00
$C_9H_8O_3$. Calculated (%) .	65.60	4.87

SUMMARY

1. The polycondensation of phenoxyacetic acid with formaldehyde in presence of mineral acids was studied; it was found that when a solution of phenoxyacetic acid in formalin is heated, the reaction proceeds most rapidly in presence of hydrochloric acid, and yields fusible polymers, soluble in aqueous alkalies, with molecular weights between 570 and 970, provided that the molar ratio of phenoxyacetic acid to formaldehyde is equal to or greater than 1; 1 mole of formaldehyde always binds more than 1 mole of phenoxyacetic acid, while the molecular weight of the resins formed decreases with increase of the excess amount of phenoxyacetic acid present on the original mixture. These results, and analysis of the soluble resins, show that, like novolacs, they are mixtures of polymers of the type $H[C_6H_3(OR)CH_2]_nC_6H_4OR$ (where $R = -CH_2COOH$) in which an average of 3 to 6 molecules of phenoxyacetic acid are cross-linked by methylene bridges through their aromatic nuclei.

2. When the soluble resins are heated with paraform in presence of sulfuric acid, infusible and insoluble polymers are formed, which swell in aqueous alkalies, and which have the properties of weakly acidic ion exchangers with an exchange capacity of 5.8 meq/g; they take up streptomycin selectively from culture media.

LITERATURE CITED

- [1] Zbl., I,307 (1925); Frdl., 14, 626; German Patent 403264, 406152.

[2] A. A. Vansheldt, *Plastics* 3, 17 (1934); in the book: *Plastics* [in Russian], vol. 2 (1937) p. 183; *Org. Chem. Ind.* 7, 388 (1937); *Proc. December Session Acad. Sci. USSR* (1939) p. 71; *J. Gen. Chem.* 12, 489 and 500 (1942).

[3] C. F. Koelsch, *J. Am. Chem. Soc.* 53, 304 (1931).

[4] A. A. Vansheldt, A. A. Vasil'ev and O. I. Okhrimenko, *Theory and Practice of the Use of Ion-Exchange Materials, Collected Papers* [in Russian] (Izd. AN SSSR, Moscow, 1955).

Received April 14, 1958

HYPOCHLORINATION OF PROPYLENE

V. S. Étlis and L. N. Grobov

The production of a number of important substances derived from propylene oxide has recently been achieved on the industrial scale [1, 2]. One method for the production of this valuable material is dehydrochlorination of propylene chlorohydrin. The latter may be made, by analogy with ethylene chlorohydrin, by hypochlorination of propylene.

The purpose of this work was to study the hypochlorination of propylene and to determine the optimum process conditions.

EXPERIMENTAL

Hypochlorination of propylene was studied with the aid of a continuous-action column of the bubbler type, 2 meters high and 40 mm in diameter. The column was jacketed to reduce heat losses. The apparatus is shown schematically in the figure.

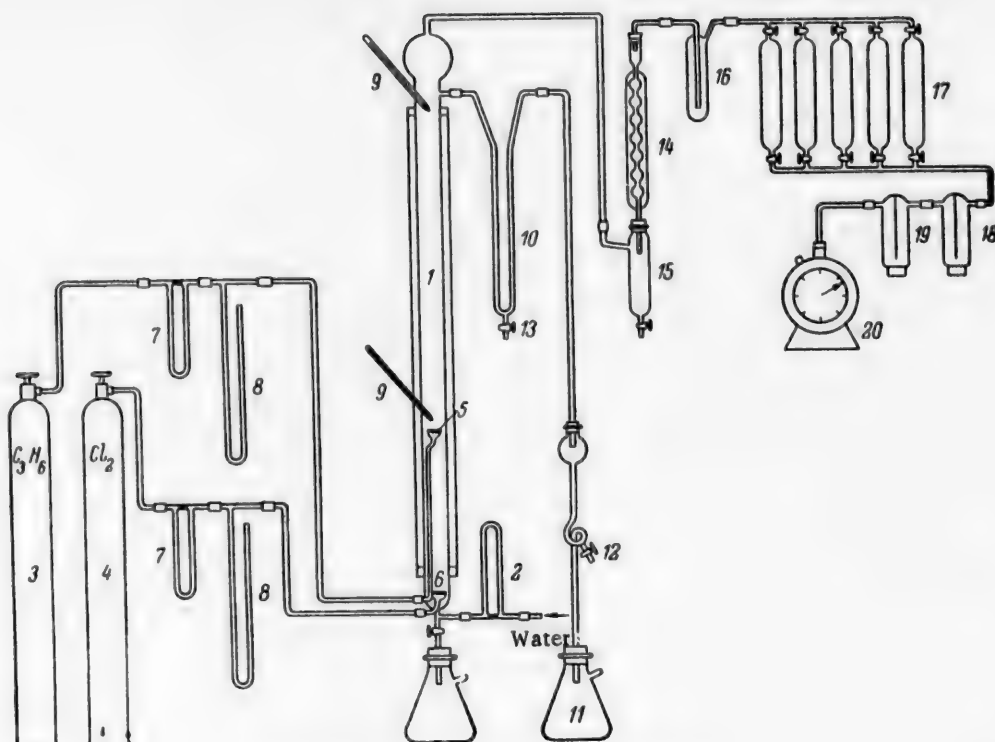
Water, the flow rate of which was measured by means of the meter 2, was fed continuously into the lower end of the column 1. Propylene and chlorine from the cylinders 3 and 4 were fed continuously into the column through the porous plates 5 and 6; chlorine was fed in at the lower end, and propylene at a point 600 mm above the entry of chlorine. The flow rates and pressures of the incoming gases were measured by means of the flow meters 7 and manometers 8. The reaction temperature was measured by the thermometers 9. The propylene chlorohydrin solution passed continuously through the upper outlet by way of the seal 10 into the flask 11. Samples were taken during the experiment out of the stopcock 12. The chlorides formed in side reactions partly overflowed together with the solution into the flask 11, and were partly retained in the seal 10, from which they could be withdrawn through the stopcock 13. The unconverted gases passed out of the top of the column through the condenser 14, where the chlorides present in the gas phase were condensed and collected in the trap 15. After the condenser the gasses passed through the control flask 16, containing a solution of starch with KI for detection of chlorine breakthrough. The pipets 17 were used for sampling the gas. After the pipets, the gases were purified and dried in the flasks 18 and 19, filled with NaOH and CaCl_2 ; they then passed through the meter 20 where their volume was measured, and escaped into the atmosphere.

The propylene-propane fraction used for the investigation had the following composition (in %): C_3H_6 81.0-89.9, C_3H_8 6.1-14.4, C_2H_4 1.0-2.6, $i\text{-C}_4\text{H}_{10}$ 0.0-1.5, $n\text{-C}_4\text{H}_{10}$ 0.3-2.5, O_2 0.2-0.5, CO_2 0.

The process was so conducted that no chlorine could be detected in the escaping gases. The reaction yielded a 4-8% solution of propylene chlorohydrin. The chloride layer (1,2-dichloropropane and di(β -chloroisopropyl) ether) was separated off. The propylene chlorohydrin was analyzed by dehydrochlorination by the action of excess alkali, with subsequent back titration*. The separated chlorides were collected and analyzed by distillation. It was found that the principal substances present in the chlorides were 1,2-dichloropropane (73 wt. %, b.p. 97-98°, d_4^{20} 1.1563, n_D^{20} 1.4388 (literature data: b.p. 97-98°, d_4^{14} 1.1659 [4]), and di(β -chloroisopropyl) ether (27 wt. %) b.p. 85-98° (45 mm), d_4^{20} 1.1238 (literature data: b.p. 187.4°, d_{20}^{20} 1.1135 [1]).

Found %: C 41.62; H 6.92; Cl 41.80; $\text{C}_6\text{H}_{12}\text{Cl}_2\text{O}$. Calculated %: C 42.10; H 7.01; Cl 41.52

* Other chlorohydrins, formed from olefins present in the propylene, were determined together with propylene chlorohydrin.



Apparatus for hypochlorination of propylene.

The chloroacetone formed by oxidation of propylene chlorohydrin was identified as the dinitrophenylhydrazone; m.p. 124° (literature data: 124-124.5° [4]).

Found % N 20.20, $C_9H_9ClN_4O_4$. Calculated %: N 20.55

To confirm that chloroacetone is formed from propylene chlorohydrin, 250 ml of propylene chlorohydrin solution containing 0.339% of carbonyl compounds calculated as chloroacetone was chlorinated for 3 hours. The contents of carbonyl compounds rose to 0.829%.

Preparation of Concentrated Propylene Chlorohydrin. In contrast to ethylene chlorohydrin [4], concentrated propylene chlorohydrin is relatively easy to prepare from dilute (6-7%) solutions. To prepare concentrated propylene chloride, 1 liter (1013.5 g) of solution containing 6.32% propylene chlorohydrin was put into the still of a Dean and Stark apparatus. After distillation, 10.45 g of 79.9% propylene chlorohydrin was withdrawn from the trap. The distillation was then continued for 40 minutes more. No layer formation was observed in the trap at this stage. The liquid (52.85 g) was run out of the trap, and 10 g of $(NH_4)_2SO_4$ was added to it. As a result, 27.08 g of 84.5% propylene chlorohydrin separated out. The distillation was then continued for 40 minutes more and 52.4 g of liquid was removed from the trap. Salting out with 20 g of $(NH_4)_2SO_4$ yielded 22.0 g of 90.3% propylene chlorohydrin. A third withdrawal of 49.8 g of liquid from the trap, salted out by means of 30 g of $(NH_4)_2SO_4$, yielded 4.5 g of 89% propylene chlorohydrin. The still contained 796 g of residual liquid free from propylene chlorohydrin.

Thus, 64.0 g of propylene chlorohydrin, taken in the form of 6.32% solution, yielded 55.1 g of 100% propylene chlorohydrin; this corresponds to an 86% yield. In the water there remained 14% of the propylene chlorohydrin, which cannot be salted out. The isolated propylene chlorohydrin had b.p. 126-127°, d_{20}^4 1.1158 and n_D^{20} 1.4393.

DISCUSSION OF RESULTS

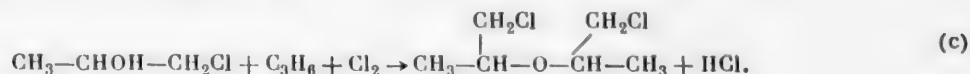
By analogy with the ethylene compound, propylene chlorohydrin is formed by the reaction



In addition, some of the propylene and chlorine is consumed in the formation of dichloropropane



Propylene chlorohydrin reacts with propylene and chlorine to form di(β -chloroisopropyl)ether:



Effect of Molar Ratio $\text{Cl}_2 : \text{C}_3\text{H}_6$ on the Molar Ratio PCH : HCl and Propylene Chlorohydrin Yield on the Converted Chlorine Experimental Temperature 35-43°, Propylene Chlorohydrin Concentration 6%, Chlorine Feed Rate 47 g/hr

Molar ratio $\text{Cl}_2 : \text{C}_3\text{H}_6$	Molar ratio PCH : HCl	Yield of PCH on Cl (%)	Molar ratio $\text{Cl}_2 : \text{C}_3\text{H}_6$	Molar ratio PCH : HCl	Yield of PCH on Cl (%)
1 : 1	0.760	63	1 : 2.4	0.953	82
1 : 1.3	0.800	72	1 : 2.5	0.908	91
1 : 1.5	0.792	72	1 : 2.5	0.975	91
1 : 1.5	0.792	73	1 : 3.3	0.945	85.5
1 : 2	0.815	86	1 : 3.2	0.960	93.5
1 : 2.2	0.902	82.5	1 : 3.8	0.960	99.5
1 : 2.3	0.965	85	1 : 4.1	1.00	100
1 : 2.4	0.905	79	1 : 4.1	1.00	99

It was desired to study various factors which influence the course of the principal reaction (a). The effect of excess propylene on the yield of propylene chlorohydrin was studied for this purpose. It follows from Equation (a) that the course of the main process may be characterized by the molar ratio $\frac{\text{propylene chlorohydrin(PCH)}}{\text{hydrogen chloride (HCl)}}$, which reaches unity in absence of the side reactions.

The results of a series of experiments are given in the table. It follows from this table that excess of propylene favors the main reaction, and when the ratio of chlorine to propylene is 1 : 4, the side reactions do not occur to any practical extent. It is also seen that the yield of propylene chlorohydrin, calculated on the chlorine consumed, also increases with increase of the $\text{C}_3\text{H}_6 : \text{Cl}_2$ ratio.

Under given conditions the yield of propylene chlorohydrin also depends on the gas feed rates.

The effects of the chlorine and propylene feed rates on the molar ratio PCH : HCl and on the temperature, at molar ratio $\text{Cl}_2 : \text{C}_3\text{H}_6 = 1 : 2.3^*$, are given below.

Cl (g/hr)	46	46.5	46.5	47	50	51	59	60.5
C_3H_6 (g/hr)	62.8	63.3	63.3	64.0	68.0	72.3	77.0	77.7
PCH : HCl	0.975	0.905	0.953	0.965	0.870	0.860	0.828	0.815
Temperature (°C) . . .	34	36	35	35	37	35	37	43

It is seen from the above that the PCH : HCl ratio falls from 0.975 to 0.815 when the chlorine rate is increased from 46 to 60.5 g per hour.

Variations of the temperature should also be noted; the temperature in our experiments altered spontaneously with variations of the feed rates.

We found that in addition to the above reactions which may occur in the hypochlorination of propylene, small amounts (from 0.5 to 1%) of chloroacetone are also formed and can be detected in the aqueous solution of propylene chlorohydrin. The formation of this compound may be regarded as the result of oxidation of 1-chloropropanol-2.

* Calculated as 100% propylene.

Distillation of the chlorinated derivatives shows that they consist mainly of 1,2-dichloropropane and di(8-chloroisopropyl)ether.

A noteworthy feature of this method for preparation of propylene chlorohydrin is the ease with which the compound can be obtained in the concentrated form.

The method used for its isolation is based on the formation of an azeotropic mixture of propylene chlorohydrin and water, which boils at 95.4° and contains 54.2% propylene chlorohydrin and 45.8% water [1], and which separates into layers when cooled. The lower layer, containing 80-85% propylene chlorohydrin, is separated off. Additional propylene chlorohydrin can be salted out of the aqueous layer by means of NaCl or $(\text{NH}_4)_2\text{SO}_4$.

SUMMARY

The influence of various factors on the hypochlorination of propylene was studied: a by-product, chloroacetone, is formed by oxidation of propylene chlorohydrin.

LITERATURE CITED

- [1] J. Bignon, Ind. chim. 40, 433, 221, 434, 249, 435, 281 (1953); Chem. and Chem. Technol. 10, 102 (1955).
- [2] P. G. Sergeev, A. A. Vinogradov, and L. M. Bukreeva, Chem. Sci. and Ind. 1, 281 (1956).
- [3] British Patent 738171 (1955); Chem. Abs. 51, 2852c (1957).
- [4] Dictionary of Organic Compounds, 1 (IL, Moscow, 1949) p. 778 [Russian translation].

Received September 7, 1957

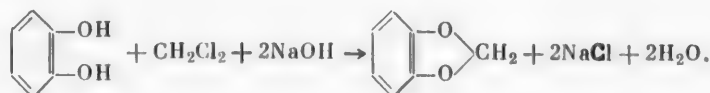
CERTAIN REACTIONS CARRIED OUT WITH METHYLENE
CHLORIDE WITHOUT THE USE OF PRESSURE IN BENZYL
ALCOHOL AS A HIGH-BOILING SOLVENT

E. D. Laskina

All-Union Scientific Research Institute of Synthetic and Natural Perfumes

Methylene chloride is one of the most easily available methylenating agents. It is known that methylenation with the aid of methylene chloride is performed only under pressure, as the boiling point of methylene chloride is considerably lower than the reaction temperature. Solvents of higher boiling points such as methylene bromide and iodide are also used for methylenation; methylene sulfate is used less often. We were interested in the methylenation reaction in relation to the preparation of the methylene ether of pyrocatechol, which is an intermediate in the synthesis of heliotropin.

The methylene ether of pyrocatechol is usually prepared by the interaction of pyrocatechol and methylene chloride in presence of caustic alkali, in ethanol or methanol solution at 100-115° under pressure [1-5]. The yield is about 30% of the theoretical on the pyrocatechol taken. The process may be schematically represented as follows:



Because of the harsh reaction conditions, large amounts of solid resinous substances are formed which interfere so much with removal of the reaction products from the autoclave that this method for preparation of the methylene ether of pyrocatechol is quite unsuitable for industrial use.

Perkin, Robinson, and Thomas attempted to prepare the methylene ether of pyrocatechol without the use of pressure, by prolonged heating of pyrocatechol and methylene chloride in absolute ethanol in presence of sodium ethylate under reflux. The ether yield was low [6].

A method for preparation of the methylene ether of pyrocatechol without the use of pressure is very desirable. In view of the fact that methylenation in autoclaves proceeds with the best results at 110-115°, it was decided to use a high-boiling solvent in order to effect the reaction at a higher temperature but without the use of excess pressure. The desired result was not achieved with the use of veratrole or chlorobenzene for this purpose; the methylene ether of pyrocatechol was not isolated. On the other hand, methylenation in benzyl alcohol was successful, but the yield of pyrocatechol methylene ether did not exceed 12-13%, while part of the unconverted methylene chloride was returned. In order to decrease the return of methylene chloride and especially to increase the ether yield, we tried addition of certain metals such as copper, silver, aluminum foil, and nickel-aluminum alloy to the reaction mixture. This series of experiments, and another series in which the effect of the alkaline reagent (caustic potash, caustic soda, potassium and sodium carbonates, slaked lime, piperidine) on the course of the reaction was tested, did not give any significant results.

Considerably better results were obtained when the methylenation was effected by means of methylene chloride in presence of sodium iodide. It is known that under certain conditions sodium iodide can react with

Substances taken for reaction (in g)					hydro-quinone	Reaction temperature (°C)	Duration of reaction (hours)	Yield of pyrocatechol methylene ether (%)	Notes
benzyl alcohol	pyrocatechol	caustic soda	sodium iodide	methylene chloride					
292	30	16	—	66,0	0.5	122-124	13.5	12.1	Reaction mass remained alkaline to phenolphthalein to the end of the experiment Amount of caustic soda increased because the reaction mass became acid during the reaction
595	60	46	30	90,5	2.0	122-124	13.5	31.5	
630	60	39	20	90	2.0	122-124	8	33.8	

organic halogen compounds containing chlorine or bromine, chlorine or bromine in the organic compound being replaced by iodine. In this instance addition of sodium iodide to the reaction mixture increased the yield of pyrocatechol methylene ether owing to formation of methylene iodide as the result of the exchange reaction between sodium iodide and methylene chloride, as shown by the data in the table.

It has been reported previously [7] that higher yields of pyrocatechol methylene ether are obtained with methylene iodide than with methylene chloride.

We found no information in the literature on the exchange reaction between methylene chloride and sodium iodide in the preparation of pyrocatechol methylene ether; it was therefore decided to study in greater detail the reaction between pyrocatechol, methylene chloride, and sodium iodide in presence of caustic alkali, in benzyl alcohol as a high-boiling solvent * without excess pressure (without the use of autoclaves) [8].

The question of the amount of sodium iodide to be taken for the reaction was very significant, as this influenced not only the yield but also the quality of the pyrocatechol methylene ether. Theoretically 1 mole of pyrocatechol requires 2 moles of sodium iodide. In practice it is sufficient to take 0.24 mole of sodium iodide per mole of pyrocatechol in order to obtain good quality pyrocatechol methylene ether in a yield of about 30% on the pyrocatechol taken. If the amount of sodium iodide taken for the reaction is increased, the amount of methylene iodide formed also increases, but it does not all react with pyrocatechol and some remains as an impurity in the pyrocatechol methylene ether. These two substances are almost impossible to separate by distillation, even with the aid of a very efficient column, because of the similarity of their boiling points. The yield of the ether with methylene iodide as an impurity is about 40-50%.

For isolation of methylene iodide in the pure state from the reaction products two series of experiments were carried out; in one series the reaction was effected without pyrocatechol, and in the other, without pyrocatechol and alkali. All the other conditions were the same as in the preparation of pyrocatechol methylene ether. Experiments in which methylene chloride and sodium iodide were heated in benzyl alcohol in presence of alkali gave dibenzylformal in 15.6% yield, and a small amount of methylene iodide, which could not be purified (under the same conditions but in absence of sodium iodide, dibenzylformal is formed in a lower yield, 12.5%). The formation of dibenzylformal may be schematically represented as follows:



* Appreciable amounts of the methylene ether of pyrocatechol could not be isolated when acetone was used as solvent for this reaction.

Methylene iodide was obtained pure in fairly good yield (45%) when methylene chloride was heated with sodium iodide in benzyl alcohol:



Simultaneously, dehydration of benzyl alcohol in presence of mineral salts resulted in the formation of dibenzyl ether (22.8%).

This method for preparation of dibenzyl ether is described in the literature [9]. Our methods for preparation of methylene iodide and dibenzylformal differ from known methods since the reactions with methylene chloride on which they depend are effected without the use of pressure.

Perkin and Scarborough prepared methylene iodide by prolonged heating of methylene chloride with sodium iodide in acetone in a hermetically sealed vessel [10] Arnhold prepared dibenzylformal by the action of heat on methylene chloride with sodium benzyolate in sealed tubes at 150° [11]. We found that dibenzylformal is not formed as a by-product in the preparation of pyrocatechol methylene ether under our conditions. However, if the sequence of reagent addition is changed, and pyrocatechol is added after a mixture of all the other components has been heated to the required temperature, a small amount of dibenzylformal is formed but the yield of pyrocatechol methylene ether is lowered.

The literature contains numerous references to the fact that the methylenation reaction is accompanied by oxidation processes, because the dihydroxybenzenes undergoing methylenation in an alkaline medium can absorb atmospheric oxygen. Therefore there are frequent descriptions of methylenation in an inert atmosphere or in an autoclave which must be filled as much as possible with the reagents and must contain the minimum possible volume of air. This was taken into consideration in our experiments on methylenation of pyrocatechol, and hydroquinone was tried as an antioxidant in order to diminish undesirable oxidation processes. The yields of pyrocatechol methylene ether were somewhat more stable on introduction of small amounts of hydroquinone into the reaction mixture.

EXPERIMENTAL

Preparation of Pyrocatechol Methylene Ether. A flask 1 liter in capacity, fitted with a mechanical stirrer, thermometer, a straight condenser, and a delivery tube reaching to the bottom of the flask, with its upper end connected to a dropping funnel, was charged with 530 g of benzyl alcohol, 32 g of caustic soda, 30 g of sodium iodide, 1 g of hydroquinone, and 30 g of methylene chloride. The reaction mixture was heated with stirring, the temperature being maintained at 122-124°. To the mixture 120 g of methylene chloride solution in benzyl alcohol (1:1) was added from the dropping funnel, care being taken that the excess methylene chloride distilled off as slowly as possible. On the following day 14 g of caustic soda and 1 g of hydroquinone was added (the reaction must be alkaline to phenolphthalein) and the mixture was heated again at the same temperature. The total time of heating at 122-124° was 14 hours. During the heating 31 g of methylene chloride was distilled off. The cooled reaction product was distilled in steam after it had been made alkaline by addition of caustic soda solution. During two hours about 110 g of a heavy oily product was distilled off; this was dried over sodium sulfate and distilled under vacuum through a rod-and-disk column (23 disks). The yield of pyrocatechol methylene ether was 21.4 g (32.2%); b.p. 63° (18 mm); n_D^{20} 1.5400, d_4^{20} 1.1972.

Found %: C 69.07; H 5.28; I 1.0. $\text{C}_7\text{H}_6\text{O}_2$. Calculated %: C 68.84; H 4.95

The analysis was performed by the micro method, by combustion of the substance in a current of oxygen and absorption of the halogen by electrolytically deposited silver.

Evidently the pyrocatechol methylene ether still contained very small amounts of methylene iodide.

According to the literature, pyrocatechol methylene ether has b.p. 77.5° (27 mm) [12], d_4^{20} 1.202 [3].

Dibenzylformal was not detected during recovery of benzyl alcohol from the residue after steam distillation. Entirely different results were obtained in another experiment. In this case the essential difference was that pyrocatechol was added gradually to a previously heated mixture of the other components (similar apparatus was used).

A flask 500 ml in capacity was charged with 110 g of benzyl alcohol, 11 g of caustic soda, 5 g of sodium iodide, and 15 g of methylene chloride. The reaction mixture was heated to 122° and a mixture consisting of 15 g of pyrocatechol, 65 g of benzyl alcohol, and 25 g of methylene chloride was added during 3.5 hours; during this time 25.8 g of methylene chloride distilled off. On the following day 4 g more of caustic soda was added before the heating was started, as the reaction mass was not alkaline. The total heating time, with stirring, at 122-124° was 10 hours. Pyrocatechol methylene ether was isolated as described above, in 2.7 g yield (16.2%). The residue in the flask after steam distillation was extracted with diethyl ether; benzyl alcohol, pyrocatechol, and dibenzylformal were found in the extract. After separation of benzyl alcohol by vacuum distillation, the mixture of pyrocatechol and dibenzylformal was diluted with ether and washed with 10% aqueous caustic soda until the alkaline layer was colorless. After evaporation of the ether 4.6 g of dibenzylformal was obtained; b.p. 153-157° (2 mm), n_D^{20} 1.5482.

Preparation of Dibenzylformal. Similar apparatus was used, with a 750 ml flask; 270 g of benzyl alcohol, 22 g of caustic soda, 30 g of sodium iodide, and 30 g of methylene chloride were heated together for 7 hours at 122-124°. As methylene chloride distilled off, a total of 72 g of a solution of methylene chloride in benzyl alcohol (1:1) was gradually added to the reaction mixture. On the following day the mixture was again heated for 7 hours after addition of 7 g of caustic soda (to an alkaline reaction to phenolphthalein). The reaction product was distilled in steam. Pure methylene iodide could not be isolated from the distillate. The residue in the flask (after steam distillation), which was alkaline to phenolphthalein, was extracted with diethyl ether; this yielded 50.2 g (15.6%) of dibenzylformal; b.p. 188.5° (13 mm), n_D^{20} 1.5480, d_4^{20} 1.0665.

Found %: C 78.98; H 7.27; $C_{15}H_{16}O_2$. Calculated %: C 78.91; H 7.06

According to the literature data, dibenzylformal has b.p. 188-190° (13 mm), d_4^{23} 1.046 [13], d_4^{20} 1.053 [11].

Dibenzylformal was prepared in exactly the same manner in absence of sodium iodide; the yield was then 12.5% on the benzyl alcohol taken.

Preparation of Methylene Iodide. A flask with tubes, 750 ml in capacity, fitted with a mechanical stirrer, thermometer, and reflux condenser, was charged with 258 g of benzyl alcohol, 40 g of sodium iodide, and 10 g of methylene chloride, and the mixture was heated with the temperature of the liquid at 124-126° for 13 hours with heating. The liquid was cooled, and the crystalline precipitate was filtered off and washed with 35 g of benzyl alcohol. The combined filtrate and washings were distilled under vacuum through a rod-and-disk column (23 disks) the following fractions being collected: 1) 4 g at 23-30° (17-14 mm); 2) 18.2 g at 70-83° (13-10 mm), n_D^{20} 1.6499; 3) 5.9 g at 82° (9 mm), n_D^{20} 1.5945; 4) 206 g at 88-92° (9 mm) with 73.6 g of residue consisting of a liquid and crystalline portion. The first fraction consisted of a mixture of water and a heavy, strongly refracting liquid. The second and third fractions were dried over calcium chloride and distilled in a vacuum to give 14.3 g (45%) of methylene iodide, b.p. 54° (7 mm).

Found %: C 4.87; H 0.99; I 96.43. CH_2I_2 . Calculated %: C 4.48; H 0.76, I 94.76

The analysis was effected by the micro method by combustion in a current of oxygen and absorption of the halogen by electrolytically deposited silver.

According to the literature, methylene iodide has b.p. 88-89° (33 mm) [14].

The fourth fraction was benzyl alcohol. From the residue after distillation (73.6 g), 54.2 g (22.8%) of dibenzyl ether was isolated. B.p. 149° (6 mm), n_D^{20} 1.5608, d_4^{20} 1.0419.

Found %: C 84.97; H 7.13; $C_{14}H_{14}O$. Calculated %: C 84.81; H 7.11

According to literature data, dibenzyl ether has b.p. 149-150° (7 mm) n_D^{20} 1.5603, d_4^{20} 1.0456 [15].

SUMMARY

1. Pyrocatechol has been methylenated by means of methylene chloride in presence of sodium iodide and caustic soda in benzyl alcohol, without pressure (without use of autoclaves) for the first time. The yield of pyrocatechol methylene ether was 32% of the theoretical on the pyrocatechol taken.

2. Methylene iodide was prepared in 45% of the theoretical yield on the methylene chloride taken, by the reaction of methylene chloride with sodium iodide in benzyl alcohol under atmospheric pressure.

3. The reaction of benzyl alcohol, taken in excess, with methylene chloride in presence of alkali under atmospheric pressure yielded dibenzylformal; the yield was 12-15% of the theoretical on the benzyl alcohol taken.

4. It is shown that dibenzylformal is not formed under the conditions described above for preparation of pyrocatechol methylene ether.

LITERATURE CITED

- [1] N. B. Ghosh, *J. Chem. Soc.* 107, 1597 (1915).
- [2] R. L. Bakhrakh, *Oil and Fat Ind.* 4, 42 (1934).
- [3] P. P. Shorygin, A. A. Simanovskaya, and A. V. Bogdanova, *J. Gen. Chem.* 8, 975 (1938).
- [4] V. N. Eliseeva and T. A. Devitskaya, *Trans. All-Union Sci. Res. Inst. Synth. and Natural Perfumes*, 2 (Food Industry Press, 1954) p. 60.
- [5] J. Draběk, *Chem. zvesti*, 10, 357 (1956).
- [6] W. N. Perkin, Jr., R. Robinson, and F. Thomas, *J. Chem. Soc.* 95, 1879 (1909).
- [7] K. N. Campbell, P. F. Hopper, and B. K. Campbell, *J. Org. Chem.* 16, 1736 (1951).
- [8] E. D. Laskina, *Soviet Author's Certif. No.* 106564 (1957).
- [9] Oddo, *Gazz.* 31, 1, 348 (1901).
- [10] W. N. Perkin, Jr. and H. A. Scarborough, *J. Chem. Soc.* 119, 1408 (1921).
- [11] M. Arnhold, *Lieb. Ann.* 240, 200 (1887).
- [12] W. J. Gensler and C. M. Samour, *J. Org. Chem.* 18, 9 (1953).
- [13] M. Descudé, *Bl. Soc. chim.* [3] 29, 48 (1908).
- [14] V. E. Tishchenko and I. L. Rabtsevich-Zubkovskii, *J. Russ. Phys.-Chem. Soc.* 46, 707 (1914).
- [15] D. N. Kursanov and V. N. Setkina, *Proc. Acad. Sci. USSR* 65, 849 (1949).

Received November 29, 1957

ARYLATION OF METHYLDICHLORSILANE BY AROMATIC HYDROCARBONS

K. A. Andrianov, I. A. Zubkov, V. A. Semenova,
and S. I. Mikhailov

It is stated in the patent literature that benzene and other aromatic hydrocarbons react with trichlorosilane and methyldichlorosilane in presence of aluminum chloride [1-3], boron trifluoride and boric acid [4-6], and boron trichloride [7]. Raney nickel was used in one investigation in the preparation of methylphenyldichlorosilane from methyldichlorosilane and benzene [8]. Because of the exceptionally great technological importance of the arylation of alkylhalosilanes, we studied the arylation of methyldichlorosilane by benzene, toluene, diphenyl, and naphthalene in presence of boric acid.

TABLE 1
Characteristics of Distillation Products

Substance	Formula	Boiling point (°C)	Pressure (mm)	d_{20}^{20}	Refractive index	Molar refraction	
						calculated	found
Tolymethyldichlorosilane	$\text{C}_6\text{H}_5\text{CH}_2\text{SiCl}_2$	161-165	7.0	1.2068	1.5330	53.13	53.10
Diphenylmethyldichlorosilane	$\text{C}_6\text{H}_5\text{CH}_2\text{SiCl}_2$	154-157.5	1.0	1.2100	1.5846	72.74	73.20
Naphthylmethyldichlorosilane	$\text{C}_{10}\text{H}_7\text{CH}_2\text{SiCl}_2$	152-158	4.0	Crystalline product, m.p. 26.2 °C			

Experiments showed that when benzene reacts with methyldichlorosilane in presence of 1-2% of boric acid at 250°, there is formed about 30% of phenylmethyldichlorosilane, a considerable amount of phenyltrichlorosilane, and gaseous reaction products which contain 86.2% hydrogen and 2.8% methane.

Toluene reacts with methyldichlorosilane at 300° in presence of boric acid to give tolylmethyldichlorosilane and gaseous products (77.5% hydrogen and 15.3% methane).

The reaction of diphenyl with methyldichlorosilane at 250-260° yields diphenylmethyldichlorosilane, diphenylbis(methyldichlorosilane), and gaseous products (79.9% hydrogen and 7.6% methane).

The reaction of naphthalene with methyldichlorosilane at 300-340° yields naphthylmethyldichlorosilane, a considerable amount of high-boiling products which do not distill under vacuum, and gaseous products (74.0% hydrogen and 16.7% methane).

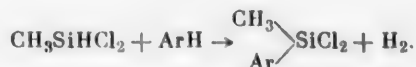
It was found that benzene and toluene react better than naphthalene and diphenyl with methyldichlorosilane.

TABLE 2

Rectification Data for 752 g of Liquid Products

Fractions	Boiling range (°C)	Pressure (mm)	Weight (g)	Yield (%)	Chlorine content (%)	Product
I	37—47	747	75	10.2	65.5	CH ₃ SiHCl ₂ + HSiCl ₃
II	58.5—74	747	154.2	20.9	55.1	(CH ₃) ₂ SiCl ₂ + traces of CH ₃ SiCl ₃
III	79—80.5	747	168.5	22.9	0.2	Benzene
IV	170—172	747	17	2.31	—	Not investigated
V	118—139	130—135	70.7	9.6	44.4	Phenyltrichlorosilane + CH ₃ C ₆ H ₅ SiCl ₂
VI	144—143.5	155—140	144.1	19.6	38.6	} CH ₃ C ₆ H ₅ SiCl ₂
VII	147—150	155—160	38.5	5.23	37.8	
Residue in still	—	—	30	4.04	—	—

In arylation of methylchlorosilane by toluene, diphenyl, and naphthalene, hydrogen atoms attached to silicon are replaced by aryl groups:



The products formed in these reactions indicate that other processes also occur. Disproportionation reactions and thermal rearrangements develop to a considerable extent under the reaction conditions. This is confirmed by the formation of phenyltrichlorosilane, methyltrichlorosilane, dimethyldichlorosilane, and of the methane obtained during the reaction. Considerable amounts of high-boiling reaction products are also formed. The amounts of methane and high-boiling nondistillable reaction products increase with the reaction temperature. Fractionation of the reaction products yielded compounds which correspond in composition to tolylmethyldichlorosilane, diphenylmethyldichlorosilane, and naphthylmethyldichlorosilane.

TABLE 3

Rectification of Fraction I Under 752 mm Pressure

Fractions	Boiling range (°C)	Weight (g)	Yield (%)	Chlorine product (%)	Product
I	32—40.5	7.6	4.2	59.5	—
II	40.5—46	10.2	5.65	61.1	CH ₃ SiHCl ₂
III	65—67	25.3	14.0	65.2	CH ₃ SiCl ₃ + traces of (CH ₃) ₂ SiCl ₂
IV	67—70	5.2	2.88	56.32	—
V	70	9.0	5.48	55.1	(CH ₃) ₂ SiCl ₂
VI	109	47.0	26.1	1.97	} toluene
VII	110	39.2	21.7	0.62	
Residue in still	—	31.99	17.7	20	—

Phenylmethyldichlorosilane always contains a small amount of phenyltrichlorosilane, which cannot be separated by rectification because of the close boiling points. It was found in the distillation of tolylmethyldichlorosilane, diphenylmethyldichlorosilane, and naphthylmethyldichlorosilane that, despite the good agreement between the molar refraction data (found and calculated), these compounds do not distill over one-degree ranges, but over narrow ranges of temperature, between 3.5 and 6° (Table 1). This indicates that other substances, probably isomers, are present. Nitration and sulfonation experiments did not yield any positive results in attempts to determine the position of the silicon atom in the aromatic nuclei. In all cases complex mixtures of polymeric products were formed, and individual compounds could not be isolated. Characteristics of the compounds formed are given in Table 1.

TABLE 4

Rectification of 81.8 g of Fraction II Under 7 mm Pressure

Fractions	Boiling range (°C)	Weight (g)	Yield (%)	Chlorine content (%)
I	83—88	12.3	15.05	28.76
II	161—165	30.7	37.5	35.64
III	170—200	31	37.9	36.11

EXPERIMENTAL

Methyldichlorosilane of b.p. 41.0°, containing 63.2% chlorine, was used for the experiments.

Preparation of Phenylmethyldichlorosilane. A 2-liter autoclave was charged with 500 g of methyldichlorosilane, 400 g of benzene, and 5 g of boric acid; the mixture was heated for 9.5 hours at 250°, the pressure in the autoclave being 80 atmos. The autoclave was then cooled to 20° (residual pressure 48 atmos). 877 g of substance was removed from the autoclave, put into a Würtz flask, and distilled from the solid residue (111 g). The liquid products (752 g) were rectified through a column of 15 theoretical plates (Table 2).

The 144–143.5° fraction (155–140 mm) was analyzed.

Found %: Cl 37.8; Si 13.50 d_{20}^{20} 1.1850, η_D 1.5130. Calculated %: Cl 37.2; Si 14.65

Spectroscopic analysis showed the presence of phenyltrichlorosilane.

Analysis of the gaseous products showed that they contained H₂ 86.2%, CH₄ 2.5%, air 3.0%.

TABLE 5

Distillation of Fraction I Under 749 mm Pressure.

Fraction	Boiling range (°C)	Weight (g)	Yield (%)	Chlorine content (%)	Product
I	32—40.2	20	8.79	66.5	CH ₃ HSiCl ₂ + HSiCl ₃
II	40.2—45	94.3	41.3	60.2	CH ₃ HSiCl ₂
III	45—62	27.10	11.9	68.2	CH ₃ SiCl ₃ + (CH ₃) ₂ SiCl ₂
IV	62—65	40.40	17.7	51.72	(CH ₃) ₂ SiCl ₂
V	65—67	17.10	7.5	26.12	—
Residue in still	—	2.59	0.55	—	—

TABLE 6

Distillation of Residue

Fraction	Boiling range (°C)	Pressure (mm)	Weight (g)	Yield (%)	Chlorine content (%)	Product
I	80—140	2	83.02	14.4	18.0	Presence of impure diphenyl shown by qualitative reaction
II	153—156	5	32.0	5.58	25.20	
III	163—152	5—2	86.3	15.0	24.38	
IV	152—194	1.0	148.5	25.9	28.33	
Residue in still	—	—	134.8	23.5	—	—

Preparation of Tolylmethyldichlorosilane. An autoclave, 8 liters in capacity, was charged with 1500 g of methyldichlorosilane, 1440 g of toluene, and 3 g of boric acid. The reaction was continued at 250° for 4 hours;

TABLE 7

Distillation of Fraction IV Under 1 mm Pressure

Fraction	Boiling range (°C)	Weight (g)	Yield (%)	Chlorine content (%)
I	108—154	7.3	5.68	—
II	154—157.5	62.8	48.8	26.82
III	165—174	23.8	18.5	27.70
IV	174—200	13.2	10.2	33.86
V	200—230	6.3	4.8	35.92
Residue in still	—	6.8	5.3	—

Note: Fraction I had m.p. 33.8 °C

Note. Fraction I had m.p. 33.8°.

the pressure in the autoclave was 80 atmos. The autoclave was cooled down to 20° (residual pressure 48 atmos), and 2825 g of substance was removed from the autoclave; the following fractions were obtained from it: Fraction I, boiling up to 150°, 1656.2 g, Fraction II, boiling in the range of 150–310°, 944.3 g.

Fraction I was rectified to give a total yield of 180.4 g of products; the rectification results are given in Table 3.

Fraction II, boiling in the 150–310° range, was distilled under vacuum from a Claisen flask with a fractionating column (Table 4).

TABLE 8

Distillation of Fraction I Under 750 mm Pressure

Fraction	Boiling range (°C)	Weight (g)	Yield (%)	Chlorine content (%)	Products
I	37—40	14.0	4.76	60.60	—
II	40—40.2	48.20	16.4	61.46	CH ₃ SiHCl ₂
III	40.2—41.2	127.0	43.2	65.61	CH ₃ SiHCl ₂ + CH ₃ SiCl ₃
IV	41.2—66	9.85	3.35	62.0	} CH ₃ SiCl ₃ + (CH ₃) ₂ SiCl ₂
V	78	39.25	13.36	62.65	
VI	78.5	15.0	5.10	27.63	—
Residue in still	—	10.85	3.69	20.66	—

A second distillation of Fraction II gave a product boiling at 161–165°. Analysis of it gave: d_{20}^{20} 1.2068, n_D^{20} 1.5330, MR found 53.10, MR calculated 53.13.

Found %: C 46.72; 46.67; H 4.87; Si 14.50; Cl 34.90. Calculated %: C 46.80; H 4.87; Si 13.64; Cl 34.60

Molecular weight of tolylmethyldichlorosilane: found 217,236; calculated 205.

Analysis of the gaseous products by means of the VTI apparatus gave: hydrogen 77.5%, methane 15.3%, unsaturated hydrocarbons and HCl absent.

Preparation of Diphenylmethyldichlorosilane. An autoclave 8 liters in capacity was charged with 1205 g of diphenyl, 1800 g of methyldichlorosilane, and 3 g of boric acid. The reaction was continued for 4 hours at 250–260°, at 80 atmos pressure in the autoclave. The residual pressure in the autoclave cooled to 20° was 29 atmos. 2462 g of substance was discharged from the autoclave; 185.5 g was put in a Würtz flask and distilled to give the fractions: Fraction I, boiling range 38–200°, 84 g; Fraction II, boiling range 200–270°, 41.5 g; residue boiling above 270°, 58 g.

TABLE 9

Distillation of Residue Under 2 mm Pressure

Fraction	Boiling range (°C)	Weight (g)	Yield (%)	Chlorine content (%)
I	118—133	8.44	7.17	25.2
II	133—140	43.6	37.1	—
III	140—222	18.69	15.9	—
Residue in still	—	41.85	35.6	—

Fraction I (228 g) was fractionated through a column of 10 theoretical plates (Table 5).

The residue boiling above 270° (574 g) was distilled under vacuum (Table 6).

Fraction IV was redistilled. The amount taken for the fractionation was 128.4 g (Table 7).

The fraction boiling at 154–157.5° (at 1 mm) had the following composition.

$C_{12}H_9$ $SiCl_2$. Found %: C 57.94; Si 10.55; H 4.85; Cl 27.70. Calculated %: C 58.42; Si 10.72; H 4.49
 CH_3 Cl 26.59

Molecular weight: found 272.2, calculated 267; MR found 73.2, MR calculated 72.74 (after repeated distillations).

Preparation of Naphthylmethylchlorosilane. An autoclave 8 liters in capacity was charged with 1500 g of naphthalene, 1620 g of methylchlorosilane, and 2.7 g of boric acid. The mixture was heated for 8 hours at 300°, the autoclave pressure rose to 80 atmos, the residual pressure in the autoclave cooled to 20° was 38 atmos. The product in the autoclave was removed and fractionated. Fraction I, boiling range 38–150°; Fraction II, boiling range 150–270°; residue, boiling above 270°.

The first fraction (294.2 g) was fractionated through a column of 10 theoretical plates (Table 8).

The residue from the first distillation, boiling above 270°, was fractionated under vacuum; 117.52 g was taken (Table 9).

TABLE 10

Distillation of Fractions II and III Under 4 mm Pressure

Fraction	Boiling range (°C)	Weight (g)	Yield (%)	Chlorine content (%)
I	65—115	1.87	3.0	30.0
II	152—158	41.88	67.2	30.6
III	158—187	3.052	4.85	24.58
IV	187—190	1.71	2.75	38.0
V	190—195	2.03	3.27	39.1
VI	195—200	7.29	11.7	36.7
Residue in still	—	1.15	1.85	—

Note. Fraction II had m. p. 26.2°

Fractions II and III were redistilled under vacuum; 62.29 g was taken (Table 10).

Analysis of Fraction II.

$C_{10}H_7$ $SiCl_2$. Found %: C 55.0; 55.09; Si 11.0; 11.6; H 4.50; 4.45; Cl 30.6. Calculated %: C 54.47; CH_3 Si 11.61; H 4.14; Cl 29.46

Molecular weight (cryoscopically in benzene): 249, ~~253~~; calculated, 241.

The gaseous products contained hydrogen 74.0%, methane 16.7%, and air 5.9%.

Experiments on nitration and sulfonation of tolylmethyldichlorosilane, naphthylmethyldichlorosilane, and diphenylmethyldichlorosilane yielded resinous products, so that the position of silicon relative to the other substituents in the nucleus could not be determined.

SUMMARY

1. Reactions of toluene, diphenyl, and naphthalene with methyldichlorosilane in presence of boric acid yielded tolylmethyldichlorosilane, diphenylmethyldichlorosilane, and naphthylmethyldichlorosilane.
2. The physical constants — boiling points, densities, and refractive indices — of the compounds synthesized for the first time, were determined.

LITERATURE CITED

- [1] A. Barry, U.S. Patent 2546330; Chem. A. 45, 8041 (1951).
- [2] A. Barry, British Patent 446466; Chem. A. 45, 5184 (1951).
- [3] A. Barry, British Patent 649972; Chem. A. 45, 5184 (1951).
- [4] A. Barry, U. S. Patent 2626266; Chem. A. 48, 7636 (1954).
- [5] A. Barry, British Patent 446666; Chem. A. 45, 7336 (1951).
- [6] A. Barry, British Patent 446629; Chem. A. 7336 (1951).
- [7] D. Brewer, U. S. Patent 2600198; Chem. A. 47, 1736 (1953).
- [8] E. A. Chernyshev and A. D. Petrov, Bull. Acad. Sci. USSR, Div. Chem. Sci. 5, 630 (1956).*

Received December 19, 1957

*Original Russian pagination. See C.B. Translation.

OXIDATION OF A MIXTURE OF CYCLOHEXANE AND CYCLOHEXANOL TO ADIPIC ACID

I. V. Berezin, E. T. Denisov, E. N. Suvorova,
Z. S. Smolyan and N. M. Émanuél'

One of the important tasks confronting chemistry at the present time is development of methods for production of monomers for plastics and synthetic fibers. Utilization of various wastes formed in processes of modern organic chemistry is significant in relation to this problem. One such waste product is the head fraction obtained by distillation of phenol hydrogenation products ("anol head"), which consists of a mixture of cyclohexane and cyclohexanol.

It is now well known that oxidation of cyclohexane by atmospheric oxygen under pressure yields valuable products such as cyclohexanone and adipic acid [1]. Liquid-phase oxidation of "anol head" could also be expected to yield these products. A study was therefore carried out of the oxidation kinetics of "anol head", and it was shown that adipic acid can be obtained by oxidation of this material.

"Anol head" comprises about 30% of the total products of phenol hydrogenation, and consists of 80 molar % of cyclohexanone and 20 molar % of cyclohexanol. Water and isopropylcyclohexane are present as impurities.

The oxidation was performed in an autoclave unit described in the literature [2] by the action of an equimolecular mixture of nitrogen and oxygen under 20 atmos pressure, at an air rate of 30 liters/hour, and an oxidation temperature of 130-150°.

In each experiment 250 ml of the raw material was put into the autoclave. Samples of the oxidized mixture were taken during each experiment, and analyzed for hydroperoxide, ketone, alcohol, acids, and esters by methods described in the literature [3, 4]. The amount of carbon dioxide liberated during each experiment was determined by absorption in baryta water.

Experiments on the oxidation of "anol head" at various temperatures showed that its oxidation rate at 130° is close to the oxidation rate of pure cyclohexane, while at higher temperatures it is oxidized even more rapidly than cyclohexane. However, because of the exothermic nature of the reaction and its high rate it is difficult to maintain a constant temperature — the heat balance is disturbed and the temperature of the reaction mixture rises.

Figure 1,a shows kinetic curves for accumulation of the oxidation products and the kinetic curve for conversion of cyclohexanol in the oxidation of "anol head" at 130°. It is seen that the oxidation reaction develops autocatalytically, and the

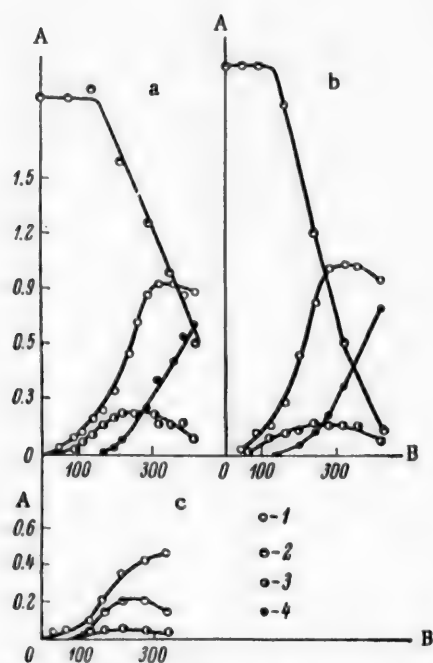


Fig. 1. Kinetic curves for accumulation of reaction products in oxidation of "anol head" (a), a mixture of pure cyclohexane and cyclohexanol (b), and pure cyclohexane (c) at 130°. A) Contents of reaction products (millimoles/ml); B) time (min); 1) ketone; 2) alcohol; 3) hydroperoxide; 4) acids.

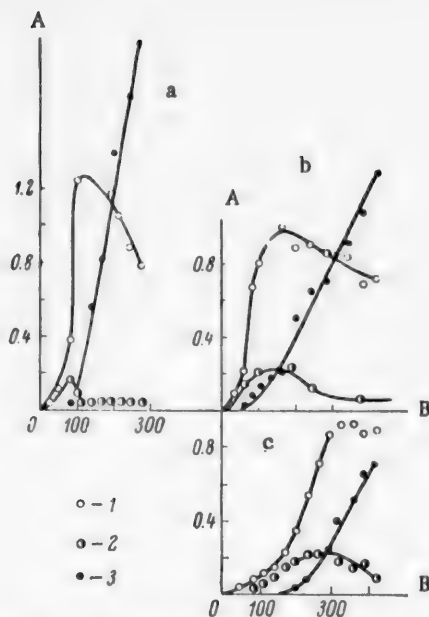


Fig. 2. Oxidation kinetics of "anol head" under different temperature conditions: a) 150°; b) 150° (80 minutes) and 130° (the remaining reaction time); c) 130°. A) Contents of reaction products (millimoles/ml); B) time (minutes); 1) ketone; 2) hydroperoxide; 3) acids.

the oxidation kinetics of the artificial mixture and of "anol head" (the kinetic curves are similar, the ketone and peroxide maxima have very similar values, and adipic acid accumulates at very similar rates).

This result shows that the kinetic relationships in the oxidation of "anol head" are determined by the relative proportions of cyclohexanol and cyclohexane in the original mixture. Other substances present in "anol head" do not influence the oxidation kinetics. The higher maximum ketone and hydroperoxide concentrations found in the oxidation of "anol head" than in the oxidation of pure cyclohexane are due to the presence of a high concentration of cyclohexanol in the original mixture. The influence of the composition of the original mixture on the maximum concentrations of the intermediate products was noted earlier in studies of the catalytic oxidation of cyclohexane [5]; it is probably associated with changes in the composition of the radicals in the oxidized system.

The oxidation rate greatly increases if the oxidation temperature is raised from 130 to 150°. The heat evolution as the result of the developing reaction is so great that the autoclave must be cooled in water to keep the temperature constant. Kinetic curves for the accumulation of oxidation products during the reaction at 150° are shown in Fig. 2,a.

The oxidation kinetics of "anol head" at 130° is represented by the curves in Fig. 2,c. Whereas at 150° the period of autocatalysis is 1 hour for ketone formation and 2 hours for acid formation, at 130° the period of autocatalysis increases to 3.5-4.5 hours.

The autocatalytic period of the reaction can be shortened considerably by the use of a variable temperature regime. Figure 2,b shows kinetic curves for an experiment in which the oxidation was effected at 150° during the first 80 minutes, with subsequent oxidation at 130°. It is seen that in this case the autocatalytic period is the same as in the experiment at 150°, while the subsequent course of the reaction is analogous to its course at 130°. The maximum ketone and hydroperoxide concentrations are the same in both experiments, and so is the constant rate of acid formation (0.22 mole/liter · hour). By oxidation under a variable temperature regime,

kinetic curves for the intermediate products — hydroperoxide and cyclohexanone — pass through maxima; dicarboxylic acids are in practice the final products. On the whole, the situation is similar to the oxidation of pure cyclohexane, apart from the kinetic curve for cyclohexanol. However, there are also some differences, as can be seen by comparison of Fig. 1,a, with Fig. 1,c, which shows the oxidation kinetics of pure cyclohexane under the same conditions. There are the following differences between the respective kinetics. The maximum ketone concentration in the oxidation of "anol head" is 0.9 mole/liter, or double that found in the oxidation of pure cyclohexane, when it is 0.45 mole/liter. The maximum hydroperoxide concentration is also considerably higher in the oxidation of "anol head" than in the oxidation of cyclohexane, and is 0.2 mole/liter as compared with 0.05 mole/liter for pure cyclohexane. These differences are probably associated with differences in composition between "anol head" and pure cyclohexane. Since "anol head" contains small amounts of other impurities in addition to cyclohexanol, it was of interest to oxidize a mixture of pure cyclohexane and cyclohexanol, identical in composition with "anol head", and thus determine the role of the other impurities in the oxidation kinetics of "anol head" and the effect of large amounts of cyclohexanol on the oxidation kinetics. An experiment was therefore carried out on the oxidation of a mixture of 20% cyclohexanol and 80% cyclohexane at 130°, 20 atmos pressure, and an air rate of 30 liters/hour.

The kinetics of accumulation of the oxidation products in this experiment is shown in Fig. 1,b. Comparison of Figs. 1,a and 1,b shows that there is almost no difference between

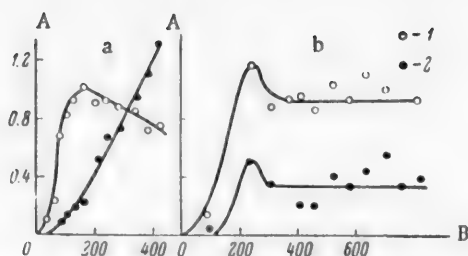


Fig. 3. Kinetic curves for accumulation of ketone and acids in the reaction zone; a) without removal of adipic acid, and b) with continuous removal of adipic acid at oxidation temperature at 130°. A) contents of reaction products (millimoles/liter); B) time (minutes); 1) ketone; 2) acids.

Oxidation of "anol head" yields a fairly complex mixture of products. Thus, oxidation of "anol head" for 7 hours at 130° gave 12.3 molar % of cyclohexanone, 10.5 molar % of cyclohexanol, 7.4 molar % of dicarboxylic acids, 4.9% of esters, 1.2% of hydroperoxide, and 64% of cyclohexane (calculated per mole of the raw material). The presence of ketone and alcohol in almost equal amounts in the oxidized mixture makes isolation of cyclohexanone from the mixture difficult because of the close boiling points of these substances. Of the other oxidation products, adipic acid is the easiest to separate. It is precipitated out of the aqueous layer on cooling. After it had been washed with hot cyclohexane, this acid had equivalent weight 73-75 g (from results of different experiments) and melted at 145°. Recrystallization of this acid from hot nitric acid gives pure adipic acid of m.p. 151° and equivalent weight 73.2 g. Therefore oxidation of "anol head" is most suitable for production of adipic acid.

Available data on the oxidation mechanism of cyclohexane indicate that under the oxidation conditions adipic acid is burned out with formation of carbon dioxide and lower dicarboxylic acids [7]. Determination of the amount of CO₂ liberated in experiments on the oxidation of "anol head" showed that in this case there was also considerable combustion of adipic acid to give lower dicarboxylic acids. It is therefore uneconomical to continue the oxidation until the oxidized mixture has a high acid content. The best procedure is to carry out the oxidation with continuous removal of the acids from the reaction zone. The following method may be used for removal of the acids.

The oxidized mixture is removed from the reactor continuously, or intermittently at definite time intervals. The mixture is homogeneous under the reaction conditions, but when cooled to room temperature it separates into hydrocarbon and aqueous layers. The ketone, alcohol, and hydroperoxide remain predominantly in the hydrocarbon layer and are returned into the reaction zone. Adipic acid passes mainly into the aqueous layer and is partially precipitated from it. In this way the final reaction products — adipic acid and water — are removed from the reaction zone, whereas the intermediate products — ketone, alcohol, and peroxide — are returned to the reaction zone and ensure a high rate of formation of adipic acid.

An experiment on the oxidation of the raw material with continuous removal of adipic acid and water was carried out as follows (the oxidation was performed at 130°).

From the moment when appreciable amounts of acid had been formed, 40 ml lots of the oxidized mixture were taken out at 20-minute intervals; the upper layer (32-36 ml) was separated from the lower layer and from precipitated adipic acid, fresh raw material was added to make the volume up to 40 ml, and the liquid was returned to the reactor. The volume of the oxidation mixture in the reactor was kept constant (220-240 ml). Kinetic curves for accumulation of ketone and acid in an experiment under the usual conditions and in the experiment with continuous removal of the acid are given in Fig. 3. The scattering of the experimental points is caused not by analytical errors, but by variations in the concentrations of the oxidation products before and after addition

It is possible to reach a higher conversion of the original hydrocarbon during the same time of oxidation. Thus, at 130° "anol head" can be 25.6% oxidized in 7 hours, whereas in oxidation for 80 minutes at 150° and the rest of the time at 130° the degree of oxidation is 35% in 5 hours. Oxidation of "anol head" at 130° in presence of a catalyst (0.015% of manganese stearate) developed even more slowly than the reaction without catalyst. For example, the ketone concentration 4 hours after the start of the reaction was 0.2 mole/liter in catalyzed oxidation, and 0.55 mole/liter in the noncatalyzed reaction. Therefore salt catalysts, of the type of Co and Mn salts, are unsuitable as accelerators for oxidation of "anol head". The retarding effect of manganese stearate catalyst is probably due to the fact that the presence of cyclohexanol in high concentration retards the conversion of manganese to a higher valence state and prolongs the stage in which the reaction is retarded by the bivalent form of the catalyst [6].

of fresh raw material. It is clear from the graph that the maximum ketone concentration is the same (1 mole/liter) with continuous removal of acid and in ordinary oxidation. The kinetic curves for acid accumulation in these two experiments differ considerably. The rate of acid accumulation with continuous removal of acids is approximately the same as in the experiments under the usual conditions, and is 0.20 mole/liter · hour. Adipic acid comprises 65 molar % of the total acids.

As was to be expected, continuous removal of adipic acid from the reaction zone lowers its combustion considerably, as is clear from the data on gas liberation. Whereas in the usual oxidation of "anol head" at 130° the average rate of CO₂ liberation is 1.5 molar % per hour, with continuous removal of adipic acid it is 0.5 molar % per hour.

Thus, if the oxidation of "anol head" is effected with continuous removal of adipic acid from the reaction zone, its combustion to lower dicarboxylic acids is diminished, and the reaction can be carried out as a continuous process.

SUMMARY

1. Experiments on the oxidation of "anol head" at 130, 150, and 150-130° were carried out; kinetic curves for accumulation of the reaction products were plotted, and it was shown that adipic acid can be produced by oxidation of this material.

2. It is shown that the characteristics of the oxidation kinetics of this raw material are entirely determined by the concentration of the cyclohexanol contained in it.

3. Oxidation of "anol head" with continuous removal of adipic acid is the most rational method for production of adipic acid from this raw material, as combustion of adipic acid to lower dicarboxylic acids is greatly diminished and the whole process becomes continuous.

LITERATURE CITED

- [1] I. V. Berezin, E. G. Denisov, and N. M. Émanuél' in the book: Questions of Chemical Kinetics, Catalysis, and Reactivity [In Russian] (Izd. An SSSR, 1955) p. 273.
- [2] I. V. Berezin, A. A. Emelin, and A. A. Konstantinov, Azerbaidzhan Petroleum Economy 6, 15 (1954).
- [3] I. V. Berezin, Candidate's Dissertation [in Russian] (MGU, 1953).
- [4] I. V. Berezin, Proc. Acad. Sci. USSR 99, 563 (1954).
- [5] E. T. Denisov and N. M. Émanuél', J. Phys. Chem. 30, 2327 (1956).
- [6] E. T. Denisov and N. M. Émanuél', J. Phys. Chem. 30, 2499 (1956).
- [7] I. V. Berezin, L. S. Vartanyan, B. G. Dzantiev, I. F. Kazanskaya and N. M. Émanuél', J. Phys. Chem. 31, 340 (1957).

Received November 1, 1957

INFLUENCE OF CHEMICAL STRUCTURE OF SULFENAMIDE COMPOUNDS ON VULCANIZATION ACTIVITY

M. S. Fel'dshtein, B. A. Dogadkin, I. I. Éitingon,
G. P. Shcherbachev, and N. P. Strel'nikova

Scientific Research Institute of the Tire Industry

In our earlier papers [1, 2] we described the vulcanization characteristics of butadiene-styrene rubber mixes in presence of sulfenamide accelerators — benzothiazolesulfendiethylamide and benzothiazolesulfencyclohexylamide. These accelerators caused a characteristic retardation of the acceleration kinetics at the initial stage of vulcanization, with the formation of more stable —C—C— linkages as the result of radical polymerization processes

in addition to the formation of —C—S_n—C— linkages. This action of the accelerators results in a considerable improvement of the technical properties of the vulcanizates, including increases of the thermal resistance and fatigue strength, and better homogeneity of laminated rubber products [2, 3].

Considerable interest attached to studies of the action of sulfenamide compounds differing in chemical structure, with the object of determining the relationship between their vulcanization activity and chemical structure. Here vulcanization activity implied not only the influence of these compounds on the kinetics of sulfur addition to rubber, but also their effect on structurization processes.

EXPERIMENTAL

The principal substances studied were representatives of the two classes of sulfenamide compounds — derivatives of mercaptobenzothiazole and of dimethyldithiocarbamic acid. As the table shows, the accelerators studied differed in the composition of the substituents in the amino group.

Each of the sulfenamide derivatives of mercaptobenzothiazole was synthesized by one of the following three methods.

1. Oxidative condensation of mercaptobenzothiazole with a secondary amine, with the use of sodium hypochlorite or iodine as oxidizing agent [4]:

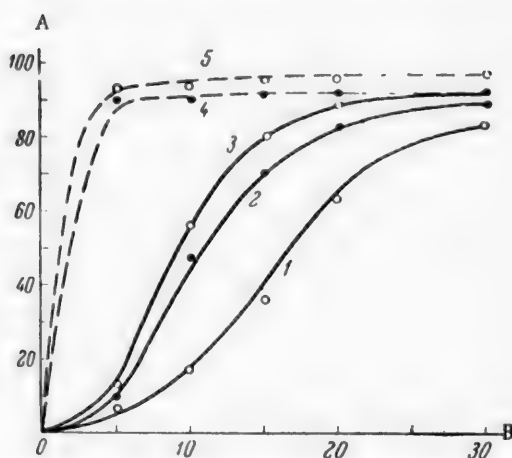
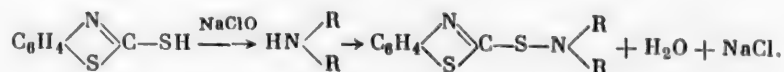
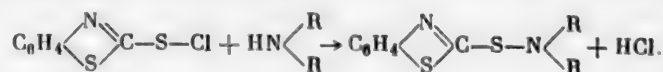
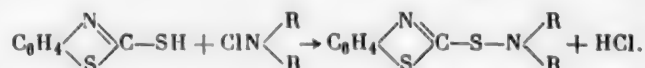


Fig. 1. Influence of sulfenamide compounds on the kinetics of sulfur addition: A) amount of sulfur reacted, $S_{\text{bound}}/S_{\text{total}}$ (%); B) vulcanization time (minutes); compounds and amounts added (wt. parts): 1) benzothiazolesulfenamide 0.7; 2) benzothiazolesulfendimethylamide 0.8; 3) benzothiazolesulfendiethylamide 0.9; 4) dimethyldithiocarbamylsulfendimethylamide 0.6; 5) dimethyldithiocarbamylsulfendiethylamide 0.72.

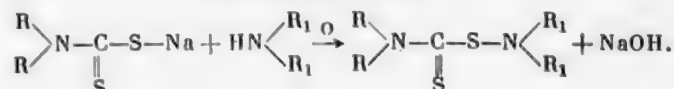
2. Condensation of benzothiazolesulfonyl chloride with the amine, for example:



3. Condensation of mercaptobenzothiazole with the corresponding chloramine:



Sulfenamide derivatives of dialkyldithiocarbamic acid were also prepared by oxidative condensation of the sodium salts with substituted amines in a weakly alkaline medium:



Sulfenamide Compounds

Derivatives of mercaptobenzothiazole	Derivatives of dimethyldithiocarbamic acid
Benzothiazolesulfenamide	Dimethyldithiocarbamylsulfenamide
$\text{C}_6\text{H}_4 \begin{array}{c} \diagup \text{N} \\ \diagdown \text{S} \end{array} \text{C}=\text{S}-\text{NH}_2$	$\begin{array}{c} \text{CH}_3 \\ \diagup \\ \text{N}-\text{C}-\text{S}-\text{NH}_2 \\ \diagdown \\ \text{CH}_3 \end{array} \begin{array}{c} \text{S} \\ \end{array}$
Benzothiazolesulfendimethylamide	Dimethylthiocarbamylsulfendimethylamide
$\text{C}_6\text{H}_4 \begin{array}{c} \diagup \text{N} \\ \diagdown \text{S} \end{array} \text{C}=\text{S}-\text{N} \begin{array}{c} \diagup \text{CH}_3 \\ \diagdown \text{CH}_3 \end{array}$	$\begin{array}{c} \text{CH}_3 \\ \diagup \\ \text{N}-\text{C}-\text{S}-\text{N} \begin{array}{c} \diagup \text{CH}_3 \\ \diagdown \text{CH}_3 \end{array} \\ \diagdown \\ \text{CH}_3 \end{array} \begin{array}{c} \text{S} \\ \end{array}$
Benzothiazolesulfendiethylamide (Sulfenamide BT)	Dimethylthiocarbamylsulfendiethylamide
$\text{C}_6\text{H}_4 \begin{array}{c} \diagup \text{N} \\ \diagdown \text{S} \end{array} \text{C}=\text{S}-\text{N} \begin{array}{c} \diagup \text{C}_2\text{H}_5 \\ \diagdown \text{C}_2\text{H}_5 \end{array}$	$\begin{array}{c} \text{CH}_3 \\ \diagup \\ \text{N}-\text{C}-\text{S}-\text{N} \begin{array}{c} \diagup \text{C}_2\text{H}_5 \\ \diagdown \text{C}_2\text{H}_5 \end{array} \\ \diagdown \\ \text{CH}_3 \end{array} \begin{array}{c} \text{S} \\ \end{array}$
Benzothiazolesulfencyclohexylamide	—
$\text{C}_6\text{H}_4 \begin{array}{c} \diagup \text{N} \\ \diagdown \text{S} \end{array} \text{C}=\text{S}-\text{N}-\text{CH} \begin{array}{c} \text{CH}_2-\text{CH}_2 \\ \quad \\ \text{CH}_2-\text{CH}_2 \end{array} \text{CH}_2$ H	—
Benzothiazolesulfenpiperide	—
$\text{C}_6\text{H}_4 \begin{array}{c} \diagup \text{N} \\ \diagdown \text{S} \end{array} \text{C}=\text{S}-\text{N} \begin{array}{c} \text{CH}_2-\text{CH}_2 \\ \quad \\ \text{CH}_2-\text{CH}_2 \end{array} \text{CH}_2$	—
Benzothiazolesulfendiphenylamide	—
$\text{C}_6\text{H}_4 \begin{array}{c} \diagup \text{N} \\ \diagdown \text{S} \end{array} \text{C}=\text{S}-\text{N}(\text{C}_6\text{H}_5)_2$	—
Benzothiazolesulfenphenylamide	—
$\text{C}_6\text{H}_4 \begin{array}{c} \diagup \text{N} \\ \diagdown \text{S} \end{array} \text{C}=\text{S}-\text{N}-\text{C}_6\text{H}_5$ H	—
Benzothiazolesulfenmorpholide	—
$\text{C}_6\text{H}_4 \begin{array}{c} \diagup \text{N} \\ \diagdown \text{S} \end{array} \text{C}=\text{S}-\text{N} \begin{array}{c} \text{CH}_2-\text{CH}_2 \\ \quad \\ \text{CH}_2-\text{CH}_2 \end{array} \text{O}$	—

The effectiveness of sulfenamide compounds as vulcanization accelerators was tested on mixes of butadiene-styrene rubber (SKS-30A) thermally plasticized to Karrer plasticity of 0.5. Butadiene-styrene rubber was chosen for the investigation because sulfenamide compounds are particularly effective vulcanization accelerators for mixes of rubbers of this type. The amounts of accelerators used were the molar equivalents of the normally-required

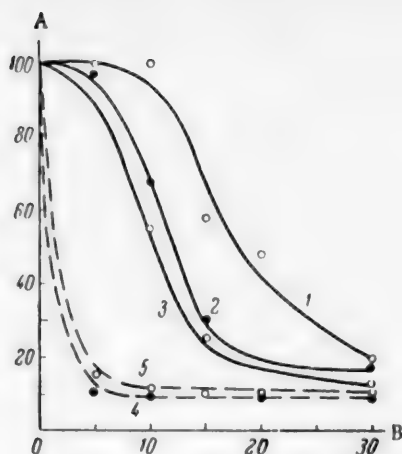


Fig. 2. Effect of vulcanization time on the solubility of mixes in chloroform: A) solubility in chloroform (%); B) vulcanization time (minutes); curve numbers as in Fig. 1.

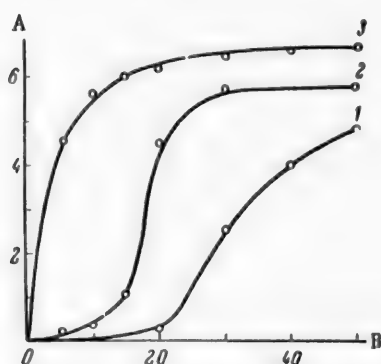


Fig. 3. Effect of sulfenamide compounds on the kinetics of variation of the equilibrium modulus: A) equilibrium modulus (kg/cm^2); B) vulcanization time (minutes); compounds and amounts added (wt. parts): 1) benzothiazolesulfenamide 0.7; 2) benzothiazolesulfendiethylamide 0.9; 3) dimethylthiocarbamylsulfendimethylamide 0.6.

concentrations of benzothiazolesulfendiethylamide (Sulfenamide (BT), the properties of which were studied in detail earlier [2, 3]. The mixes contained 1.5 weight parts of sulfur, the accelerator, 5.0 weight parts of zinc oxide, and 2.0 weight parts of stearic acid per 100 weight parts of rubber. In addition to these components, loaded mixes contained channel black and Rubberax. The loaded mixes contained 2.0 weight parts of sulfur.

The influence of sulfenamide compounds on the vulcanization kinetics of nonloaded mixes is represented by data on sulfur addition in Fig. 1, by variations of solubility in chloroform in Fig. 2, and variations of the equilibrium modulus in Fig. 3. It follows from the data in Fig. 1 and 2 that the curves for the vulcanization kinetics of mixes containing accelerators of the benzothiazolesulfenamide type reveal the existence of an initial period of retarded vulcanization. Thus, after 5 minutes of vulcanization the amount of reacted sulfur in such mixes does not exceed 10% of the amount added, and the mixes are completely soluble in chloroform. The retarded period of vulcanization is illustrated especially clearly by the data on variations of equilibrium modulus (Fig. 3). Whereas a mix, containing benzothiazolesulfendiethylamide, only attains its final value of the equilibrium modulus after 10 minutes of vulcanization, and in mixes with benzothiazolesulfenamide the modulus is zero, even after 20 minutes of heating, in a mix with dimethyldithiocarbamylsulfendimethylamide the equilibrium modulus reaches $4.7 \text{ kg}/\text{cm}^2$ after only 5 minutes of vulcanization.

Dialkyldithiocarbamylsulfenamides have a different influence on the vulcanization kinetics. Taken in molecular equivalents of the amounts of benzothiazolesulfenamides used, they cause a very high rate of the reaction of sulfur addition to rubber, so that the vulcanization process is almost complete within the first 5-10 minutes of heating at 143° (Figs. 1-3). Thus, the most important distinction between the effects of thiocarbamylsulfenamides and benzothiazolesulfenamides is that the former lead to the formation of a spatial vulcanization structure at the earliest stage, whereas with benzothiazolesulfenamides the vulcanization process is characterized by a definite induction period.

During recent years it has been shown [5-7] that sulfur in the molecules of sulfur-containing accelerators is exchanged with elemental sulfur at vulcanization temperatures. Some workers [5] consider that exchange is a means of activation of sulfur in the vulcanization process.

It was of interest to determine the relationship between vulcanization activity of accelerators and the rate of isotope exchange with sulfur. The substances taken for the investigation were benzothiazolesulfendimethylamide and dimethylthiocarbamylsulfendimethylamide, which are representatives of two classes of sulfenamide compounds which differ in their influence of vulcanization kinetics. The exchange reaction was effected in benzene solution (in sealed tubes) at 110 and 130° . The mixtures were vulcanized in a press and in solution at the temperatures used for the exchange. It was not possible to carry out experiments at the usual vulcanization temperature (143°) because of the rapid decomposition of sulfenamides, especially benzothiazolesulfendimethylamide. The

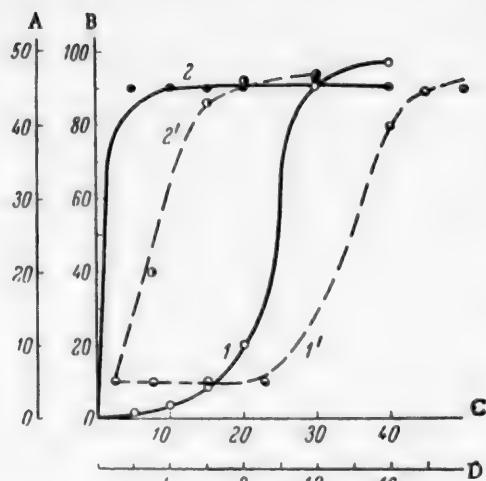


Fig. 4. Kinetics of isotope exchange between accelerators and elemental sulfur, and of rubber-sulfur interaction, at 130°: A) I/I_0 (%); B) amount of sulfur reacted, $S_{\text{bound}}/S_{\text{total}}$ (%); C) vulcanization time (minutes); D) heating time (hours); 1,1') benzothiazolesulfendimethylamide; 2,2') dimethylthiocarbamylsulfendimethylamide; 1,2) sulfur addition; 1',2') isotope exchange.

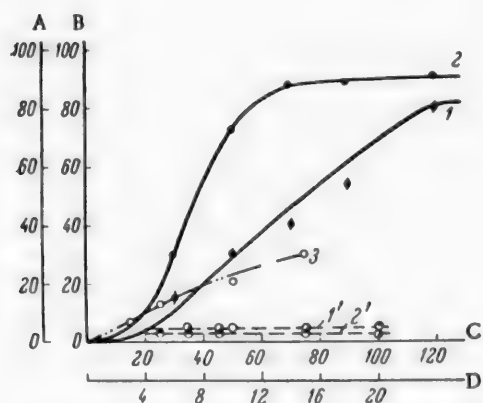


Fig. 5. Kinetics of isotope exchange between accelerators and elemental sulfur, and of rubber-sulfur interaction, at 110°: coordinates as in Fig. 4; 1,2) sulfur addition during vulcanization in press; 3) the same, in solution; 1',2') isotope exchange; 1,1') benzothiazolesulfendimethylamide; 2,2',3) dimethylthiocarbamylsulfenyldimethylamide.

results* obtained on the kinetics of exchange between accelerators and sulfur and on vulcanization kinetics (amounts of sulfur added to the rubber) are given in Figs. 4 and 5. It follows from Fig. 4 that the kinetic curves for vulcanization at 130° are similar in form to the kinetic curves for the exchange reaction. At the lower temperature (110°) vulcanization in the press is also fairly rapid (Fig. 5). Vulcanization in solution is considerably slower. However, even in this case, as the data on the course of changes of solubility in chloroform show (Fig. 6), a considerable degree of structure formation is attained in presence of dimethylthiocarbamylsulfendimethylamide accelerator. It follows that at 110° vulcanization takes place, whereas no isotope exchange is observed between the accelerators investigated and elemental sulfur.

With regard to the influence of alkyl substituents in the amino group on the vulcanization activity of benzothiazolesulfenamides, it must be noted that the longest induction period in vulcanization is observed in presence of unsubstituted benzothiazolesulfenamide (Fig. 1). Other compounds, containing methyl or ethyl radicals in the amino group, show a tendency to shorten the induction period of vulcanization with increase in the molecular weight of such radicals. It must be remembered that the length of the induction period naturally depends on the vulcanization temperature and the amount of accelerator added to the mix. However, in the case of benzothiazolesulfenamides an induction period is found over the entire range of accelerator concentrations used in practice. This is shown by the curves in Fig. 7, which represent the kinetics of sulfur addition at vulcanization temperature 143° with different amounts of benzothiazolesulfendiethylamide and their molar equivalents of dibenzothiazole disulfide and diphenylguanidine. It is clear from Fig. 7 that, in contrast to mixes containing dibenzothiazole disulfide and diphenylguanidine, the vulcanization kinetics of mixes containing various amounts of benzothiazolesulfendiethylamide can be represented by S-shaped curves with distinct initial retarded vulcanization periods.

The experimental data presented below, represent the vulcanization activities of certain cyclic and heterocyclic derivatives of benzothiazolesulfenamide. The vulcanization activities (based on data on solubilities in chloroform) of benzothiazolesulfenpiperidide, benzothiazolesulfencyclohexylamide, and the diethylamide derivative are compared in Fig. 8, a. Whereas in presence of the latter two accelerators the mixes remain almost completely soluble in chloroform after 5 minutes of vulcanization, in the case of benzothiazolesulfenpiperidide the solubility falls to 25% during the same vulcanization time. The kinetic curve for vulcanization (based on data on sulfur

* These results were obtained with the assistance of D. M. Pevzner.

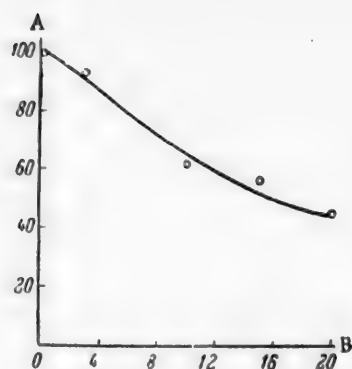


Fig. 6. Effect of dimethylthiocarbamylsulfendimethylamide on structure formation during vulcanization in solution at 110°: A) solubility of film in chloroform (%); B) duration of heating of the solution (hours).

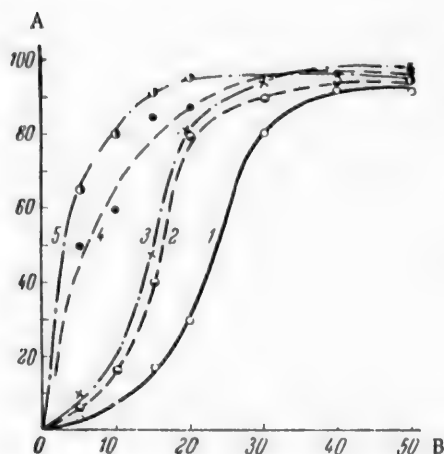


Fig. 7. Effects of the nature and content of the accelerator on the kinetics of rubber addition: A) amount of sulfur reacted, $S_{\text{bound}}/S_{\text{total}}$ (%); B) vulcanization time (minutes); accelerators and amounts added (weight parts): 1) benzothiazolesulfendiethylamide 0.8; 2) the same, 1.0; 3) the same, 1.2; 4) dibenzothiazole disulfide 0.6 and diphenylguanidine, 0.6; 5) the same, 0.6 and 0.75.

The presence of morpholine groups in sulfenamide compounds also has a retarding influence on vulcanization kinetics. In this class of compounds, the product of oxidative condensation of mercaptobenzothiazole and morpholine — benzothiazolesulfenmorpholide — was synthesized and studied. Fig. 11 shows data on the kinetics of sulfur addition in the vulcanization of nonloaded mixes containing benzothiazolesulfenmorpholide (Curve 2) and benzothiazolesulfendiethylamide (Curve 1). The induction period of vulcanization is somewhat longer for the mix

addition) of a mix containing benzothiazolesulfencyclohexylamide shows a shorter induction period of vulcanization (Fig. 8, b) than the curve for a mix containing its molar equivalent of benzothiazolesulfendiethylamide. If the accelerator molecule contains the piperidine group, there is no induction period. The vulcanization kinetics of butadiene-styrene rubber in presence of benzothiazole-sulfenpiperidide (Fig. 8, b) is similar in character to the vulcanization kinetics of mixes containing thiocarbamylsulfenamide accelerators.

Introduction of two phenyl radicals into the amino group of a sulfenamide compound results in almost total loss of vulcanization activity. Thus, a nonloaded mix, containing benzothiazolesulfendiphenylamide, had relative elongation over 1700% and residual elongation of 110% after 100 minutes of heating at 143°. The bound-sulfur content was within the range characteristic of mixes without vulcanization accelerators. The absence of any appreciable structuring effect is clearly seen in presence of this compound in loaded mixes containing channel black (Fig. 9). Replacement of one phenyl radical in the benzothiazolesulfendiphenylamide molecule by a hydrogen atom produces a compound — benzothiazolesulfenphenylamide — which is an effective vulcanization accelerator. It is clear from the data in Fig. 9, that the structuring action (as indicated by the modulus) of benzothiazolesulfenphenylamide approaches that of benzothiazolesulfendiethylamide (Sulfenamide BT).

In connection with this difference in the effectiveness of sulfenamide derivatives of mercaptobenzothiazole in which amide hydrogen is replaced by one or two phenyl groups respectively, it was of undoubted interest to investigate the activities of analogous compounds in which the corresponding hydrogen atoms are replaced by hydrogenated phenyl nuclei, such as cyclohexyl and dicyclohexyl. It is clear from Fig. 10 that benzothiazolesulfendicyclohexylamide is inferior to benzothiazolesulfencyclohexylamide as a vulcanization accelerator.

Thus, it follows from these data that compounds formed by the introduction of only one phenyl or cyclohexyl radical into the amino group of benzothiazolesulfenamide are more active accelerators than compounds in which the amino hydrogen is replaced by two phenyl or cyclohexyl groups.

It should be noted in this connection that the compounds formed by replacement of hydrogen by hydrogenated radicals have higher vulcanization activities than the phenyl derivatives. This is seen especially clearly in a comparison of the vulcanizing effects of benzothiazolesulfendicyclohexylamide and of benzothiazolesulfendiphenylamide, as the latter is almost ineffective as a vulcanization accelerator.

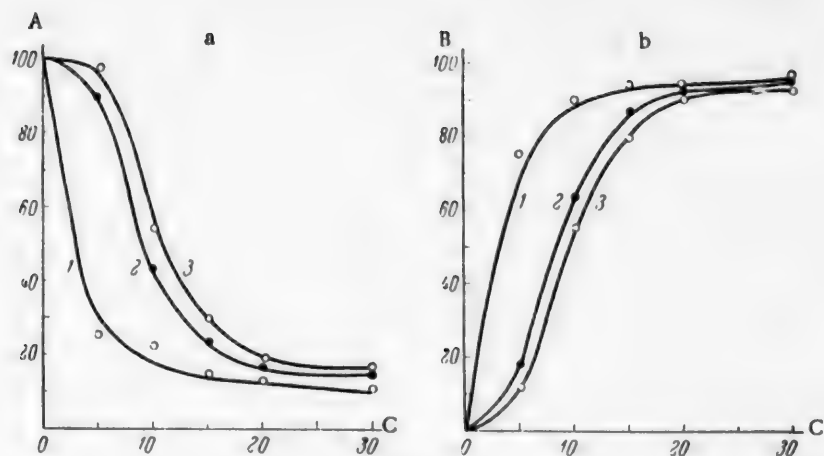


Fig. 8. Vulcanization kinetics of mixes containing benzothiazolesulfenpiperidine (1), benzothiazolesulfen-cyclohexylamide (2), and benzothiazolesulfendiethylamide (3). A) Solubility in chloroform (%); B) amount of sulfur reacted, $S_{\text{bound}}/S_{\text{total}}$ (%); C) vulcanization time (minutes).

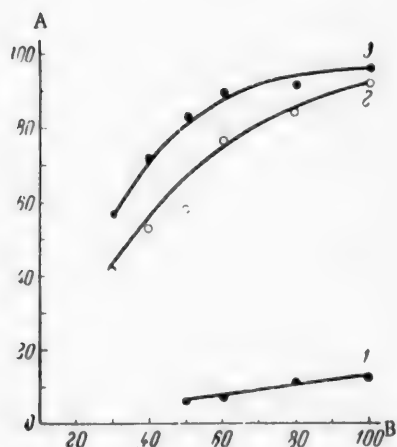


Fig. 9

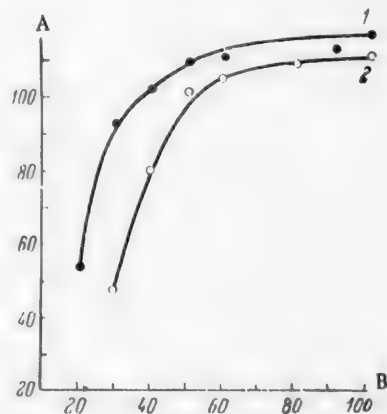


Fig. 10

Fig. 9. Influence of phenyl radicals on the vulcanization activity of benzothiazolesulfenamides (in mixes with channel black): A) equilibrium modulus at 300% elongation (kg/cm^2); B) vulcanization time (minutes); compounds and amounts added (wt. parts): 1) benzothiazolesulfendiphenylamide, 1.4; 2) benzothiazolesulfenphenylamide 1.1; 3) benzothiazolesulfendiethylamide 1.0.

Fig. 10. Vulcanization activities of benzothiazolesulfencyclohexylamide (1) and benzothiazolesulfendicyclohexylamide (2) in mixes with channel black; coordinates as in Fig. 9.

with benzothiazolesulfenmorpholidethan for the mix with benzothiazolesulfendiethylamide. However, the time needed to reach the vulcanization optimum (as shown by the physical data) is almost the same for the two mixes. The vulcanizates made with the use of benzothiazolesulfenmorpholide are equivalent in physical and mechanical properties to vulcanizates with benzothiazolesulfendiethylamide.

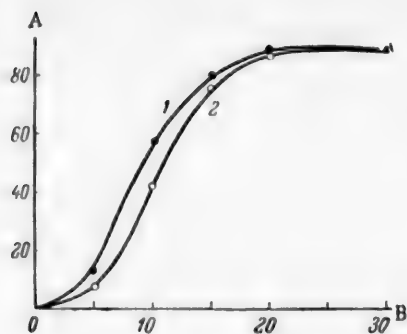


Fig. 11

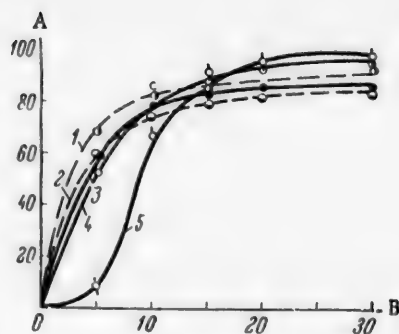


Fig. 12

Fig. 11. Kinetics of sulfur addition in presence of benzothiazolesulfendiethylamide (1) and benzothiazolesulfenmorpholide (2): A) amount of sulfur reacted $S_{\text{bound}}/S_{\text{total}}$ (%), B) vulcanization time (minutes).

Fig. 12. Vulcanization kinetics of mixes of the inner-tube type: coordinates as in Fig. 11; compounds and amounts added: 1) dimethylthiocarbamylsulfendiethylamide 0.8; 2) tetramethylthiuram disulfide 0.35 and dibenzothiazole disulfide 0.30; 3) dimethylthiocarbamylsulfendimethylamide 0.40; 4) dibenzothiazole disulfide 1.0 and diphenylguanidine 1.0; 5) benzothiazolesulfendiethylamide 1.2.

In conclusion, it should be noted that the vulcanization accelerators described are suitable from the technical aspect. Sulfenamide derivatives of mercaptobenzothiazole which slow down vulcanization at the start of the process, prevent premature vulcanization almost entirely and ensure that the mixes remain longer in the viscofluid state, which is important in the production of monolithic multilayer products [3]. Because of this, some of the mercaptobenzothiazole derivatives — benzothiazolesulfendiethylamide, benzothiazolesulfencyclohexylamide, and recently benzothiazolesulfenmorpholide — have been extensively used in the production of automobile tire treads.

By the nature of the vulcanization kinetics (of butadiene-styrene rubber) in presence of sulfenamide derivatives of dithiocarbamic acid, these compounds may be useful in inner-tube stocks (Fig. 12). It is known that a short vulcanization time is used in the production of inner tubes. Because of this, the vulcanization system used in such stocks should ensure a high rate of vulcanization. Examples (comparison standards) are provided by the accelerator groups used in industry: dibenzothiazole disulfide — tetramethylthiuram disulfide, and dibenzothiazole disulfide — diphenylguanidine. The use of benzothiazolesulfendiethylamide in mixes of this type involves certain difficulties, because retarded vulcanization occurs in presence of this accelerator (Fig. 12). On the other hand, mixes containing thiocarbamylsulfenamide accelerators are close in their vulcanization kinetics to the comparison mixes, and therefore conform to the vulcanization requirements of inner-tube stocks.

LITERATURE CITED

- [1] B. Dogadkin, M. Fel'dshtein, A. Dobromyslova, V. Shkurina, and M. Kaplunov, Proc. Acad. Sci. USSR 92, No. 1, 61 (1953).
- [2] B. Dogadkin, M. Fel'dshtein, and D. Pevzner, J. Appl. Chem, 28, No. 5, 533 (1955).*
- [3] B. Dogadkin, M. Fel'dshtein, and D. Pevzner, Proc. Conference on Bonding Strength Between Elements of Multilayer Articles [In Russian] (Goskhimizdat, 1956).
- [4] E. Carr, O. Smith, and A. Alliger, J. Org. Chem, 14, 6, 921 (1949).
- [5] G. Blokh et al., Light Industry 7 and 10 (1952); 1 (1954); J. Chem. Ind, 2 (1956).

*Original Russian pagination. See C. B. Translation.

- [6] E. Gur'yanova et al. J. Phys. Chem. 28, No. 1, 60 and 67 (1954); 28, No. 12, 2116 (1954).
[7] J. Auerbach, Ind. Eng. Chem. 45, 7, 1526 (1953).

Received December 11, 1957

COMPOSITION OF THE PRODUCTS OF CYCLOHEXANOL
DEHYDROGENATION OVER A ZINC CATALYST AND CONVERSION
OF THE RESULTANT STILL RESIDUE INTO CYCLOHEXANONE

L. Kh. Freidlin, V. Z. Sharf, and Z. S. Smolyan

Catalytic dehydrogenation of cyclohexanol to cyclohexanone has become of great industrial importance in relation to the development of caprolactam production. The available literature data on dehydrogenation of cyclohexanol refer mainly to the influence of the nature of the catalyst and process conditions on the yield of cyclohexanone. The composition of the reaction products has not been studied in detail.

In the Japanese patent [1] a Cu-Al-Ni (58:48:2) catalyst is recommended for dehydrogenation of cyclohexanol. The cyclohexanone yield is 85%. An American patent [2] recommends a catalyst made by reduction of a mixture of copper and zinc oxides (50:50) at 400-450°. The cyclohexanone yield was 65% at 395°.

The production of cyclohexanone by dehydration of cyclohexanol is complicated by a number of parallel and consecutive reactions. The chief of these are: dehydrogenation of the cyclohexanol naphthene nucleus, redistribution of hydrogen in cyclohexanone, dehydration of cyclohexanol, and condensation of cyclohexanone.

Terent'ev and Guseva [3] found that cyclohexanone undergoes a conversion similar to irreversible catalysis in presence of platinized carbon even at 200°, with formation of phenol (28%) and cyclohexanol (35%). The latter is dehydrated to cyclohexene, which is further isomerized to benzene and cyclohexane.

Cyclohexanol and cyclohexanone yields phenol in presence of a complex catalyst consisting of Ni, Cu, Cr₂O₃, and alkali sulfates [4] and Raney-type catalysts [5]. Raney catalysts also yield a neutral oil which is presumed to contain cyclohexyl ether and cyclohexylphenyl.

Nazarov and his associates [6] showed that cyclohexanone is converted into phenol (75%) and cyclohexane over aluminum oxide under dynamic conditions at 320-450° and at atmospheric pressure. In a search for the source of formation of the condensation products formed in dehydrogenation of cyclohexanol, Masina [7] found that when cyclohexanol and cyclohexanone are passed over nickel or cobalt catalysts at 380-450° the greater amount of these products is formed from cyclohexanone. Formation of condensation products has also been observed in presence of catalysts which do not have dehydrogenating properties. For example, Petrov found that on prolonged contact (24 hours) with aluminum oxide under 30 atmos pressure at 320° cyclohexanone is converted into cyclohexylidenecyclohexanone-2 and into condensation products of three and four molecules of cyclohexanone [8]. Moreover, formation of cyclohexylidenecyclohexanone-2 was also observed [9] in absence of catalyst, when cyclohexanone was boiled under reflux (10% formed in 115 hours).

In this investigation we studied the composition of the products formed in the industrial process of cyclohexanol dehydrogenation over zinc catalyst. The principal reaction product is cyclohexanone, the yield of which is 80-85% of the theoretical. About 15% of the cyclohexanol remains unchanged. The catalyzate contains 0.3-0.5 % cyclohexene and 0.1-0.15% phenol.

After distillation of cyclohexene, cyclohexanone, and cyclohexanol, a higher-boiling residue remains in the still. Investigation of its composition showed that over 50% of it consists of cyclohexylidenecyclohexanone-2. It was of practical interest to determine whether it is possible to convert the main component of the still residue into cyclohexanone. We therefore developed a continuous method for hydrolysis of cyclohexylidenecyclohexanone-2

whereby about 40% of the still residue is converted into cyclohexanone. About 10% of cyclohexanol is formed at the same time. In addition, cyclohexyl ether in 2-3% yield was isolated from the still residue.

EXPERIMENTAL

Composition of Catalyzate. The catalyst consisted of iron turnings or sheet iron, coated with a thin layer of metallic zinc. Cyclohexanol was dehydrogenated at 380-420° at space velocity 1 hour⁻¹. The reaction products were separated by rectification; first water and cyclohexene were driven off at atmospheric pressure in the form of an azeotrope of b.p. 70-71°. The amount of cyclohexene in the catalyzate is usually 0.3-0.5%, and of water 0.1-0.2%. The product was then rectified by means of a column with an efficiency of 35 theoretical plates (TP). Cyclohexanone was usually isolated at 100 mm and 91°. It was found to contain 98-98.5% of cyclohexanone, by the oxime method. The yield was 80-85% on the cyclohexanol passed. At 106° and the same pressure 10-15% of unchanged cyclohexanol was distilled off. After distillation of the cyclohexanol, the still contained a high-boiling residue, corresponding to 1-1.5% of the cyclohexanol taken.

Composition of the Still Residue. The residue was distilled from a Claisen flask at 20 mm. Two broad fractions were collected: I, boiling up to 140°, and II, boiling between 140 and 160°. The residue was not investigated.

Fraction I was distilled through a column of 15 TP efficiency at 2-3 mm; at 70-74° phenol was collected in 0.1-0.15% yield on the catalyzate.

Fraction II comprised over 60% of the still residue. It was distilled through a column of 35 TP at 20 mm. At 129-130° a substance (10% by weight) was isolated, with the following properties: n_D^{20} 1.4921, d_4^{20} 0.962; it was shown by the oxime method to contain 83.7% of a ketone, calculated as cyclohexylidenecyclohexanone-2. It is soluble in organic solvents and insoluble in water; its 2,4-dinitrophenylhydrazone melted at 156-157°. This carbonyl compound was not identified. Further rectification of Fraction II gave cyclohexylidenecyclohexanone-2 in approximately 80% yield, corresponding to a 50% content of this ketone in the still residue. A second distillation yielded a substance with the following properties: b.p. 153-154° at 20 mm, n_D^{20} 1.5051, d_4^{20} 1.005. The oxime method showed a 99-100% ketone content, calculated as cyclohexylidenecyclohexanone-2. The following derivatives were prepared: 2,4-dinitrophenyl hydrazone of m.p. 122° and oxime of m.p. 153-154°.

Analysis of oxime: Found %: C 74.70; H 9.82; N 6.65. $C_{12}H_{19}ON$. Calculated %: C 74.60; H 9.83; N 7.25

A mixed sample with pure cyclohexylidenecyclohexanone-2 oxime gave no melting point depression.

Fraction II was hydrogenated at 180° over $Ni-Cr_2O_3$ catalyst. A substance with the following properties was isolated from the catalyzate after repeated rectification: b.p. 149-150° at 20 mm, m.p. 30°, n_D^{20} 1.4992, d_4^{20} 0.9838, MR: found 54.02; calculated 54.74.

Analysis of the substance: Found %: C 78.69; H 11.49. $C_{12}H_{22}O$. Calculated %: C 79.10; H 12.09

These properties were close to the properties of cyclohexylcyclohexanol-2, prepared earlier by hydrogenation of cyclohexylidenecyclohexanone: m.p. 30-31°, b.p. 265-270° at 760 mm [10].

Preparation of Cyclohexanone by Hydrolytic Decomposition of Cyclohexylidenecyclohexanone-2 Present in the Still Residue from Cyclohexanone Production

We showed earlier that cyclohexylidenecyclohexanone-2 can be converted hydrolytically into cyclohexanone in 80-90% yield [11].

A recent patent [12] also describes a process for production of cyclohexanone by hydrolytic decomposition of the 200-260° fraction of the still residues, containing cyclohexylidenecyclohexanone-2.

It was of interest to determine whether this method can be used for obtaining cyclohexanone from still residues in cyclohexanone production.

The effects of process conditions on cyclohexanone yield were first studied (see table). The experiments were performed in an autoclave.

The cyclohexanone formed was distilled off in the form of an azeotropic mixture with water, of b.p. 96-97° and determined by the oxime method. After cyclohexanone-water azeotrope, the cyclohexanol-water azeotrope of b.p. 97-98° distills over. The amount of cyclohexanol was 20% of the amount of cyclohexanone isolated.

Results of Autoclave Experiments

Temperature (°C)	Volume ratio of NaOH solution and still residue	Contact time (minutes)	Cyclohexanone yield (%)
230	2.5	60	27.8
250	2.5	30	40.8
260	1.0	30	36.5
270	2.5	30	39.6
300	2.5	30	40.5

It follows from the table that under the optimum conditions: temperature 250-270°, contact time 30-40 minutes, and 2.5:1 ratio of caustic soda (1% aqueous solution) to still residue, the cyclohexanone yield was 40% by weight.

It was necessary to find whether it might be advisable first to isolate the fraction containing cyclohexylidenecyclohexanone-2 from the still residue, and then to hydrolyze it. The original still residue (60.6 g) was distilled at 15 mm to give the following fractions:

Fraction	B.p. (°C)	Amount (g)
I	65-100	1.8
II	100-141	35.8
III	141-144	12.7
Residue	—	9.4
Losses	—	0.9

Fractions II and III were separately hydrolyzed in the autoclave. The cyclohexanone yields were 48 and 60% respectively. Thus, a total of 25 g of cyclohexanone was obtained, which corresponds to 41.5% yield on the still residue taken. It is seen that hydrolysis of previously isolated fractions which could contain cyclohexylidenecyclohexanone-2 gives about the same yield of cyclohexanone as the still residue itself.

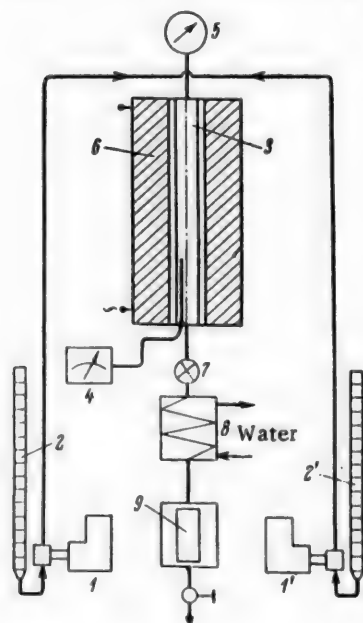


Diagram of continuous unit.

Prolonged experiments were then carried out in a continuous unit (see diagram). The still residue and 1% sodium hydroxide solution were drawn by means of the hydraulic pumps 1 and 1' from two burets 2 and 2', and fed under pressure through steel capillaries into the upper end of the reactor 3, 20 mm in diameter and 400 mm long. The temperature was measured by means of the thermocouple 4 inserted in the reactor wall. The reactor was fitted with a manometer 5 and heater 6 with automatic temperature regulation. The reaction mixture was discharged continuously from the reactor through a fine-control valve 7 and condenser 8, and collected in the receiver 9. In this way the reaction components were fed in and the reaction products withdrawn continuously. The experiments were conducted at 260-280°, with a contact time of 30 minutes and 2:1 ratio of aqueous sodium hydroxide (1%) to still residue. Samples were taken during operation of the unit, and their cyclohexanone contents were determined. The cyclohexanone yield in all the experiments was 39-41 wt. % on the amount of still residue passed.

As was shown earlier, about 50% of Fraction II and III did not react during the hydrolysis and was not distilled with water. After

repeated distillation of the unconverted portion of the still residue, we isolated, in addition to cyclohexylidene-cyclohexanone-2, dicyclohexyl ether in about 3% yield calculated on the original still residue. After distillation over sodium the ether had the following constants: b.p. 114-116° (15 mm), n_D^{20} 1.4744. Literature data: b.p. 115.8° (15 mm), n_D^{20} 1.4741 [13].

Found %: C 79.15; H 12.10. $C_{12}H_{22}O$. Calculated %: C 79.11; H 12.08

SUMMARY

1. The composition of the products formed in industrial dehydrogenation of cyclohexanol over zinc catalyst was studied; in addition to cyclohexanone, the yield of which is 80-85%, and unconverted cyclohexanol (10-15%), the reaction products contain cyclohexene (0.3-0.5%), water (0.1-0.2%), phenol (0.1-0.15%), cyclohexyl ether (0.02-0.03%), and cyclohexylidenecyclohexanone-2 (0.5-1%).

The relatively small amounts of by-products indicate that the zinc catalyst is highly selective.

2. The still residue, containing about 50% of cyclohexylidenecyclohexanone-2, can be converted by hydrolysis, without previous isolation of the latter, into cyclohexanone in 40% yield. A similar result was obtained in a continuous unit.

LITERATURE CITED

- [1] Japanese Patent 6613 (153); Chem. A. 49, 9689f (1955).
- [2] U. S. Patent 2552300; Chem. A. 46, 134d (1952).
- [3] A. P. Terent'ev and A. N. Guseva, Proc. Acad. Sci. USSR 52, 135 (1946).
- [4] U. S. Patent 2588359; Chem. A. 46, 5226g (1952).
- [5] Nobuto Ohta and Masaki Sato, Repts. Govt. Chem. Ind. Research Inst. Tokyo, 48, 177 (1953).
- [6] I. N. Nazarov, I. L. Kotlyarevskii, and N. V. Kuznetsov, J. Gen. Chem, 22, 1147 (1952).*
- [7] M. P. Masina, J. Gen. Chem. 8, 1264 (1938).
- [8] A. D. Petrov, J. Russ. Phys.-Chem. Soc. 60, 1435 (1928).
- [9] C. D. Hurd, J. Am. Chem. Soc. 61, 3359 (1939).
- [10] O. Wallach, Ber., 40, 70 (1907).
- [11] L. Kh. Freidlin and V. Z. Sharf, Bull. Acad. Sci. USSR 4, 512 (1957).*
- [12] Federal German Patent 927668; Referat. Zhur. Khim. 15, 48274 (1956).
- [13] W. Schrauth and W. Wege, Ber. 57, 858.

Received July 26, 1957

*Original Russian pagination. See C. B. Translation.

ANTISEPTIC PROPERTIES OF COAL-TAR COMPONENTS

G. D. Kharlampovich, M. V. Gofman, M. M. Raukas,
and N. D. Rus'yanova

The S. M. Kirov Polytechnic Institute of the Urals

Various coal tar-oils are widely used for rotproofing of wood. However, not enough is known as yet about the antiseptic effects of individual coal-tar components or the mutual influence of these components in the complex mixtures which coal-tar oils are. Investigation of the antiseptic action of phenols, bases, and neutral components of these oils, and of mixtures of these, is not only of great practical importance but also of independent scientific interest.

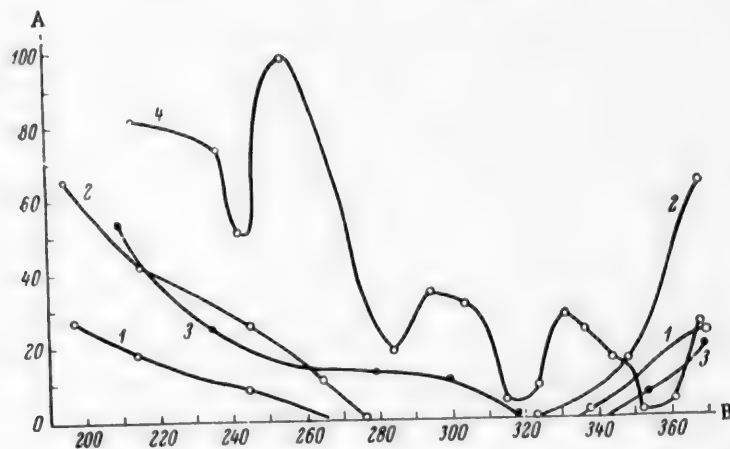


fig. 1. Effect of the boiling ranges of coal-tar fractions on their antiseptic action on the fungus *Coniophora cerebella*: A) relative weight loss (%), B) average boiling point of fraction ($^{\circ}\text{C}$); antiseptics and their concentrations (%): 1) phenols, 1.7%; 2) phenols, 1%; 3) bases, 1.7%; 4) neutral compounds, 1.7%.

We studied the action of various coal-tar oils and of individual components isolated from these oils on the fungi *Coniophora cerebella* and *Merulius domesticus*, which destroy wood.

The experimental procedure is described in one of our earlier papers [1]. The resistance of the specimens was also estimated from their relative weight losses (ratio of the weight loss of an impregnated specimen to the weight loss of a control specimen). The exposure time was 100 days in all cases. Experiments in which the weight loss was 5% and over were taken into consideration. If the weight loss was less than 5%, it was assumed that the specimen was not attacked by the fungus.

Study of the Antiseptic Properties of Individual Compounds

For elucidation of the effect of the nature of the antiseptic, the antiseptic properties of a number of pure compounds and of mixtures of known composition were studied. The results of these experiments are given in Table 1.

TABLE 1

Antiseptic Action of Coal-Tar Components on the Fungus *Contiophora cerebella*

Antiseptic	Conc. of antiseptic (%)	Relative weight loss (%)	Limiting dose of antiseptic (%)	Antiseptic	Conc. of antiseptic (%)	Relative weight loss (%)	Limiting dose of antiseptic (%)
Phenols				Bases			
Phenol	{ 1.5 2.5	{ 36 18	{ >2.5	Acridine	{ 1.7 3.0	{ 8.0 0.0	{ ~1.7
o-Cresol	{ 1.5 2.4	{ 24 12	{ >2.4	Quinoline	{ 1.7 2.5	{ 35.0 26.0	{ >2.5
Mixed xylenols	{ 1.5 1.8	{ 15 9	{ ~1.8	Dihydroacridine	{ 3.0	108.0	Inactive
Polyalkyl phenols (225-260°)	{ 1.2 1.7	{ 23.9 9	{ ~1.7	Neutral Compounds			
α-Naphthol	{ 0.5 1.0	{ 20.0 0.0	{ 0.5- -1.0	α-Methylnaphthalene	2.0	81.2	
β-Naphthol	{ 0.5 0.75	{ 8.0 0.0	{ ~0.5	β-Methylnaphthalene	2.0	65.0	
p-Phenylphenol	{ 0.3 0.6	{ 23.0 0.0	{ 0.3- -0.6	Indole	2.0	70.0	
Methylnaphthols	{ 0.3 0.6	{ 15.0 0.0	{ 0.3- -0.6	Acenaphthene	2.0	28.2	
Methylphenylphenols	{ -0.6 1.0	{ 29.0 0.0	{ 0.6- -1.0	Fluorene	2.0	35.0	
Phenanthrol-2	{ 2.0 3.5	{ 20.0 0.0	{ 2.0- -3.5	Diphenylene oxide	2.0	50.8	
				Phenanthrene	{ 1.5 2.0	{ 0.0 0.0	
				Anthracene	2.0	66.5	
				Carbazole	2.0	128.3	

Note. Weight loss of control specimen = 65%.

The following conclusions may be drawn from the above results.

1. Phenols are more active antiseptics than bases or natural compounds. The antiseptic effects of bases and neutral compounds are approximately equal.
2. Alkylation increases the antiseptic activity of phenols; the activity is increased even more by introduction of a benzene ring.

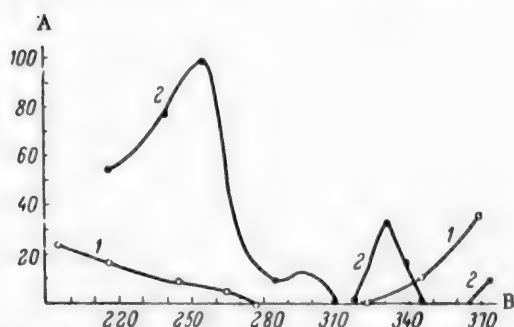


Fig. 2. Effect of the boiling ranges of coal-tar fractions on their antiseptic action on the fungus *Merulius domesticus*. A) Relative weight loss (%); B) average boiling point of fraction (°C); antiseptics and their concentrations (%): 1) phenols, 1.7%; 2) neutral compounds, 1.7%.

3. Naphthols and their homologs are better antiseptics than phenol derivatives. However, the activity is lower for compounds with more complex molecules (phenanthrol, methylphenylphenols).

4. Compounds with condensed systems of benzene rings are more active than compounds with separated benzene rings. If the benzene rings in a condensed system are separated by a nonaromatic ring, the activity is lowered sharply. Thus, anthracene, diphenylene oxide and fluorene are less active than acenaphthene and phenanthrene. The sharp decrease in activity caused by hydrogenation of the middle ring in acridine is also significant.

5. Wood specimens impregnated with carbazole or dihydroacridine are attacked much more rapidly than controls. Thus, compounds containing the imino group are nutrient media for the fungi and accelerate their growth.

Study of the Influence of the Boiling Ranges of Coal-Tar Products on Their Antiseptic Action

In order to determine the optimum ranges for collection of fractions used as antiseptics, we studied the antiseptic effects of various fractions of phenols, bases, and neutral coal-tar components, obtained by fractionation of the raw material through a laboratory packed column with an efficiency of 25 theoretical plates. The results of these experiments are given in Fig. 1 and Fig. 2.

TABLE 2

Effect of Removal of Individual Components on the Antiseptic Action of Wastes on the Fungus *Contophora cerebella*

Components	Contents of principal product (%)	Concentration of anti-septic (%)	Relative weight loss (%)	Limiting concentration (%)
Phenols				
α -Naphthol fraction (278-285°)	65	{ 0.6 1.0	{ 35.0 0.0	{ 0.6-1.0
α -Naphthol fraction after removal of 80% of the α -naphthol	13	{ 0.6 1.0	{ 24.0 0.0	{ 0.6-1.0
β -Naphthol fraction (275-295°)	45	{ 0.3 0.6	{ 32.0 0.0	{ 0.3-0.6
β -Naphthol fraction (60% of β -naphthol removed)	18	{ 0.3 0.6	{ 34.0 0.0	{ 0.3-0.6
p-Phenylphenol fraction (308-320°)	40	{ 0.3 0.6	{ 24.0 0.0	{ 0.3-0.6
308-320° fraction (50% of p-phenylphenol removed)	20	{ 0.3 0.6	{ 21.0 0.0	{ 0.3-0.6
Bases				
Acridine fraction (330-350°)	35	2.0	0.0	
50% of acridine removed	17	2.0	7.2	
90% of acridine removed	4	2.0	14.3	
Neutral compounds				
Anthracene fraction (335-343°)	46	2.0	27.4	
Same, without anthracene	10	2.0	12.0	

These results show that with the use of fractions, as with the use of the individual compounds, the activity of phenols is higher than that of bases or neutral compounds.

Each group of tar components has a definite activity maximum, which is in the 310-360° range for neutral compounds, in the 260-335° range for phenols, and in the 320-350° range for bases. The activity minimum in the 250-270° range found for neutral compounds is due to the presence of indole in this fraction, and the minimum in the 325-340° range, to the presence of anthracene.

The toxicity of neutral oils boiling below 310° is low, and they can really only serve as diluents.

Influence of Phenols and Bases on the Antiseptic Properties of Oils

This question is still obscure. It was considered for a long time that the activity of oils is determined by the presence of phenols and bases in them. However, there have been recent reports that removal of phenols does not affect the activity of anthracene oil [2].

It was even stated in a review article on tar processing [3] that hydroxylic compounds have an adverse effect on the antiseptic properties of coal-tar oils.

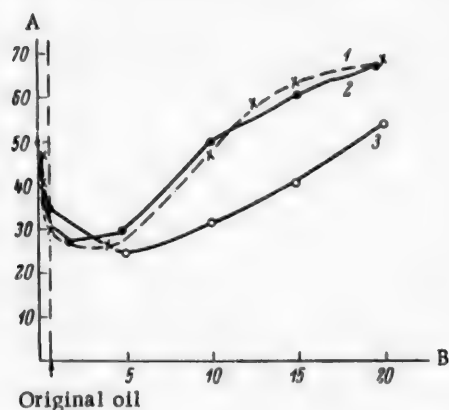


Fig. 3. Effect of phenols on the antiseptic action of anthracene oil: A) activity coefficient (100/limiting concentration); B) phenol content (%); oil with base content (%): 1) 0.2 (Contophora cerebella fungus); 2) 6.0 (same fungus); 3) 6.0 (Merulius domesticus fungus).

In the present investigation the main experiments were carried out on standard anthracene oil containing 0.9% phenols and 6.0% bases. The effects of removal of phenols and bases, and of addition of a broad fraction of high-boiling phenols (270-320°), on the activity were studied.

The results of these experiments are plotted in Fig. 3. They lead to the following conclusion.

Removal of phenols, if their content is below 10%, increases the antiseptic activity of the oil. Therefore removal of phenols and bases from ordinary preserving oils would yield more active antiseptics, and not lower the oil quality.

The existence of antagonism between phenols and neutral components of oils must be regarded as established. There is no evidence in favor of the hypothesis that antagonism exists between phenols and bases, or bases and neutral oils.

Antagonism occurs only at relatively low phenol concentrations (up to 10%). Oil toxicity increases with further increase of the phenol content. Thus, oils containing over 10% phenols are especially active antiseptics.

Antiseptic Action of Wastes After Isolation of Pure Products

Many methods have now been developed for isolation of individual coal-tar components in the pure state. For more economical production all the wastes should be utilized.

The effects of removal of certain valuable components on the activity of a number of fractions of neutral oils, phenols, and bases were tested in this connection. The results of the experiments are given in Table 2.

It follows from these data that in most cases the wastes are not inferior in antiseptic properties to the original fractions, and sometimes are even better than the latter. Wastes are quite suitable as components for antiseptic mixtures. The only exception is the 330-350° base fraction, the activity of which falls sharply after removal of acridine.

LITERATURE CITED

- [1] M. V. Gofman and G. D. Kharlampovich, J. Appl. Chem. 30, No. 4, 660 (1957).*
- [2] G. B. Campbell, Am. Ry. Eng. Assoc. Bull. 484, 343 (1949); Chem. A. 18, 669 (1950).
- [3] Coke and Gas. 3, 93 (1950).

Received October 4, 1957

*Original Russian pagination. See C. B. Translation.

DETERMINATION OF MOLECULAR WEIGHTS OF HUMIC PREPARATIONS CRYOSCOPICALLY IN PYROCATECHOL

T. A. Kukharensko and L. N. Ekaterinina

It is known that determination of the molecular weights of humic acids and other humic preparations presents considerable difficulties. Humic acids are insoluble in the organic solvents used for determinations of molecular weight by the cryoscopic and ebullioscopic methods. Literature data on the molecular weights of humic acids are highly contradictory.

The value usually taken for the molecular weight of humic acids (1200-1400) is not adequately justified, as it is partly based on calculations [1] or was found for derivatives of humic acids (nitrohumic acids [2]). Moreover, considerably higher molecular weights — of the order of tens of thousands [3] — and considerably lower, in the hundreds, have been reported.

Smith and Howard [4, 5] and Polansky and Kinney [6] found that di- and trihydric phenols and their derivatives are good solvents for humic acids made by oxidation of coal. Of the solvents used by them, pyrocatechol is the most satisfactory because of its thermal stability and low melting point. Smith and Howard developed a method for determination of the molecular weights of humic acids cryoscopically in pyrocatechol, and designed an apparatus for the purpose. Their values for the molecular weights of different humic acids from oxidized coal varied between 200 and 300.

We attempted to determine the molecular weights of humic acids from peats, brown coals, and weathered coals, and also of hymatomelanic acids isolated from weathered coals. In view of the considerable effect of moisture on molecular weight determinations, the samples were dried carefully to constant weight under vacuum at 70°, and then in a desiccator at room temperature over phosphorus pentoxide. Humic acids dissolved in pyrocatechol to give homogeneous solutions.

The molecular weights given in Table 1 show permissible variations between duplicate experiments. As was to be expected, humic acids from peat have lower molecular weights than humic acids from brown coal. The molecular weights of humic acids from weathered coal vary according to the degree of weathering; a sample from coal close to the surface has lower molecular weight than a sample from a greater depth. Hymatomelanic acids have lower molecular weights than humus acids from the same coal. It was noted, however, that the molecular weights of humic acids are not comparable with the equivalent weights of the samples determined by the reaction with barium hydroxide, which involves all the acidic groups of the molecule, and by the reaction with calcium acetate, which involves the carboxyl groups only. Moreover, the molecular weights found are lower than the molecular weights of hydrocarbons formed by exhaustive hydrogenation of humic acids from peat, brown coal, and weathered coal, determined by Savel'ev [7] cryoscopically in benzene, and found to be 283, 334, and 323 respectively. Neither did the values obtained correspond to the high-molecular nature of humic acids which is attributed to them on the basis of a number of their properties. Table 1 shows that methyl esters of humic acids, prepared by exhaustive methylation of humic acids by methyl alcohol, have considerably higher molecular weights than nonmethylated humic acids. This gave rise to the suggestion that humic acids may react with pyrocatechol to form esters. The possibility of chemical reaction with pyrocatechol is denied by the authors cited, although their investigations of the reaction products were confined to qualitative solubility tests on the reaction product and the original substance.

To test this hypothesis, we studied the reactions between humic acids and pyrocatechol. Humic acids from Galician moss peat and weathered coal from the "Baidavskaya" pit were heated with a 20-fold quantity of

TABLE 1

Molecular Weights of Humic Acids* in Pyrocatechol

Substance	Concentration (g/100 g)	ΔT	Molecular weight	Chemical equivalent	
				by Ba(OH) ₂	by Ca(CH ₃ COO) ₂
Humic acids of Galician moss peat	0.97, 1.23	0.30, 0.40	230, 220	134	349
Humic acids from Aleksandriya earthy brown coal	1.07, 1.26	0.25, 0.27	305, 295	138	300
Humic acids from weathered Kuznetsk coal from the "Baidaevskaya" pit	1.35, 1.24	0.45, 0.39	214, 223	177	317
Humic acids from weathered Kuznetsk coal from the "Maneikha" pit (3 meters from roof)	1.55, 1.32	0.34, 0.29	326, 318	131	212
Humic acids from weathered Kuznetsk coal from the "Severnaya" pit (105 cm from roof)	0.83, 0.97	0.20, 0.28	299, 247	157	186
Humus acids from the same coal	0.88, 0.52	0.28, 0.12	304, 312	—	—
Hymatomelanolic acids from the same coal	0.94, 0.63	0.36, 0.32	186, 142	—	—
Humic acids from weathered Kuznetsk coal from the "Severnaya" pit (15 cm from roof)	1.07, 1.24	0.30, 0.38	256, 232	146	193
Humus acids from the same coal	0.41, 0.89	0.10, 0.22	292, 280	—	—
Product formed by methylation with methyl alcohol of humic acids from weathered Kuznetsk coal from the "Baidaevskaya" pit	0.65, 0.46	0.10, 0.07	465, 472	—	—

* In accordance with Oden's classification [1], we subdivide humic acids into alcohol-soluble hymatomelanolic acids and alcohol-insoluble humus acids.

pyrocatechol for 30 minutes at 120° on a glycerol bath. The reaction product was washed free from pyrocatechol with dry ethyl ether (confirmed by ferric chloride test). The yield was 87.1% from humic acids of weathered coal, and 91.2% from peat. The filtrate from the ether washing was colored; this showed degradation of the humic acids as the result of interaction. The reaction products were analyzed for carbon and hydrogen contents, active acid groups were determined by the sorption method, and the molecular weight was determined cryoscopically in pyrocatechol. The results are presented in Table 2 and compared with corresponding data for the original humic acids.

Table 2 shows that the carbon contents of the reaction products were lower than those of the original humic acids, the carboxyl group contents were considerably lower (one sample was almost free from carboxyl groups), while the phenolic hydroxyl contents were higher. The molecular weights of the reaction products of humic acids with pyrocatechol were lower by one half.

These results lead to the conclusion that the reaction probably occurs between the carboxyl groups of the humic acids and the phenolic hydroxyls of pyrocatechols. This may give rise to substances of the ester type and water, with a consequent decrease in molecular weight.

TABLE 2

Characteristics of the Original Humic Acids and Products of Their Reaction with Pyrocatechol

Sample	Molecular weight (average)	Contents (%)		Contents of active acid groups (meq/g)		
		C	H	total	carboxyl	phenolic hydroxyl (by difference)
Humic acids of weathered coal	218	68.58	3.25	5.62	3.15	2.47
Reaction product of humic acids of weathered coal with pyrocatechol	105	64.45	3.80	6.02	0.22	5.80
Humic acids of peat	225	62.13	4.70	7.41	2.86	4.55
Reaction product of humic acids of peat with pyrocatechol	99	56.18	5.31	7.67	1.35	6.32

The hypothesis that water is formed in the reaction between humic acids and pyrocatechol was confirmed by determinations of moisture by the Dean and Stark method. The moisture contents were 3.01% in the reaction product of pyrocatechol and humic acids from weathered coal, and 7.46% in the reaction product of pyrocatechol and humic acids from peat.

TABLE 3

Molecular Weights of Hymatomelanic Acids

Source of hymatomelanic acids	Content of hymatomelanic acids in humic acids (%)	Molecular weight
Humic acids from "Elektroperedacha" peat	8.31	300, 285
Humic acids from weathered Kuznetsk coal, near roof of "Maneikha" pit	24.60	372, 342
Product formed by decomposition of humic acids (from weathered Kuznetsk coal from "Baidavskaya" pit) by metallic sodium in liquid ammonia	4.76	286, 266

To confirm that the reaction takes place between the carboxyl groups of humic acids and the phenolic hydroxyls of pyrocatechol, the reaction product was saponified by 0.2 N alcoholic caustic potash on a boiling water bath for 30 minutes. The saponification equivalents were: for the original humic acids of peat, 7.73 meq/g; for the reaction product, 8.62 meq/g; for the original humic acids from weathered coal, 7.45 meq/g, and for their reaction product, 8.40 meq/g; thus, the saponification equivalents are higher for the reaction products of humic acids with pyrocatechol than for the original humic acids, but the difference is considerably less than is to be expected on the assumption that an ester is formed by the carboxyl groups of the humic acids. Evidently ester formation was incomplete under the conditions used, as compared with the conditions used in the molecular weight determinations.

For determination of molecular weights of humic acid fractions soluble in organic solvents, of the type of hymatomelanic acids, we used dioxane for the first time as the cryoscopic liquid; this solvent has m.p. 11.75° and does not react with acids.

The molecular weights determined with the aid of this solvent are given in Table 3.

SUMMARY

It was shown in this investigation that humic acids react with pyrocatechol; it is therefore evident that pyrocatechol cannot be used as a solvent in the cryoscopic method for determination of molecular weights of humic substances.

LITERATURE CITED

- [1] S. Oden, *Die Huminsäuren*, Leipzig (1919).
- [2] W. Fuchs, *Die Chemie d. Kohle*, Berlin (1931).
- [3] W. Schele, *Koll. Beihefte* 46, 369 (1937).
- [4] R. C. Smith and H. C. Howard, *J. Am. Chem. Soc.* 57, 513 (1935).
- [5] R. C. Smith and H. C. Howard, *J. Am. Chem. Soc.* 58, 740 (1936).
- [6] T. S. Polansky and C. R. Kinney, *Fuel* 4, 409 (1952).
- [7] T. A. Kukharensko and A. S. Savel'ev, *Proc. Acad. Sci. USSR* 4, 729 (1952).

Received December 17, 1957

PRODUCTION OF FORMALDEHYDE IN A FLOW UNIT BY OXIDATION OF METHANE, CATALYZED BY NITROGEN OXIDES

N. S. Enikolopyan, N. A. Kleimenov, L. V. Karmilova,
A. M. Markevich, and A. B. Nalbandyan

During the past 50 years the problem of methane oxidation has been the subject of numerous research in the fields of chemistry and chemical kinetics; there have been two predominant directions in this work. The first direction was concerned with phenomenology of the reaction, identification of the intermediate and final products, and attempts to establish the mechanism of oxidation [1-7]. The aim of the second was to find methods for obtaining good yields of valuable oxygen-containing compounds (formaldehyde and methyl alcohol) by slow oxidation of methane. This direction is closely connected with the important problem of chemical conversion of natural and petroleum gases.

Searches for routes and optimum conditions for the formation of various intermediate products in the oxidation of methane involve considerable difficulties, caused by the reactivity of the starting substances and intermediate oxidation products. In view of the inertness of the methane molecule ($Q_{C-H} = 101 \pm 2$ kcal to remove the first H atom) the main determining step is chain initiation. The primary CH_3 radical formed from methane is highly active, and therefore elementary reactions involving this radical, which determine the further course of oxidation, proceed at high rates. Numerous attempts to obtain formaldehyde and methanol by noninitiated thermal oxidation, which commenced with the work of Bone [1], proved unsuccessful. The great majority of subsequent investigations were concerned with searches for the best methods for initiating the reaction and lowering the reaction temperature. Solutions to this problem were sought by means of heterogeneous [8, 9] and homogeneous [10-12] catalytic oxidation of methane, the use of pressures for oxidation reactions [13, 14], and use of special initiation methods (ozone [15-17], photochemical methods [18-21], electric discharge [22-24], etc.). Various combinations of these methods were also often used.

Considerable successes in the problem of formaldehyde production from methane under normal pressures have been achieved with the use of homogeneous catalysts, especially such catalysts as hydrogen chloride and nitrogen oxides. The best results in oxidation of methane catalyzed by hydrogen chloride were obtained by Medvedev [25, 26], who combined the action of HCl and of solid catalysts (tin, lead, and iron borates and phosphates). In the best experiments with a dilute methane-air mixture ($CH_4 = 13.8\%$) containing 0.3% HCl, he succeeded in converting up to 5% of the methane into formaldehyde per pass, with up to 58% total useful conversion of the methane reacted. He established the existence of an effective concentration of the homogeneous catalyst, above which the yield of formaldehyde decreases, and the carbon monoxide content in the reaction products rises. However, this method was not operated industrially because of the difficulty in maintaining the precise temperature conditions in a large unit.

Promising results in the oxidation of natural gas with the use of nitrogen oxide catalysts were obtained by Bibb [27, 28]. By passing a mixture containing 29% of natural gas (24.5% CH_4 and 4.75% C_2H_6), 70% air, and 1-2% nitrogen oxides at 770° through 4 consecutive reactors, he obtained 123.3 g of CH_2O per m^3 of natural gas.

Bibb concluded from his results that nitrogen oxides constitute a promising catalyst in the oxidation of methane to oxygen-containing products. However, as has been pointed out in the literature, the high yields of CH_2O attained in these experiments may have been due to the presence of higher hydrocarbons, the molar content of which exceeded that of the formaldehyde formed.

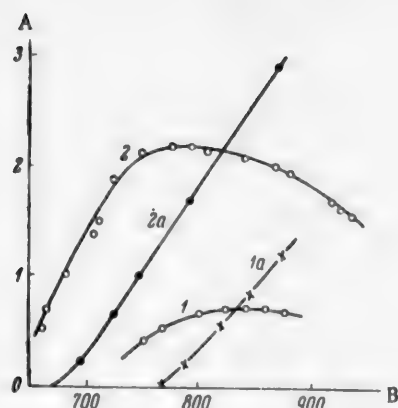


Fig. 1. Effect of temperature in the yields of methane oxidation products in a reactor of 1Kh18N9T steel of higher carbon content, in relation to surface treatment. Original mixture (%): CH_4 33.3, air 66.6, NO 0.1; contact time 0.07 second; A) yield of CH_2O (% on CH_4) and yield of CO and CO_2 (% on mixture); B) temperature ($^\circ\text{C}$). 1,1a) Yields of CH_2O and CO in untreated vessel; 2,2a) yields after treatment with $\text{K}_2\text{B}_4\text{O}_7$.

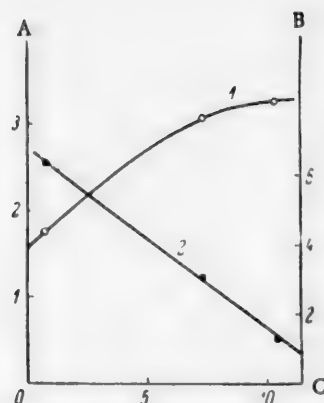


Fig. 2. Variation of the degree of methane conversion with surface - volume ratio in a packed steel vessel ($d = 40$ mm) at $t = 760^\circ$. Original mixture (%): CH_4 33.3, air 66.6, NO 0.12; contact time 0.1 second; A) yield of CH_2O (% on CH_4); B) yield of CO (% on CH_4); C) s/v ratio (cm^{-1}); yields: 1) CH_2O ; 2) CO.

Bibb's views were criticized by Smith and Milner [29], who reached the opposite conclusion as the result of their experiments; they considered that catalysis by nitrogen oxides is unpromising, because they are consumed (reduced to nitrogen) during the reaction. However, it was shown by subsequent experiments performed by D. M. Rudkovskii and ourselves, that their views on the reduction of nitrogen oxides are erroneous.

D. M. Rudkovskii and his associates worked in 1946 on the oxidation of methane by atmospheric oxygen in presence of nitrogen oxides. By passing an air-methane mixture containing 0.2-0.25% nitrogen oxides through 3 reactors in series, they showed that about 4.8% of the methane passed through a reactor is converted to formaldehyde. Formaldehyde is now being produced on the pilot scale from natural gas in Rumania. The process is based on the patents of a German firm [30]. A tubular reactor ($d = 81$ mm) is used; with 10-fold circulation of methane-air mixture (18% CH_4 , 9% O_2 , 67.9% N_2 , 3% CO, 1.6% CO_2), containing 0.08% NO, contact time 0.15-0.2 seconds, and temperature $600-620^\circ$, about 8% of the methane passed through the reactor is converted into formaldehyde. Important disadvantages of the process are formation of considerable amounts (up to 30% of the methane passed) of carbon monoxide, dioxide, and water, and the low formaldehyde concentration ($\sim 0.2\%$) in the exit gases, which makes separation of formaldehyde from the gas phase difficult.

This paper contains certain results of laboratory experiments on the formation of formaldehyde by oxidation of methane by atmospheric oxygen in presence of nitrogen oxides as catalyst.*

EXPERIMENTAL

Method of Investigation. The oxidation of methane was effected under flow conditions with the reaction mixture close to atmospheric pressure, at $600-800^\circ$. The experimental unit and methods used for analysis of the reaction products are described in earlier papers [6]. Most of the experiments were performed in vessels filled with inert packing ($s/v = 10-40 \text{ cm}^{-1}$).

* Members of the All-Union Scientific Research Institute for Gases of the Ministry of the Petroleum Industry, S. S. Anisyan, S. Ya. Beider, and N. I. Vinnikova, and members of the State Institute for the Planning of Rubber Industry Plants of the Ministry of the Chemical Industry, A. S. Zhadaev, N. N. Chernov, and M. N. Shendrik took part in various sections of the work.

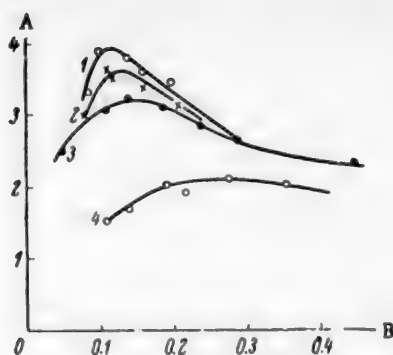


Fig. 3. Kinetics of formaldehyde formation of different compositions of the methane-air mixtures at $t = 650^\circ$: A) CH_2O yield (% on CH_4); B) contact time (seconds); methane content (%): 1) 8; 2) 16; 3) 33.3; 4) 50.

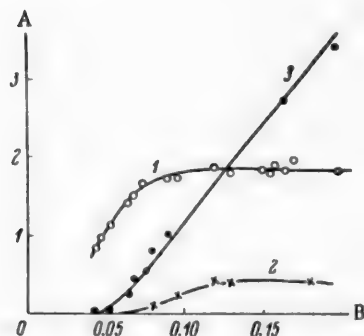


Fig. 4. Kinetics of methane oxidation at $t = 650^\circ$ for 1:1 CH_4 -air mixture, NO 0.1%. A) Yields of CH_2O , CO, and CH_3OH (% on CH_4); B) contact time (seconds); yields: 1) CH_2O ; 2) CH_3OH ; 3) CO.

Effect of Potassium Perborate. In flow experiments, under atmospheric pressure in a packed quartz vessel, on the effect of temperature on formaldehyde yield we found, in agreement with the results of others [31, 32] that the reproducibility of the results was very bad and that the surface gradually became stabilized. However, this stabilization of the vessel surface by the proceeding reaction proved to be erratic. For reproducible yields of formaldehyde it was necessary to find a reliable method for consistent stabilization of the reaction-vessel surface.

On the assumption that lack of reproducibility is caused by heterogeneous processes during the chain oxidation of methane, and in the light of the results of Lewis and Elbe [33] and Nalbandyan [34, 35], according to whom the probability of recombination of hydrogen atoms is lower on a quartz surface treated with $\text{K}_2\text{B}_4\text{O}_7$, we studied the effect of such treatment on the kinetics of methane oxidation and on the formaldehyde yield. Experiments with quartz and metal reactors showed that treatment of the vessel surface with 2% aqueous $\text{K}_2\text{B}_4\text{O}_7$ solution considerably raises the oxidation rate of methane and simultaneously increases the formaldehyde yield. This is illustrated in Fig. 1, where the yields of methane oxidation products are plotted against the temperature, for the reaction in a steel vessel (carbon-enriched smelting of 1Kh18N9T steel). It follows from the graph that the percentage conversion of methane into formaldehyde is more than trebled after treatment of the vessel, while the position of the maximum CH_2O yield is shifted to a lower temperature (780 from 850°).

However, potassium perborate treatment does not eliminate fully the specific influence of the reactor material on oxidative conversion. In a quartz vessel the best CH_2O yield is obtained at a lower temperature ($t_{\text{max}} \sim 630-650^\circ$).

Effect of Packing of the Vessels. Most investigators have observed that the reaction of methane oxidation is suppressed when the vessel dimensions are reduced or when packing is introduced; this is undoubted. proof of the radical mechanism of the reaction. We studied the effect of packing on the yield of formaldehyde in methane oxidation.

The reaction was conducted in a vessel packed with porcelain Raschig rings of different sizes, under otherwise constant conditions, and the relationship between the degree of oxidation of methane and CH_2O and CO yields on the one hand, and the surface-volume (s/v) on the other, was determined. This relationship is plotted in Fig. 2. It can be seen that the extent of the reaction depends sharply on the s/v ratio; the most favorable proportions of formaldehyde and carbon monoxide (maximum CH_2O and minimum CO) are attained at high s/v ratios.

On the basis of these results packed vessels treated with potassium tetraborate were used in all the subsequent experiments on the optimum conditions for the formation of formaldehyde from methane in relation to the composition of the reacting mixture, temperature, and concentration of the homogeneous catalysts. The reproducibility was consistently good.

Effect of Mixture Composition. The effect of the composition of the original mixture on the yields was studied in detail in order to find the optimum methane-oxygen ratio. The methane content of the mixture was varied from 8 to 90%.

Fig. 3 shows kinetic curves for formaldehyde formation, plotted for methane-air mixtures of different compositions. It is seen that the degree of conversion of methane into formaldehyde increases with dilution of the

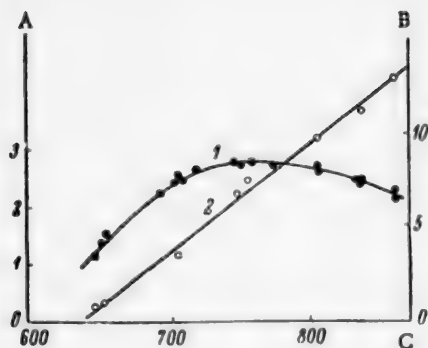


Fig. 5. Effect of temperature on the yield of formaldehyde and carbon monoxide in the oxidation of CH_4 in a reaction vessel of 1Kh18N9T. Original mixture (%): CH_4 33.3, air 66.6, NO 0.1; contact time 0.07 second; A) yield of CH_2O (% on CH_4); B) yield of CO (% on CH_4); C) temperature ($^{\circ}\text{C}$); yields: 1) CH_2O ; 2) CO.

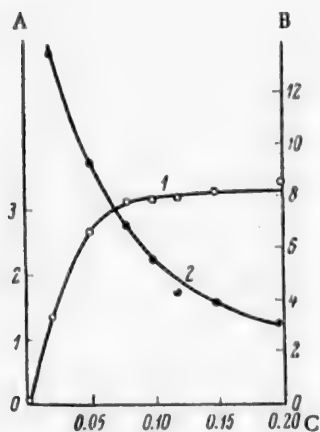


Fig. 6. Effect of concentration of homogeneous catalyst on the formaldehyde yield at $t = 700^{\circ}$. Original mixture (%): CH_4 18, O_2 9, N_2 73; contact time 0.09 second; A) yield of CH_2O (% on CH_4); B) CH_2O :NO ratio; C) NO concentration (% on original mixture); 1) yield of CH_2O ; 2) variations of the relative yield of CH_2O per catalyst molecule (CH_2O :NO).

mixture. In dilute mixtures the formaldehyde yield reaches 4% on the methane passed. The maximum yield in mixtures containing from 8 to 33.3% CH_4 is reached in contact times of the order of 0.1-0.15 second, and in rich mixtures (50% CH_4) in 0.25 second. Accumulation of the other oxidation products, CH_3OH and CO, for an equimolecular mixture is shown graphically in Fig. 4. It follows from these data that, in agreement with Medvedev's results, the degree of useful conversion of methane increases as the mixture becomes poorer in the combustible gas, but the concentration of formaldehyde in the exit gas is then lower, so that it is more difficult to collect. Because of this the subsequent experiments on formaldehyde production were performed with mixtures containing 33% methane, when the formaldehyde concentration in the gas reaches 1% by volume.

The effect of temperature for a reaction vessel made from steel with a high carbon content is shown in Fig. 1. The nature of the relationship does not alter with vessels of high-quality 1Kh18N9T steel, but the formaldehyde yield increases, reaching 2.8% (Fig. 5) and over. It should be noted that the temperature range may be used for the reaction for an almost constant yield of CH_2O is fairly wide, and is about 100° .

Effect of Concentration of the Homogeneous Catalyst. To investigate the behavior of nitrogen oxides in the reacting system and to find their optimum concentration in the gas-air mixture, the effect of NO concentration on the formaldehyde yield was studied for mixtures of different composition in the temperature range from 650 to 750° . The results are plotted in Fig. 6, where curve 1 represents variations of the formaldehyde concentration in the gas with the NO content in the mixture. Variations of the relative yield of formaldehyde per molecule of catalyst (CH_2O :NO) are represented by curve 2.

It follows from these results that the CH_2O yield in the noncatalyzed reaction at $t = 700^{\circ}$ and $\tau = 0.09$ second is almost zero (0.16% on the methane passed). The yield of CH_2O rises sharply, almost linearly, with addition of nitrogen oxides to the mixture. On further increase of the catalyst concentration the yield increases only slightly. At the same time the relative yield of formaldehyde per NO molecule falls sharply.

These were the unfavorable conditions used by Smith and Milner, who added about 1% of nitrogen oxides to the mixture.

Our other experiments show that there is an optimum catalyst concentration (close to 0.1% in the mixture) at which, in a single pass of a gas-air mixture containing 33.3% CH_4 and 66.6% air, up to 10 formaldehyde molecules are formed per molecule of nitric oxide, and the degree of useful conversion of methane reaches 3%. With repeated circulation up to 30-35 molecules of CH_2O per catalyst molecule can be obtained. The existence of an optimum catalyst concentration is apparently associated with the catalytic effect of nitric oxide on the second

stage of the process, oxidation of the formaldehyde formed; this is confirmed by the sharp increase of the proportion of CO in the reaction products at high NO concentrations.

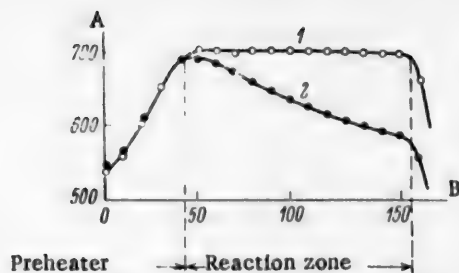


Fig. 7. Temperature distribution along the reactor axis: A) temperature ($^{\circ}\text{C}$); B) reactor length (cm); 1) original mixture (%): CH_4 33.3, air 66.6, NO 0.12, and products (%): CH_2O 2.7 and CO 1.2; 2) the same mixture without NO, and products (%): $\text{CH}_2\text{O} = \text{CO} = 0$.

The experiments were conducted with a 1:2 CH_4 :air mixture. Figure 7 shows the temperature distribution along the reactor axis. Curve 1 corresponds to the process with a mixture containing 0.12% nitrogen oxides; the contents of CH_2O and CO in the products were respectively 2.7 and 1.2% on the methane fed into the reactor. In other words, about 70% of the converted methane is oxidized to CH_2O . If the supply of nitrogen oxides is discontinued, the reaction stops — the CH_2O and CO contents fall to zero and the temperature in the reaction zone falls accordingly (Curve 2).

SUMMARY

1. The optimum conditions for formaldehyde formation by oxidation of methane in presence of nitric oxide catalyst were studied, and it was found that the rate and course of oxidation depend on the magnitude and nature of the surface of the reaction vessel. It was shown that surface treatment with $\text{K}_2\text{B}_4\text{O}_7$ increases and stabilizes the CH_2O yield and lowers the reaction temperature by 80–100°. The tetraborate coating was shown to be stable. The formaldehyde yield is sharply increased and the degree of methane oxidation is decreased with the use of packed vessels treated with $\text{K}_2\text{B}_4\text{O}_7$.
2. A relationship has been established between the formaldehyde yield and the concentration of homogeneous catalyst in the mixture, and it is shown that this concentration has an optimum value. The relative yield of formaldehyde ($\text{CH}_2\text{O}:\text{NO}$) in a single pass reaches 10–12 molecules per molecule of catalyst present.
3. The degree of conversion of methane into formaldehyde is higher in more dilute mixtures. The optimum composition of the methane–air mixture was found, at which maximum productivity and the greatest useful conversion of methane are obtained.
4. Optimum conversion of methane into formaldehyde can be obtained over a temperature range of about 100°.
5. It is shown that the reaction can be conducted stably in metal vessels.
6. The laboratory data were confirmed by trials in a pilot unit of a capacity of 13 m^3 of gas–air mixture per hour.

LITERATURE CITED

- [1] W. A. Bone, H. Davies, H. Gray, H. Heustock, and J. Dawson, *Phil. Trans. Roy. Soc. A.*, 288 (1915); W. A. Bone, *J. Chem. Soc.*, 81, 535 (1902); W. A. Bone and R. Allum, *Proc. Roy. Soc. A.*, 134, 578 (1932).

- [2] C. Hinshelwood and H. Fort, *Proc. Roy. Soc. A*, 129, 284 (1930).
- [3] R. Norrish, *Discus. Far. Soc.* 10, 296 (1951).
- [4] N. N. Semenov, *Chain Reactions* [in Russian] (State Chem. Tech. Press, Leningrad, 1934); *Progr. Chem.* 20, 673 (1951).
- [5] I. N. Antonova, V. A. Kuz'min, R. I. Moshkina, M. B. Neiman, A. B. Nalbandyan, and G. I. Feklisov, *Bull. Acad. Sci. USSR, Div. Chem. Sci.* 5, 789 (1955).*
- [6] L. V. Karmilova, A. B. Nalbandyan, and N. S. Enikolopyan, *J. Phys. Chem.* 30, 798 (1956).
- [7] A. Egerton, G. J. Minkoff, and K. C. Salooja, *Proc. Roy. Soc. A.*, 235, 158 (1956).
- [8] L. F. Marek and D. A. Gan, *Catalytic Oxidation of Organic Compounds* [in Russian] (ONTI, 1936).
- [9] L. Ya. Margolis, *Progr. Chem.* 20, 176 (1951).
- [10] A. P. Kreshkov, *J. Gen. Chem.* 10, 1605 (1940); *J. Chem. Ind.* 11, 1702 (1939).
- [11] T. E. Laying and R. Soukup, *Ind. Eng. Chem.* 20, 1052 (1928).
- [12] A. Matui and M. Jasida, *J. Chem. Soc. Ind. Japan* 43, 117B (1940).
- [13] D. Newitt and A. Haffner, *Proc. Roy. Soc. A.*, 134, 591 (1932); D. Newitt and P. Szego, *Proc. Roy. Soc. A.*, 147, 555 (1934).
- [14] M. S. Furman, *J. Chem. Ind.* 1, 2 (1946).
- [15] R. V. Wheeler and T. S. Blair, *J. Soc. Chem. Ind.* 41, 331 (1922).
- [16] P. Monceaux, *Mem. Serv. Chim. d'État. (Paris)* 33, 423 (1947).
- [17] N. A. Kleimenov, I. N. Antonova, A. M. Markevich, and A. B. Nalbandyan, *J. Phys. Chem.* 30, 794 (1956).
- [18] N. V. Fok, *Candidate's Dissertation* [in Russian] (Inst. Chem. Phys. Acad. Sci. USSR, 1951).
- [19] N. V. Fok and A. B. Nalbandyan, in the book: *Questions of Chemical Kinetics, Catalysis, and Reactivity* [in Russian] (Izd. AN SSSR, Moscow, 1955) p. 219.
- [20] A. B. Nalbandyan, *Proc. Acad. Sci. USSR* 60, 607 (1948).
- [21] J. A. Gray, *J. Chem. Soc.* 3150 (1952).
- [22] M. Kushnerov and A. Shekhter, *Proc. Acad. Sci. USSR* 32, 560 (1941).
- [23] E. Brigger and H. Hofer, *Helv. Chim. Acta* 23, 800 (1940).
- [24] Gutehoffnungshütte Oberhausen, *British Patents* 343461, 352978, 375076, 375314 (1928); *French Patents* 694380 (1930) and 684969 (1929).
- [25] S. S. Medvedev, *Trans. Karpov Phys.-Chem. Inst.* 3, 54 (1924); *Natural Gases* 4, 5, 29 (1932); *Soviet Patent* 3605 (1927).
- [26] S. S. Medvedev and E. A. Robinson, *Trans. Karpov Phys.-Chem. Inst.* 4, 117 (1925).
- [27] K. H. Bibb, *Ind. Eng. Chem.* 24, 10 (1932); *U. S. Patent* 1392886 (1921); *Canadian Patent* 302672 (1930).
- [28] K. H. Bibb and J. Lucas, *Ind. Eng. Chem.* 21, 633 (1929).
- [29] D. E. Smith and R. T. Milner, *Ind. Eng. Chem.* 23, 357 (1931).
- [30] Gutehoffnungshütte Oberhausen, *German Patents* 649330 (1930), 700823 (1931), 770179 (1934), 788533 (1935).
- [31] D. E. Hoare, *Trans. Far. Soc.* 49, 628 (1953).

*Original Russian pagination. See C. B. Translation.

[32] D. E. Hoare and A. D. Walsh, Proc. Roy. Soc. A., 215, 454 (1952); Fifth Symposium (International) on Combustion, N. Y. 955 (1956).

[33] B. Lewis and G. Elbe, J. Chem. Phys. 10, 366 (1942).

[34] A. B. Nalbandyan and S. M. Shubina, J. Phys. Chem. 20, 1249 (1949).

[35] N. S. Enikolopyan and A. B. Nalbandyan, Proc. Acad. Sci. Armenian SSR 7, 57 (1947).

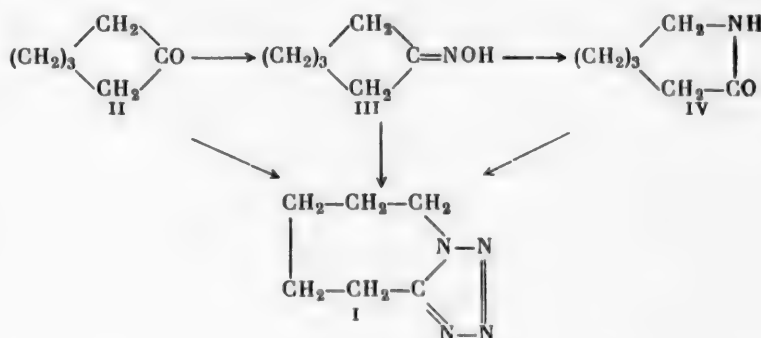
Received September 30, 1957

SYNTHESIS OF α,β -CYCLOPENTAMETHYLENETETRAZOLE (CORAZOLE)

R. G. Glushkov and E. S. Golovchinskaya

The S. Ordzhonikidze All-Union Chemical and Pharmaceutical Research Institute

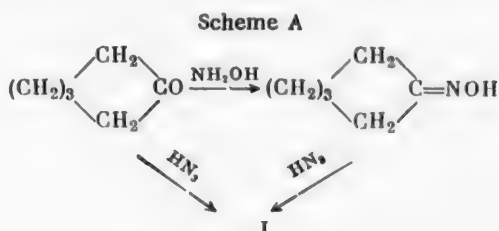
Starting materials for the synthesis of α,β -cyclopentamethylenetetrazole (I) can be cyclohexanone (II), its oxime (III), or the lactam of ϵ -leucine (IV) which is formed by the oxime as the result of a Beckman rearrangement.



The synthesis of (I) was first described by Schmidt [1] in 1924, in his paper on the reaction of the $>NH$ residue formed in the decomposition of hydrazoic acid by the action of concentrated H_2SO_4 :

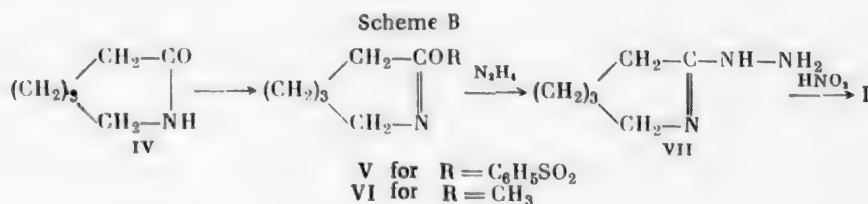


The α,β -cyclopentamethylenetetrazole synthesized in the course of that investigation, was soon acknowledged to be a powerful camphorlike cardiac drug with many valuable characteristics in its action on respiration, the central nervous system, and the circulation. Numerous patents have been published since 1924, describing different methods for preparations of (I) and of other substituted tetrazoles [2]. Most of these patents are based on the reaction of free hydrazoic acid (or its salts in presence of free mineral acids) with (II) or the oxime (III) by scheme A.



There are also several patents which describe different variants of the synthesis of (I) by a somewhat more complex scheme, in which the use of the toxic and explosive hydrazoic acid is avoided. These variants comprise several stages. They all involve the formation of various imino ethers or esters of the enol form of ϵ -leucine

lactam (o-alkyl or o-acyl lactams), interaction of the ether or ester with hydrazine, and subsequent closure of the tetrazole ring by the action of HNO_2 on the resultant 2-hydrazino- $\Delta_{1,3}$ -homopiperidine (VII) in accordance with scheme B.



Data from one of the Knoll A. G. patents [3] were used for development of a method for synthesis of (I) by scheme A, suitable for technical purposes. Several suitable modifications were introduced in order to simplify the process, reduce costs, and especially, to ensure safety of the process. In particular, in order to avoid accumulation of N_3H in the reaction mass, it proved desirable to change the sequence of reagent addition: instead of mixing of sodium azide with chlorosulfonic acid in chloroform followed by addition oxime solution to the resultant solution of N_3H , chlorosulfonic acid was added gradually to a mixture of sodium azide and a solution of (III). By this procedure the N_3H liberated from the azide reacts immediately, and its accumulation in the reaction mass is therefore improbable. The main condition for success in this case is careful maintenance of the optimum temperature conditions (30–35°); at a lower temperature (say, 27–28°) the reaction does not proceed, so that N_3H accumulates in the solution, and this results in a subsequent violent exothermic process. Conversely, at a higher temperature N_3H boils (at 57°), and therefore evaporates at the instant of its liberation from the salt without entering the reaction. Replacement of chloroform by the cheaper dichloroethane did not affect the results of the reaction, which is on the whole a simple and convenient method for synthesis of (I), suitable for large-scale operation.

One variant of production of (I) by scheme B is acylation of (IV) by benzenesulfonyl chloride in presence of pyridine, treatment of the reaction mass with hydrazine acetate, and cyclization of the hydrazidine (VII), formed from the intermediate benzenesulfonic ester (V), by the action of HNO_2 [4].

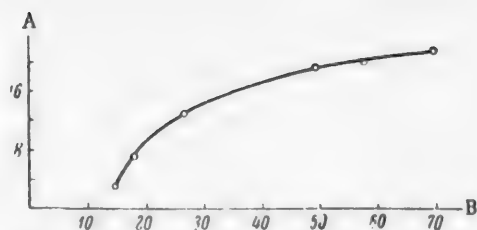
In experiments on this variant corazole was obtained in yields not higher than 18.6% of the theoretical; in addition, a certain amount of diphenyl disulfide was isolated from the reaction mixture; this compound was probably formed by the reduction of benzenesulfonyl chloride by the action of hydrazine. Attempts to use the oxime (III) in an analogous process [5] were likewise unsuccessful.

A more convenient method was based on the formation of a stable o-alkyl ether of caprolactim as an intermediate product at the first synthesis stage [6]. Some modifications of the known method for preparation of (VI) [7] and its conversion into (I) [8] resulted in quite consistent and satisfactory yields of (I) from the original (IV), and these experiments showed that this variant of the synthesis of α, β -cyclopentamethylenetetrazole may be used for practical purposes.

Because of the considerable solubility of (I) in water and in most organic solvents, the purification of the substance isolated from the reaction mass required careful attention. Repeated crystallization from diethyl ether (1:7), in which (I) is moderately soluble, gives pure corazole, but this procedure is not widely applicable. In order to replace ether by a less volatile and inflammable solvent, it was found that the unpurified reaction product can be dissolved in 1.5 parts of toluene in the cold, with subsequent precipitation of (I) from the toluene solution, decolorized by charcoal, by gradual addition of 1.5 parts of ligroine of b.p. 70–80° [(I) is almost insoluble in petroleum hydrocarbons]. This purification method was found to have the disadvantage that, although the corazole so obtained is crystalline and has a sharp melting point, it sometimes retains a faint cream color.

Quite satisfactory results were obtained by crystallization from water. The crystallization procedure used for this purpose depends on the sharp fall in the solubility of (I) in water (see figure) at temperatures below 10°. Twofold crystallization of the unpurified reaction product from small volumes of water, with careful utilization of the mother liquors and effective cooling, ensures that losses of corazole are negligible and yield a colorless preparation, which conforms to the specification of the State Pharmacopeia in all respects.

EXPERIMENTAL



Solubility of α,β -cyclopentamethylenetetrazole in water at different temperatures:

A) temperature ($^{\circ}\text{C}$); B) α,β -cyclopentamethylenetetrazole content (in weight, %).

after 1 hour to 50° ; after 1 hour at 50° 7.5 liters of water was added with stirring to the mass cooled in ice, the dichloroethane layer was separated off, and the acid aqueous solution was extracted with 5 lots of 180 ml of dichloroethane with stirring. The extract was dried by means of calcined K_2CO_3 and dichloroethane was distilled off. The total weight of the residue was 499 g (of this, 329 was obtained from the layer which separated from the acid aqueous solution, 137 g from the 1st, 2nd, and 3rd extractions, 25 g from the 4th extraction, and 8 g from the last). After twofold crystallization from water, 393.5 g of pure corazole was obtained; this is 57% of the theoretical yield.

Preparation of Corazole (Method 2) from Caprolactam. The original technical caprolactam was converted into o-methylcaprolactim by the known procedure [7] with the following modifications: the methylation was effected at $60-65^{\circ}$ with half the specified amount of benzene, and the reaction mass was neutralized by 30% K_2CO_3 solution (210 ml per mole of caprolactam) rather than 50% solution, in order to avoid side reactions. Under these conditions, the yield of distilled o-methylcaprolactim was 70-75% of the theoretical. In the subsequent reaction with hydrazine hydrate, instead of the pure substance, the undistilled reaction product, which remained after distillation of benzene (with a fractionating column under vacuum at $< 40^{\circ}$), was used.

Crude o-methylcaprolactim (made by the methylation of 2.4 moles - 271.22 g - of caprolactam in 400 ml of benzene by means of 2.4 moles - 227.6 g - of dimethyl sulfate at $60-65^{\circ}$) was added during 30 minutes with vigorous stirring (at $17-20^{\circ}$) to 2.64 moles (132 g) of hydrazine hydrate. The crystallized reaction mass was stirred at the same temperature for 1-1.5 hours more, cooled to between -3 and -5° , and to it was added a solution of 248 g of NaNO_2 in 500 ml of water and then 20% H_2SO_4 during 3-3.5 hours (about 800 ml, tests with starch-iodide paper, acid reaction to Congo red). The reaction mass was stirred for 1.5 hours, filtered, and extracted with dichloroethane; the weight of the residue after distillation of dichloroethane was 224-228 g, and after crystallization from water the yield of pure product was 177.0-179.4 g, which corresponds to 53.46-54.2% calculated on caprolactam.

Purification of Crude Corazole. A solution of 1 kg of crude corazole (prepared by method 1 and 2) was boiled for 1.5 hours in 1 liter of water with 50 g of activated carbon. The filtered solution was cooled in ice, and 750 g of the first-crystallization product was obtained (it was sometimes yellowish). The mother liquor (925 ml) was concentrated to 230 ml, and cooled in ice to yield 215 g of crude corazole; the filtrate (35 g) was discarded. A solution of 750 g of the first-crystallization product in 375 ml of distilled water was boiled with 22.5 g of charcoal, filtered, and cooled in ice. The filtered corazole was washed with 100 ml of water and dried at room temperature. The yield of white corazole from the second crystallization, m.p. $58-59^{\circ}$, was 550 g. The mother liquor from the second crystallization with the wash-liquor (total volume 450 ml) was evaporated down to 190 and cooled in ice to yield a further 153 g of crude corazole.* This was added to the 215 g isolated earlier; twofold crystallization, as described above, of all the substance isolated from the condensed mother liquors (368 g) yielded a further 237 g of white second-crystallization corazole of m.p. $58-59^{\circ}$. The total yield of second-crystallization corazole, conforming to the State Pharmacopeia specifications, was 787 g.

* The mother liquor from the second crystallization and the wash-liquor may be used for the first crystallization in the next experiment.

Reaction of Caprolactam with Benzenesulfonyl Chloride. To a solution of 20 g (0.177 mole) of caprolactam and 18.8 ml (0.21 mole) of dry pyridine in 40 ml of dry chloroform there was added 31.4 g (0.177 mole) of benzenesulfonyl chloride at 0° during 1 hours. The mixture was added gradually to a solution of 32.3 g (0.21 mole) of hydrazine acetate in 220 ml of absolute alcohol, warmed to 35-36°. The reaction mass was cooled to 0°, a solution of 12.2 g (0.177 mole) of NaNO₂ in 30 ml of water was added, then 20% H₂SO₄ solution (~ 62 ml) was added slowly, the liquid was filtered, the filtrate was evaporated under vacuum, and the residue was extracted with chloroform. After evaporation of the solvent, the residue was distilled under vacuum. This yielded 8 g of caprolactam (b.p. 95-115° at 6-7 mm, m.p. 68-71°, m.p. of mixed sample with caprolactam 67-69°), and 14.5 g of an oil of b.p. 175-190° at 6-7 mm, which was treated with water. A crystalline substance of m.p. 58-59° was isolated (mixture with corazole melted at room temperature, m.p. after crystallization from aqueous alcohol 60-61°). The properties of this substance correspond to the properties of diphenyl disulfide [9].

Found %: S 29.89 C₁₂H₁₀S₂. Calculated %: S 29.36

The aqueous filtrate after separation of diphenyl disulfide was treated with 4% aqueous HgCl₂ solution to give 13.47 g of the double salt of corazole with HgCl₂ of m.p. 171-173° [10]; this corresponds to 4.55 g of corazole, which is 18.6% of the theoretical yield.

SUMMARY

Two variants of the synthesis of α,β -cyclopentamethylenetetrazole (corazole), suitable for practical use, have been developed. The starting material is cyclohexanone oxime in one case, and ϵ -leucine lactam in the other. The product is purified by crystallization from small volumes of water.

LITERATURE CITED

- [1] K. Schmidt, Ber. 54, 704 (1924).
- [2] J. Marcus, Rev. Chim. 1, 29 (1957).
- [3] German Patent 574943; Friedl. 19, 1437.
- [4] German Patent 537739; Friedl. 17, 2609.
- [5] German Patent 532969; Friedl. 18, 3051.
- [6] R. Benson and T. Cairns, J. Am. Chem. Soc. 70, 2115 (1948).
- [7] Organic Syntheses 4 (1953), p. 305 [Russian translation].
- [8] R. Stolle, Ber. 60, 1032 (1930).
- [9] C. Graeve, Lieb. Ann. 174, 189 (1874).
- [10] German Patent 439041; Friedl. 15, 333.

Received November 29, 1957

A NEW SYNTHESIS OF SULFANTHROL

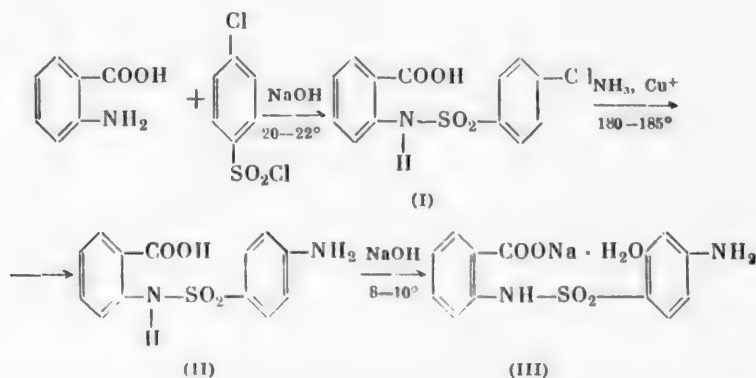
N. N. Dykhanov and A. S. Dykhanova

The Central Laboratory of the "Akrikhin" Pharmaceutical Factory, Moscow

In the production of sulfanilamide drugs, the main starting materials have always been the relatively costly and scarce acyl anilides. It has long been desirable and necessary to replace them by other, more readily available and cheaper materials.

At the present time the most promising types of intermediates available in our country for the production of sulfanilamide drugs are chlorobenzene or p-chlorobenzenesulfonic acid. Grigorovskii and his associates (including one of the present authors) have developed convenient industrial methods for the production of the acid chloride [1] and amide [2] of p-chlorobenzenesulfonic acid, and found the optimum conditions for the ammonolysis of p-chlorobenzenesulfonamide [3] and some of its derivatives [4, 5]. On the basis of these investigations the synthesis of sulfanilamide has been effected, with good economic characteristics, both from chlorobenzene and from technical p-chlorobenzenesulfonic acid on the pilot scale [6].

If a new form of raw material is used for sulfanilamide production, it will become necessary to convert the production of other sulfanilamide drugs to the same material, and we therefore effected the synthesis of another such drug, namely sulfanthrol, according to the scheme:



p-(N-o-Carboxyphenyl)chlorobenzenesulfonamide (I) was prepared in 85-90% yield by the interaction of 1.1 mole of p-chlorobenzenesulfonchloride with 1 mole of anthranilic acid in aqueous caustic soda solution at 20-22°.

Ammonolysis of p-(N-o-carboxyphenyl)chlorobenzenesulfonamide was effected by the heating of 1 mole of this compound with 8 moles of 25% aqueous ammonia solution in presence of 0.25 mole of cuprous chloride in a steel bomb at 180-185°. Under the stated conditions the reaction is complete in 3 hours. The maximum pressure in the bomb reaches 21 atmos. The yield of N¹-(o-carboxyphenyl)sulfanilamide (II) was 73.5-77% of the theoretical.

To convert N¹-(o-carboxyphenyl)sulfanilamide into its sodium salt (sulfanthrol), the substance was dissolved in a small excess of 10% aqueous caustic soda solution heated to 90-95°; after treatment with activated carbon, the salt was crystallized on cooling to 8-10°.

The quality of the sulfanthrol (III) so prepared conformed to all the specifications of the pharmacopœia.

EXPERIMENTAL

p-(N-o-Carboxyphenyl)chlorobenzenesulfonamide. A three-necked 750 ml flask, fitted with a stirrer and thermometer, contained 350 ml of 5% aqueous caustic soda solution and 13.7 g (0.1 mole) of anthranilic acid. To the stirred solution 26.5 g of moist crude 88% p-chlorobenzenesulfonyl chloride (equivalent to 23.3 g or 0.11 mole of the 100% compound) was added by small portions at 20-22°. The reaction mixture was kept weakly alkaline to phenolphthalein by periodic additions of the same caustic soda solution. After the sulfonyl chloride had been added, the reaction mixture was stirred for 2 hours at room temperature.

The resultant suspension of the sodium salt of p-(N-o-carboxyphenyl)chlorobenzenesulfonamide was heated to 95-100°, mixed with 2 g of activated charcoal, and filtered. To the filtrate*, cooled to 65-70°, 10% hydrochloric acid was added to a weak acid reaction to Congo red. The precipitated p-(N-o-carboxyphenyl)chlorobenzene-sulfonamide was filtered off, washed thoroughly with water, and dried at 105° to constant weight. This gave 27-28 g of substance of m.p. 202-204°; the yield was 85-90% of the theoretical calculated on anthranilic acid.

p-(N-o-carboxyphenyl)chlorobenzenesulfonamide is readily soluble in alcohol, acetone, and pyridine; it is insoluble in water, ether, and aromatic hydrocarbons; it crystallizes from alcohol (1:5) in the form of small colorless needles, m.p. 206-207°.

Found %: C 50.19; H 3.27; N 4.28; Cl 11.49 $C_{13}H_{10}O_4NClS$. Calculated %: C 50.08; H 3.20; N 4.49; Cl 11.37.

The sodium salt of p-(N-o-carboxyphenyl)chlorobenzenesulfonamide is readily soluble in water and pyridine; it is insoluble in alcohol, acetone, ether, and aromatic hydrocarbons; it crystallizes from water (1:3) in colorless leaflets. When dried, first at 65-70° and then at 120° to constant weight, the salt does not contain water of crystallization and melts with decomposition at 327-330°.

Found %: C 46.69; H 2.59; N 4.30; Cl 10.75 $C_{13}H_9O_4NClSNa$. Calculated %: C 46.78; H 2.71; N 4.19; Cl 10.62

N¹-(o-Carboxyphenyl)sulfanilamide. This compound was prepared by ammonolysis of p-(N-o-carboxyphenyl)-chlorobenzenesulfonamide. The ammonolysis was effected in a bomb of "EYa-1T" stainless steel, 430 ml in capacity, fitted with an electric heater, a thermometer socket, a manometer, and a needle valve for removal of excess ammonia.

The bomb was charged with 62.3 g of p-(N-o-carboxyphenyl)chlorobenzenesulfonamide, 125 ml of 25% aqueous ammonia [27.5 g (NH₃)] and 5 g of cuprous chloride. The closed bomb was heated to 180-185° and held at that temperature until the pressure ceased to fall (about 3 hours). The maximum pressure in the bomb reached 21 atmos, and toward the end of the reaction the pressure fell to 16 atmos.

After the end of the reaction, the bomb was cooled to 70° and then warmed slowly, while excess ammonia was released through the valve until there was no excess pressure at 100°. The bomb was then cooled to room temperature and opened. The reaction mass consisted of a suspension of crystalline ammonium salt of N¹-(o-carboxyphenyl)sulfanilamide in a dark-blue, weakly ammoniacal mother liquor.

The ammonium salt of N¹-(o-carboxyphenyl)sulfanilamide was filtered off, pressed out thoroughly, washed with 25-30 ml of cold water (43-45 g of the dry salt was obtained), and put in 150 ml of 10% aqueous caustic soda heated to 95-100°. The solution was heated to boiling, and air was blown through until the ammonia odor disappeared; 5 g of activated charcoal was then added to the solution, which was boiled for 15 minutes and filtered while hot.

The calculated quantity of 10% hydrochloric acid was added to the stirred filtrate, cooled to 65-70°, and the suspension which formed was cooled to 15-20°. The precipitated N¹-(o-carboxyphenyl)sulfanilamide was filtered off**, washed with water, and dried at 105° to constant weight.

* When the filtrate is cooled to 5-10°, the salt is again partially precipitated.

** If hydrochloric acid is added to a solution of the sodium salt of N¹-(o-carboxyphenyl)sulfanilamide until weakly acid to Congo red, the sparingly soluble hydrochloride of N¹-(o-carboxyphenyl)sulfanilamide is precipitated, m.p. 204-205° (from alcohol, 1:10).

This gave 38-40 g of substance* of m.p. 219-222°, which was then converted into sulfanthrol as described below.

After separation of the ammonium salt of N¹-(o-carboxyphenyl)sulfanilamide, the mother liquor still contained a certain amount of this salt, ammonium chloride, and the cuprous catalyst; to it 10% hydrochloric acid was added to a weakly acid reaction to Congo red. The precipitated crude hydrochloride of N¹-(o-carboxyphenyl)sulfanilamide was separated from the liquid phase (9-12 g of moist substance), dissolved in 25 ml of 10% aq. caustic soda solution, boiled for 30 minutes with 0.5 g of activated charcoal and 0.05 g of sodium hydrosulfite, and filtered again. The calculated quantity of 10% hydrochloric acid was added to the filtrate to precipitate pale-brown crude N¹-(o-carboxyphenyl)sulfanilamide in 6-9 g yield (dry weight). A single crystallization from 50% alcohol (1:5) with activated charcoal (0.5 g) as clarifying agent yielded 4.5-5.5 g of substance of m.p. 220-223°.

The total yield of N¹-(o-carboxyphenyl)sulfanilamide was 43-45 g, which corresponds to 73.5-77% of the theoretical.

Sodium Salt of N¹-(o-carboxyphenyl)sulfanilamide or Sulfanthrol. 29.2 g of N¹-(o-carboxyphenyl)sulfanilamide of m.p. 219-223° was dissolved at 90° in 50 ml of 10% aqueous caustic soda solution, the solution was stirred with 1.5 g of activated charcoal to clarify it (10-15 minutes), filtered, and the filtrate was cooled to 8-10°. The precipitated sulfanthrol was filtered off, washed with 15 ml of ice-cold water, pressed out thoroughly, and dried at 80-90° to constant weight. The yield was 20-25 g of sulfanthrol, of pharmacopeia grade.

After separation of sulfanthrol from the filtrate, unchanged N¹-(o-carboxyphenyl)sulfanilamide was isolated from the latter (9-10 g dry weight), and used in subsequent preparations of sulfanthrol. The total yield of sulfanthrol was about 96% of the theoretical calculated on N¹-(o-carboxyphenyl)sulfanilamide.

LITERATURE CITED

- [1] A. M. Grigorovskii, N. N. Dykhanov, and Z. M. Kimen, J. Appl. Chem. 28, 616 (1955).**
- [2] A. M. Grigorovskii, N. N. Dykhanov, and Z. M. Kimen, J. Gen. Chem 27, 531 (1957).**
- [3] A. M. Grigorovskii and N. N. Dykhanov, J. Appl. Chem 30, 1215 (1957).**
- [4] A. M. Grigorovskii and N. N. Dykhanov, J. Appl. Chem 30, 1352 (1957).**
- [5] A. M. Grigorovskii and T.N. Akif'eva, J. Appl. Chem 29, 154 (1956).**
- [6] A. M. Grigorovskii and P. A. Gangrskii, Med. Ind. USSR 3, 25 (1955).
- [7] M. V. Rubtsov and V. M. Fedosova, J. Gen. Chem. 14, 854 (1944).**

Received 1957

* After 2 or 3 recrystallization from alcohol (1:5), the substance melts at 225°, in agreement with literature data [7]. However, this degree of purity is not required for the production of sulfanthrol of pharmacopeia standard.

** Original Russian pagination. See C. B. Translation.

BRIEF COMMUNICATIONS

PREPARATION OF SPECTRALLY PURE RHODIUM

V. V. Lebedinskii, E. V. Shenderetskaya, and
A. G. Maforova

The N. S. Kurnakov Institute of General and Inorganic Chemistry,
Academy of Sciences, USSR

The triamine trichloride method, proposed by V. V. Lebedinskii, is widely used for the preparation of chemically pure rhodium. However, although the rhodium prepared by this method corresponds to the chemically pure rating, it does not conform to the high purity standards required in the construction of certain physical instruments. For removing the remaining (very slight) impurities, we have devised a method for additional purification of rhodium by means of sulfite compounds.

The principal method for separation of base elements from metals of the platinum group is the nitrite method.

The principle of this method is that 45% solution of sodium nitrite is added to a solution of chlororhodic acid in hydrochloric acid, in the proportion of 4 to 6 g of sodium nitrite to 1 g of metal present in the solution. All the platinum-group elements form soluble complex compounds. Rhodium and iridium are present in the solution as $\text{Na}_3[\text{Rh}(\text{NO}_2)_6]$ salts, platinum and palladium as $\text{Na}_2[\text{Pt}(\text{NO}_2)_4]$ salts and base elements are precipitated as the hydroxides.

The reaction is conducted at the boil until a straw-yellow solution is formed:



It follows from the above equation that, when sodium nitrite is added to a solution of $\text{H}_3[\text{RhCl}_6]$, hydrochloric acid is formed, which decomposes sodium nitrite, and therefore excess of sodium nitrite is taken for the reaction. After separation of base-metal hydroxides, ammonium chloride is added to the filtrate to give a solution containing 12% ammonium chloride. Ammonium sodium hexanitrorhodate $(\text{NH}_4)_2\text{Na}[\text{Rh}(\text{NO}_2)_6]$ is precipitated. The precipitate is filtered off and washed with 4-5% ammonium chloride solution and distilled water:



When the ammonium sodium hexanitrorhodate is precipitated, the salts of bivalent platinum and palladium remain in solution because of their high solubility.

For further purification of rhodium from traces of noble metals, ammonium sodium hexanitrorhodate is converted into trinitritotriamine rhodium $[\text{Rh}(\text{NH}_3)_3(\text{NO}_2)_3]$. For this, ammonium sodium hexanitrorhodate is added by small portions to a boiling solution of ammonia, and the liquid is boiled until the precipitate is completely dissolved. 1.6 ml of ammonia and 20 ml of water should be taken per 1 g of salt. When the ammonium sodium hexanitrorhodate has dissolved, the solution is boiled until trinitritotriamine rhodium begins to crystallize; the mother liquor is then decanted and boiled until a fresh portion of precipitate appears. The precipitate is filtered off and washed with distilled water:



The rhodium is purified further by conversion of its trinitritotriamine into the trichlorotriamine.

The precipitate of trinitrototriammine rhodium is covered with hydrochloric acid of 1:2 dilution and boiled until evolution of nitrogen oxides ceases. The reaction proceeds according to the equation:



The solution with the precipitate is then cooled and filtered; the filtrate is orange in color. The trichlorotriammine rhodium is again treated with hydrochloric acid and this procedure is repeated until the hydrochloric acid solution filtered from the trichlorotriammine is almost colorless.

After these operations, the trichlorotriammine rhodium may be regarded as chemically pure, but it still contains some hundredths of one per cent of noble and base metals. These small amounts of impurities can be removed by conversion of trichlorotriammine rhodium into a sulfite compound.

As a result of a series of investigations we reached the conclusion that trichlorotriammine rhodium is the most convenient starting material for preparation of high-purity rhodium.

When trichlorotriammine rhodium is dissolved in ammonium sulfite, platinum, palladium, iron, copper, and other metals remain in the residue, while rhodium and iridium dissolve in excess ammonium sulfite.

Trichlorotriammine rhodium is dissolved in boiling ammonium sulfite solution, and the mixture is boiled until the ammine is completely dissolved. This results in the formation of ammonium trisulfitorhodate, which is easily soluble in saturated ammonium sulfite solution:



The liquid is filtered to remove the precipitate (containing Pt, Pd, Cu, etc.), and again heated to boiling, with hydrochloric acid. When hydrochloric acid is added to the solution, a small amount of trichlorotriammine rhodium may be formed (as the result of insufficient boiling of trichlorotriammine rhodium with ammonium sulfite). In that case the precipitated trichlorotriammine rhodium is filtered off, and the solution is heated with hydrochloric acid until ammonium chlororhodate is precipitated.

A sample of the ammonium chlororhodate is taken separately and tested for purity. If the chlororhodate is found to be pure, it is filtered off, washed with dilute ammonium chloride solution, and heated to the metal. If iridium is detected in the ammonium chlororhodate, the purification should be effected by way of ammonium trisulfitorhodate $(\text{NH}_4)_3[\text{Rh}(\text{SO}_3)_3]$. For this, the impure ammonium chlororhodate is decomposed by chlorination with the aid of aqua regia until the ammonium ions are completely destroyed. The solution is evaporated almost to dryness, diluted with water, filtered, and ammonium sulfite is added in the proportion of 15 ml of saturated ammonium sulfite solution to 1 g of rhodium.

When the liquid is heated on the water bath, ammonium trisulfitorhodate is formed; this is readily soluble in a large excess of ammonium sulfite and in hydrochloric acid, and is almost insoluble in water:



Iridium remains in solution, forming readily soluble chlorosulfite complex compounds. The ammonium trisulfitorhodate is filtered off, washed with water, and tested for purity.

If the compound is free from impurities and conforms to the required purity standards, it is converted into ammonium chlororhodate and heated to the metal.

If traces of iridium are still detected, the sulfite purification must be repeated. If the rhodium is contaminated with other metals, in addition to iridium, the purification should be repeated by the trichlorotriammine method.

In conclusion, the results of spectrum analysis of a sample of purified rhodium are given below.

The original trichlorotriammine rhodium contained the following impurities: Pt and Pd 0.02%, Ir 0.02%, Cu 0.02%, Fe traces. After the first sulfite purification the copper content fell to 0.01%. Platinum and iron remained as traces. Palladium and iridium were not detected.

After a second sulfite purification, copper could not be detected by spectrum analysis. Platinum metals and iron were not found either.

Received November 17, 1958

PREPARATION OF SPECTRALLY PURE PALLADIUM

A. M. Rubinshtein and S. K. Sokol

The N. S. Kurnakov Institute of General and Inorganic Chemistry,
Academy of Sciences, USSR

Modern methods for preparation of pure palladium can yield palladium of fairly high purity. However, even the best product contains 99.98-99.99% palladium. Platinum, gold and rhodium, in decreasing order, are always present as impurities in palladium. As it was required to investigate the standard physical properties of palladium, we were concerned with the problem of preparing spectrally pure palladium.

The problem was difficult because not only was it necessary to develop a new method for preparation of physically pure palladium, but absolutely pure reagents were needed, which we had to prepare ourselves.

All the experiments were conducted in vessels free from traces of other noble metals.

The essential problem was to find means for removing traces of platinum and gold in presence of a high palladium content.

Technical palladium, from which the spectrally pure metal was to be prepared, was dissolved in aqua regia; the solution was then evaporated with hydrochloric acid and hot water to remove excess HNO_3 and to decompose nitroso compounds. The following compounds are formed in solution: $\text{H}_2[\text{PdCl}_4]$, $\text{H}_2[\text{PtCl}_6]$, $\text{H}[\text{AuCl}_4]$, $\text{H}_3[\text{RhCl}_6]$; of these, $\text{H}_2[\text{PtCl}_6]$, $\text{H}[\text{AuCl}_4]$ and $\text{H}_3[\text{RhCl}_6]$ are present in very small amounts.

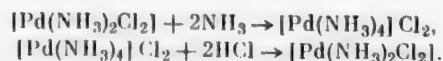
Special conditions are required for complete removal of platinum, rhodium, and gold from the solution, as their concentrations are very low while the concentration of palladium salts is high.

Because of this, separation of platinum from such solution by the use of NH_4Cl solution for precipitation of $(\text{NH}_4)_2[\text{PtCl}_6]$ does not give successful results. Part of the platinum always remains in solution. We therefore proposed, before precipitation of platinum as $(\text{NH}_4)_2[\text{PtCl}_6]$ to subject the $\text{H}_2[\text{PdCl}_4]$ solution to the action of gaseous chlorine to oxidize part of the $\text{H}_2[\text{PdCl}_4]$ to $\text{H}_2[\text{PdCl}_6]$. This reaction proceeds very readily - in our experiment about 10% of the total $\text{H}_2[\text{PdCl}_4]$ was oxidized to $\text{H}_2[\text{PdCl}_6]$. When NH_4Cl solution acts on $\text{H}_2[\text{PdCl}_6]$ solution, insoluble ammonium chloropalladate $(\text{NH}_4)_2[\text{PdCl}_6]$ is precipitated; this takes all the chloroplatinate with it, as $(\text{NH}_4)_2[\text{PtCl}_6]$ and $(\text{NH}_4)_2[\text{PdCl}_6]$ are isomorphous.

Platinum cannot be detected in the solution after separation of the precipitate of $(\text{NH}_4)_2[\text{PdCl}_6]$ and $(\text{NH}_4)_2[\text{PtCl}_6]$. If the solution, after separation of the chloropalladate and chloroplatinate, is oxidized again, the precipitated $(\text{NH}_4)_2[\text{PdCl}_6]$ is quite free from platinum.

Palladium, containing about 1% platinum, was tested. From 196.3 g of palladium we obtained a precipitate of $(\text{NH}_4)_2[\text{PdCl}_6]$ and $(\text{NH}_4)_2[\text{PtCl}_6]$, which gave 6.63 g of metal when heated; this metal contained 28.87% Pt. The second chloropalladate gave 4.35 of metal on heating. This contained only 0.00005 g of platinum, which corresponded to 0.01% platinum in the palladium. In the third chloropalladate fraction platinum could not be detected by chemical methods. It follows therefore that, when part of the palladium is precipitated as chloropalladate, all of the platinum is precipitated with it, and the solution no longer contains platinum. The solution $\text{H}_2[\text{PdCl}_4]$ is heated (to remove excess chlorine and to reduce $\text{H}_2[\text{PdCl}_6]$ to $\text{H}_2[\text{PdCl}_4]$) and treated with ammonia. A precipitate of Vauquelin's salt $[(\text{NH}_3)_4\text{Pd}][\text{PdCl}_4]_2$ is first formed, and then dissolves in excess NH_4OH on heating to form $[\text{Pd}(\text{NH}_3)_2\text{Cl}_2]$. Base metal impurities are precipitated as hydroxides.

The solution of $[\text{Pd}(\text{NH}_3)_4]\text{Cl}_2$ is treated with hydrochloric acid. The palladosammine $[\text{Pd}(\text{NH}_3)_2\text{Cl}_2]$ is precipitated as a result. The palladosammine is reprecipitated several times from ammonia and hydrochloric acid by the reactions:



It was observed during the reprecipitation of the palladosammine that after filtration of the $[\text{Pd}(\text{NH}_3)_4]\text{Cl}_2$ solution a very small precipitate remained, the amount of which decreased in consecutive reprecipitations. Investigation of this precipitate showed it to contain a small amount of gold.

Spectrum analysis of the palladosammine showed that it contained a very small amount of gold. Other platinum metals were not detected. Moreover, no traces of copper, nickel, iron, or other base metals were found.

Thus, it proved possible to obtain palladium containing no impurities other than gold.

It was necessary to work out a method for preliminary removal of gold from palladium before extraction of platinum.

For this, we proposed treatment of the $\text{H}_2[\text{PdCl}_4]$ solution with hydrogen sulfide before oxidation by chlorine. By the action of hydrogen sulfide, gold is reduced to the metal while platinum and palladium are partially precipitated as sulfides. The gold formed by reduction is always finely divided and is very difficult to filter off. In this instance, the reduction of gold is accompanied by precipitation of platinum and palladium sulfides. The precipitate entrains all the finely divided gold from solution. The amount of palladium precipitated as sulfide is very small. In this manner it is possible to remove all the gold before precipitation of platinum. After separation of the sulfides and gold, the solution is oxidized by gaseous chlorine, and 25% NH_4Cl solution is added to precipitate the chloropalladate, which contains all the platinum as chloroplatinate.

After separation of this precipitate the solution is treated with ammonia and then with hydrochloric acid to precipitate the palladosammine.

The palladosammine is reprecipitated 3-5 times from ammonia and hydrochloric acid. No impurities were detected in the palladosammine obtained by this method.

The palladosammine is heated with great care in an alumina crucible. The palladium must be cooled rapidly after the heating to minimize the amount of palladium oxides formed.

The resultant mixture of metallic palladium and palladium oxides, of various colors from green to blue, is molded, fused in a high-frequency furnace, and subjected to mechanical treatment.

Investigations of the physical properties of this palladium, carried out in the Institute of Measures and Measuring Instruments, showed it to be spectrally pure. About 200 g of spectrally pure palladium was obtained by this method.

Received November 19, 1958

ELECTROLYTIC PREPARATION OF POTASSIUM PERBORATE

N. E. Khomutov and A. T. Sklyarov

Although the electrolytic process for production of sodium perborate was developed many years ago, it is still far from perfect, as the current efficiencies for the final product do not exceed 40-50% and costly platinum anodes are required for the process. Further improvement of the electrolytic process for the production of perborates is held back because the influence of the experimental conditions on the course of the anode processes, on which this method is based, is not fully understood. Further experimental data in this field are needed also for a correct understanding of the mechanism of anodic formation of perborates.

The theories, which have been advanced to explain the anodic formation of perborates [1-3], including the universal theory of electrooxidation proposed by Glasstone and Hickling [4], could not account for all the observed facts and have not been universally accepted [5].

In this connection the electrolysis of solutions of carbonates, borates, and their mixtures is being studied in our laboratory. The results of these investigations have been partially reported earlier [6]. The present communication contains some results obtained in a study of the influence of electrolyte composition on the anodic oxidation of borate-carbonate solutions.

Analysis of earlier kinetic data [6] showed that the rate of the anode processes increase with increasing contents of borax and carbonate in solution. These results suggest that higher current efficiencies should be expected with the use of higher concentrations of borax and carbonates in the original electrolyte. Since the solutions of borax and soda mixtures used in industry are very close to saturation, the aim of the present work was to study the possibility of using the very soluble potassium carbonate instead of soda as the electrolyte.

Electrolyte composition (moles/liter)	Current efficiency (%)
Borax 0.10 + potash 1.17	49.8
Borax 0.33 + potash 3.61	88.5
Borax 0.52 + potash 3.61	93.0

Our electrolysis experiments were conducted in a U-shaped glass vessel of 400 ml capacity; one branch of the vessel contained a cylindrical porous ceramic vessel, which served as the cathode compartment. The other branch of the vessel acted as the anode compartment. The U-shaped tube was contained in a vessel cooled by running water. The cathode was an iron plate with a working area of 1 cm². The current source was a VSA-3m selenium rectifier. The temperature in the electrolytic cells was maintained at the required level

by regulation of the water flow. The temperature was measured within the vessel itself. Reagents of chemically-pure grade were used for preparation of the solutions.

The course of the anode processes was observed by measurements of current efficiencies for active oxygen in the solution. For this, samples were taken from the electrolyzed solutions after thorough stirring, acidified with sulfuric acid, and titrated by potassium permanganate. The anodes were made from different materials, in the form of wires, plates, or rods. The working anode surface was 1-0.5 cm².

A positive result was obtained in the study of the possible use of mixtures of borax and potash as electrolytes. It was found that with the use of such mixtures, solutions of considerably higher concentrations could be obtained than with the use of borax-soda mixtures. The table gives current efficiencies for active oxygen determined for solutions of potash-borax mixtures of three different compositions. The anode in this case was a

platinum plate with a working area of 0.6 cm^2 . The temperature during electrolysis did not exceed 9° . The current density was 0.5 amp/cm^2 . The current efficiency was determined after 1.5 amp-hr of electricity had been passed.

The data in the table show that with the use of concentrated solutions of potash-borax mixtures as electrolytes, very high current efficiencies for active oxygen can be attained at a platinum anode.

Experiments on electrolysis of borax-potash mixtures, with the use of carbon and lead anodes, showed that the current efficiencies were again higher than the corresponding values for borax-soda solutions, and reached over 10% of the theoretical in highly concentrated solutions.

Active oxygen was also formed, with low current efficiencies, if silver and nickel anodes were used. When magnetite, iron, bismuth, tungsten, molybdenum, copper, or tantalum were used as anode materials, active oxygen was not formed either in borax-potash or in borax-soda solutions.

Our results obtained with the use of borax-potash mixtures show that such mixtures can be used for electrolytic production of perborates. In consequence of these results our investigations of the electrolysis of potash-borax mixtures are continuing.

A series of polarization determinations was carried out for solutions of different borax-potash mixtures with platinum, carbon, and lead anodes. Analysis of the polarization data showed that polarization values are lower in borax-potash solutions than in soda-borax solutions, and that the relationship between the anode potential and the logarithm of the current density is linear and conforms to the Tafel equation. The constant b in the Tafel equation in this case exceeds 0.5.

LITERATURE CITED

- [1] F. Foerster, Z. ang. Chem. 34, 354 (1921).
- [2] W. G. Polack, Z. Elektroch. 21, 253 (1915).
- [3] K. Arndt, Z. Elektroch. 22, 63 (1916).
- [4] S. Glasstone and A. Hickling, Progr. Chem. 10, 108 (1941).
- [5] M. Haisinsky, Discuss. Faraday Soc. 1, 254 (1947).
- [6] N. E. Khomutov and M. F. Sorokina, J. Phys. Chem. 32, 1956 (1958).

Received February 18, 1958

SEPARATE DETERMINATION OF CYCLOHEXANONE AND CYCLOHEXANOL IN AQUEOUS SOLUTIONS

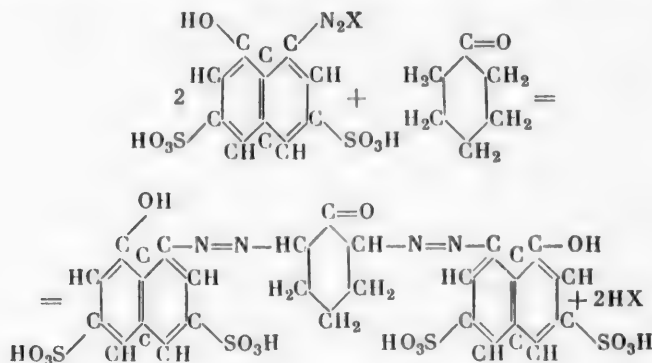
A. S. Masiennikov

Laboratory of the Prophylactic Disinfection Section of the Gor'kii Regional Sanitary and Epidemic Station

Analytic methods for cyclohexanone and cyclohexanol, based on reactions on their functional groups [1, 2], are complex in procedure, generally involve nonaqueous media, and are suitable for high concentrations.

Other methods, based on various condensation and polymerization reactions [3-5], are applicable only to determinations of either of the substances individually or in the presence of small amounts of the other.

We showed earlier [6] that cyclohexanone can form an azo dye when coupled with the diazonium salt of H acid (1-naphthylaminoethoxy-3,6-disulfonic acid), in accordance with the equation



Subsequent investigations showed that this reaction can be used for separate determination of cyclohexanone and cyclohexanol in aqueous solutions. For determination of cyclohexanol, the latter was oxidized quantitatively to cyclohexanone by a solution of chromic anhydride in sulfuric acid. The chromic anhydride for this was prepared from potassium dichromate as described by Karyakin [7], without isolation in the free state from solution. After separation of potassium hydrogen sulfate, the filtrate was diluted 25-fold by concentrated sulfuric acid and used for oxidation of cyclohexanol.

Under the usual conditions, for determination of cyclohexanone by the reaction with H acid diazonium salt, the cyclohexanol present is partly converted into cyclohexanone and tends to lead to high results. Addition of acetic anhydride and urotropin to the solution prevents this process, without affecting adversely the course of analysis. Cyclohexanone and cyclohexanol may be determined either by the usual colorimetric methods, or by colorimetric titration with standard aqueous solutions of the azo dye, formed by the coupling of cyclohexanone with the diazonium salt of H acid. The azo dye required for preparation of the standard solution, can be prepared as described in our preceding paper [6].

EXPERIMENTAL

The artificial aqueous solutions, containing cyclohexanone and cyclohexanol, were prepared from chemically pure reagents, the constants of which agreed with literature data. Cyclohexanone, b.p. 155°, n_D^{20} 1.450; cyclohexanol, b.p. 161°, n_D^{20} 1.465.

Results of Separate Determinations of Cyclohexanone and Cyclohexanol by the Reaction With the Diazonium Salt of H Acid and Colorimetric Titration

Taken (μ g)		Cyclohexanone found		Cyclohexanol found	
cyclo-hexanone	cyclo-hexanol	in μ g	in %	in μ g	in %
1	100	1.1	110	92	92
5	95	4.5	90	88	97.7
10	90	10.5	105	92	102.2
20	80	19.5	97.5	78	97.5
30	75	31	103.3	76	101.3
40	70	42	105	72	102.3
50	60	49	98	63	105
60	50	62	103.3	48	96
70	40	68	97.1	43	107.5
80	30	82	102.5	28	93.3
90	20	89	98.8	22	110
100	10	99	99	11	110

Determination of Cyclohexanone in Presence of Cyclohexanol

Reagents: acetic anhydride, 10% aqueous solution of urotropin (hexamethylenetetramine), freshly-prepared 1% sodium metabisulfite solution, 25% aqueous sodium hydroxide solution, freshly-prepared solution of H acid diazonium salt (prepared by the mixing, in 1:1 ratio, of a 1% sodium nitrite solution and 0.25 % solution of the monosodium salt of H acid in 0.05 N sulfuric acid), standard aqueous solution of cyclohexanone, containing 0.1 mg per ml for ordinary colorimetric determinations, or a millimolar solution of the azo dye (0.758 mg of dye per ml of solution) for determination by colorimetric titration.

Analytical procedure. One drop (about 0.02 ml) of acetic anhydride and 0.2 ml of 10% urotropin solution are added to 1 ml of the test solution, containing from 1 to 100 μ g of cyclohexanone in a test tube. The liquids are mixed and 0.2 ml of 1% sodium metabisulfite solution, 0.2 ml of caustic soda, and 0.5 ml of the solution of H acid diazonium salt are added. After 5 minutes the solution is diluted with water to 10 ml and examined colorimetrically.

In determination of cyclohexanone by colorimetric titration, 1 ml of water is taken in another tube, and the same amounts of the reagents are added to the test sample. After dilution with water to 10 ml, standard solution of the azo dye is added until the color matches that of the test sample. 1 ml of millimolar solution of the azo dye corresponds to 98 μ g of cyclohexanone.

Results of cyclohexanone determinations by colorimetric titration are given in the table.

Determination of Cyclohexanol in Presence of Cyclohexanone

Reagents: 50% sodium hydroxide solution, 10% sodium sulfite solution, solution of H acid diazonium salt as used for cyclohexanone determination, solution of chromic anhydride (about 5 mg per ml) in concentrated sulfuric acid, standard solution of cyclohexanone or azo dye as for cyclohexanone determination.

Analytical procedure. The cyclohexanone content is determined in a separate sample. Then 1 ml of the test solution is put in a test tube, 0.3 ml of chromic anhydride solution in concentrated sulfuric acid is added, and the liquid is mixed and left to stand for 20 minutes. After 20 minutes 0.2 ml of 10% sodium sulfite solution is added (with three 0.5 ml portions of alkali, with 5-minute intervals between the additions) and 1 ml of H acid diazonium salt solution; the liquid is mixed. After 5 minutes it is diluted with water to 10 ml and examined colorimetrically.

Colorimetric titration for determination of cyclohexanol is carried out as described for the analysis of cyclohexanone. 1 ml of a millimolar solution of the azo dye corresponds to 100 μ g of cyclohexanol.

In calculations of the results of determinations of cyclohexanol in presence of cyclohexanone, the amount of cyclohexanone found in the sample without oxidation must be subtracted from the amount found in the sample oxidized by chromic anhydride. The difference, multiplied by the factor 1.02, corresponds to the amount of

cyclohexanol in 1 ml of the test solution. The results of cyclohexanol determinations in presence of cyclohexanone are given in the table.

SUMMARY

1. A method has been developed for separate determinations of cyclohexanone and cyclohexanol in aqueous solutions, by means of the reaction with H acid diazonium salt; with this method the determinations can be carried out either by the usual colorimetric methods or by colorimetric titrations with standard aqueous solutions of the azo dye formed by the coupling of cyclohexanone with H acid diazonium salt.
2. The error in determination of microgram quantities of cyclohexanone and cyclohexanol does not exceed 10%.

LITERATURE CITED

- [1] H. A. Joles and A. W. Lon, *Ind. Eng. Chem., Anal. Ed.* 2, 102 (1939).
- [2] P. Elwing and B. Warshawsky, *Ind. Eng. Chem., Anal. Ed.* 1, 20 (1942).
- [3] J. F. Freon, W. E. Grutchfeld, and K. V. Kutzmeller, *J. Ind. Hyg. and Toxicol.* 25, 393 (1943).
- [4] S. Nagare and J. Mitchel, *Anal. Chem.* 25, 1376 (1953).
- [5] A. S. Maslennikov, *Industrial Laboratory* 20, No. 1, 40 (1954).
- [6] A. S. Maslennikov, *J. Appl. Chem.* 31, No. 8, 1277 (1958).*
- [7] Yu. V. Karyakin, *Pure Chemical Reagents* [in Russian] (1936) p. 79.

Received March 1, 1958

*Original Russian pagination. See C. B. Translation.

APPARATUS FOR PREPARATION OF SALTS BY ANODIC SOLUTION OF METALS

V. I. Kravtsov and Yu. N. Polovoi

Metals and solutions of the appropriate acids are often used as starting materials for preparation of pure metal salts. However, the spontaneous solution of certain pure metals in acids, with liberation of hydrogen, is an extremely slow process [1]. Among such metals are those with high hydrogen overvoltages (Cd, Zn, Pb, Sn) [2].

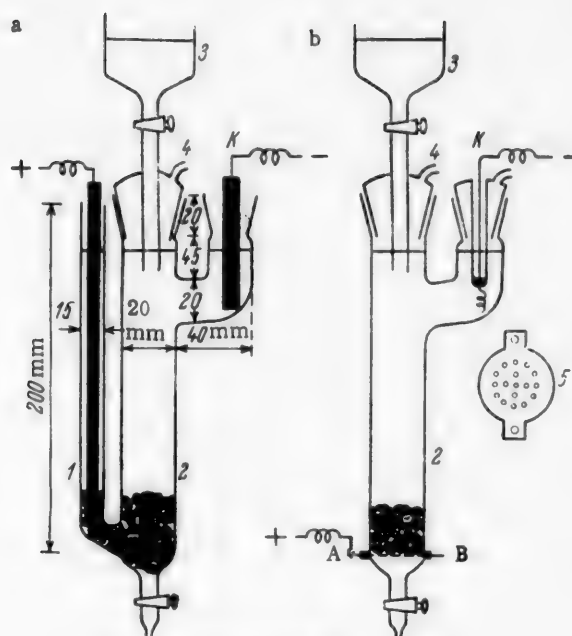
In a number of cases anodic solution is suitable method for preparation of salts from metals; the present paper deals with the applicability of this method for preparation of cadmium sulfate.

The mechanism of anodic solution of cadmium in H_2SO_4 solutions has been the subject of several investigations [3-7]. It follows from the available literature data that the φ -log i curves, representing the anode process of cadmium dissolution, have a linear region with the coefficient $b \approx 0.03$ V, the value of which shows that the stage of diffusion of cadmium ions into the solution determines the rate of the whole process [3, 7].

The cells used for preparation of cadmium sulfate are shown in the diagram. A layer of granulated cadmium was put into cell a so that it filled the lower parts of tubes 1 and 2. Then the anode A and cathode K were inserted into the apparatus (the electrodes were metallic cadmium rods) and acid was poured in through the funnel 3. The tube 4 served as an outlet for the gases liberated at the anode. The contact between the anode A and granulated cadmium, which served as the soluble anode, was checked for reliability and direct current at ~ 15 V was then passed through the cell. When the cell, in which the diameter of the working tube was 20 mm, (see figure) was used, the optimum current strength was 1.5 amp. At this current strength a temperature of $80-90^\circ$ was established in the cell. Higher current strengths caused intensive agitation of the solution, so that cadmium ions entered the cathode compartment more easily and the current efficiency for cadmium sulfate decreased.

The dissolving granules of metallic cadmium formed $CdSO_4$ solution, which collected at the bottom of the apparatus because of its high density. In 3 N H_2SO_4 solution a fairly distinct boundary could be observed after 1-2 hours of anodic dissolution above the layer of granulated cadmium between the heavy solution containing predominantly cadmium sulfate and the lighter solution, containing predominantly sulfuric acid. As the concentrated solution, containing $CdSO_4$ appears, it should be run off through the stopcock into a receiver, because otherwise there is a sharp increase in the amount of metallic cadmium liberated in spongy form together with hydrogen at the cathode. If conditions ensuring minimum agitation of the electrolyte are maintained, the deposit of spongy cadmium at the cathode grows rather slowly and does not give rise to any great inconveniences because it is easily detached from the cathode and, after the included hydrogen has been pressed out, it can be dissolved at the anode.

When 3 N H_2SO_4 solution was used under the conditions described above, the samples initially taken had the approximate composition 4.5 N $CdSO_4$ + 1 N H_2SO_4 , i.e., about 80% of the total electrolyte concentration was cadmium sulfate. In subsequent samples the decrease of the total electrolyte concentration was accompanied by a decrease in acidity, but the increase of the percentage content of cadmium sulfate was slight. To balance the loss of the expended sulfuric acid, sulfuric acid solution of higher concentration (~ 4 N) was poured into the apparatus during operation; this concentration corresponded to the average total concentration of the product. Experiments with 8 N H_2SO_4 did not give satisfactory results, as the acid concentration in samples did not fall below 5-6 N.



General view of the cell.

A cell of type b (see diagram) can be recommended for preparation of salts from metals which for any reason cannot be formed into conducting rods. In this case the anode connection is the plate 5 made from platinum, tantalum, or some other sufficiently inert metal, with a number of orifices. The diaphragm 5 is fixed between two ground-glass plates. This may be effected by means of Bakelite varnish, which is fairly resistant to acids after thermal polymerization. The cathode may be platinum or some other metal inert in the given electrolyte. If a tantalum diaphragm is used, care must be taken that the main mass of the metal at the anode does not dissolve, because otherwise the anode potential may reach values at which tantalum becomes passive.

The proposed method for preparation of cadmium sulfate has the advantage that, when cadmium is anodically dissolved, a considerable proportion of the impurities present in the original metal does not pass into solution. Thus, spectrum analysis showed that cadmium sulfate made by anodic solution of analytical-grade cadmium in reagent-grade sulfuric acid contained $\sim 0.003\%$ Cu, $\sim 0.003\%$ Pb; the Fe content was below 0.001% , and was not detected by spectrum analysis. The original cadmium, according to spectroscopic data, contained 0.03% Pb, 0.05% Cu and $\sim 0.002\%$ Fe. These results show that the contents of such impurities as Pb, Cu and Fe in cadmium sulfate, made by anodic dissolution of cadmium, are decreased roughly tenfold. The impurities, which accumulate on the anode in the form of black sludge, should be removed at intervals from the anode compartment.

The cells described in this paper may be used for production of salts of either base or noble metals which dissolve at the anode.

In conclusion, we thank Professor Ya. V. Durdin for valuable advice in the course of this work.

LITERATURE CITED

- [1] A. N. Frumkin, Proc. 2nd Conference on Metal Corrosion, 1 [In Russian] (1940).
- [2] A. N. Frumkin, V. S. Bagotskii, Z. A. Iofa, and B. N. Kabanov, Kinetics of Electrode Processes [In Russian] (Izd. MGU, 1952).
- [3] O. Gatty and E. Spooner, The Electrode Potential Behavior of Corroding Metals in Aqueous Solutions, 420 (1938).
- [4] G. Kimball and A. Glassner, J. Chem. Phys. 8, 820 (1940).

- [5] Ya. M. Kolotyrkin and L. A. Medvedeva, *J. Phys. Chem* 27, 1344 (1953).
- [6] Ya. M. Kolotyrkin and L. A. Medvedeva, *J. Phys. Chem* 29, 1477 (1955).
- [7] V. I. Kravtsov and I. S. Loginova, *J. Phys. Chem* 31, 2438 (1957).

Received October 23, 1957

REACTION OF AMMONIA WITH THE OXIDE OF PETROSELINIC ACID

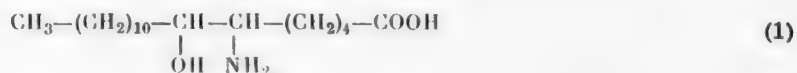
G. V. Pigulevskii, I. L. Kuranova, and E. V. Sokolov

It was reported in our previous papers [1, 2] that the oxides of oleic acid (cis- Δ^9 -octadecenoic acid) and elaidic acid (trans- Δ^9 -octadecenoic acid) add on ammonia with formation of the corresponding hydroxy amino acids.

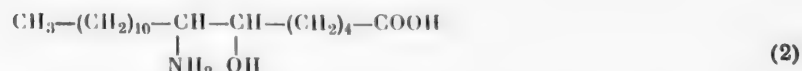
The present paper deals with a study of the action of ammonia on the oxide of petroselinic acid (cis- Δ^6 -octadecenoic acid).

The oxide of petroselinic acid of m.p. 59-60° was prepared by oxidation of the acid by peracetic acid. The reaction between ammonia and the oxide was conducted at 130°. The product had m.p. 133-134° after recrystallization from alcohol; it was soluble in dilute acids, alkalies, and alcohol, and was insoluble in water, ether, and benzene.

The hydroxyaminostearic acid, synthesized by means of the reaction of ammonia with petroselinic acid oxide, had the composition $C_{18}H_{37}O_3N$, according to elementary analysis and may have the structure:



or



Oxidation of the substance by lead tetraacetate [3] yielded lauric aldehyde (semicarbazone m.p. 102-102.5° [4], 2,4-dinitrophenylhydrazone, m.p. 106° [5]) and a nitrogen-containing compound, which yielded adipic acid on hydrolysis.

The nitrile of lauric acid, which should be formed if the compound had structure (2), was not detected.*

We assume on the basis of the oxidation results that hydroxyaminostearic acid of m.p. 133-134° has the structure 6-amino-7-hydroxyoctadecanoic acid (1).

We synthesized the hydrochloride of hydroxyaminostearic acid, of composition $C_{18}H_{36}O_3NCl$ and m.p. 81.5-83°.

EXPERIMENTAL

Petroselinic acid oxide of m.p. 59-60° was prepared by oxidation of petroselinic acid** by peracetic acid by the method described previously [2]. Petroselinic acid oxide was prepared for the first time by oxidation of petroselinic acid by perbenzoic acid [6]. The purity of the substance was determined by elementary analysis.

* Lauric acid nitrile was specially synthesized in order to test its volatility in steam. We found no information in the literature with regard to this property. It was found that the nitrile is quantitatively volatile in steam.

** Petroselinic acid of m.p. 32° and iodine number 87 was isolated from coriander oil.

Found %: C 72.53; 72.50; H 11.27; 11.50 $C_{18}H_{34}O_3$. Calculated %: C 72.42; H 11.45

The reaction between ammonia and petroselinic acid oxide was carried out under the conditions described earlier [2]. A substance was obtained which, after repeated recrystallization from alcohol, melted at 133-134°. Further recrystallization did not raise the melting point; the yield was 61%.

Found %: C 68.44; 68.45; H 11.58; 11.86; N 4.40; 4.68 $C_{18}H_{37}O_3N$. Calculated %: C 68.52; H 11.82; N 4.44

Oxidation by Lead Tetraacetate. 50 ml of glacial acetic acid was added to 6.7 g of hydroxyaminostearic acid in a round-bottomed flask fitted with a reflux condenser. To this solution 18.8 g of lead tetraacetate was added in small portions during two hours at room temperature. The reaction mixture was then diluted with 50 ml of water and distilled in steam. From 200 ml of distillate 2 g of an oily colorless substance with a sharp odor was obtained. It gave a positive test with Schiff's reagent. Qualitative tests showed the presence of very small traces of nitrogen; this was confirmed by quantitative determination of nitrogen. The substance gave the silver mirror reaction; with semicarbazide it formed a semicarbazone, which melted at 102-102.5° after crystallization from methyl alcohol.

Found %: N 17.70; 17.43 $C_{18}H_{27}ON_3$. Calculated %: N 17.45

In addition, the 2,4-dinitrophenylhydrazone was prepared; m.p. 106°, in agreement with literature data [5].

The residue in the flask after steam distillation was extracted with ether; the ether extract was washed thoroughly with water acidified with hydrochloric acid, and then again with water to a neutral reaction. The extract was dried over sodium sulfate and the ether was evaporated off; the residue, which was a thick brown mass shown by the Lassaigne test to contain nitrogen, was hydrolyzed in 2 N alcoholic potassium hydroxide (30 ml) on heating on a water bath. Ammonia was liberated copiously during hydrolysis. At the end of the hydrolysis, alcohol was evaporated off to dryness; the potassium salt was dissolved in water, dilute hydrochloric acid was added to an acid reaction, and the liquid was extracted with ethyl acetate. The residue after evaporation of the solvent was a resinous mass from which a white solid substance was extracted by treatment with boiling water.

Paper chromatography [7] (with butanol saturated with water as the solvent and known adipic acid as the reference substance) showed that this substance was adipic acid.

Preparation of Hydrochloride of the Composition $C_{18}H_{35}O_3NH_2 \cdot HCl$. To 4 g of hydroxyaminostearic acid there was added 20 ml of ethyl acetate containing 0.5 g of gaseous hydrogen chloride. Crystals were precipitated; these were filtered off and recrystallized from ethyl acetate and ether. Melting point 81.5-83°.

Found %: Cl 10.10; 10.09 $C_{18}H_{35}O_3NCl$. Calculated %: Cl 10.08

SUMMARY

The reaction of ammonia with petroselinic acid (cis- Δ^6 -octadecenoic acid) oxide results in the formation of 6-amino-7-hydroxyoctadecanoic acid with m. p. 133-134°. The hydrochloride of this acid was prepared.

LITERATURE CITED

- [1] G. V. Pigulevskii and I. L. Kuranova, Proc. Acad. Sci. USSR 82, 601 (1952).
- [2] G. V. Pigulevskii and I. L. Kuranova, J. Gen. Chem. 24, 2006 (1954).*
- [3] G. V. Pigulevskii and I. L. Kuranova, J. Appl. Chem. 28, 213 (1955).
- [4] F. Sigmund, Monatsh. 52, 185 (1929).
- [5] C. F. H. Allen, J. Am. Chem. Soc. 52, 2958 (1930).
- [6] A. Steger and J. van Loon, Rec. trav. chim. 46, 703 (1927); G. V. Pigulevskii and N. I. Simonova, J. Gen. Chem. 9, 1928 (1939).
- [7] H. F. Linskens, Papierchromatographie in der Botanik, Berlin (1955).

Received July 2, 1958

*Original Russian pagination. See C. B. Translation.

CONDENSATION OF ISOPHTHALIC ALDEHYDE WITH NITROMETHANE

V. V. Perekalin and O. M. Lerner

Thiele [1, 2] was the first to study the reaction of the simplest dialdehydes of the benzene series — terephthalic and orthophthalic aldehydes — with nitromethane. Subsequently this reaction was studied by others [3-5].

The condensation of the third isomeric aldehyde, isophthalic, with nitromethane was first studied by Ruggli and Schetty [6], in order to synthesize and study the properties of 1,3-bis-(β -nitrovinyl)benzene (I). They found that, under the conditions used previously by Worrall for the synthesis of β -nitrostyrene [7], isophthalic aldehyde condenses with nitromethane, forming the dinitrodiolefin (I) in only 7% yield.

They were able to raise the yield of (I) to 35% by the use of methylamine and benzylamine as catalysts.

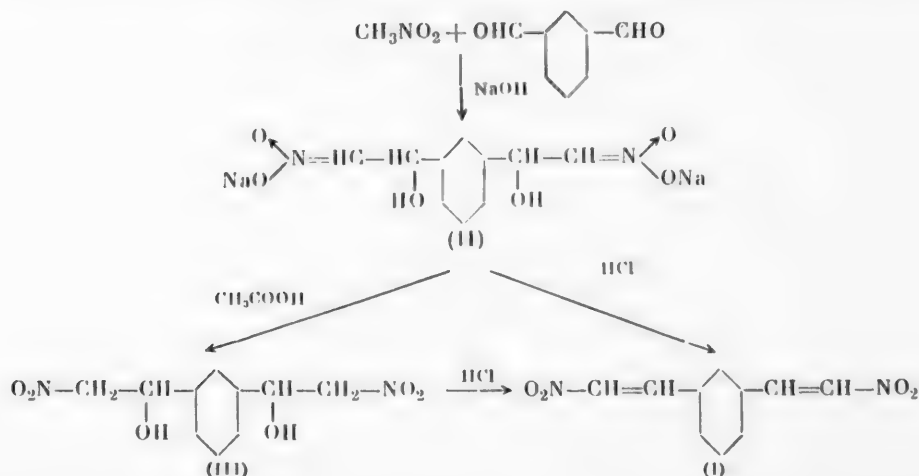
In continuation of our work on dinitrodiolefins [5, 8], we also studied this reaction.

It was found that, by analogy with the procedure developed by us for condensation of terephthalic aldehyde with nitromethane [5], the reaction with isophthalic aldehyde should also be carried out with the use of excess concentrated caustic soda solution as the condensing agent. The yield of (I) then increases to 67%.

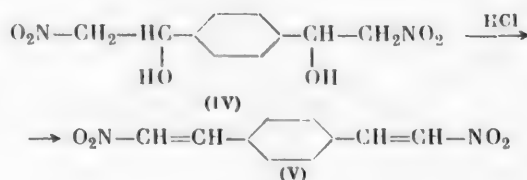
As in the case of the simplest aromatic aldehydes, under the influence of caustic soda there is first formed the product of aldol condensation of isophthalic aldehyde with nitromethane — the disodium salt of aci-1,3-bis-(α -hydroxy- β -nitroethyl)-benzene (II). The action of dilute hydrochloric acid on an aqueous solution of (II) causes separation of the sparingly soluble dinitrodiolefin (I); the action of dilute acetic acid gives 1,3-bis-(α -hydroxy- β -nitroethyl)-benzene (III), not previously described.

To confirm the structure of (III), the conditions for this conversion into the dinitrodiolefin (I) were studied.

Use was made of the recently developed method for dehydration of aryl nitroethanols [9] by means of an aqueous alcoholic solution of hydrochloric acid to convert the dinitroglycol (III) directly into the dinitrodiolefin (I).



This dehydration procedure was successfully applied in the conversion of 1,4-bis-(α -hydroxy- β -nitroethyl)-benzene (IV) [5] into 1,4-bis-(β -nitrovinyl)-benzene (V).



EXPERIMENTAL

Condensation of Isophthalic Aldehyde with Nitromethane. A three-necked 100 ml flask fitted with a stirrer and thermometer was charged with 5.4 g (0.04 mole) of isophthalic aldehyde and 35 ml of methanol. The reaction mass was cooled to -5° , and 4.8 g (0.12 mole) of caustic soda in 8 ml of water was added with vigorous stirring in such a manner that the reaction temperature did not exceed $15-18^\circ$. The resultant solution was again cooled to -5° , and 5 g (0.082 mole) of nitromethane was added rapidly (within 15-20 seconds). The temperature rose spontaneously to 10° . The solution was stirred for 15 minutes at 5° , and 60 ml of ice water was then added. The solution of disodium salt of aci-1,3-bis-(α -hydroxy- β -nitroethyl)-benzene can be converted either into 1,3-bis-(β -nitrovinyl)-benzene (I), or into 1,3-bis-(α -hydroxy- β -nitroethyl)-benzene (III), according to the procedure used subsequently.

Preparation of 1,3-bis-(β -nitrovinyl)-benzene (I). After addition of the reaction mass to a cooled solution of 4 N hydrochloric acid, a yellow precipitate of the dinitrodiolefin (I) separated out; this was filtered off, washed with water, pressed out thoroughly, and crystallized from acetone. This gave 5 g of fine orange crystals of m.p. 204° . A mixed sample of this substance with known 1,3-bis-(β -nitrovinyl)-benzene gave no melting point depression. Evaporation of the acetone mother liquor, or addition of ethanol, yielded an additional 0.9 g of the dinitrodiolefin of m.p. $201-203^\circ$. Total yield was 5.9 g, or 67% of theoretical.

Preparation of 1,3-bis-(α -hydroxy- β -nitroethyl)-benzene (III). This solution, prepared earlier, was added gradually to 50 ml of 40% acetic acid; a white crystalline precipitate of the dinitroglycol (III) formed slowly. After 10-15 hours the substance was separated by filtration from the cooled liquor and dried in air. The yield was 5.6 g, or 55% of the theoretical.

1,3-bis-(α -hydroxy- β -nitroethyl)-benzene is a cream-colored crystalline substance of m.p. $100-102^\circ$ (from dichloroethane with subsequent addition of chloroform); it is readily soluble in ethanol, benzene, chloroform, and ethyl acetate.

Found %: N 10.91; 10.95 $\text{C}_{10}\text{H}_{12}\text{O}_6\text{N}_2$. Calculated %: N 10.93

Conversion of 1,3-bis-(α -hydroxy- β -nitroethyl)-benzene into 1,3-bis-(β -nitrovinyl)-benzene. A flask, 50 ml in capacity, fitted with a stirrer and reflux condenser, contained 2.5 g of the dinitroglycol (III), 10 ml of ethanol, 10 ml of water, and 10 ml of concentrated hydrochloric acid. The reaction mass was boiled for 7 hours. On the following day the precipitate was filtered off, washed, and crystallized from acetone. The compound melted at 204° and did not give a melting point depression with the dinitrodiolefin (I).

Conversion of 1,4-bis-(α -hydroxy- β -nitroethyl)-benzene into 1,4-bis-(β -nitrovinyl)-benzene. The reaction conditions were similar to those described in the preceding paragraph. The dinitroglycol (IV) was boiled for 7 hours, and the precipitate formed was crystallized from acetone-ethanol mixture. A compound of m.p. $229-230^\circ$ was obtained; this gave no melting point depression with known 1,4-bis-(β -nitrovinyl)-benzene (V).

LITERATURE CITED

- [1] J. Thiele, Ber. 32, 1293 (1899).
- [2] J. Thiele and E. Weitz, Ann. 377, 1 (1910).
- [3] D. Worrall, J. Am. Chem. Soc. 62, 3253 (1940).
- [4] O. Schales and H. Grafe, J. Am. Chem. Soc. 74, 4486 (1952).

- [5] V. V. Perekalin and O. M. Lerner, *J. Gen. Chem.* 28, 1815 (1958).*
- [6] P. Ruggli and O. Schetty, *Helv. Chim. Acta* 23, 718 (1940).
- [7] D. Worrall, in the book: *Organic Syntheses* 1, (IL, Moscow, 1949), p. 308 [Russian translation].
- [8] V. V. Perekalin and O. M. Lerner, *J. Appl. Chem.* 29, 1610 (1956).*
- [9] A. Dornow and G. Petsch, *Arch. Pharm.* 284, 153 (1951); *C. A.* 46, 8621 (1952).

Received July 11, 1958

*Original Russian pagination. See C. B. Translation.



Physical Chemistry

**PHYSICAL CHEMISTRY Section
of the
PROCEEDINGS OF THE ACADEMY OF SCIENCES
OF THE USSR (DOKLADY)**

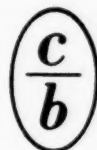
including all reports on:

**Chemical Kinetics
Interface Phenomena
Electrochemistry
Absorption Spectra
and related subjects**

As in all sections of the Proceedings, the papers are by leading Soviet scientists. Represents a comprehensive survey of the most advanced Soviet research in physical chemistry. The 36 issues will be published in 6 issues annually. Translation began with the 1957 volume. Translation by Consultants Bureau bilingual chemists, in the convenient C. B. format.

Annual subscription	\$160.00
Single issues	35.00
Individual articles	5.00

Cover-to-cover translation, scientifically accurate. Includes all diagrammatic and tabular material integral with the text; clearly reproduced by multilith process; staple bound.



CONSULTANTS BUREAU, INC.
227 W. 17th St., NEW YORK 11, N. Y.



Chemistry Collections

IN ENGLISH TRANSLATION

Consultants Bureau's chemistry collections, a unique venture in the translation-publishing field, consist of articles on specialized subjects, selected by specialists in each field, from Soviet chemical journals published in translation by CB. These collections are then presented in symposium form.

Periodically we shall issue new collections taken from the latest volumes of our journals, not only on subjects already covered but also on those which prove most valuable to current scientific research. The following is one of the most recent additions to our list of collections (information on forthcoming titles available on request).

SOVIET RESEARCH IN FUSED SALTS (1956)

42 papers taken from the following Soviet chemistry journals, 1956: Soviet Journal of Atomic Energy; Journal of General Chemistry; Journal of Applied Chemistry; Bulletin of the Academy of Sciences, USSR, Division of Chemical Sciences; Proceedings of the Academy of Sciences, USSR, Chemistry Section. The entire collection consists of one volume, in two sections.

I Systems (23 papers)	\$ 30.00
II Electrochemistry: Aluminum and Magnesium, Corrosion, Theoretical; Thermodynamics; Slags, Mattes (19 papers)	20.00
THE COMPLETE COLLECTION	\$ 40.00

also available in translation . . .

SOVIET RESEARCH IN FUSED SALTS (1949-55)

125 papers taken from the following Soviet chemistry journals, 1949-55: Journal of General Chemistry; Journal of Applied Chemistry; Bulletin of Academy of Sciences, USSR, Div. Chemical Sciences; Journal of Analytical Chemistry. Sections of this collection may be purchased separately as follows:

Structure and Properties (100 papers)	\$110.00
Electrochemistry (8 papers)	20.00
Thermodynamics (6 papers)	15.00
Slags and Mattes (6 papers)	15.00
General (5 papers)	12.50
THE COMPLETE COLLECTION	\$150.00

NOTE: Individual papers from each collection are available at \$7.50 each. Tables of contents sent upon request.

CB collections are translated by bilingual scientists, and include all photographic, diagrammatic and tabular material integral with the text. Reproduction is by multilith process from "cold" type; books are staple bound in durable paper covers.

CONSULTANTS BUREAU, INC.

227 WEST 17TH STREET, NEW YORK 11, N. Y.

